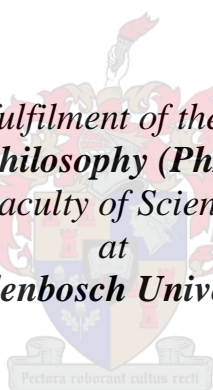


# **Novel analytical methods for the determination of antiretroviral drugs and their metabolites in environmental water samples**

by

**Tlou Thatayotlhe Mosekiemang**

*Thesis presented in fulfilment of the requirements for the degree of **Doctor of Philosophy (PhD) in Chemistry** in the Faculty of Science at **Stellenbosch University***



Supervisor: Prof. André de Villiers  
Co-supervisor: Prof. Marietjie Stander

**December 2021**

## **Declaration**

By submitting this dissertation electronically, I declare that the entirety of the work contained therein is my own, original work, that I am the sole author thereof (save to the extent explicitly otherwise stated), that reproduction and publication thereof by Stellenbosch University will not infringe any third party rights and that I have not previously in its entirety or in part submitted it for obtaining any qualification.

**Date:** December 2021

## Abstract

The occurrence and persistence of pharmaceuticals in aquatic environments is a topical public health issue because of their perpetual discharge into the environment as intact- or biotransformed products. The environmental effects for most these compounds are known, but much concern relates to the recently introduced pharmaceutical classes such as antiretroviral drugs (ARVDs), as well as their metabolites and transformation products. The potential presence of transformation products and metabolites of most ARVDs in wastewater samples is currently largely unknown. Most of the analytical methods developed to monitor ARVDs in aqueous environmental samples are targeted at selected compounds of a few therapeutic classes, warranting the need to expand their scope. ARVDs vary significantly in terms of molecular size,  $pK_a$  and polarity, which further complicates the development of universal analytical methods for ARVD determination.

The first task of this study was to develop a liquid chromatography-tandem mass spectrometric (LC-MS/MS) multiresidue method for the analysis of multiclass ARVDs and selected metabolites in wastewater samples. This necessitated the development of two separate sample preparation methods: one based on reversed phase (RP) solid phase extraction (SPE) sample clean-up and pre-concentration, and a second based on direct injection to correct for losses of polar ARVDs due to low breakthrough volumes on SPE. Application of the developed method to samples obtained from two wastewater treatment plants (WWTPs) in the Western Cape differing by advanced tertiary treatment processes allowed the first confirmation and quantification of two phase I ARVD metabolites, 8,14-dihydroxy efavirenz and 12-hydroxynevirapine. Furthermore, quantitative results confirm that levels of ARVDs in South African wastewaters are generally comparable to the rest of the world, and that they were mostly effectively removed by established treatment processes, with the exception of efavirenz and nevirapine. High concentrations were measured in the dry season, and the polar ARVDs were measured at high concentrations. WWTP treatment by *uv*-irradiation was found to be more effective at removing ARVDs compared to chlorination.

In the second part of the study, supercritical fluid chromatography (SFC)-MS/MS was evaluated as an alternative to LC-MS/MS for the analysis of ARVDs in wastewater. Although the scope of the developed SFC-MS/MS method was more limited compared to LC, there was a high level of agreement in the quantitative data (recoveries, repeatability, and reproducibility) obtained by the two methods. These findings demonstrate for the first time the suitability of SFC-MS/MS for environmental analysis of ARVDs and their metabolites.

Finally, a non-targeted LC-high resolution MS (HR-MS) method incorporating ion mobility spectrometry (IMS) was developed to screen for additional ARVDs and metabolites in wastewater samples. Based on IMS-filtered HR-MS low and high collision energy spectra and IMS collision cross section values, and using a suitable mass defect filter, several novel hydroxylated-, sulphated,

carboxylated and glucuronidated metabolites for efavirenz, nevirapine, ritonavir and abacavir were identified for the first time in wastewater.

## Opsomming

Die voorkoms en hardnekkigheid van farmaseutiese produkte in akwatiese omgewings is 'n aktuele openbare gesondheids kwessie as gevolg van hul storting in die omgewing, beide as onveranderde- en biogetransformeerde produkte. Die omgewingsimpak van die meeste van hierdie verbindings is reeds bekend, maar heelwat kommer bestaan in verband met onlangs bekendgestelde farmaseutiese produkte soos antiretrovirale middels (ARVDs) asook hul metaboliëte en transformasieprodukte. Die potensieë teenwoordigheid van hierdie transformasieprodukte en metaboliëte van die meeste ARVDs in afvalwatermonsters is tans grotendeels onbekend. Meeste van die analitiese metodes wat ontwikkel is om ARVDs in waterige omgewingsmonsters te monitor, is gemik op geselekteerde verbindings van beperkte terapeutiese klasse en dit regverdig die behoefte aan die uitbreiding daarvan. ARVDs wissel aansienlik in terme van molekulêre grootte,  $pK_a$  en polariteit en dit bemoeilik die ontwikkeling van universele analitiese metodes vir ARVD-bepaling verder.

Die eerste mikpunt van hierdie studie was om 'n vloeistofchromatografie-tandem massaspektrometriese (LC-MS/MS) multiresidu-metode te ontwikkel vir die analise van multi-klas ARVDs en geselekteerde metaboliëte in afvalwatermonsters. Dit het die ontwikkeling van twee afsonderlike monstervoorbereidingsmetodes genoodsaak: een is gebaseer op omgekeerde fase (RP) soliede fase ekstraksie (SPE) skoonmaak en voorkonsentrasie van die monster, en 'n tweede gebaseer op direkte inspuiting om verliese van polêre ARVDs, as gevolg lae deurbreekvolumes met SPE, te vermy. Die toepassing van die ontwikkelde metodes op monsters verkry vanaf twee afvalwaterbehandelingsaanlegte in die Wes-Kaap, wat verskil in hul gevorderde tersiëre behandelingsprosesse, het die eerste bevestiging en kwantifisering van twee fase I ARVD-metaboliëte, 8,14-dihydroxy efavirenz en 12-hydroxynevirapine, moontlik gemaak. Verder bevestig kwantitatiewe resultate dat vlakke van ARVDs in Suid-Afrikaanse afvalwater oor die algemeen vergelykbaar is met die res van die wêreld, en dat hulle meestal effektief verwyder word deur gevestigde behandelingsprosesse, met die uitsondering van efavirenz en nevirapine. Hoër konsentrasies is in die droë seisoen gemeet en die polêre ARVDs is ook in hoër konsentrasies gevind. Daar is waargeneem dat behandeling deur *uv*-bestraling meer effektief is vir verwydering van ARVDs as chlorinerings.

In die tweede deel van die studie is superkritiese vloeistofchromatografie (SFC)-MS/MS geëvalueer as 'n alternatief tot LC-MS/MS vir die analise van ARVDs in afvalwater. Alhoewel die omvang van die ontwikkelde SFC-MS/MS-metode meer beperk was in vergelyking met LC, was daar 'n hoë mate van ooreenstemming in die kwantitatiewe data (herwinbaarheid, herhaalbaarheid en reproduseerbaarheid) wat deur die twee metodes verkry is. Hierdie bevindings toon vir die eerste keer die geskiktheid van SFC-MS/MS vir die analise van ARVDs en hul metaboliëte in die omgewing.

Ten slotte is 'n ongeteikende LC-hoë resolusie MS (HR-MS) metode wat ioonmobiliteitspektrometrie (IMS) insluit ontwikkel om addisionele ARVDs en hul metaboliëte in afvalwatermonsters te probeer opspoor. Gebaseer op IMS-gefiltreerde HR-MS lae en hoë botsingsenergiespektra en IMS-

botsingsdeursnee-waardes, en met behulp van 'n geskikte massa-defekfilter, is verskeie nuwe gehidroksileerde, gesulfateerde, gekarboksileerde en geglukuroniseerde metaboliëte van efavirenz, nevirapien, ritonavir en abacavir vir die eerste keer in afvalwater geïdentifiseer.

## Acknowledgements

I would like to express my sincere gratitude to the following people and institutions for valuable contributions throughout this study:

- I will forever be indebted to my supervisors: Prof. André de Villiers and Prof. Marietjie Stander for admitting me into their research group despite a very different topic from the rest of the group members. Thanks for your patience and hand-held guidance throughout this study. Again, thanks for the financial support that had enabled me to stay registered when I have exhausted all avenues of securing tuition fees. I will forever be grateful for your support.
- In the same way I am indebted to other staff members at Stellenbosch University many of whom contributed immensely to this study: Malcolm Taylor for sharing his immense expertise of MassLynx™ and more recently our discussion regarding MetaboLynx™, Erick van Schalkwyk with whom I learnt most aspects of trouble shooting, Prof. Burger and Dr A. Tredoux for their presence in the lab meant a lot to us. This refers also to my fellow group members; Sithandile, Gaalebalewe, Pieter, Magriet, William, Aron, Esther and Keabetswe for your friendship.
- Gratitude's are also due to Mrs. Norma Derby (Coordinator, African Partnerships, Stellenbosch International Office), Prof. O. Dikinya (HoD, Environmental Science, University of Botswana), Prof. R. Madibela (Botswana University of Agriculture and Natural Science), and Ms Neo Seroke (Manager, Training and Development, University of Botswana). I appreciated your encouragements, well wishes, and regular contact with me whilst away from home.
- Most importantly, I appreciate the financial support received from TRECCAfrica II initiative, National Research Foundation of South Africa (NRF), and the University of Botswana.

## List of abbreviations

7,14-dihydroxy EFZ: 7,14-dihydroxy efavirenz

8,14-dihydroxy EFZ: 8,14-dihydroxy efavirenz

8,14-dihydroxy EFZ-sulphate: 8,14-dihydroxy efavirenz-sulphate

7-hydroxy EFZ: 7-hydroxy efavirenz

8-hydroxy EFZ: 8-hydroxy efavirenz

2-hydroxy NVP: 2-hydroxy nevirapine

3-hydroxy NVP: 3-hydroxy nevirapine

12-hydroxy NVP: 12-hydroxy nevirapine

3TC: lamivudine

ABC: abacavir

APCI: atmospheric pressure chemical ionisation

API: atmospheric pressure ionisation

APPI: atmospheric pressure photoionization

ART: antiretroviral therapy

ARV: antiretroviral

ARVDs: antiretrovirals drugs

ATV: atazanavir

CCS: collision cross section

DI: direct injection

DIA: data independent acquisition

EFZ: efavirenz

ESI: electrospray ionisation

ESI+: positive ESI

ESI-: negative ESI



EtOAc: ethyl acetate

FA: formic acid

FTC: emtricitabine

HR-MS: high resolution mass spectrometry

ILIS: Isotopically labelled internal standard

IMS: ion mobility spectrometry

LOD: limit of detection

Log  $K_{ow}$ : Water-Octanol partition coefficient

LOQ: limit of quantification

LC: liquid chromatography

LPV: lopinavir

MDF: mass defect filter

MDL: method detection limit

ME: matrix effects

MRM: multiple reaction monitoring

MS: mass spectrometer

MS/MS: tandem mass spectrometry

MQL: method quantification limit

$m/z$ : mass-to-charge ratio

NVP: nevirapine

NRTI: nucleoside/nucleotide reverse transcriptase inhibitor

*n*NRTI: non-nucleoside reverse transcriptase inhibitor

PI: protease inhibitor

q: qualifier ion

Q: quantifier ion

Q-TOF: quadrupole time-of-flight

RP: reversed phase

RP-LC: reversed phase liquid chromatography

RP-SPE: reversed phase solid phase extraction

RTV: ritonavir

SFC: supercritical fluid chromatography

SPE: solid phase extraction

$t_A$ : arrival time

TOF: time-of-flight

$t_R$ : retention time

TWIMS: travelling wave ion mobility spectrometer

UHPLC: ultra high performance liquid chromatography

WWTP: wastewater treatment plant

ZDV: Zidovudine

# Table of Contents

<b>Declaration</b>	i
<b>Abstract</b>	ii
<b>Opsomming</b>	iv
<b>Acknowledgements</b>	vi
<b>List of abbreviations</b>	vii
<b>General introduction and objectives</b>	1
<b>1.1 Introduction</b>	2
<b>1.2 Aims and objectives.</b>	5
<b>1.3 References</b>	6
<b>Chapter 2</b>	10
<b>Literature Review</b>	10
<b>2.1 Brief overview of antiretrovirals</b>	11
<b>2.2 Metabolism and excretion</b>	14
<b>2.3 Wastewater treatment</b>	15
<b>2.4. Analysis of wastewater</b>	17
2.4.1 <i>Sample collection and storage</i>	17
2.4.2 <i>Sample clean-up and extraction</i>	18
2.4.2.1 <i>SPE conditioning and sample loading</i>	19
2.4.2.2 <i>Theoretical overview of the breakthrough phenomenon</i>	19
2.4.2.3 <i>Analyte elution step</i>	21
2.4.2.4 <i>Eluent drying and residue resuspension.</i>	22
2.4.3 <i>Direct injection</i>	28
2.4.4 <i>Lyophilisation</i>	28
2.4.5 <i>Instrumental analyses of ARVDs in environmental samples</i>	30
2.4.5.1 <i>Liquid chromatography (LC)</i>	30
2.4.5.2 <i>Gas chromatography</i>	31
2.4.5.3 <i>Supercritical fluid chromatography (SFC)</i>	31
2.4.6 <i>Mass spectrometric detection of ARVDs in environmental samples</i>	32
2.4.6.1 <i>Ionisation modes</i>	32
2.4.7 <i>Tandem mass spectrometry</i>	34
2.4.8 <i>Method validation of quantitative data</i>	36
2.4.9 <i>High resolution mass spectrometry</i>	38
2.4.10 <i>Processing of HR-MS data using advanced data analysis tools.</i>	40
2.4.11 <i>Ion mobility spectrometry</i>	42
<b>2.5 Summary</b>	44
	x

<b>2.6</b>	<b>References</b>	46
	<b>Chapter 3</b>	60
	<b>Simultaneous quantification of commonly prescribed antiretroviral drugs and their selected metabolites in aqueous environmental samples by direct injection and solid phase extraction liquid chromatography - tandem mass spectrometry<sup>#</sup></b>	60
	<b>Abstract</b>	61
	<b>3.1. Introduction</b>	62
	<b>3.2. Materials and methods</b>	64
	3.2.1 <i>Reagents and chemicals</i>	64
	3.2.2 <i>Sample collection</i>	64
	3.2.3 <i>Instrumentation and experimental conditions</i>	65
	3.2.4 <i>Quantitation and method validation</i>	65
	3.2.5 <i>Direct injection LC-MS/MS: Procedure and evaluation of recovery and matrix effects</i>	66
	3.2.6 <i>SPE-LC-MS/MS: Procedure and evaluation of recovery and matrix effects</i>	66
	<b>3.3 Results and discussion</b>	67
	3.3.1 <i>Solubility profiling of the target analytes</i>	67
	3.3.2 <i>Chromatographic performance</i>	67
	3.3.3 <i>Evaluation of direct injection LC-MS/MS for the analysis of wastewater samples</i>	68
	3.3.4 <i>Optimisation and evaluation of SPE sample preparation for surface water samples</i>	69
	<b>3.3.5 Method validation</b>	70
	3.3.5.1 <i>Calibration and method selectivity</i>	70
	3.3.5.2 <i>Accuracy, intermediate precision and matrix effects</i>	70
	3.3.6 <i>Occurrence of ARVDs and selected metabolites in wastewater samples from two wastewater plants in South Africa</i>	71
	3.3.6.1 <i>Seasonal patterns of occurrence of ARVDs and their metabolites</i>	74
	3.3.6.2 <i>Comparison of quantitative data for ARVDs with previous studies</i>	75
	<b>3.4 Conclusions</b>	77
	<b>3.5 References</b>	79
	<b>Supplementary information for:</b>	83
	<b>Simultaneous quantification of commonly prescribed antiretroviral drugs and their selected metabolites in aqueous environmental samples by direct injection and solid phase extraction liquid chromatography - tandem mass spectrometry</b>	83
	<b>Chapter 4</b>	99
	<b>Evaluation of supercritical fluid chromatography-tandem mass spectrometry (SFC-MS/MS) for the analysis antiretrovirals and their selected metabolites in wastewater</b>	99
	<b>Abstract</b>	100
	<b>4.1 Introduction</b>	101

<b>4.2 Experimental</b>	102
4.2.1 Chemicals and reagents	102
4.2.2 SFC experimental conditions and column evaluation	103
4.2.3 Mass spectrometric optimisation	104
4.2.4 Preparation of calibration standard solutions	104
4.2.5 Sample collection and preparation	105
4.2.5.1 Lyophilisation	105
4.2.5.2 Solid phase extraction	105
4.2.6 Reconstitution of dried extracts	105
4.2.7 Evaluation of method performance	106
<b>4.3 Results and Discussion</b>	106
4.3.1 Optimisation of SFC-MS/MS conditions	106
4.3.2 Comparison of SPE and lyophilisation for sample preparation	110
4.3.3 Method evaluation and validation	113
4.3.4 Comparison of quantitative results: SFC-MS/MS and UHPLC-MS/MS	117
4.3.5 Overall method performance	117
<b>4.4 Conclusions</b>	118
<b>4.5 References</b>	119
<b>Chapter 4</b>	125
<b>Supplementary information for:</b>	125
<b>Evaluation of supercritical fluid chromatography-tandem mass spectrometry (SFC-MS/MS) for the analysis antiretrovirals and their selected metabolites using SFC-MS/MS</b>	125
<b>Chapter 5</b>	137
<b>Ultra high pressure liquid chromatography coupled to travelling wave ion mobility-time of flight mass spectrometry for the screening of pharmaceutical metabolites in wastewater samples: application to antiretrovirals.</b>	137
<b>Abstract</b>	138
<b>5.1 Introduction</b>	139
<b>5.2 Experimental</b>	141
5.2.1 Chemicals	141
5.2.2 Sample preparation	142
5.2.3 UHPLC settings	142
5.2.4 TWIMS-Q-TOF settings	143
<b>5.3 Results and discussion</b>	143
5.3.1 Analytical procedure for the untargeted screening of ARVD metabolites in wastewater samples. 143	
5.3.2 Identification of ARVD metabolites	149

5.3.2.1 <i>Efavirenz metabolites</i>	149
5.3.2.1.1 <i>Monohydroxylated metabolites of efavirenz</i>	149
5.3.2.1.2 <i>Dihydroxylated metabolites of efavirenz</i>	152
5.3.2.1.3 <i>Phase II metabolites of efavirenz</i>	153
<i>Glucuronide metabolite</i>	153
<i>Sulphated metabolites</i>	154
5.3.2.2 <i>Nevirapine metabolites</i>	156
5.3.2.3 <i>Ritonavir metabolite</i>	159
5.3.2.4 <i>Abacavir metabolite</i>	159
5.3.3 <i>Occurrence of the ARVD metabolites</i>	159
<b>5.4 Conclusions</b>	160
<b>5.5 References</b>	161
<b>Supplementary information for:</b>	168
<b>Ultra high pressure liquid chromatography coupled to travelling wave ion mobility-time of flight mass spectrometry for the screening of pharmaceutical metabolites in wastewater samples: application to antiretrovirals.</b>	168
<b>References</b>	175
<b>General Conclusions and Recommendations</b>	176
<b>6.1 General conclusions</b>	177
<b>6.2 Recommendations for future studies</b>	178

# Chapter 1

---

## General introduction and objectives

## 1.1 Introduction

The main drivers of aquatic pollution by pharmaceutical compounds are human excretion of unchanged drugs and metabolites, disposal of expired/unwanted drugs into the sewer system and partial removal of these drugs by established wastewater treatment processes (Nannou *et al.*, 2020, 2019; Ncube *et al.*, 2018). After ingestion, and by the end of a therapeutic process, drugs are eliminated intact or as metabolites from the body through various clearance routes, chief of which is excretion in urine and faecal matter (Ncube *et al.*, 2018). Discharge of effluent into rivers and streams is a widely used disposal method that constitutes a major pathway for the contamination of pristine surface waters (Botero-Coy *et al.*, 2018). The environmental impacts of most pharmaceuticals are well documented, and in advanced economies they are registered as priority compounds on the watchlist of environmental persistent substances for which advanced tertiary treatment of effluent by *uv*-irradiation, chlorine oxidation, *etc.* is required before discharge (Russo *et al.*, 2018; Zhou *et al.*, 2019). For example, X-ray agents are well known carcinogens (Buseti *et al.*, 2008), antibiotics are believed to cause antibiotic resistance in bacteria and are blamed for more cases of difficult-to-treat infections (Botero-Coy *et al.*, 2018). Regarding the new drugs, not a lot is known about their environmental toxicity and persistence. The same applies to their metabolites, because humans excrete both parent and metabolite, and available data shows that they have not been studied to same extent as the parent compounds (Brown and Wong, 2015). A typical example is the antiretroviral drugs (ARVDs), which have received significant research focus in the last decade (Abafe *et al.*, 2018; Boulard *et al.*, 2018; Funke *et al.*, 2016; K'oreje *et al.*, 2018; Muriuki *et al.*, 2020; Ngumba *et al.*, 2016; Prasse *et al.*, 2010; Wood *et al.*, 2015). However, little is known regarding the environmental impact and fate of ARVD metabolites (Funke *et al.*, 2016; Madikizela *et al.*, 2020; Nannou *et al.*, 2019).

ARVDs are an emerging class of pharmaceuticals used for the treatment of HIV/AIDS. As a consequence, high consumption per capita occurs especially in regions with high incidence rates of this disease (Andrade *et al.*, 2011; Nannou *et al.*, 2019; Ncube *et al.*, 2018). This prompted significant research interest in the study of their occurrence in aquatic environments, in particular in wastewater (Abafe *et al.*, 2018) and surface water (Prasse *et al.*, 2010; Wood *et al.*, 2015), and their removal rates during wastewater treatment (K'oreje *et al.*, 2018; Madikizela *et al.*, 2020; Russo *et al.*, 2018; Zhou *et al.*, 2019). Until now, there is no data regarding the environmental occurrence of ARVD metabolites, despite indications that they are metabolized via phase I and II biotransformation pathways to facilitate body clearance (Nannou *et al.*, 2020, 2019). ARVDs are a diverse group of pharmaceuticals comprised of several therapeutic classes such as nucleoside reverse transcriptase inhibitors (NRTIs), non-nucleoside reverse transcriptase inhibitors (*n*NRTIs), protease inhibitors (PIs), integrase inhibitors (INIs), co-receptor inhibitors (CRIs) and fusion inhibitors (FIs), which are structurally and physico-



chemically dissimilar (Andrade *et al.*, 2011). This diversity may present a unique analytical challenge to develop multiresidue methods targeting the analysis of all the classes simultaneously, especially considering the heterogeneity of wastewater matrix in which they are carried (Mosekiemang *et al.*, 2019). Presumably, this explains the scarcity of multiresidue methods suitable for the analysis of multi-class ARVDs - as opposed to an abundance of methods targeting selected therapeutic classes only.

Liquid chromatography coupled to mass spectrometry (LC-MS) is the most widely used instrument in the analysis of ARVDs in wastewater samples (Ngumba *et al.*, 2016). Preceding LC-MS analysis is a lengthy and often complicated sample clean up, analyte extraction and pre-concentration step, which may not be straightforward due to the extreme variation in polarity and pK<sub>a</sub> displayed by ARVDs (Backe and Field, 2012). Moreover, these compounds are normally present in wastewater at varying concentrations, typically in the range ng/mL-µg/mL, with pre-concentration a mandatory step for analytes present at ng/mL levels (Ngumba *et al.*, 2016). In this situation, the implementation of solid phase extraction (SPE), the most common form of sample pre-treatment for these analyses, may present both advantages and disadvantages (Backe and Field, 2012; Brewer and Lunte, 2015). SPE offers good enrichment of trace level analytes to detectable levels, although this might also be a drawback for compounds present at higher levels due to amplification of concentrations to levels detrimental to the instrument (*i.e.* saturation of the ion source and promotion of carry-over effect due to contamination of the flow path). Furthermore, the extreme polarity range of ARVDs presents a challenge due to poor retention of polar compounds on the generic reversed phase (RP)-SPE sorbents (Nannou *et al.*, 2019). For instance, NRTIs are extremely polar due to the presence of pyrimidine bases (*e.g.* thymine, cytosine, adenine, *etc.*) and a deoxyribose sugar, resulting in poor recoveries on RP-SPE sorbents due to low breakthrough volumes (Aminot *et al.*, 2015; Brewer and Lunte, 2015). While poor recoveries may be accurately compensated for by addition of suitable isotopically labelled internal standards (ILIS) during sample preparation, they are seldom available and expensive.

Pre-concentration may however not be required for analytes occurring at µg/mL levels, because they fall within detectable limits of LC-MS instruments (Nannou *et al.*, 2019; Ngumba *et al.*, 2016). Simple methods such as direct injection and large volume injection LC, that do not rely on analyte enrichment, have recently been developed for this reason (Boulard *et al.*, 2018; Funke *et al.*, 2016; Mosekiemang *et al.*, 2019; Wooding *et al.*, 2017),

Supercritical fluid chromatography (SFC) offers an attractive alternative to LC-MS/MS owing to the chromatographic advantages conferred by high diffusivity of CO<sub>2</sub>-based mobile phase (Desfontaine *et al.*, 2015). SFC hyphenated to MS/MS is relevant in environmental analysis because of inherently low solvent consumption, the capability of very fast analyses and complementary selectivity. To date, however, the technique is relatively unexplored in the environmental context despite growing interest in its application to pharmaceutical analyses. The same is true for hydrophilic interaction

chromatography (HILIC), which has not been used to the same extent as RP-LC, despite its benefits for the analysis of extremely polar pharmaceuticals, their metabolites and transformation products (Boulard *et al.*, 2018; Funke *et al.*, 2016).

Quantitative analyses of ARVDs in wastewater samples is usually achieved by LC-MS/MS on triple quadrupole instruments operated in the multiple reaction monitoring (MRM) mode (Ngumba *et al.*, 2016). This is a highly sensitive approach relying on tandem-in-space MS steps to monitor two or more ion transitions for a selected analyte. The technique is also highly selective and achieves low detection limits, but is not suitable for the detection of analytes that are not included in the MRM method even if they are present in a wastewater sample (Hermes *et al.*, 2018). The use of high resolution mass spectrometry (HR-MS), especially in multi-stage instruments such as quadrupole-time-of-flight (Q-TOF) systems, is an alternative strategy to expand spectral coverage for untargeted analyses due to the ability to perform full scan MS and MS/MS experiments to produce accurate mass precursor and product ion spectra necessary for structural elucidation of unknown compounds (Nannou *et al.*, 2019). Such an approach shows promise for the identification of ARVD metabolites and transformation products, given the scarcity of information on their occurrence in aqueous samples (Funke *et al.*, 2016; Mosekiemang *et al.*, 2019). ARVD metabolites are mostly hydroxylated-, sulfated- and glucuronic acid derivatives of the parent drugs, and as such numerous regioisomers are expected. These isomers cannot be distinguished by HR-MS because positional isomers have identical molecular formula and often similar fragmentation spectra (Hollender *et al.*, 2017). Tandem HR-MS instruments may be operated in data dependent- (DDA) and data independent acquisition (DIA) modes (Kinyua *et al.*, 2015; Wrona *et al.*, 2005). DDA provides better MS/MS spectra, since precursor ions subjected to fragmentation are selected beforehand to increase selectivity and reduce spectral noise. In the DIA mode, all ions are subjected to alternating low and high collision energy fragmentation, which in the case of highly complex samples and/or poor chromatographic resolution may result in highly complex fragmentation spectra that may be difficult to interpret (Hollender *et al.*, 2017). In this instance, spectral deconvolution may be achieved by implementation of an additional separation platform such as ion mobility spectrometry (IMS). IMS involves an electrophoretic separation of gas phase ions under a static or oscillating electric field in the presence of a buffer gas to separate ions according to charge, size, and conformation (Dodds and Baker, 2019). IMS offers the capability to separate co-eluting isomeric and isobaric compounds according to differences in their gas phase mobility properties, and can be used to filter full-scan MS data according to drift or arrival time to provide high quality fragmentation spectra (Hollender *et al.*, 2017). IMS is a promising technique with clear potential in wastewater analysis, but somewhat surprisingly has not gained sufficient attention in this field.

Considering the above, it is apparent that there is no one universal method that could be implemented for the analysis of ARVDs and their metabolites in wastewater; instead, a multifaceted approach comprising several complementary methods is needed.

## 1.2 Aims and objectives.

The main aim of this study was to develop novel chromatographic methods based on liquid chromatography tandem (LC-MS/MS), supercritical fluid chromatography (SFC)-MS/MS, and ion mobility spectrometry (IMS)-high resolution MS (HR-MS) for targeted quantitative, and untargeted screening analysis of ARVDs and their metabolites in wastewater samples. To achieve this, the following objectives were set:

- i) To develop and validate a multiresidue method for the analysis of ARVDs and selected metabolites using UHPLC-MS/MS.
- ii) To evaluate the potential of a combination of lyophilisation and SFC-MS/MS as an alternative method to LC-MS/MS for the analysis of ARVDs and selected metabolites in wastewater.
- iii) To perform a comprehensive untargeted screening for ARVDs and their metabolites in wastewater using high resolution mass spectrometry (HR-MS) coupled to IMS.

### 1.3 References

- Abafe, O.A., Späth, J., Fick, J., Jansson, S., Buckley, C., Stark, A., Pietruschka, B., Martincigh, B.S., 2018. LC-MS/MS determination of antiretroviral drugs in influents and effluents from wastewater treatment plants in KwaZulu-Natal, South Africa. *Chemosphere* 200, 660–670. <https://doi.org/10.1016/j.chemosphere.2018.02.105>
- Aminot, Y., Litrico, X., Chambolle, M., Arnaud, C., Pardon, P., Budzinski, H., 2015. Development and application of a multi-residue method for the determination of 53 pharmaceuticals in water, sediment, and suspended solids using liquid chromatography-tandem mass spectrometry. *Anal. Bioanal. Chem.* 407, 8585–8604. <https://doi.org/10.1007/s00216-015-9017-3>
- Andrade, C.H., de Freitas, L.M., de Oliveira, V., 2011. Twenty-six years of HIV science: An overview of anti-HIV drugs metabolism. *Brazilian J. Pharm. Sci.* 47, 209–230. <https://doi.org/10.1590/S1984-82502011000200003>
- Backe, W.J., Field, J.A., 2012. Is SPE necessary for environmental analysis? A quantitative comparison of matrix effects from large-volume injection and solid-phase extraction based methods. *Environ. Sci. Technol.* 46, 6750–6758. <https://doi.org/10.1021/es300235z>
- Botero-Coy, A.M., Martínez-Pachón, D., Boix, C., Rincón, R.J., Castillo, N., Arias-Marín, L.P., Manrique-Losada, L., Torres-Palma, R., Moncayo-Lasso, A., Hernández, F., 2018. An investigation into the occurrence and removal of pharmaceuticals in Colombian wastewater. *Sci. Total Environ.* 642, 842–853. <https://doi.org/10.1016/j.scitotenv.2018.06.088>
- Boulard, L., Dierkes, G., Ternes, T., 2018. Utilization of large volume zwitterionic hydrophilic interaction liquid chromatography for the analysis of polar pharmaceuticals in aqueous environmental samples: Benefits and limitations. *J. Chromatogr. A* 1535, 27–43. <https://doi.org/10.1016/j.chroma.2017.12.023>
- Brewer, A.J., Lunte, C., 2015. Analysis of Nucleosides in Municipal Wastewater by Large-Volume Liquid Chromatography Tandem Mass Spectrometry. *Anal. Methods* 7, 5504–5510. <https://doi.org/10.1039/C5AY00929D>
- Brown, A.K., Wong, C.S., 2015. Current trends in environmental analysis of human metabolite conjugates of pharmaceuticals. *Trends Environ. Anal. Chem.* 5, 8–17. <https://doi.org/10.1016/j.teac.2015.01.002>
- Busetti, F., Linge, K.L., Blythe, J.W., Heitz, A., 2008. Rapid analysis of iodinated X-ray contrast media in secondary and tertiary treated wastewater by direct injection liquid chromatography-tandem mass spectrometry. *J. Chromatogr. A* 1213, 200–208. <https://doi.org/10.1016/j.chroma.2008.10.021>

- Desfontaine, V., Guillarme, D., Francotte, E., Nováková, L., 2015. Supercritical fluid chromatography in pharmaceutical analysis. *J. Pharm. Biomed. Anal.* 113, 56–71.  
<https://doi.org/10.1016/j.jpba.2015.03.007>
- Dodds, J.N., Baker, E.S., 2019. Ion Mobility Spectrometry: Fundamental Concepts, Instrumentation, Applications, and the Road Ahead. *J. Am. Soc. Mass Spectrom.* 30, 2185–2195.  
<https://doi.org/10.1007/s13361-019-02288-2>
- Funke, J., Prasse, C., Ternes, T.A., 2016. Identification of transformation products of antiviral drugs formed during biological wastewater treatment and their occurrence in the urban water cycle. *Water Res.* 98, 75–83. <https://doi.org/10.1016/j.watres.2016.03.045>
- Hermes, N., Jewell, K.S., Wick, A., Ternes, T.A., 2018. Quantification of more than 150 micropollutants including transformation products in aqueous samples by liquid chromatography-tandem mass spectrometry using scheduled multiple reaction monitoring. *J. Chromatogr. A* 1531, 64–73. <https://doi.org/10.1016/j.chroma.2017.11.020>
- Hollender, J., Schymanski, E.L., Singer, H., Ferguson, P.L., 2017. Non-target screening with high resolution mass spectrometry in the environment: Ready to go? *Environ. Sci. Technol.* [acs.est.7b02184](https://doi.org/10.1021/acs.est.7b02184). <https://doi.org/10.1021/acs.est.7b02184>
- K'oreje, K.O., Kandie, F.J., Vergeynst, L., Abira, M.A., Van Langenhove, H., Okoth, M., Demeestere, K., 2018. Occurrence, fate and removal of pharmaceuticals, personal care products and pesticides in wastewater stabilization ponds and receiving rivers in the Nzoia Basin, Kenya. *Sci. Total Environ.* 637–638, 336–348. <https://doi.org/10.1016/j.scitotenv.2018.04.331>
- Kinyua, J., Negreira, N., Ibáñez, M., Bijlsma, L., Hernández, F., Covaci, A., Van Nuijs, A.L.N., 2015. A data-independent acquisition workflow for qualitative screening of new psychoactive substances in biological samples. *Anal. Bioanal. Chem.* 407, 8773–8785.  
<https://doi.org/10.1007/s00216-015-9036-0>
- Madikizela, L.M., Ncube, S., Chimuka, L., 2020. Analysis, occurrence and removal of pharmaceuticals in African water resources: A current status. *J. Environ. Manage.* 253, 109741.  
<https://doi.org/10.1016/j.jenvman.2019.109741>
- Mosekiemang, T.T., Stander, M.A., de Villiers, A., 2019. Simultaneous quantification of commonly prescribed antiretroviral drugs and their selected metabolites in aqueous environmental samples by direct injection and solid phase extraction liquid chromatography - Tandem mass spectrometry. *Chemosphere* 220, 983–992. <https://doi.org/10.1016/j.chemosphere.2018.12.205>
- Muriuki, C., Kairigo, P., Home, P., Ngumba, E., Raude, J., Gachanja, A., Tuhkanen, T., 2020. Mass loading, distribution, and removal of antibiotics and antiretroviral drugs in selected wastewater

- treatment plants in Kenya. *Sci. Total Environ.* 743, 140655.  
<https://doi.org/10.1016/j.scitotenv.2020.140655>
- Nannou, C., Ofrydopoulou, A., Evgenidou, E., Heath, D., Heath, E., Lambropoulou, D., 2020. Antiviral drugs in aquatic environment and wastewater treatment plants: A review on occurrence, fate, removal and ecotoxicity. *Sci. Total Environ.* 699, 134322.  
<https://doi.org/10.1016/j.scitotenv.2019.134322>
- Nannou, C., Ofrydopoulou, A., Evgenidou, E., Heath, D., Heath, E., Lambropoulou, D., 2019. Analytical strategies for the determination of antiviral drugs in the aquatic environment. *Trends Environ. Anal. Chem.* 24, e00071. <https://doi.org/10.1016/j.teac.2019.e00071>
- Ncube, S., Madikizela, L.M., Chimuka, L., Nindi, M.M., 2018. Environmental fate and ecotoxicological effects of antiretrovirals: A current global status and future perspectives. *Water Res.* 145, 231–247. <https://doi.org/10.1016/j.watres.2018.08.017>
- Ngumba, E., Kosunen, P., Gachanja, A., Tuhkanen, T., 2016. A multiresidue analytical method for trace level determination of antibiotics and antiretroviral drugs in wastewater and surface water using SPE-LC-MS/MS and matrix-matched standards. *Anal. Methods* 8, 6720–6729.  
<https://doi.org/10.1039/c6ay01695b>
- Prasse, C., Schlusener, M.P., Schulz, R., Ternes, T.A., 2010. Antiviral drugs in wastewater and surface waters: a new pharmaceutical class of environmental relevance. *Environ. Sci. Technol.* 44, 1728–1735. <https://doi.org/10.1021/es903216p>
- Russo, D., Siciliano, A., Guida, M., Andreozzi, R., Reis, N.M., 2018. Removal of antiretroviral drugs stavudine and zidovudine in water under UV 254 and UV 254 / H<sub>2</sub>O<sub>2</sub> processes : Quantum yields, kinetics and ecotoxicology assessment. *J. Hazard. Mater.* 349, 195–204.  
<https://doi.org/10.1016/j.jhazmat.2018.01.052>
- Wood, T.P., Duvenage, C.S.J., Rohwer, E., 2015. The occurrence of anti-retroviral compounds used for HIV treatment in South African surface water. *Environ. Pollut.* 199, 235–243.  
<https://doi.org/10.1016/j.envpol.2015.01.030>
- Wooding, M., Rohwer, E.R., Naude, Y., 2017. Determination of endocrine disrupting chemicals and antiretroviral compounds in surface water: A disposable sorptive sampler with comprehensive gas chromatography -Time-of-flight mass spectrometry and large volume injection with ultra-high performance. *J. Chromatogr. A* 1496, 122–132. <https://doi.org/10.1016/j.chroma.2017.03.057>
- Wrona, M., Mauriala, T., Bateman, K.P., Mortishire-Smith, R.J., O'Connor, D., 2005. “All-in-One” analysis for metabolite identification using liquid chromatography/hybrid quadrupole time-of-flight mass spectrometry with collision energy switching. *Rapid Commun. Mass Spectrom.* 19,

2597–2602. <https://doi.org/10.1002/rcm.2101>

Zhou, C., Wang, Y., Chen, J., Niu, J., 2019. Porous Ti / SnO<sub>2</sub> -Sb anode as reactive electrochemical membrane for removing trace antiretroviral drug stavudine from wastewater. *Environ. Int.* 133, 105157. <https://doi.org/10.1016/j.envint.2019.105157>

## **Chapter 2**

---

### **Literature Review**



## 2.1 Brief overview of antiretrovirals

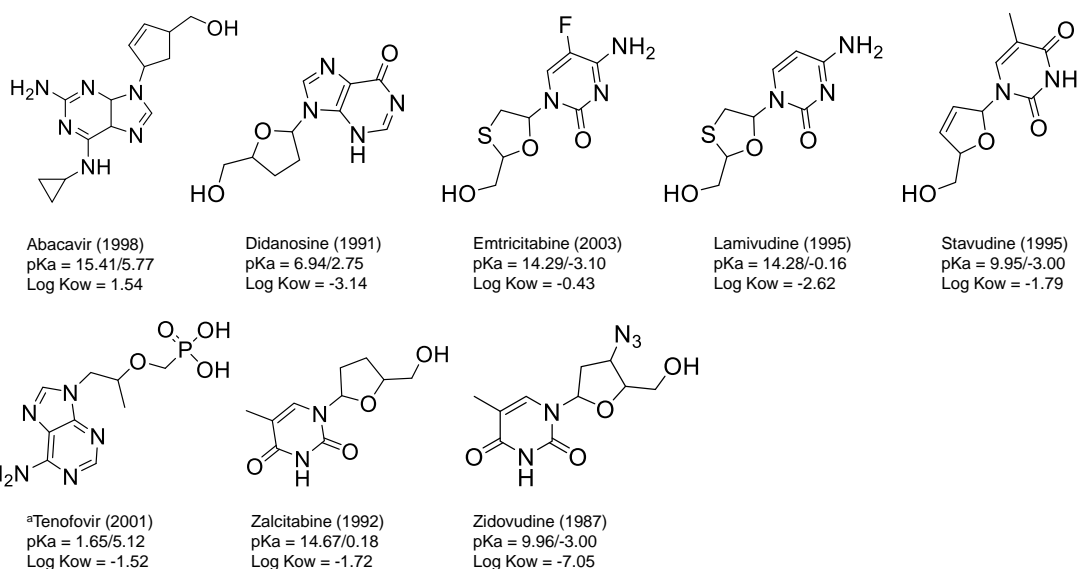
Antiretroviral drugs (ARVDs) are medications used in the treatment of human immune deficiency virus type 1 (HIV-1), although they are not sufficiently potent to eliminate the virus from infected cells (De Clercq, 2009). HIV-1 attacks the CD2-T-cells responsible for the proper functioning of the body's immune system. ARVDs act as inhibitors of the HIV-1 replication- and/or development mechanisms. This was shown in 1985, when it was discovered that zidovudine (ZDV), initially an anti-cancer drug, possessed crucial anti-HIV traits (Andrade *et al.*, 2011; De Clercq, 2009). Since then, the Food Drug Administration (FDA) has already approved ~30 ARVDs with various modes of action (**Figure 2.1**), designed to target the virus at the various stages of its life cycle (Vella *et al.*, 2012). Until now, four distinct approaches have been identified according to which ARVDs function: (1) viral load reduction (virological), (2) reduction in infection rates (epidemiological), (3) improvement and/or resuscitation of the immune system (immunological), and (4) reduction in side effects and/or delay in the onset of full-blown illness (therapeutical). The main goal is to reduce the infectivity and delay the onset of illness. ARVDs are classified according to their modes action: the nucleoside/nucleotide reverse transcriptase inhibitors (NRTIs), the non-nucleoside reverse transcriptase inhibitors (*n*NRTIs), the protease inhibitors (PIs), the integrase inhibitors (INIs), the fusion inhibitors (FIs), and the co-receptor inhibitors (CRIs). These classes possess specific antagonistic roles that impede the normal functioning and development of HIV-1 within the host cell. Therefore, antiretroviral therapy (ART) is generally aimed at lessening morbidity and mortality by targeting the virulence of the virus at its various stages of development. ARVDs are structurally and physico-chemically diverse, both within and between classes, except for NRTIs which display a considerable within class similarity (**Figure 2.1**). Except for NRTIs all other classes are chemically lipophilic (Colombo *et al.*, 2005).

NRTI drugs are generally inactive in their original form and must be converted into bioactive deoxynucleoside triphosphates in the body, which are incorporated into the viral reverse transcriptase where they act as a chain terminator for the reverse transcription mechanism (Andrade *et al.*, 2011; Cihlar and Ray, 2010). FIs prevent entry of the virus into the host cell by blocking the host cell receptor sites (Andrade *et al.*, 2011). PIs contain a hydroxyethylene scaffold, which, when incorporated into the HIV-1-protease, impairs its ability to facilitate maturation of viral protein (Kumar *et al.*, 2004). This briefly illustrates the diversity in modes of action of different ARVDs. To exploit these diverse mechanisms in treatment, a synergistic approach known as combinational therapy or highly active antiretroviral therapy (HAART) was adopted, in which a typical prescription comprises of two to three different therapeutic classes, *e.g.* two NRTI drugs and another drug from a different therapeutic class (Mirochnick *et al.*, 2009; Vella *et al.*, 2012). This broad-spectrum strategy has proved to be effective in addressing mutation related drug resistance and is based on the principle of reducing the risk of resistance: in the event one drug failing, other components of the formulation should remain potent to the virus. This strategy also ensures that the virus is targeted at different critical stages of its life cycle.

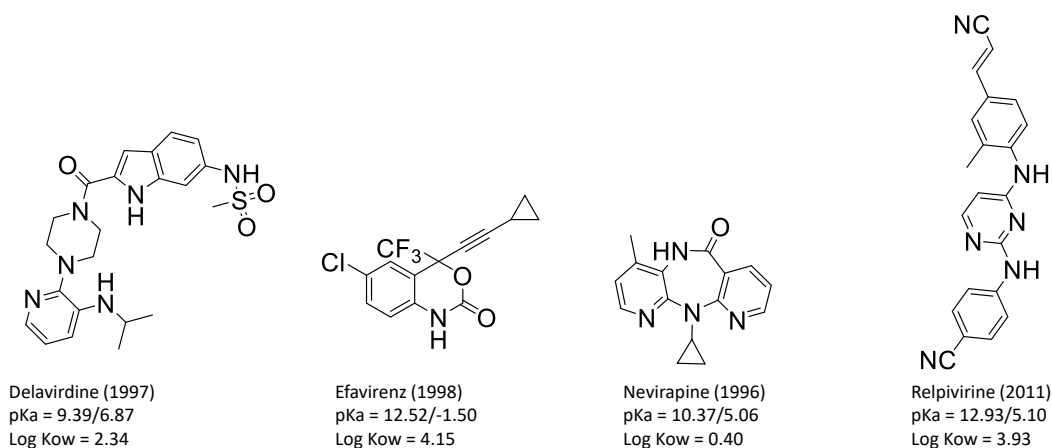
To reduce the risk of drug resistance, strict adherence to therapy is encouraged by current initiatives to ensure improved access to this therapy in regions with high incidence rates (De Clercq, 2009; World Health Organization *et al.*, 2013). This wholesale roll-out of ARVDs initiated by WHO (2016), coupled with the strict adherence obligation, makes these drugs a significant pharmaceutical class in terms of global consumption *per capita* (De Clercq, 2009).

Overall, the concerted initiatives against HIV prevalence have been successful, as evidenced by reduced rates of transmission, reduced mortality and a general increase in the number patients enrolled in ART.

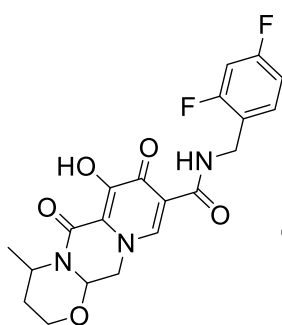
### A) <sup>α</sup>Nucleotide/Nucleoside Reverse Transcriptase Inhibitors



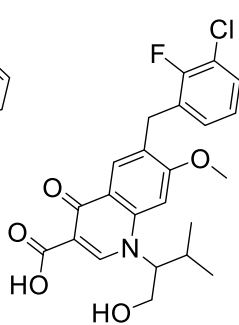
### B) Non-Nucleoside reverse transcriptase inhibitors



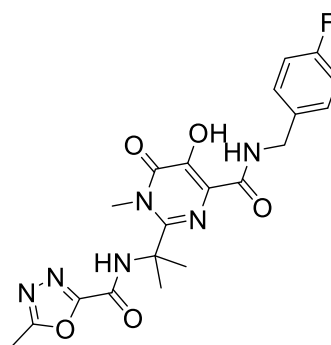
C) Integrase Inhibitors



Dolutegravir (2013)  
pKa = 10.1/-0.51  
Log Kow = 1,62

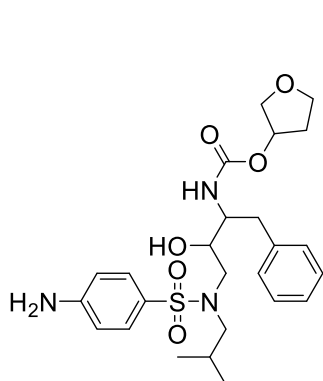


Elvitegravir (2014)  
pKa = 6.16/-0.53  
Log Kow = not available

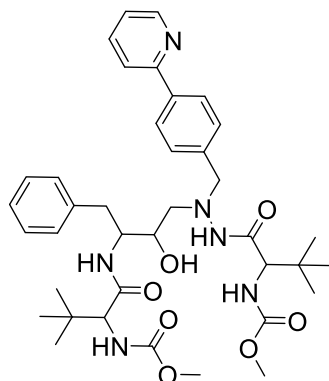


Raltegravir (2007)  
pKa = 5.62/-1.50  
Log Kow = 0,40

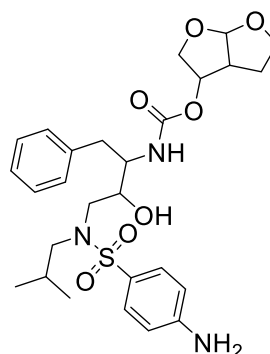
D) Protease Inhibitors



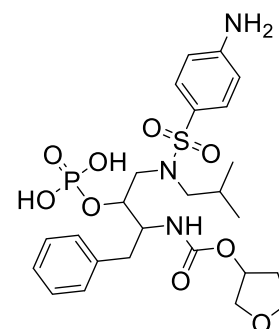
Amprenavir (1999)  
pKa = 13.61/2.39  
Log Kow = 2.20



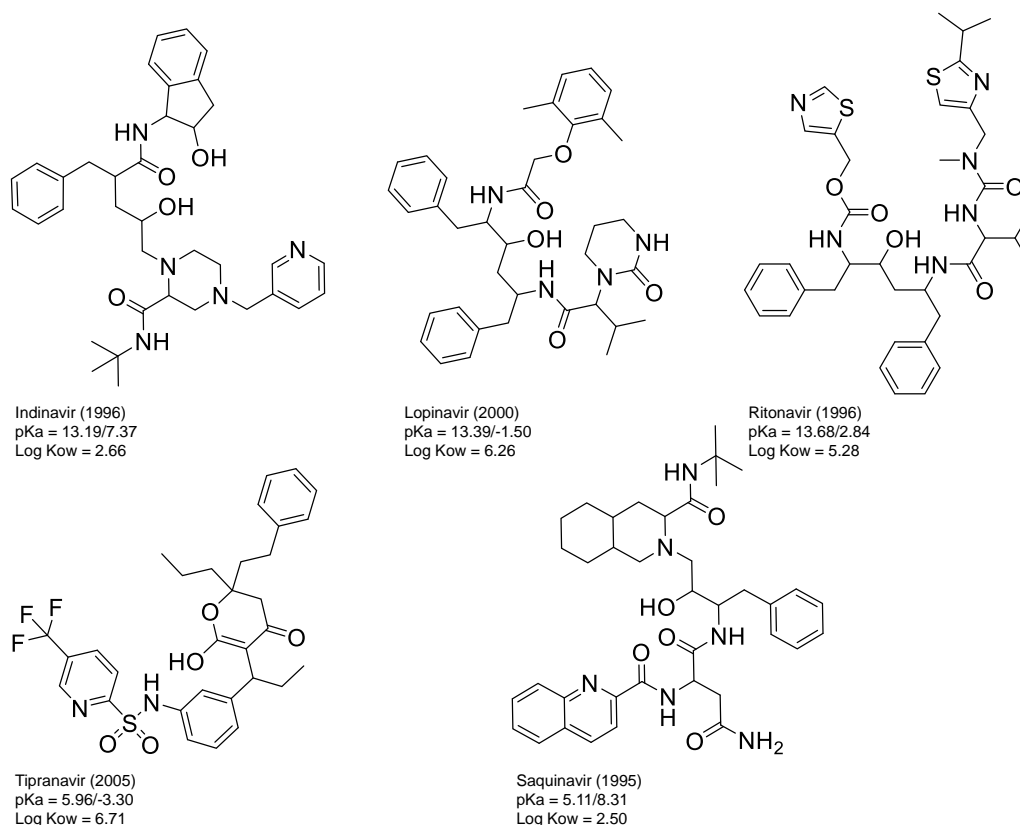
Atazanavir (2003)  
pKa = 5.12/4.33  
Log Kow = 2.88



Darunavir (2006)  
pKa = 13.59/2.39  
Log Kow = 1.88



Fosamprenavir (2003)  
pKa = 1.22/2.45  
Log Kow = 1.62



### E) Fusion Inhibitors

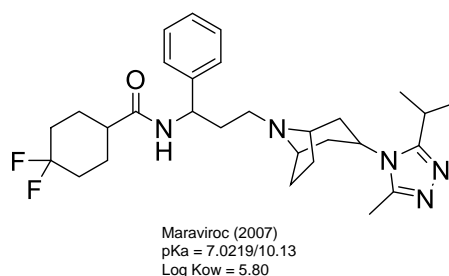


**Figure 2.1:** Molecular structures for ARVDs showing dates of approval by the Food Drug and Administration (FDA, pK<sub>a</sub> and Log K<sub>ow</sub> estimated according to US Environmental Protection Agency (2012). The pK<sub>a</sub> values represents the strongest acid/base according to the Drug bank database (<https://www.drugbank.ca/drugs/>, accessed July 2020).

## 2.2 Metabolism and excretion

Generally, metabolism of ARVDs, just like other pharmaceutical drugs, is a two-phase enzymatic process, referred to as phases I and II (Andrade *et al.*, 2011; Veal and Back, 1995). In Phase I, biotransformation reactions are catalysed by the cytochrome P450 (CYP) group of enzymes in which polar (-SH, -NH<sub>2</sub>, -COOH or -OH) functional groups are attached to the parent compound, while the phase II reactions incorporate larger water-soluble functional groups such as the glucuronic acid, sulphate or glycine to the parent compound (Andrade *et al.*, 2011; Cihlar and Ray, 2010; Mutlib *et al.*,

1999). All these reactions facilitate body clearance, which involves elimination of both parent ARVDs and metabolites along with excreta. This explains why these drugs are significant constituents of wastewater, particularly in HIV-stricken regions such as sub-Saharan Africa (Nannou *et al.*, 2020; Ncube *et al.*, 2018).

A typical metabolic process involving ARVDs is shown in **Figure 2.2**, which describes the biotransformation process for zidovudine, a pioneering drug in the NRTI therapeutic class. The process shows two types of metabolites: the phosphorylated metabolites are intracellular species and therefore retained in the body (and not expected to occur in wastewater), and the inactive and more hydrophilic glucuronidated and hydroxylated metabolites, which are predominantly eliminated from the body via the known clearance routes. The latter forms are environmentally relevant because they enter the sewer along with excreta. Until now, information regarding the extent of body clearance for ARVDs has not been reviewed in detail, which precludes a correlation between the typical concentrations of parent ARVDs and metabolites found in wastewater and pharmacokinetic data. Indeed, this constitutes a literature gap and warrants a dedicated study.

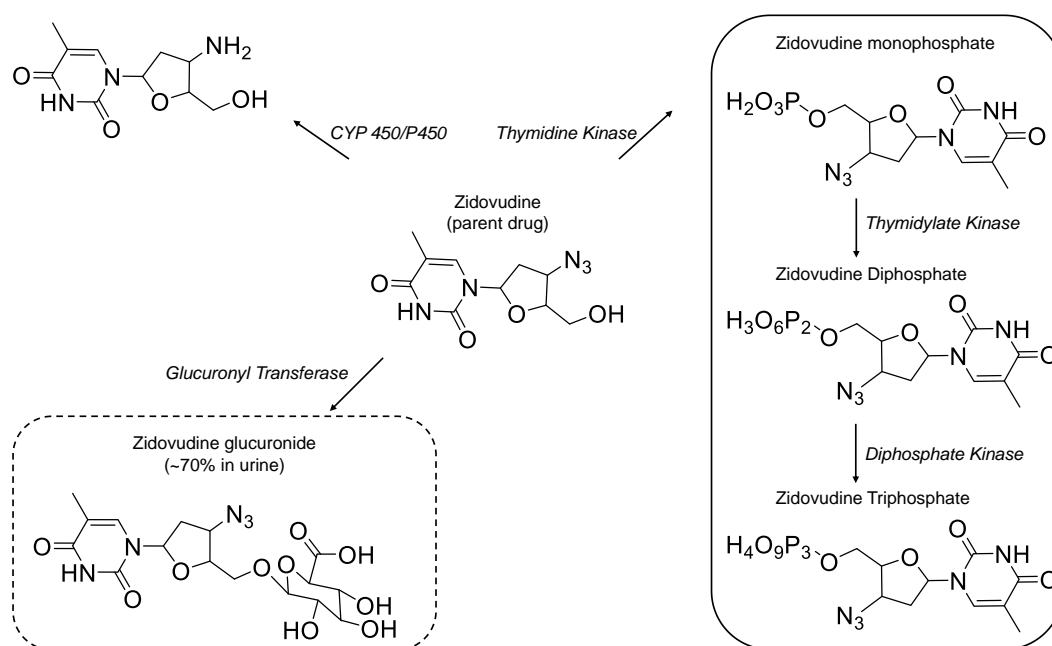


**Figure 2.2:** A summary of the metabolism pathways for zidovudine. The bold perimeter shows active intracellular phosphorylated metabolites, while the dotted perimeter shows the excretory glucuronidated metabolite. Adapted with slight modifications from Veal and Back (1995).

### 2.3 Wastewater treatment

Discharge of spent water produced from subsistence and industrial activities is loosely referred to as wastewater (Atinkpahoun *et al.*, 2018; Bengtsson and Tillman, 2004). It is mostly composed of dirty

water with significant proportions of solids. Therefore, it is highly variable in composition and heterogeneous (Vieno *et al.*, 2007). Wastewater is highly regulated because of its potential to propagate or nurture microorganisms that are detrimental to human life, and strict regulations are in place to ensure it is treated and disposed safely into the environment (Salgot *et al.*, 2018). Despite the strict legislation surrounding this, it has since emerged that wastewater treatment processes are often not effective at eliminating organic pollutants, which may include pharmaceuticals, pesticides, fire retardants, *etc.* (Peng *et al.*, 2014; Prasse *et al.*, 2010). Consequently, these organic pollutants continue to be detected in treated effluent and depending on their environmental stability they may remain intact for many years, posing a threat of bioaccumulation in various environmental compartments.

Wastewater treatment entails physical and biological treatment processes (Salgot *et al.*, 2018). The physical processes involve separation of solids (filtration and grit removal) in the preliminary stages. The influent is then held in settling tanks where components of the influent are separated according to size and density (biodegradable solids settle at the bottom, while surfactants and grease float at the top). The resulting bilayer is separated by slowly pumping out the supernatant liquid which is comprised of predominantly water and other low-density components. This process is repeated several times until a considerable proportion of solids are removed and the turbidity of the influent is near clear.

At this stage, the influent proceeds to the secondary stage, which may either be biological treatment or membrane bioreactor (MBR) treatment. The latter is a relatively new and capital-intensive technology, and still very rare by African standards, except for few piloting plants in Western Cape, South Africa - two of which were study areas for this work. Biological or activated sludge treatment, on the other hand, is when a broth of micro-organisms is inoculated into influent, followed by oxygenation (aerobic system) or deoxygenation processes (anaerobic system) (Salgot *et al.*, 2018). In aerobic systems, the air is forced into the influent-containing tanks to encourage aerobic microbial growth, while in anaerobic systems, oxygen-purging reactions (fermentation) are encouraged to support growth of anaerobic microbes. The underlying principle for both systems is to encourage bacteria-based degradation of compounds contained in the influent. These biotic degradation processes are time-dependent and the duration to complete each process is called the hydraulic retention time (HRT), or sludge retention time (SRT). In the case of treatment of solids, longer the hydraulic/sludge retention times are better because this affords adequate time for a complete biodegradation process (Vieno *et al.*, 2007). This means that sludges with high SRTs develop a rich microbial diversity and thus a higher pollutant removal potential than sludges with low SRTs. The same applies to HRT in that the longer the aerobic/anaerobic process is allowed, the better the chances of organic pollutant removal (Falås *et al.*, 2016; Vieno *et al.*, 2007). It has been confirmed that compounds such as fluoxetine that have a slow degradation kinetics will experience less effective biodegradation at shorter SRTs (Luo *et al.*, 2014). The same effect has been observed for some ARVDs (efavirenz and nevirapine) (Abafe *et al.*, 2018; Wood *et al.*, 2016). On the other hand, secondary treatment by MBR entails removing of dissolved and sludge-bound pollutants by

filtration. Here, the assumption is that residual organic pollutants that may have resisted biodegradation are adsorbed to filterable suspended solids (Luo *et al.*, 2014) and subsequently eliminated.

Finally, in the tertiary treatment stage, eutrophication nutrients (phosphates and nitrates) are removed by altering the pH. At high pH, nitrates readily convert to ammonia, which can easily be blown out during aeration (Funke *et al.*, 2016). Alternatively, at low pH, nitrates convert to nitrogen gas and nitrous oxide via a reduction reaction. Phosphates are precipitated by a forced reaction using calcium or iron containing salt (Mirzaei *et al.*, 2017).

Before discharge, the effluent is disinfected with oxidants to eliminate residual microbes. This is achieved by advanced tertiary stage oxidative processes such as chlorination (Acero *et al.*, 2010), *uv*-irradiation (Paredes *et al.*, 2018; Russo *et al.*, 2018), ozonation (Borowska *et al.*, 2016), *etc.* The objective of tertiary stage treatment is purification of effluent and elimination of residual non-biodegradable organic pollutants before discharge into the environment. Russo *et al.* (2018) conducted a lab-scale experiment to evaluate the efficiency of *uv*-wavelength-irradiance at 254 nm with or without a dose of peroxide (H<sub>2</sub>O<sub>2</sub>) for the removal of stavudine and zidovudine in treated effluent. The results demonstrated that these compounds were indeed partially eliminated using *uv*-irradiation, but better results were achieved when combining *uv*-irradiance with H<sub>2</sub>O<sub>2</sub>.

## **2.4. Analysis of wastewater**

### *2.4.1 Sample collection and storage*

Wastewater is a very heterogenous and dynamic matrix (Choi *et al.*, 2018; Salgot *et al.*, 2018) due to variabilities in composition and volumes of inflow and outflow streams. This usually complicates the interpretation of results because of limited knowledge of the spatial and temporal variation trends in the overall pharmaceutical concentrations between influent and effluent streams (Nannou *et al.*, 2019). The main goal of sample collection is to obtain a sample that is representative of the catchment area serviced by a particular wastewater treatment plant (WWTP) (Ort *et al.*, 2010). This task is normally achieved at designated sample collection points within a WWTP by either obtaining a once-off sample (a grab sample), or by collecting numerous grab samples of constant volumes at regular time intervals (usually ~24 h) and pooling them into a composite sample. An alternative is to use a passive sampler, which offers automated operation, but is seldom used in environmental sampling due to high cost of acquisition. A passive sampler is a submersible device used to accumulate sample aliquots at varying depths and predetermined time intervals in a flowing stream, thereby allowing collection of a more representative sample as a weighted function of sampling time and flow rate (Ort, 2010).

Sampling techniques reported in published methods for the determination of ARVDs in wastewater were mostly based on grab sampling, with a few recent studies that opted for miniaturized analyte extraction methods such as molecularly imprinted polymers (MIPs) (Mtolo *et al.*, 2019) and sorptive

microextraction devices (Mlunguza *et al.*, 2020; Wooding *et al.*, 2017). **Table 2.4** presents a detailed summary of all the sampling techniques used for the detection of ARVDs.

For most studies, grab and composite samples were filtered to remove suspended solids using various commercially available glass fibre filters of a range of pore sizes before storage, normally at 4°C, and processed within 24h. Sample volumes obtained ranged from 50-1000 mL with 100 mL sample volume particularly used for effluent samples and 50 mL for raw wastewater samples. The differences in sample volumes processed are presumably based on the assumption that raw wastewater may contain higher concentrations of pharmaceutical compounds compared to effluent samples.

#### 2.4.2 *Sample clean-up and extraction*

Several analyte extraction techniques have been successfully implemented to extract, purify and preconcentrate various ARVDs from wastewater. These include the use of passive samplers based on polydimethylsiloxane (PDMS) (Wooding *et al.*, 2017), hollow fibre microextraction (Mlunguza *et al.*, 2020), molecularly imprinted polymers (Mtolo *et al.*, 2019; Terzopoulou *et al.*, 2016) and offline solid phase extraction (SPE) (Abafe *et al.*, 2018; K'oreje *et al.*, 2016, 2012; Muriuki *et al.*, 2020; Ngumba, 2018; Ngumba *et al.*, 2016a, 2016b; Peng *et al.*, 2014; Prasse *et al.*, 2010; Wood *et al.*, 2015). A detailed summary of the sample extraction techniques used in ARVD analyses is presented in **Table 2.1**. SPE is by far the most preferred sample preparation method. In fact, sample clean-up by SPE is beneficial for many reasons, chief of which is the excellent selectivity of the technique, given the array of potential interferences that may be present in environmental samples. SPE also allows for a phase-transition from the aqueous sample medium to a suitable medium that matches the mobile phase, *e.g.* a highly organic medium for hydrophilic interaction chromatography (HILIC) (Boulard *et al.*, 2018; Prasse *et al.*, 2010). However, SPE also involves multiple steps, each of which may be prone to analyte loss. For instance, at the sample loading step, analytes may be lost due to low affinity of the sorbent, inadequate bed wetting/conditioning, or exceedance of the breakthrough volume (**Section 2.4.2.2**). Also, during the evaporation and dissolution of the dried residue (if used), analyte losses may occur due to high vapour pressures or partial solubility of analytes.

Several stationary phase chemistries have been evaluated for SPE of ARVDs, typically based on the recoveries they provide. The Oasis HLB phase – a copolymer phase of divinylbenzene and vinylpyrrolidone – has been the preferred cartridge for the analyses of ARVDs in several studies (Abafe *et al.*, 2018; K'oreje *et al.*, 2016, 2012; Wood *et al.*, 2015). The high recoveries obtained on this cartridge may be attributed to its ability to extract simultaneously a broad spectrum of acidic, neutral and basic polar analytes over a full pH scale (Nannou *et al.*, 2019), although poor relative recoveries are obtained for the extremely polar ARVDs indinavir, maraviroc (Aminot *et al.*, 2015) and lamivudine (Boulard *et al.*, 2018; Wood *et al.*, 2015). This has prompted exploration of alternative sorbents (Nannou *et al.*, 2020, 2019), including cation exchange Oasis MCX (Aminot *et al.*, 2015), Isolute ENV+



(Funke *et al.*, 2016; Prasse *et al.*, 2010) and Strata SDB-L. Interestingly, the experimental procedures implemented differed considerably amongst the listed studies for ARVD determination, as discussed in further detail for the different steps involved in SPE below.

#### 2.4.2.1 SPE conditioning and sample loading

Most authors opted to use acetonitrile (ACN) and methanol (MeOH) of different volumes depending on cartridge/sorbent bed sizes for the conditioning step, but methods differed in terms of pH adjustment of the sample before loading (**Table 2.1**). For instance, K'oreje *et al.* (2016, 2012) used a 50 mL neutralized (pH 7) wastewater sample to which 1 g/L Na<sub>2</sub>EDTA.2H<sub>2</sub>O was added before percolation onto an Oasis HLB cartridge (200 mg, 6 mL) for the analysis of lamivudine, nevirapine, stavudine, and efavirenz. Ngumba *et al.* (2016b, 2016a) used 500 mL samples on the same cartridge to evaluate the effect of sample pH between 3 and 11 on retention of the same compounds (and efavirenz) and obtained the best recovery for all analytes at pH 9. Wood *et al.* (2015) loaded 500 mL of non pH adjusted wastewater sample onto Oasis HLB cartridges (200 mg, 6 mL). Boulard *et al.* (2018) evaluated Stata XCW (6 mL, 500 mg), Oasis MCX (3 mL, 60 mg), Oasis WCX (6 mL, 500 mg), Oasis HLB (6 mL, 200 mg) and Isolute ENV+ (6 mL, 500 mg) cartridges using 100 mL sample volumes adjusted to pH's in the range 2-8. With no reasons advanced for the preferred sample volumes, it is assumed that most studies relied on the manufacturer's recommended loading capacities for the cartridges. The sample loading flow rates used in all studies ranged from 1-10 mL/min. Interestingly, no details were provided for the suitability of the selected flow rates considering that breakthrough volume (an important parameter of frontal chromatography) is dependent on flow rate (refer to a further discussion on breakthrough below). Aminot *et al.* (2015), evaluated analyte losses during loading, particularly losses due to exceedance of the breakthrough volume on Oasis MCX 60-mg cartridges (Waters, St Quentin en Yvelines, France). The consensus regarding flow rate is it should be as slow as possible. This data is not available for most ARVDs, although it is qualitatively now known that the highly polar nucleosidic ARVDs such as lamivudine and emtricitabine are poorly retained on generic reversed phase (RP)-based sorbents (Boulard *et al.*, 2018; Mosekiemang *et al.*, 2019; Prasse *et al.*, 2010; Wood *et al.*, 2015). This necessitates a dedicated study to profile ARVDs according to breakthrough volumes on a variety of commercially available sorbent beds.

#### 2.4.2.2 Theoretical overview of the breakthrough phenomenon

The breakthrough volume ( $V_B$ ) is a very important measurable parameter that is used to characterize SPE sorbent beds (Moldoveanu and David, 2015). Breakthrough volumes of analytes on a given sorbent bed are determined from a plot of loaded sample volume (mL) *versus* the ratio of analyte concentration in the SPE effluent ( $C$ ) to its concentration in the sample ( $C_0$ ) to produce a breakthrough volume curve (**Figure 2.3**). This process simulates SPE as a frontal LC-type separation, although it will not account

for analyte loss due to typical operational flaws such as fast flow rates and insufficient bed equilibration, or exceedance of loading capacity. The breakthrough volume is defined as the maximum sample volume that can be loaded on the sorbent bed and yield a 100% recovery (i.e. before elution of the analyte occurs) (Bielicka-Daszkiwicz *et al.*, 2013; Bielicka-Daszkiwicz and Voelkel, 2009). **Figure 2.3** illustrates that if a sample containing a retainable analyte of concentration  $C_0$  is continuously fed onto the SPE bed, it will be retained on the sorbent provided that the concentration of the analyte in the sample and the flow rate at which it is percolated are reasonably low and the retention factor ( $K$ ) is high. As sample loading progresses, traces of the analyte will start to appear in the SPE effluent, but at lower concentrations ( $C$ ) relative to the sample - this marks the onset of breakthrough, and the volume of sample loaded up to this point corresponds to the breakthrough volume ( $V_B$ ). The system reaches  $C/C_0 \sim 50\%$  at a point denoted as the retention volume ( $V_R$ ), when half the concentration of the analyte in the sample is found in the SPE effluent. The concentration of the analyte in the SPE effluent will steadily increase with the loaded volume until it is almost equal to the concentration of the analyte in the sample, at a point referred to as the holdup volume ( $V_M$ ), i.e.  $C/C_0 \sim 100\%$ . Practically, the larger the breakthrough volume, the greater the pre-concentration factor that can be attained in SPE. This means that for a given SPE process, the  $V_B$  should be as large as possible.

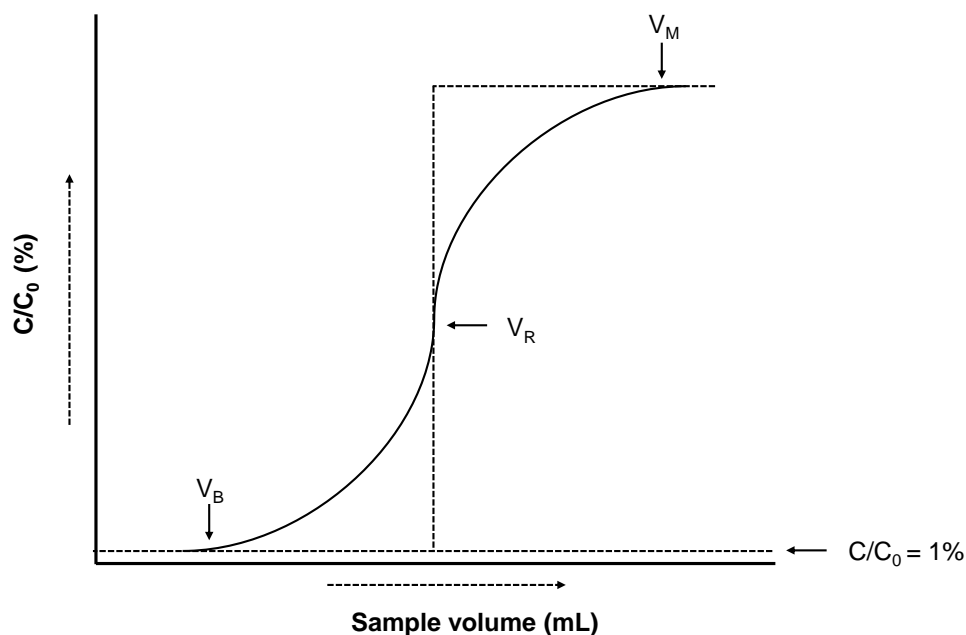


**Figure 2.3:** A typical breakthrough curve illustrating the derivation of the breakthrough volume, retention volume and the sorbent holdup volume. Adapted with modifications from Bielicka-Daszkiwicz and Voelkel (2009).

Several equations have been developed to calculate breakthrough volume; one approach is discussed here. According to **Eq. 2.1**, the breakthrough volume ( $V_B$ ) is estimated as a function of the plate number ( $N$ ) of a sorbent bed.

$$V_B = V_R \left( a_0 + \frac{a_1}{N} + \frac{a_2}{N^2} \right)^{-1/2} \quad \text{Eq.2.1}$$

where  $V_R$  and  $N$  have been defined,  $a_0$ ,  $a_1$ , and  $a_2$  are coefficients, determined for various values of  $b$  and are available in literature (Bielicka-Daszkiwicz and Voelkel, 2009). The retention volume ( $V_R$ ) is related to the capacity factor ( $k$ ) through **Eq.2.2**.

$$V_R = V_M (1 + k) \quad \text{Eq.2.2}$$

where  $V_M$  is the hold-up volume for the sorbent.

The capacity factor ( $k$ ) and holdup volume ( $V_M$ ) can be calculated from the extraction recovery:

$$R = \frac{V_M}{V_0} k \quad 100\% \quad \text{Eq. 2.3}$$

where  $R$  is the extraction recovery (%) and  $V_0$  is the sample volume (mL).

Then, theoretical plates ( $N$ ) can be estimated according to **Eq. 2.4**:

$$N = L/2d_p \quad \text{Eq. 2.4}$$

where  $L$  is the column length (sorbent bed size) and  $d_p$  is the particle size.

Aminot *et al.* (2015) reported breakthrough data for abacavir, indinavir, lamivudine, nelfinavir, nevirapine, ritonavir, saquinavir and zidovudine using a cation exchange Oasis MCX 60-mg cartridge. The authors estimated  $V_B$  at 1000 mL for most compounds on this cartridge. Breakthrough data for other ARVDs and on other phases is still lacking.

#### 2.4.2.3 Analyte elution step

Preceding the elution step is the washing and drying of the loaded sorbent using either vacuum drying (Abafe *et al.*, 2018; Aminot *et al.*, 2018, 2016, 2015; K'oreje *et al.*, 2016, 2012; Muriuki *et al.*, 2020; Ngumba *et al.*, 2016b, 2016a) or nitrogen gas drying (Prasse *et al.*, 2010; Wood *et al.*, 2015). Analyte elution is another critical step prone to analyte loss since incomplete elution will result in low recoveries. Several solvents mixtures of different elution strengths have been used to elute ARVDs from SPE cartridges. For example, for RP-SPE Abafe *et al.* (2018) used a mixture of equal proportions of MeOH and ethyl acetate (EtOAc), Aminot *et al.* (2018, 2016, 2015) used EtOAc/acetone (1:1, v/v) followed by dichloromethane (DCM)/MeOH/acetic acid (48/48/2, v/v/v), while Prasse *et al.* (2010) used a mixture of MeOH/acetone (50/50, v/v) + 0.2% FA. K'oreje *et al.* (2016, 2012) used only MeOH to elute

efavirenz, lamivudine, nevirapine and zidovudine. Overall, mostly acidic mixtures were used to desorb ARVDs from RP-sorbents.

#### *2.4.2.4 Eluent drying and residue resuspension.*

Unless the eluted sample is directly suitable for analysis, SPE effluents are typically dried in an inert environment using a gentle stream of nitrogen. The residue is dissolved in a suitable medium, ideally as close as possible to the solvent composition of the chromatographic mobile phase *i.e.* predominantly aqueous for RP-LC and highly organic for HILIC and normal phase (NP) LC. This step is prone to analyte loss due to inadequate dissolution of residues (Li *et al.*, 2015), or potential loss of volatile analytes. This aspect is discussed in detail in **Chapter 3**, while **Table 2.1** provides a summary of the solvent compositions used for the resuspension of ARVDs.

**Table 2.1:** A summary of sample preparation methods and chromatographic conditions previously used for the analysis of ARVDs in environmental samples.

Therapeutic class (compounds <sup>a</sup> ) and log $K_{ow}$ , water solubility range	Sample volume: pH adjustment SPE/direct injection/lyophilisation Elution solvent Residue reconstitution solvent Preconcentration factor	Column, stationary phase, and dimensions	Mobile phase (solvents A/B), flow rate, run time, column temp and injection volume	Reference
<b>NTRI</b> (ZDV,3TC); <b>nNRTI</b> (EFZ, NVP); <b>II</b> (RGV); <b>FI</b> (MVC); <b>PI</b> (ATZ, DNV, IDV, LPV, RTV, SQV) Log $K_{ow}$ -7.05 to 6.27, Water solubility $7.0 \times 10^4$ to $1.1 \times 10^{-4}$	<b>Sample volume:</b> 100 mL: pH not adjusted. <b>SPE:</b> Oasis HLB (200 mg, 6 mL) <b>Elution solvents:</b> 5 mL MeOH and 3 mL EtOAc <b>Reconstitution solvent:</b> 1 mL MeOH <b>Pre-concentration factor:</b> 100×	Hypersil Gold, C18, $50 \times 2.1$ mm, $1.9 \mu\text{m } d_p$  <b>Guard column:</b> Not specified	<b>Solvent A:</b> 0.1% FA in H <sub>2</sub> O <b>Solvent B:</b> 0.1% FA in MeOH <b>Flow rate:</b> 0.2 mL/min. <b>Run time:</b> 10.50 min. <b>Column temp.:</b> 25°C <b>Injection volume:</b> 20 $\mu\text{L}$	(Abafe <i>et al.</i> (2017)
<b>NRTI</b> (3TC, ABV, ZDV); <b>nNRTI</b> (NVP); <b>PI</b> (IDV, NFV, RTV, SQV) Log $K_{ow}$ -7.05 to 8.98, Water solubility $7.0 \times 10^4$ to $1.1 \times 10^{-4}$ mg/L	<b>Sample volume:</b> 100 mL: pH 2 <b>SPE</b> Oasis MCX (60 mg, 3 mL) <b>Elution solvents:</b> 3 mL EtOAc /acetone (50/50, v/v) and 3 mL MeOH/DCM/NH <sub>4</sub> OH (48/48/4, v/v/v)/ <b>Reconstitution solvents:</b> 0.3 mL water/ACN (90/10) <b>Pre-concentration factor:</b> >333×	Zorbax SB-C18, $50 \times 2.1$ mm, 1.8 $\mu\text{m } d_p$  <b>Guard column:</b> Not specified	<b>Solvent A:</b> 0.1% FA in H <sub>2</sub> O <b>Solvent B:</b> 0.1% FA in ACN <b>Flow rate:</b> 0.6 mL/min. <b>Run time:</b> 17 min. <b>Column temp.:</b> 30°C <b>Injection volume:</b> 5 $\mu\text{L}$	Aminot <i>et al.</i> (2015, 2016)

Therapeutic class (compounds <sup>a</sup> ) and log K <sub>ow</sub> , water solubility range	Sample volume: pH adjustment SPE/direct injection/lyophilisation Elution solvent Residue reconstitution solvent Preconcentration factor	Column, stationary phase, and dimensions	Mobile phase (solvents A/B), flow rate, run time, column temp and injection volume	Reference
<b>NRTI</b> (ABV, 3TC, FTC) transformation products and metabolites (3TC carboxylate, ABV-carboxylate, FTC carboxylate, FTC S-oxide)	<p><b>Sample volume:</b> 100 mL: pH 2-8</p> <p><b>SPE:</b> Strata XCW (500 mg, 6 mL) Oasis MCX (60 mg, 3 mL) Oasis HLB (200 mg, 6 mL) Isolute ENV+ (500 mg, 6 mL)</p> <p><b>Elution solvents:</b> Not specified</p> <p><b>Reconstitution solvents:</b> Not specified</p> <p><b>Lyophilisation sample volume:</b> 10 mL: pH unadjusted</p> <p><b>Elution and Reconstitution solvents:</b> Not specified</p>	<p>Zwitterionic HILIC Nucleodur (250 × 3 mm, 3.0 μm <i>d<sub>p</sub></i>) Luna HILIC (150 × 3 mm, 3.0 μm <i>d<sub>p</sub></i>)</p> <p><b>Guard column:</b> EC HILIC Nucleodur (4 × 3 mm, 3 μm <i>d<sub>p</sub></i>)</p>	<p><b>Solvent A:</b> 10 mM NH<sub>4</sub>-formate with 0.1% FA <b>Solvent B:</b> 7.5 mM NH<sub>4</sub>-formate in ACN/Milli-Q (90:10, v/v) with 0.1% FA <b>Flow rate:</b> 0.5 mL/min. <b>Run time:</b> 33 min. <b>Column temp.:</b> 25°C <b>Injection volume:</b> 70 μL</p>	(Boulard <i>et al.</i> , 2018)
<b>NRTI</b> (3TC, ZDV); <b>nNRTI</b> (NVP) Log K <sub>ow</sub> -1.4 to 3.89 Water solubility 7.0 × 10 <sup>4</sup> to 1.0 × 10 <sup>2</sup> mg/L	<p><b>Sample volume:</b> 500 L: pH 9</p> <p><b>SPE:</b> Oasis HLB (200 mg, 6 mL)</p> <p><b>Elution solvents:</b> 5 mL 2% MeOH in 5% Aq. NH<sub>4</sub>OH</p> <p><b>Reconstitution solvents:</b> 1 mL ACN/Water (20/80 v/v)</p> <p><b>Pre-concentration factor:</b> 500×</p>	<p>Waters XBridge, C18, 100 × 2.1 mm, 3.5 μm <i>d<sub>p</sub></i></p> <p><b>Guard column:</b> Not specified</p>	<p><b>Solvent A:</b> 0.1% FA in H<sub>2</sub>O <b>Solvent B:</b> 0.1% FA in ACN <b>Flow rate:</b> 0.25 mL/min. <b>Run time:</b> 19 min. <b>Column temp.:</b> 30°C <b>Injection volume:</b> 10 μL</p>	(Muriuki, <i>et al.</i> , (2020)

Therapeutic class (compounds <sup>a</sup> ) and log K <sub>ow</sub> , water solubility range	Sample volume: pH adjustment SPE/direct injection/lyophilisation Elution solvent Residue reconstitution solvent Preconcentration factor	Column, stationary phase, and dimensions	Mobile phase (solvents A/B), flow rate, run time, column temp and injection volume	Reference
<b>NRTI</b> (d4T, 3TC, ZDV); <b>nNRTI</b> (EFZ, NVP) Log K <sub>ow</sub> -7.05-4.15 Water solubility $2.0 \times 10^4$ - $9.3 \times 10^{-2}$ mg/L	<b>Sample volume:</b> 500 mL: pH 7 <b>SPE:</b> Oasis HLB (200 mg, 6 mL) <b>Elution solvents:</b> 2 × 5 mL MeOH <b>Reconstitution solvents:</b> 2.5 mL ACN/H <sub>2</sub> O (10/90 v/v) <b>Pre-concentration factor:</b> 200×	Phenomenex Luna, C18, 150 × 2.0 mm, 3 μm d <sub>p</sub>  <b>Guard column:</b> Not specified	<b>Solvent A:</b> MeOH <b>Solvent B:</b> 0.1% FA in MeOH <b>Flow rate:</b> 0.17 mL/min <b>Run time:</b> 65 min. <b>Column temp.:</b> 35°C <b>Injection volume:</b> 10 μL	K'oreje <i>et al.</i> , 2018, 2016, 2012)
<b>NRTI</b> (3TC, FTC, ZDV, ZDVG), <b>nNRTI</b> (EFZ, 8,14-diOH-EFZ, 12-OH-NVP, NVP), <b>PI</b> (RTV, RTVM) Log K <sub>ow</sub> -1.4 to 8.98 Water solubility $7.0 \times 10^4$ to $1.1 \times 10^{-4}$ mg/L	<b>Sample volume:</b> 1.3 mL: pH 7 <b>Direct injection:</b> Water/MeOH (70/30 v/v) <b>SPE:</b> Strata SDB-L (200 mg, 6 mL) <b>Sample volume:</b> 50 mL: pH 7 <b>Elution solvents:</b> MeOH/DCM/FA (49/49/2, v/v/v) <b>Reconstitution solvents:</b> Water/MeOH (70/30 v/v) <b>Pre-concentration factor:</b> 50×	Aquity HSS T3, C18, 150 × 2.1 mm, 1.8 μm d <sub>p</sub>  <b>Guard column:</b> Acquity UPLC HSS T3 VanGuard (5 × 2.1 mm, 1.8 μm d <sub>p</sub> )	<b>Solvent A:</b> 0.1% FA in H <sub>2</sub> O <b>Solvent B:</b> ACN <b>Flow rate:</b> 0.25 mL/min. <b>Run time:</b> 9 min. <b>Column temp.:</b> 30°C <b>Injection volume:</b> 2 μL	(Mosekiemang <i>et al.</i> , 2019)

Therapeutic class (compounds <sup>a</sup> ) and log K <sub>ow</sub> , water solubility range	Sample volume: pH adjustment SPE/direct injection/lyophilisation Elution solvent Residue reconstitution solvent Preconcentration factor	Column, stationary phase, and dimensions	Mobile phase (solvents A/B), flow rate, run time, column temp and injection volume	Reference
<b>NRTI</b> (3TC, ZDV); <b>nNRTI</b> (NVP) Log K <sub>ow</sub> -1.4 to 3.89 Water solubility $7.0 \times 10^4$ to $1.0 \times 10^2$ mg/L	<b>Sample volume:</b> 500 mL: pH 9 <b>SPE:</b> Oasis HLB (200 mg, 6 mL) <b>Elution solvents:</b> 5 mL 2% MeOH in 5% Aq. NH <sub>4</sub> OH <b>Reconstitution solvents:</b> 3 mL water ACN/water (80/20 v/v) <b>Pre-concentration factor:</b> 500×	Waters XBridge, C18, 100 × 2.1 mm, 3.5 μm <i>d<sub>p</sub></i>  <b>Guard column:</b> Not specified	<b>Solvent A:</b> 0.1% FA in H <sub>2</sub> O <b>Solvent B:</b> 0.1% FA in ACN <b>Flow rate:</b> 0.25 mL/min. <b>Run time:</b> 19 min. <b>Column temp.:</b> 30°C <b>Injection volume:</b> 10 μL	(Ngumba <i>et al.</i> , 2018, 2016b, 2016a)
<b>NRTI</b> (d4T, ZDV) Log K <sub>ow</sub> -0.72 to 9.72 Water solubility $1.0 \times 10^2$ to $2.0 \times 10$ mg/L	<b>Sample volume:</b> 200 mL wastewater: pH 8 500 mL well water: pH 8 <b>SPE:</b> Isolute ENV+ (500 mg, 6 mL) <b>Elution solvents:</b> 5 × 2 mL MeOH/Acetone (50:50, v/v) + 0.2% FA <b>Reconstitution solvents:</b> 1 mL 5 mM NH <sub>4</sub> Ac <b>Pre-concentration factor:</b> 100× & 500×	Phenomenex Synergi Hydro-RP, C18, 50 × 2.0 mm, 2.5 μm <i>d<sub>p</sub></i>  <b>Guard column:</b> C18 guard column, 4 × 3.0 mm	<b>Solvent A:</b> 5 mM NH <sub>4</sub> Ac <b>Solvent B:</b> MeOH <b>Flow rate:</b> 0.25 mL/min <b>Run time:</b> 15 min. <b>Column temp.:</b> 25°C <b>Injection volume:</b> Not specified.	(Peng <i>et al.</i> , 2014)
<b>NRTI</b> (d4T, ZDV) <b>nNRTI</b> (NVP) Log K <sub>ow</sub> -0.72 to 9.72 Water solubility $1.0 \times 10^2$ to $2.0 \times 10$ mg/L	<b>Sample volume:</b> 200-500 mL wastewater; pH 8 <b>SPE:</b> Isolute ENV+ (500 mg, 6 mL) <b>Elution solvents:</b> 5 × 2 mL MeOH/Acetone (50:50, v/v) <b>Reconstitution solvents:</b> 1 mL 5 mM NH <sub>4</sub> Ac	Synergi Hydro RP, C18 (150 × 3.0 mm, <i>d<sub>p</sub></i> )	<b>Solvent A:</b> 5 mM NH <sub>4</sub> -formate <b>Solvent B:</b> MeOH <b>Flow rate:</b> 0.4 mL/min. <b>Run time:</b> 22 min. <b>Column temp.:</b> 40°C <b>Injection volume:</b> Not specified	Prasse <i>et al.</i> , 2010



Therapeutic class (compounds <sup>a</sup> ) and log K <sub>ow</sub> , water solubility range	Sample volume: pH adjustment SPE/direct injection/lyophilisation Elution solvent Residue reconstitution solvent Preconcentration factor	Column, stationary phase, and dimensions	Mobile phase (solvents A/B), flow rate, run time, column temp and injection volume	Reference
<b>NRTI</b> (3TC, FTC, TNV); <b>nNRTI</b> (EFZ, NVP) Log Kow -1.44 to 4.7 Water solubility $11.2 \times 10^5$ to $9.3 \times 10^{-2}$ mg/L	<b>Sample volume:</b> 1000 mL/pH not adjusted. <b>SPE:</b> Bond Elut Plexa (200 mg, 6 mL) <b>Elution solvents:</b> not stated. <b>Reconstitution solvents:</b> 0.2 mL water/ACN (90/10, v/v) <b>Pre-concentration factor:</b> 5000×	Bond Elut Plexa, C18, 100 × 2.1 mm, 2.6 μm d <sub>p</sub>	<b>Solvent A:</b> 5 mM NH <sub>4</sub> -formate <b>Solvent B:</b> 1.5% FA in MeOH <b>Flow rate:</b> 0.3 mL/min. <b>Run time:</b> 15.5 min. <b>Column temp.:</b> 25°C <b>Injection volume:</b> 10 μL	Rimayi <i>et al.</i> , 2018
<b>NRTI</b> (3TC, d4T, FTC, ZAL, ZDV), <b>nNRTI</b> (EFZ, NVP), <b>PI</b> (IDV, LPV, RTV)	Sample volume: 500 mL, pH not adjusted/ <b>SPE:</b> Oasis HLB (200 mg, 6 mL) <b>Elution solvents:</b> 5 mL MeOH <b>Reconstitution solvents:</b> 0.2 mL water/ACN (90/10, v/v) 2500× preconcentration factor	Zorbax Eclipse C8, 50 × 3.0 mm, 1.8 μm d <sub>p</sub>	<b>Solvent A:</b> 0.1% FA <b>Solvent B:</b> 0.1% FA in ACN <b>Flow rate:</b> 0.4 mL/min. <b>Run time:</b> 40 min. <b>Column temp.:</b> 22°C <b>Injection volume:</b> 15 μL	(Wood <i>et al.</i> , 2015)

<sup>a</sup>ABV – abacavir; ABV-COOH – carboxy abacavir; ABV-COOH-desCP – descyclopropyl abacavir; ABV-COOH-OH – carboxy hydroxy abacavir; ATV – atazanavir; d4T – stavudine; DDC – zalcitabine; DDI – didanosine; DRV – darunavir; EFZ – efavirenz; 8,14-diOH EFV – 8,14 dihydroxy efavirenz; ETR – etravirine; FPV – fosamprenavir; FTC – emtricitabine; FTC-COOH – carboxy emtricitabine; FTC-COOH-S-oxide – carboxy emtricitabine-S-oxide; FTC-S-oxide – emtricitabine-S-oxide; IDV – indinavir; 3TC – lamivudine; LPV – lopinavir; MRV – maraviroc; NFV – nelfinavir; nevirapine – NVP; 12-OH-nevirapine – 12 hydroxy nevirapine; RAL – raltegravir, TFV – tenofovir; ZDV – zidovudine; ZDV-COOH – carboxy zidovudine.

### 2.4.3 Direct injection

Apart from the sample pre-treatment involving SPE, direct injection (DI) or large volume direct injection (LVDI) are alternative methods that could be employed in wastewater analysis. LVDI is defined as sample introduction that involves injection of sample volumes larger than 10% of the void volume of the analytical column (Busetti *et al.*, 2012). This method therefore typically entails injection of sample volumes in the range 100-5000  $\mu\text{L}$ , as opposed to DI, which entails injection of conventional sample volumes in the range of 1-20  $\mu\text{L}$  (Chiaia *et al.*, 2008; Martínez Bueno *et al.*, 2011; Ng *et al.*, 2020; Zhang *et al.*, 2020). Sample filtration and the use of appropriate guard columns are required to avoid damage to the column and instrument. These techniques have been utilized as early as 1975 to avert losses of polar analytes (Little and Fallick, 1975), and recently by Funke *et al.* (2016) and Mosekiemang *et al.* (2019) for ARVD analysis by RP-LC, and Boulard *et al.* (2018) and Prasse *et al.* (2010) by HILIC. The main limitation of DI is the lack of sensitivity, because pre-concentration is not performed as is commonly the case for SPE (Busetti *et al.*, 2008). For this reason, DI can be combined with a suitable non-selective pre-concentration step such as lyophilisation, although this approach is seldom used in environmental analysis.

### 2.4.4 Lyophilisation

Lyophilisation is a sample desiccation process in which water is evaporated from a sample matrix by sublimation. Thereafter, the dried extract is reconstituted in a small volume (relative to the original volume), thereby elevating the concentrations of analytes. Briefly, an aqueous sample is frozen prior to lyophilisation, normally using liquid nitrogen (Luque De Castro and Izquierdo, 1990; Ramirez *et al.*, 2014). Maintaining the sample in the frozen state throughout the lyophilisation process is crucial to facilitate the process. This suggests that the sample matrix should not contain any solvents with a lower freezing point than that of water. **Figure 2.4** shows the phase transitions of water as a function of pressure (Atm.) and temperature ( $^{\circ}\text{C}$ ). As can be seen, the pressure should be kept below the triple point (6.11 mBar/ $6.0 \times 10^{-3}$  Atm. for water) for sublimation to occur. In the practical context, the frozen sample mounted on the freeze drier operated below the triple point of water will force a solid-to-gas phase transition thereby eliminating water from the sample and leaving behind the analyte and other residues.

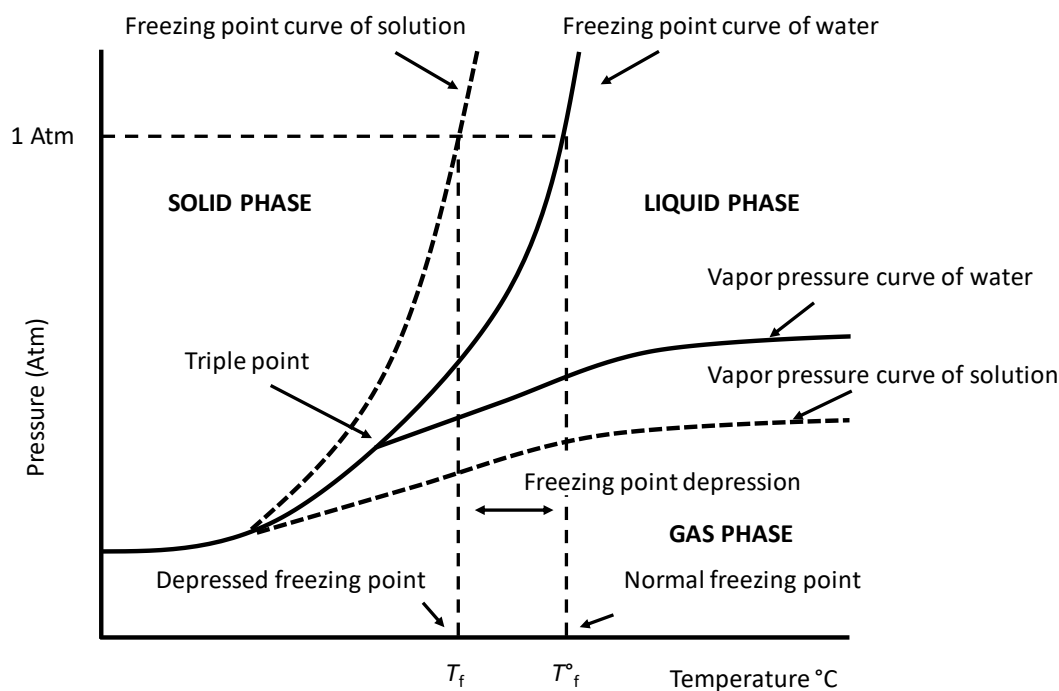


**Figure 2.4:** A typical phase diagram for pure water illustrating solid-to-gas phase transition suitable for an effective lyophilisation process. Adapted with modification from Syslová *et al.* (2011).

Lyophilisation is a suitable method for concentrating non-volatile, heat or light labile compounds dissolved in water (Syslová *et al.*, 2011). However, this form of sample preparation is relatively unexplored in environmental analysis, especially in the case of ARVDs, which precludes a fair appraisal of its (de)merits. Boulard *et al.* (2018) used lyophilisation in combination with zwitterionic HILIC analysis for the analysis of abacavir, abacavir carboxylate, emtricitabine, emtricitabine carboxylate, emtricitabine S-oxide and lamivudine in wastewater, and reported improved recoveries compared to SPE (Boulard *et al.*, 2018). Compounds with higher vapour pressures than the operating pressure of the freeze drier (0.03-0.1 mBar) will clearly be lost due to volatilization. Significant losses of, for example polychlorinated biphenyls during lyophilisation has been reported and been ascribed to their relatively high vapour pressures (de Voogt *et al.*, 2000). Nevertheless, at typical operating pressures, this is not expected to be an issue for most ARVDs because of their relatively low vapour pressures (**Table 2.2**).

**Table 2.2:** Typical vapour pressures of ARVDs.

Compound	Class	Vapor pressure <sup>1</sup> (mm Hg)	Stability at freeze drying pressure (0.03 mBar = $2.2 \times 10^{-2}$ mm Hg)
abacavir	NRTI	No data	×
didanosine	NRTI	6.6	×
emtricitabine	NRTI	$1.7 \times 10^{-8}$	✓
lamivudine	NRTI	$8.3 \times 10^{-16}$	✓
stavudine	NRTI	$9.5 \times 10^{-12}$	✓
tenofovir	NRTI	No data	×
zalcitabine	NRTI	$5.8 \times 10^{-8}$	✓
zidovudine	NRTI	$5.2 \times 10^{-20}$	✓
delavirdine	nNRTI	No data	×
efavirenz	nNRTI	$3.8 \times 10^{-7}$	✓
etravirine	nNRTI	No data	×
nevirapine	nNRTI	$3.4 \times 10^{-9}$	✓
relpivirine	nNRTI	$3.4 \times 10^{-12}$	✓
dolutegravir	INSTI	$1.4 \times 10^{-17}$	✓
elvitegravir	INSTI	No data	×
raltegravir	INSTI	$4.5 \times 10^{-22}$	✓
amprenavir	PI	$9.9 \times 10^{-18}$	✓
atazanavir	PI	$1.0 \times 10^{-26}$	✓
darunavir	PI	No data	×
fosamprenavir	PI	$1.1 \times 10^{-11}$	✓
indinavir	PI	No data	×
lopinavir	PI	$3.4 \times 10^{-24}$	✓
ritonavir	PI	$1.1 \times 10^{-27}$	✓
tipranavir	PI	$4.4 \times 10^{-21}$	✓
saquinavir	PI	$2.0 \times 10^{-31}$	✓
maraviroc	FI	$1.1 \times 10^{-11}$	✓

<sup>1</sup>vapor pressure values were obtained from PubChem open chemistry database

(<https://www.ncbi.nlm.nih.gov/pccompound>, accessed 7/8/2020).

(✓) denotes the compound is either lyophilizable or (×) unknown due to lack of data.

The fact that very small amounts of solvent (typically to redissolve the residue) are required to process samples by lyophilisation makes it an attractive ‘green’ technique for reducing the cost per analysis; a consideration of relevance in environmental analysis where large volumes of samples are typically processed. However, lyophilisation lacks the sample clean-up aspect, a potential drawback that may explain the lack of its application in environmental analysis (de Voogt *et al.*, 2000; Luque De Castro and Izquierdo, 1990; Ramirez *et al.*, 2014).

#### 2.4.5 Instrumental analyses of ARVDs in environmental samples

The instrument of choice for the analysis of non-volatile organic compounds in aqueous environmental samples is liquid chromatography (LC) coupled to a mass spectrometer (MS) due to its unrivalled sensitivity and selectivity in the detection of analytes occurring at trace level concentrations (Bade *et al.*, 2015; Hernández *et al.*, 2014, 2011; Nannou *et al.*, 2019). In the discussions that follow regarding the applications of LC-MS in the analyses of ARVDs in wastewater samples, the initial focus will be an overview of the chromatographic methods used thus far, followed by a focused discussion regarding the application of various types of mass spectrometry in this field. The scope of this review includes all reports on the subject in the period 2010-2020.

##### 2.4.5.1 Liquid chromatography (LC)

Reversed phase liquid chromatography (RP-LC) is the most widely used technique in the separation of organic compounds in wastewater samples, including pharmaceuticals, and ARVDs in particular. Hydrophilic interaction chromatography (HILIC) has also featured in the analysis of highly polar ARVDs and their metabolites (Boulard *et al.*, 2018; Prasse *et al.*, 2010). Research interest in the analysis of ARVDs rose to prominence since 2010 (Prasse *et al.*, 2010). In this period, ultra high pressure liquid chromatography (UHPLC) became the standard instrument (Petrovic *et al.*, 2010). The analytical benefits of UHPLC include high chromatographic efficiency, improved peak resolution, elution of narrower, sharper peaks and especially a reduction in analysis time (de Villiers *et al.*, 2006; Shaaban and Górecki, 2012). All these parameters are crucial in quantitative environmental analysis, where high throughput and good peak quality is a requirement for accurate peak integration. It is well known that fast analysis can be achieved by a reduction in the particle size of the column packing material (de Villiers *et al.*, 2006). Small particles sizes provide shorter diffusion distances and a more uniform flow through the column, thus less peak broadening, resulting in reduced A- and C- terms of the van Deemter equation. The drawback is that such phases require higher operating pressures due to lower column permeability, as described by the Darcy's law (**Eq. 2.8**). This equation relates pressure drop across a column ( $\Delta P$ ) to column permeability ( $K_0$ ), mobile phase viscosity ( $\eta$ ), column length ( $L$ ), particle diameter ( $d_p$ ) and mobile phase linear velocity ( $u_0$ ):

$$\Delta P = \frac{K_0 \eta L}{d_p^2} u_0 = \frac{K_0 \eta H}{d_p^2} u_0 \quad \text{Eq. 2.5}$$

Accordingly, a pressure drop across a column is directly proportional to the column length and inversely proportional to the square root of particle size. Practically, fast analysis may be achieved by reducing column length concurrently with the plate height, *i.e.* smaller particle sizes. The gain in speed is due to a combination of shorter columns operated at higher flow rates. Reducing solvent viscosity by increasing the column temperature can be used to further increase throughput. **Table 2.1** had provided

an overview of the stationary phases and the corresponding run times obtained for the analyses of ARVDs in environmental samples.

#### 2.4.5.2 Gas chromatography

Gas chromatography (GC) has seen limited application in the analysis of ARVDs. GC has been successfully used to separate and quantify some of the thermally stable ARVDs such as efavirenz and nevirapine (Schoeman *et al.*, 2017; Wooding *et al.*, 2017). Schoeman *et al.* (2017) used GC hyphenated to time-of-flight MS (TOF-MS), whereas Wooding *et al.* (2017) used comprehensive two-dimensional GC (GC×GC) hyphenated to TOF-MS because of the complexity of the wastewater matrix. In the multidimensional GC method, compounds are typically separated according to boiling point in one dimension, and polarity in the other. The two columns used in each dimension are connected via a (typically cryogenic) modulator whose function is to trap analytes from the first dimension and refocus/reinject them into the second dimension. The effect of combining two separations is that compounds co-eluting in one dimension may be resolved in the other, and as such the benefits of GC×GC include improved resolution and peak capacity compared to one-dimensional GC. As expected, a plethora of compounds were tentatively identified in wastewater GC×GC, and a selected few were conclusively identified and quantified (Wooding *et al.*, 2017).

#### 2.4.5.3 Supercritical fluid chromatography (SFC)

SFC is nowadays considered an alternative separation platform to LC and has been mostly used in the analysis of ARVDs in plasma and other human secretions (Akbal and Hopfgartner, 2017), or for impurity profiling in lab water (Alexander *et al.*, 2013; Romand *et al.*, 2016). The technique is yet to be implemented for the same analyses in wastewater. In SFC, separations are achieved using small amounts of polar organic solvent (MeOH, ACN *etc*) and supercritical CO<sub>2</sub>, resulting in a mobile phase with lower viscosity and higher diffusivity than is the case in LC (Alexander *et al.*, 2012; Desfontaine *et al.*, 2015; Grand-Guillaume Perrenoud *et al.*, 2012b). CO<sub>2</sub> is an inert gas and is preferred due to its achievable critical pressure ( $P_c$ , 74 bar) and temperature ( $T_c$ , 31°C), which are relatively easily achievable with conventional chromatographic instrumentation. Alternative supercritical mobile phases include ammonia (NH<sub>3</sub>), methane (CH<sub>4</sub>), propane (C<sub>3</sub>H<sub>8</sub>) and ethylene (C<sub>2</sub>H<sub>4</sub>), but toxicity, corrosiveness and flammability largely preclude their use (Grand-Guillaume Perrenoud *et al.*, 2014; Nováková *et al.*, 2014).

SFC is a powerful technique for fast and high resolution separations of a wide range of compounds, including weakly polar and thermolabile compounds in complex samples. The low viscosity and elevated analyte diffusion coefficients of the supercritical mobile phase allows for fast separations, especially when using sub-2 µm packed columns. A comparison between SFC and UHPLC is illustrated in **Figure 2.5**, where it is clear that the former technique offers higher optimal mobile phase velocities

and comparable plate heights (i.e. efficiency). Further advantages of SFC include the excellent separations of structural related compounds (isomers, chiral compounds, *etc.*) and low susceptibility to matrix effects (Svan *et al.*, 2018).

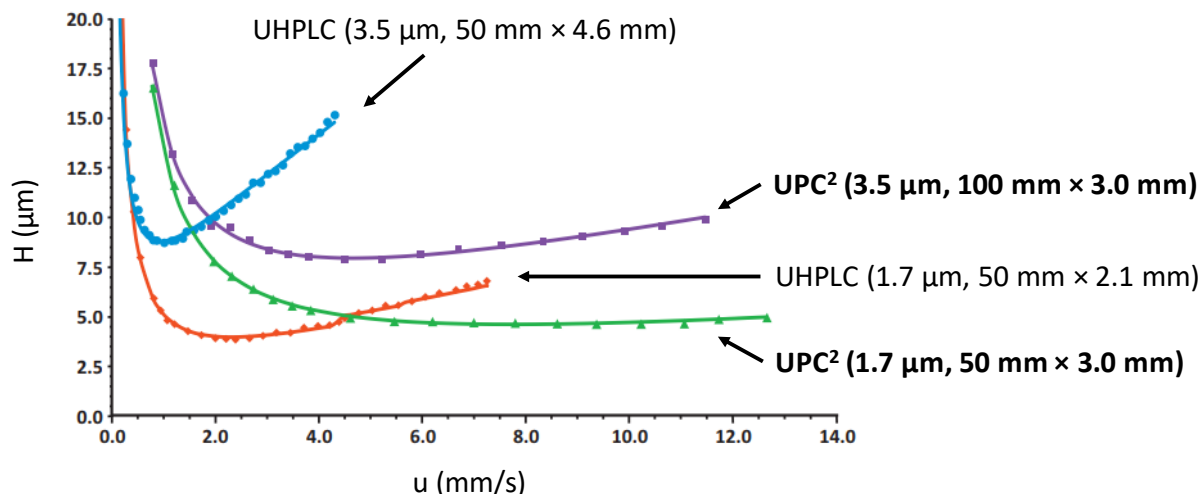


**Figure 2.5:** Plate height curves for butylparaben obtained on a SFC (UPC<sup>2</sup>) system equipped with columns of 3.5  $\mu\text{m}$  (purple trace) and 1.7  $\mu\text{m}$  particle sizes (green trace) and UHPLC equipped with columns of 3.5  $\mu\text{m}$  (blue trace) and 1.7  $\mu\text{m}$  particle sizes (green trace). Reprinted with permission from Grand-Guillaume Perrenoud *et al.* (2014).

The performance of SFC for the separations of basic, polar pharmaceuticals ( $\text{pK}_a > 7$ ) is however often limited by poor peak shapes and tailing, as observed for lamivudine and efavirenz (Alexander *et al.*, 2013; Mosekiemang *et al.*, 2019). In this work, peak shapes could not be improved by addition of a 10 mM  $\text{NH}_4$ -acetate and 0.1% isopropyl amine to the mobile phase, normally suggested as a remedy (Alexander *et al.*, 2013). It is believed that peak deterioration is a result of the formation of carbamic acid by a reaction between  $\text{CO}_2$  and amines, which can be minimised by addition of MeOH (Grand-Guillaume Perrenoud *et al.*, 2012a). Dispas and co-workers reported an improvement in peak shapes for PIs (**Figure 2.1**) use a mobile phase make-up of  $\text{H}_2\text{O}$ -MeOH, (5:95, *v/v*) with 0.1% FA, with post-column addition of 25 mM  $\text{NH}_4$ -acetate (Dispas *et al.*, 2018). Although most applications of SFC to ARVD analysis employ MS, Russo *et al.* (2018) reported the use of a photodiode array detector ( $\lambda$  254 nm) for the detection of stavudine and zidovudine in surface water.

#### 2.4.6 Mass spectrometric detection of ARVDs in environmental samples

##### 2.4.6.1 Ionisation modes

LC systems hyphenated to MS are composed of a separations module, an ion source, the most common of which are any of the three configurations of atmospheric pressure ionization (API) (**Figure 2.6**), and

the mass analyser. The ion source serves as a gateway device for sending charged ions into the MS and is therefore an important component of LC-MS for its dual roles as an ion generator and a vacuum transition platform from atmospheric pressure to high vacuum. Various designs of ion sources are in use today, but the API devices consisting of atmospheric pressure chemical ionisation (APCI), atmospheric pressure photoionisation (APPI) and especially electrospray ionisation (ESI) are most widely used for a wide range of analytes, including pharmaceutical environmental analyses (Andra *et al.*, 2017; Hernández *et al.*, 2011; Rochat, 2018). The ionisation process in these devices typically occurs with limited fragmentation of the molecular ion, and these are therefore referred to as soft ionisation techniques (Banerjee and Mazumdar, 2012; Laaniste *et al.*, 2019).

Of the three API sources, ESI is by far the most common, also in the analysis of ARVDs (Abafe *et al.*, 2018; Aminot *et al.*, 2015; Boulard *et al.*, 2018; Funke *et al.*, 2016; K'oreje *et al.*, 2016; Ngumba *et al.*, 2016b, 2016a; Prasse *et al.*, 2010; Wood *et al.*, 2015), although APCI has also been used (Prasse *et al.*, 2010; Wooding *et al.*, 2017). APPI was most recently developed, and commercialized in 2000, and has not yet been applied in ARVD analysis.

In ESI, the LC effluent is channelled into a capillary tube held at a high potential (3-6 kV) relative to the ionisation source, where the liquid is nebulized with the help of nitrogen gas into a fine mist of highly charged ionic droplets. In the ionisation chamber, these droplets are reduced in size due to the evaporative effects of heated nitrogen (drying gas), causing concentration of the charge within them relative to the liquid surface tension (coulombic repulsion force). This progresses until the surface tension of the liquid exceeds the coulombic force, at the Raileigh limit, when the strained droplets break into clouds of sub- $\mu\text{m}$  highly charged droplets, from where gaseous analyte ions are released to be channelled through the ion optics into the mass analyser (**Figure 2.6**). A consequence of this mode of operation is that ESI is less compatible with high flow rates compared to APCI and APPI, where the mobile phase is evaporated prior to ionisation. Typical flow rates for UHPLC are mostly compatible with the modern ESI sources (Garcia-Ac *et al.*, 2011; Laaniste *et al.*, 2019; Parr *et al.*, 2018), ranging from 0.2-0.6 mL/min for the studies considered in this chapter (**Table 2.2**).

The APCI process entails nebulisation of the column effluent into a fine mist or aerosol as shown in **Figure 2.6**. Ion formation is then achieved using a corona discharge that facilitates formation of radical ions of abundant atmospheric gases such as nitrogen, oxygen and water vapor ( $\text{N}_2^{+}$ ,  $\text{NO}^+$ ,  $\text{H}_2\text{O}^+$ ), which are then responsible for the ionisation of analytes through a series of proton or charge transfer or associative/dissociative electron capture reactions. The resulting highly charged ions are then transmitted into the MS. Unlike ESI, APCI is compatible with high flow rates (Garcia-Ac *et al.*, 2011). APCI is capable of ionising non-to-moderately polar and thermally stable compounds of up to  $\sim 1000$  Da (**Figure 2.6**). Its resilience to matrix effects makes it suitable for environmental analyses (Garcia-Ac *et al.*, 2011; Prasse *et al.*, 2010). For example, Wooding *et al.* (2017) used APCI in the analysis of



multi-class pharmaceuticals, including efavirenz and nevirapine, while Prasse *et al.* (2010) used APCI for the analysis of multi-class ARVDs.

APPI is complementary to ESI and APCI, and is mostly used for ionisation of relatively non-polar, low molecular compounds (**Figure 2.6**). This method uses a vacuum ultraviolet Krypton discharge lamp to emit 10 eV photons, which react with either the analytes directly, or through charge transfer from dopant molecules such as toluene (Kauppila *et al.*, 2014; Robb *et al.*, 2000; Ross and Wong, 2010). Solvents with ionisation energies below the photon energy may be used as dopants. Although untested, this form of ionisation may be relevant to ARVD analysis, considering the extreme low polarities of some therapeutic classes such as PIs.

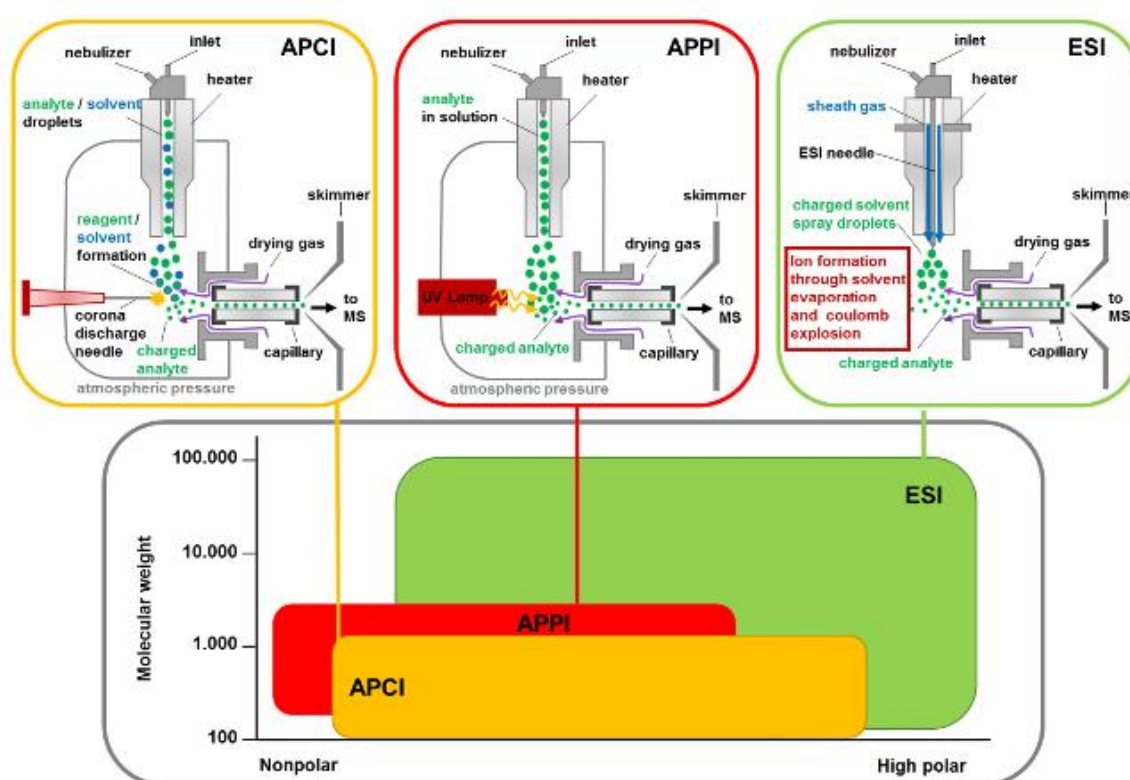


**Figure 2.6:** The different designs of the APCI, APPI and ESI ion sources and a graphical presentation of their suitability for the analysis of compounds according to polarity range and mass. Reprinted with permission from Parr *et al.* (2018).

#### 2.4.7 Tandem mass spectrometry

Research on monitoring ARVDs in wastewater has involved largely quantitative, targeted analyses, which are mostly accomplished using tandem mass spectrometry instruments due to their ability to selectively detect analytes at ultra-trace level concentrations. In theory, tandem mass-spectrometry can either be performed in space or in time. Tandem-in-space is when the successive MS/MS stages occur at the different regions of the instrument, such as in triple quadrupole (QqQ) instruments. In such

systems, two mass analysers are coupled in series with an RF-only Ar/N<sub>2</sub> filled collision cell sandwiched between the two quadrupoles. In the case of Orbitrap MS, ion fragmentation processes occur inside a trap device with the trap and store events being time-regulated, a process described as tandem in time.

Triple quadrupole MS instruments are mostly used in selected/multiple reaction monitoring (S/MRM) mode to quantify ARVDs (**Table 2.4**). In this mode of operation, the precursor ion/adduct is selected in the first quadrupole (Q1), which is set to selected ion monitoring (SIM) and transmitted to the collision cell for fragmentation. After fragmentation, a specific fragment/product ion is selected in the last quadrupole (Q3), also operated in SIM mode, to be detected (Rochat, 2018). It is the monitoring of these ion transitions that confers the selectivity and sensitivity of the MRM method. Better selectivity is achieved if at least two ion transitions pairs are monitored. Typical ion transitions for ARVDs are listed in **Chapter 3**. The sensitivity of the MRM methods assessed according to their achievable limits of detections (LODs) are discussed in detail in recent review articles by Nannou *et al.* (2020, 2019): the lowest recorded LOD was 0.08 ng/mL, which is sufficiently low to detect ARVDs in wastewater samples.

Despite the excellent sensitivity and selectivity achievable by MS/MS detection in MRM mode, there are some limitations, including (i) the requirement to optimize acquisition parameters for every single analyte may be time consuming, and more importantly (ii) such method is inherently only suitable to detect analytes included in the method set up (K'oreje *et al.*, 2012). Alternative application of QqQ-MS for qualitative purposes use acquisition modes such as survey-, neutral loss-, product ion-, and precursor ion scans, but these have not been reported for ARVD analysis. This presents an opportunity for possible innovative structural elucidation experiments, particularly for the identification of novel phase II metabolites of ARVDs. For example, an initial neutral loss scan operated in series with product ion scan, whereby a predetermined neutral loss triggers MS<sup>2</sup> of the recognized ion (*e.g.* glucuronides and sulfates) might prove useful in this regard.

Interestingly, IT-Orbitrap MS has also been used to quantify ARVDs (Funke *et al.*, 2016; K'oreje *et al.*, 2012). The quantitation process involved extracted ion chromatograms (XICs) constructed using narrow mass windows from the full-scan data, with the integrated and peak areas related to concentration in the conventional manner. In terms of selectivity, HR-MS has been reported to be comparable to QqQ-MS in MRM mode, since the narrow mass extraction windows used to obtain the XICs is dependent on mass accuracy (Rochat, 2018, 2016). A comparison of achievable sensitivity levels between low- and high-resolution instruments is difficult to assess given an interplay of various factors such as instrumentation, ionisation efficiency, chromatography, *etc.*, although generally tandem MS in MRM mode offers the lowest LODs.

#### 2.4.8 Method validation of quantitative data

Quantitative data should be subjected to some form of credibility check, which entails assessment of all aspects related to reliability, accuracy, and reproducibility – referred to as method validation (Kruve *et al.*, 2015; Magnusson, 2014). Numerous method validation guidelines are available, but all are in agreement that method validation must test for selectivity and specificity, linearity of the calibration curve, limits of detection/quantification, inter- and intra-day precision, recovery and matrix effects (IUPAC, 2000). Selectivity and sensitivity provide assurance of the identity of the analyte in the presence of interferents (Antignac *et al.*, 2003; Kruve *et al.*, 2015). It is a requirement that method validation must convincingly demonstrate selectivity even in the presence of potential interferents (Araujo, 2009). Although it is possible that interferents such as metabolites may appear in an MRM chromatogram intended for the parent compound (when they share the same transition ions), they should not interfere with quantification due to the differences in retention time ( $t_R$ ) (Funke *et al.*, 2016). In addition, MRM methods provide ion ratio data, which can be used to monitor selectivity, since these ratios are expected to remain resilient to fluctuations in concentration and matrix effects (Antignac *et al.*, 2003).

A test for linearity of a calibration curve is another critical parameter to be ascertained. This entails a correlation of the instrument response to a series of known concentrations; the relationship is expected to be linear ( $\mathbf{y} = \mathbf{m}\mathbf{x} + \mathbf{c}$ ). If this is not the case, a high order regression model such as weighted least squares linear regression may be used. A simple way of determining the linearity of a calibration curve is to use a plot of residuals (Eq. 2.6) to check if the error of replicated calibration points is constant over the calibration range (*i.e.* homoscedastic) or whether the residual error increases with concentration (*i.e.* heteroscedastic).

$$\mathbf{S}(\mathbf{r}) = \sqrt{\frac{\sum (\mathbf{y}_i - \hat{\mathbf{y}}_i)^2}{\mathbf{n} - 2}} \quad \text{Eq. 2.6}$$

where  $\mathbf{y}_i$  is the observed value of  $\mathbf{y}$  (instrument response) for a given value of  $\mathbf{x}_i$  (concentration) and  $\hat{\mathbf{y}}_i$  is the predicted  $\mathbf{y}$  according to the equation of the trend line for a given value of  $\mathbf{x}_i$ .  $\mathbf{n}$  is the number of calibration points. Typical plots of residual errors are shown in **Figure 2.7**.

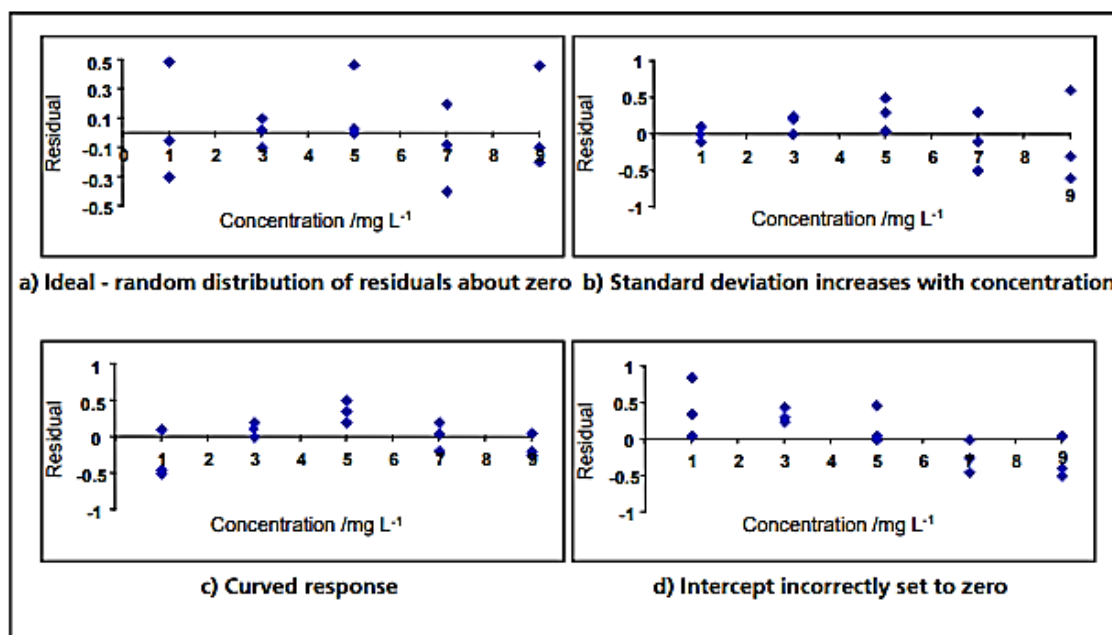


**Figure 2.7:** Examples of residual plots obtained from a 9-point calibration curve with three replicates per point. Panel (a) shows the ideal, with uniformly distributed residuals along the calibration range (homoscedasticity). The remainder of the plots depict various forms of heteroscedasticity: (b) an increase in error along a calibration range, (c) a curved response of residuals and (d) a non-zero intercept. Reprinted with modifications from Prichard and Barwick (2003).

For quantification, one of the external standard, internal standard or standard addition calibration methods can be used; each is suitable for different purposes. For example, standard addition and matrix-matched calibration are used to eliminate matrix effects (Brown and Mustoe, 2014; Cimetiere *et al.*, 2013; Martins *et al.*, 2016). In matrix-matched calibration, analytical standards are spiked into a matrix that does not contain the analytes. This contrasts with standard addition, where analytical standards are spiked in a matrix that contains the analyte. Wood *et al.* (2015) used standard addition, while Ngumba *et al.* (2016) used matrix-matched calibration for quantitative analysis of ARVDs.

Internal standard calibration is method in which a fixed concentration of a suitable internal standard (an isotopically labelled standard incorporating <sup>13</sup>C, <sup>2</sup>H, <sup>15</sup>N, *etc.* is preferred) is added across a calibration range. It is used to compensate for analyte loss due to ionisation effects and during sample preparation. The resulting calibration curve is a plot of analyte concentration as a function of the ratio of analyte to internal standard responses. So far, this has been the most widely used method for the quantitative analysis of ARVDs (Abafe *et al.*, 2018; Aminot *et al.*, 2018, 2015; Boulard *et al.*, 2018; K'oreje *et al.*, 2018, 2016, 2012; Muriuki *et al.*, 2020; Prasse *et al.*, 2010).

From the calibration curve, the method sensitivity and limit of detection (LOD) can be statistically determined. The LOD is a measure of the lowest concentration that can be reliably detected with

certainty (Evard *et al.*, 2016) and can be calculated according to **Eq. 2.7**. In relation to LOD is the limit of quantification (LOQ), calculated according to **Eq. 2.8**.

$$\text{LOD} = 3.3 \times \frac{S_d}{b} \quad \text{Eq. 2.7}$$

$$\text{LOQ} = 10 \times \frac{S_d}{b} \quad \text{Eq. 2.8}$$

where  $S_d$  is the standard deviation of the residuals  $S_{y,x}$  and  $b$  is the slope of the regression line.

Precision and accuracy are calculated using the recovery data. Precision is a measure of agreement between replicate measurements, while accuracy is a measure of the extent of deviation between the true concentration and experimental observation (Antignac *et al.*, 2003; Magnusson, 2014). It is expected that the observed concentration should be as close as possible to the nominal concentration, that is, bias should be as low as possible. It is imperative for the experiment to be replicated to allow for a measurement of precision in terms of mean and % relative standard deviation (RSD). The method is deemed precise if independently prepared sample replicates provide almost the same value. It is recommended that precision should be measured for within batch/run replicates to establish repeatability and between batches/runs to establish the reproducibility of the method.

Matrix- and neat solvent-fortified samples can also be used to evaluate matrix effects. This effect occurs when interferences co-eluting with the target analyte alter the ionisation efficiency by either enhancing or suppressing the signal. Several methods are used to evaluate this effect, including comparison of slopes of matrix-matched and neat solvent calibration curves (Kruve *et al.*, 2015). An approach less often used is to perform post-column infusion of the matrix to detect ion enhancement or suppression regions of the chromatographic run (Rossmann *et al.*, 2015). The simplest approach to evaluate matrix effects is however to compare concentrations or peak areas obtained in matrix-fortified and solvent-fortified samples (Antignac *et al.*, 2003; Araujo, 2009).

#### 2.4.9 High resolution mass spectrometry

The application of high resolution mass spectrometry (HR-MS) for untargeted analysis, structural elucidation and identification of unknown compounds has received relatively little attention in the reviewed literature reports dealing with ARVD analysis. Only two papers report the use of HR-MS to identify transformation products (TPs) of ARVDs during the wastewater treatment process. Funke *et al.* (2016) used the LTQ Orbitrap MS to identify TPs of the ARVDs abacavir, emtricitabine, lamivudine and zidovudine during treatment process, while Wood *et al.* (2016) used Q-TOF-MS to study the behaviour of nevirapine during chlorination of effluent and reported the formation of several nevirapine TPs. Other studies were merely to demonstrate the quantitative capability of the HR-MS using a range of instruments, including a magnetic sector double-focusing/ion trap hybrid MS (K'oreje *et al.*, 2018, 2016, 2012), GC-TOF (Schoeman *et al.*, 2017) and GC×GC TOF-MS (Wooding *et al.*, 2017). The lack

of literature reports demonstrating the occurrence of ARVD metabolites in wastewater provides an ideal application for untargeted HR-MS methods (as reported in **Chapter 5**).

HR-MS instruments are ideally suited for performing untargeted or suspect screening due to their capability to generate full scan high resolution data, and on tandem systems also high resolution MS/MS data. High resolution data can only go as far as providing the elemental formula of an unknown compound, and facilitates structural elucidation, but assignments based on such data remain tentative until confirmed by reference standards. A typical workflow for processing high resolution data entails inspection of the low collision energy total ion chromatogram (TIC) for peaks of interest, extraction of extracted ion chromatograms (XICs) using narrow mass extraction windows, and low collision energy spectra to obtain elemental formulae. The next step is to extract the high collision energy spectrum for the selected  $m/z$  from the high energy TIC. The limitation of this approach is that co-elution of isobaric ions cannot be identified in the low energy XIC. The low collision energy spectrum will reveal co-elution of species with different  $m/z$  by distinguishing the relevant molecular ions, but the main limitation is the complexity of the resulting high collision energy spectra. As a result, smarter data application tools have been developed to assist with simplification of the analysis of complex HR-MS data.

Data dependent acquisition (DDA) and data independent acquisition (DIA) modes are alternative strategies specifically designed to improve the quality of MS/MS data. DDA is information-dependent and functions according to pre-set criteria for selecting precursor ions to be subjected to MS/MS fragmentation. Several parameters such as retention time ( $t_R$ ), isotopic pattern, neutral loss, *etc.* are provided as input information to specify when the tandem MS instrument should switch from full-scan acquisition mode to MS/MS mode once a peak of interest is detected. The main limitations of DDA methods are that they do not always solve co-elution-related spectral complexities, and that several analyses may be required to gather data used for the pre-selection of the relevant precursor ions. This approach was used by Wood *et al.* (2016) for the identification of chlorinated TPs of nevirapine. In this case the criteria used for precursor ion selection were based on  $t_R$  and isotopic patterns for chlorine-containing TPs.

In contrast, DIA entails the alternating application of low- and high collision energies across the chromatographic run. This technique is also referred to as MS<sup>E</sup> (Waters), all-ion fragmentation (Thermo) and MS/MS<sup>ALL</sup> (Sciex). In DIA methods, selection of precursor ion beforehand is not performed, and all ions are transmitted into the collision cell and subjected to alternating low- and high energy collisions (a collision energy ramp can also be used). The low collision energy acquisition minimizes fragmentation and thus conserves the molecular ion information when using soft ionisation devices such as ESI and APCI. On the other hand, high collision acquisition promotes fragmentation in the generation of product ion spectra. DIA methods are comparatively fast, but suffer lower selectivity

compared to DDA methods, with the link between precursor- and product ions often obscured, making spectral interpretation difficult.

#### 2.4.10 Processing of HR-MS data using advanced data analysis tools.

Several post-acquisition processing tools have been developed for data mining of high resolution data. Essentially, the main objective of many of these tools is to reduce the complexity of the TIC to a manageable composite chromatogram containing only peaks of interest by way of data filtering. As such, these are data reduction tools. Examples of commercial software used for this purpose are Metabolyx (Waters), Networks (Thermo), MassHunter (Agilent Technologies) (Cuyckens *et al.*, 2009; Tiller *et al.*, 2008b, 2008a). The most common approach involves the implementation of molecular structure and mass defect filter templates to full-scan data. Mass defect refers to the difference between the exact- and the nominal mass of a compound (Andra *et al.*, 2017). This feature can differentiate target analytes from interferents because of the differences in their molecular formulae and respective mass defect patterns. When such a template is implemented either during a run or post-acquisition, interfering ions are readily removed, leaving simplified data that could facilitate the identification process (Zhang *et al.*, 2009a). For example, a family of structurally related metabolites may be recognized by their characteristic mass defect profiles in the presence of matrix background. It has been shown that the mass defects of drug metabolites fall within 50 mDa relative to that of the parent drug (Zhang *et al.*, 2009b). For example, hydroxylation changes the mass defect value by -5 mDa, glucuronidation by +32 mDa and sulfation by -43 mDa. Consequently, 50 mDa can be used as a threshold value for mass defect filters targeting the common phase I and II metabolic pathways (Andra *et al.*, 2017; Zhang *et al.*, 2003). For instance, Bateman *et al.* (2007) used such a mass defect template to identify the ARVD indinavir and its metabolites in plasma, while Castro-perez *et al.* (2009) used the technique to determine the metabolism and routes of clearance for ritonavir and its metabolites. Zhang *et al.* (2008) used a set of model drugs that included the ARVDs indinavir, lamivudine and zidovudine to demonstrate the selectivity of mass defect filtering to detect these drugs in complex biological matrices. A summary of the mass- and mass defect shifts for biotransformation products of ARVDs is presented in **Table 2.3**. As discussed previously, ARVDs undergo mainly hydroxylation biotransformation in the phase I pathway and further sulfation and glucuronidation in the phase II pathways (Andrade *et al.*, 2011), such that the corresponding mass shifts and formulae changes can readily be predicted.

**Table 2.3:** Mass and mass defect shifts for metabolites in relation to their parent compounds.

Description (Phase I/II)	Mass shift (Da)	Mass defect shift (mDa)	Formula change
Hydroxylation (phase I)	15.9949	-5.1	+O
2 × Hydroxylation (phase I)	31.9898	-10.2	+O <sub>2</sub>
Glucuronidation (phase II)	+176.0321	32.1	+C <sub>6</sub> H <sub>8</sub> O <sub>7</sub>
Sulfation (phase II)	+80.0432	-43.2	+SO <sub>3</sub>

Source: Zhang *et al.* (2009b).

**Figure 2.8** demonstrates the application of a mass defect template (using MetaboLynx™) to search for metabolites of nevirapine in a full-scan MS data obtained for the analysis of a wastewater sample processed by SPE. The metabolite list included the parent compound (C<sub>15</sub>H<sub>14</sub>N<sub>4</sub>O) and the expected metabolites according to their transformation: hydroxylation, 2× hydroxylation, sulfate conjugation and glucuronide conjugation. The mass defect filter was enabled at a tolerance limit of 50 mDa across a *t<sub>R</sub>* range of 0-44 minutes. Unexpected metabolites functionality was also enabled. As can be seen, the output composite TIC provided peaks for the expected metabolites according to the mass defect template, of which four were identified as nevirapine metabolites. The data reduction capability of mass defect filtering is evident from comparison of the base peak ion and composite TIC chromatograms (**Figure 2.8**).

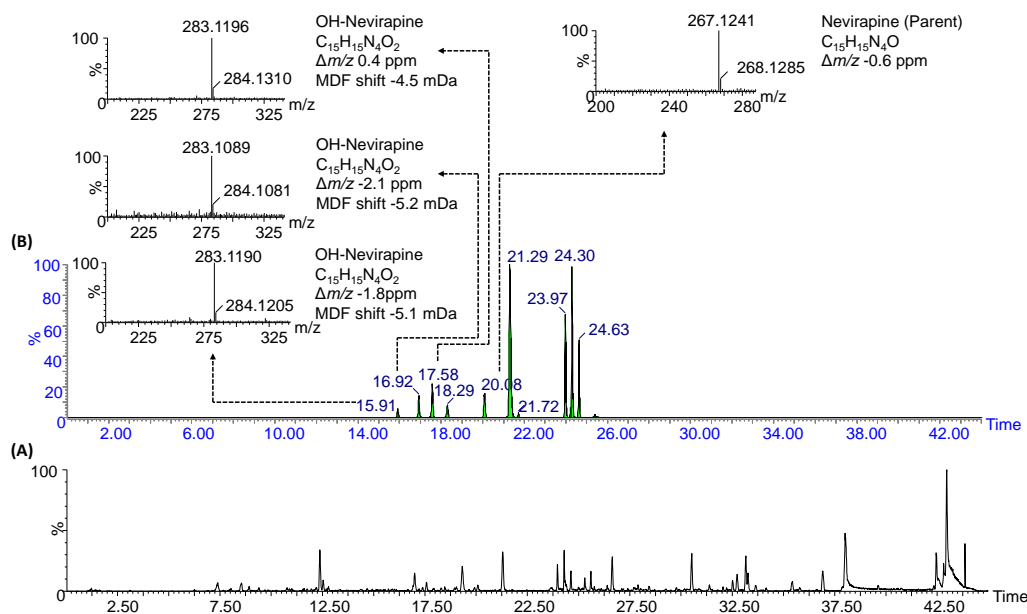


**Figure 2.8:** Post-acquisition processed LC-MS<sup>E</sup> data using Metabolynx™ software to detect nevirapine and its metabolites in raw wastewater sample processed by SPE. (A) shows the low energy base peak ion chromatogram, and (B) a simplified composite TIC containing expected metabolites obtained after



implementing a mass defect filter template ( $\pm 50$  mDa) for nevirapine ( $C_{15}H_{15}N_4O$ ) and its phase I and II metabolites. Mass spectra are shown for the identified metabolites as indicated. Source: Author's unpublished data.

#### 2.4.11 Ion mobility spectrometry

Ion mobility spectrometry (IMS) is an electrophoretic technique that separates gas phase ions on the basis of their mobility in a buffer gas in the presence of an electric field (**Figure 2.9**). Ions are separated based on their mass, charge and their averaged collisional cross section areas (Creaser *et al.*, 2004). Integration of IMS into HR-MS workflows offers several benefits: potential separation of isomers that cannot be distinguished by HR-MS, the option for signal filtering according to drift or arrival time for ions buried in matrix, and the assignment of a unique analyte identifier based on its structural conformation known as the collision cross section (CCS,  $\Omega$ ) (Campuzano *et al.*, 2012; Lanucara *et al.*, 2014; Lian *et al.*, 2018; Paglia *et al.*, 2015). Several IMS platforms are in use today, including drift tube- (DTIMS), travelling wave- (TWIMS), field asymmetric wave form- (FAIMS), differential mobility analysers (DMA), and trapped IMS (TIMS), all with associated strengths and weaknesses (Dodds and Baker, 2019).

The basic principle of operation of IMS is to separate gaseous ions under the influence of a static (DTIMS, TIMS, and DMS) or oscillating electric field (TWIMS and FAIMS). The electric field ( $\mathbf{E}$ ) induces ion migration, where the ion's mobility ( $\mathbf{K}$ ) is related to its velocity ( $\mathbf{v}_d$ ) according to **Eq. 2.9**.

$$\mathbf{K} = \frac{\mathbf{v}_d}{\mathbf{E}} \quad \text{Eq. 2.9}$$

Under the influence of the electric field and in the presence of the buffer gas, small ions tend to attain higher velocity compared to larger ions, because the larger surface area of the latter result in more collisions with the buffer gas. The mobility is also dependent on the pressure and temperature of the buffer gas, so  $\mathbf{K}$  is related to temperature and pressure via **Eq. 2.10**. By convention, temperature (273 Kelvin) and pressure (760 Torr) are normalized to standard conditions to calculate reduced mobility ( $\mathbf{K}_0$ ):

$$\mathbf{K}_0 = \mathbf{K} \frac{P T_0}{P_0 T} \quad \text{Eq. 2.10}$$

In IMS, an ion's drift or arrival time ( $t_D$  or  $t_A$ ) is measured. On DTIMS instruments, this value can be directly converted to the ion's CCS ( $\Omega$ , in units of square Angströms ( $\text{\AA}^2$ )) value via the Mason-Schamp equation (**Eq. 2.11**).

$$\Omega = \frac{3}{16} \left( \frac{2\pi}{\mu k_b T} \right)^{1/2} z e \quad \text{Eq. 2.11}$$

where  $e$  and  $z$  are the electron and ion charges, respectively,  $N_0$  is the density of the buffer gas,  $\mu$  is the reduced mass of the ion-buffer gas complex, and  $k_B$  and  $T$  are the Boltzmann's constant and temperature of the drift region, respectively. For TWIMS instruments, where a variable electric field is used, calibration is required to relate  $t_A$  to CCS. For this purpose, calibrants such as polyalanine, for which CCS values are known (typically measured on DTIMS systems), are used.

TWIMS (**Figure 2.9**) and DTIMS instruments are most widely used in environmental analysis (Hinnenkamp *et al.*, 2019; Jafari Horestani *et al.*, 2018; Stephan *et al.*, 2016), albeit that the technique has found relatively limited application compared to other fields. Regarding the analysis of ARVDs by IMS, only one report exists by Howdle *et al.* (2009), who used polyethylene glycol as shift reagent to manipulate  $t_R$  and  $t_D$  of lamivudine and its PEG-complexes. The scarcity of published work regarding the application of IMS to analyse for ARVDs also means that experimental CCS values for these compounds are lacking, with the exception of atazanavir.

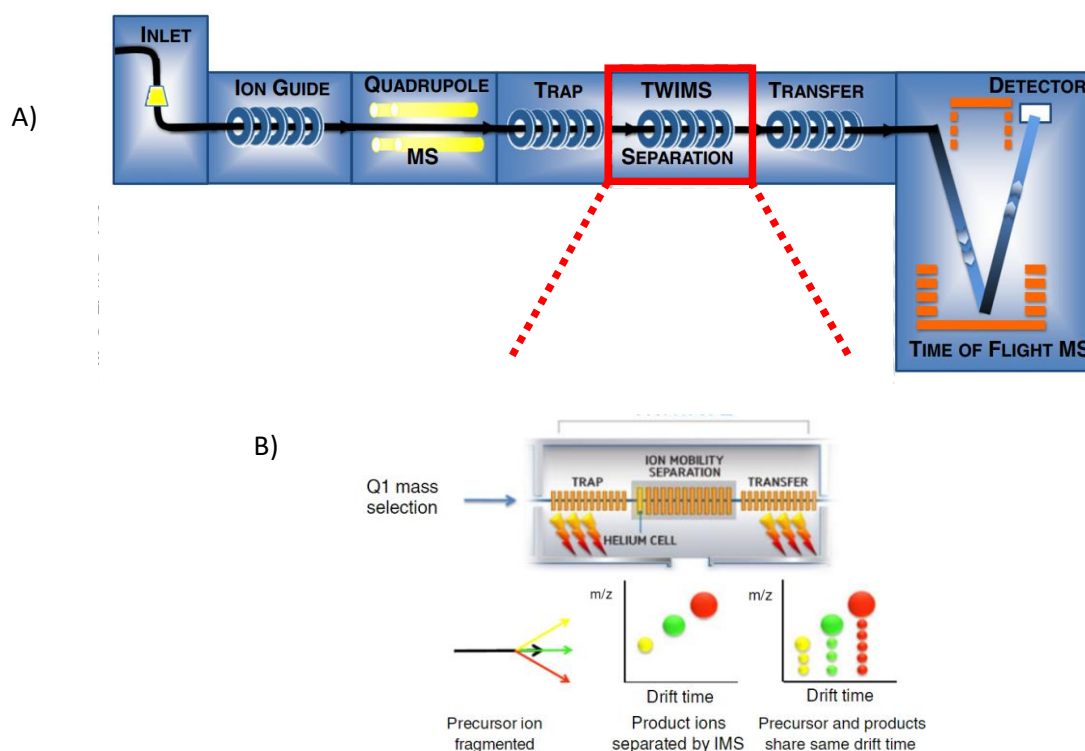


**Figure 2.9:** (A) A schematic diagram of commercially available travelling wave ion mobility spectrometry (TWIMS) integrated with an orthogonal acceleration quadrupole-time-of-flight mass spectrometer. Gas phase ions are separated in the TWIMS device (B) in which fragmentation can occur before or after IMS separation as shown by the time-aligned-parallel procedure where precursor ions and their corresponding product ions are drift time-aligned. (B) is reprinted with permission from Sun *et al.* (2011).

## 2.5 Summary

The analysis of ARVDs in the environment has been the focus of extensive research in the last decade, although the focus of much of this research has been on quantitative analysis using tandem mass spectrometry. Data regarding the occurrence of ARVDs in the environment has been summarised in recent reviews by Madikizela *et al.* (2020), Nannou *et al.* (2020, 2019), and Ncube *et al.* (2018). Like other pharmaceutical compounds, ARVDs are partially eliminated during conventional wastewater treatment processes. This is true for the polar nucleosidic NRTIs, although the mid-polar *n*NRTIs efavirenz and nevirapine show lower removal efficiencies (Schoeman *et al.*, 2017; Wood *et al.*, 2016). Overall, the concentrations of ARVDs are highly influenced by seasonal variations, with high concentrations observed in the dry season in contrast to low concentrations observed in the wet season due to rainwater dilution. Significantly, no information regarding the occurrence of ARVD metabolites in wastewater is available.

ARVDs vary significantly in terms of their physico-chemical properties (**Figure 1**), which complicates the development of analytical methods aimed at the entire array of therapeutic classes in a single analysis, especially when metabolites are of interest. For example, vastly different solubilities may complicate method development and validation (Li *et al.*, 2015). Regarding sample preparation, RP-SPE remains a popular method, despite the low retention of polar nucleosidic NRTIs such as abacavir (Aminot *et al.*, 2015; Boulard *et al.*, 2018), lamivudine and emtricitabine (Boulard *et al.*, 2018; Funke *et al.*, 2016; Wood *et al.*, 2016). A remedial intervention has been to use large volume direct injection to correct for poor recoveries of such compounds (Boulard *et al.*, 2018; Funke *et al.*, 2016). Alternative extraction techniques such as MIPS (Mtolo *et al.*, 2019), sorption microextraction (Mlunguza *et al.*, 2020; Wooding *et al.*, 2017) have also been explored for these analyses.

Reported methods for the separation of ARVDs have largely used RP-LC columns of various dimensions and particle sizes. Only two studies reported the use of HILIC for the separation of several polar NRTIs and transformation products (Boulard *et al.*, 2018; Prasse *et al.*, 2010). SFC has been used for the separation of several glucuronides, including zidovudine glucuronide (Romand *et al.*, 2016), and protease inhibitors (Akbal and Hopfgartner, 2017), efavirenz and lamivudine (Alexander *et al.*, 2013), albeit not in wastewater. This shows the potential of the technique for wastewater analysis. Similarly, a literature gap exists regarding the application of HR-MS for the screening analysis of non-target ARVDs and their metabolites. **Table 2.4** summarizes the analytical methods applied thus far for the analysis of ARVDs in wastewater.

**Table 2.4:** A summary of analytical techniques used for the analysis of ARVDs in wastewater.

Common technique	Alternative technique	
<b>(1) Sample collection</b>		
Grab samples. (500-1000 mL) (Funke <i>et al.</i> , 2016; K'oreje <i>et al.</i> , 2018, 2016, 2012; Mlunguza <i>et al.</i> , 2020; Mosekiemang <i>et al.</i> , 2019; Ngumba, 2018; Ngumba <i>et al.</i> , 2016a; Rimayi <i>et al.</i> , 2018; Schoeman <i>et al.</i> , 2017; Wood <i>et al.</i> , 2016, 2015; Wooding <i>et al.</i> , 2017; Aminot <i>et al.</i> , 2015, 2016)	Composite samples (24 h) (Funke <i>et al.</i> , 2016; Ngumba <i>et al.</i> , 2016b; Aminot <i>et al.</i> , 2015)	Passive sampler Chemcatcher® (Rimayi <i>et al.</i> , 2019)
<b>(2) Analyte extraction and pre-concentration</b>		
Solid phase extraction (SPE) (off-line <sup>a</sup> /on-line <sup>b</sup> )	Lyophilisation Large volume direct injection (Mlunguza <i>et al.</i> , 2020; Mosekiemang <i>et al.</i> , 2019)	Sorptive microextraction (PDMS (Wooding <i>et al.</i> , 2017); MIPS (Mtolo <i>et al.</i> , 2019); HF-LPME (Mlunguza <i>et al.</i> , 2020))
<b>Oasis HLB<sup>a</sup></b> (Abafe <i>et al.</i> , 2018; K'oreje <i>et al.</i> , 2018, 2016, 2012; Ngumba <i>et al.</i> , 2016a, 2016b; Wood <i>et al.</i> , 2015)		
<b>MCX<sup>a</sup></b> (Aminot <i>et al.</i> , 2016, 2015; Ngumba <i>et al.</i> , 2016b)		
<b>MAX<sup>a</sup></b> (Ngumba <i>et al.</i> , 2016b)		
<b>Strata SDB-L<sup>a</sup></b> (Mosekiemang <i>et al.</i> , 2019)		
<b>Cleanert PEP<sup>a</sup></b> (Schoeman <i>et al.</i> , 2017)		
<b>QuEChERS<sup>a</sup></b> (Schoeman <i>et al.</i> , 2017)		
<b>(3) Instrumental analysis</b>		
<b>LC-tandem MS (RP-LC, HILIC)</b> MRM-QqQ-MS: (Abafe <i>et al.</i> , 2018; Aminot <i>et al.</i> , 2016, 2015; Mosekiemang <i>et al.</i> , 2019; Ngumba <i>et al.</i> , 2016a, 2016b; Wood <i>et al.</i> , 2015) (Funke <i>et al.</i> , 2016); Boulard <i>et al.</i> , 2018; Prasse <i>et al.</i> , 2010)	<b>LC-HR-MS</b> Q-TOF-MS: Funke <i>et al.</i> , 2016; K'oreje <i>et al.</i> , 2018, 2016, 2012; Wooding <i>et al.</i> , 2017); MS <sup>n</sup> -LTQ-Orbitrap (Funke <i>et al.</i> , 2016)	<b>GC-MS</b> GC-TOF-MS: (Schoeman <i>et al.</i> , 2017), GC×GC-TOF-MS (Wooding <i>et al.</i> , 2017)

## 2.6 References

- Abafe, O.A., Späth, J., Fick, J., Jansson, S., Buckley, C., Stark, A., Pietruschka, B., Martincigh, B.S., 2018. LC-MS/MS determination of antiretroviral drugs in influents and effluents from wastewater treatment plants in KwaZulu-Natal, South Africa. *Chemosphere* 200, 660–670. <https://doi.org/10.1016/j.chemosphere.2018.02.105>
- Acero, J.L., Benitez, F.J., Real, F.J., Roldan, G., 2010. Kinetics of aqueous chlorination of some pharmaceuticals and their elimination from water matrices. *Water Res.* 44, 4158–4170. <https://doi.org/10.1016/j.watres.2010.05.012>
- Akbal, L., Hopfgartner, G., 2017. Effects of liquid post-column addition in electrospray ionization performance in supercritical fluid chromatography – mass spectrometry. *J. Chromatogr. A* 1517, 176–184. <https://doi.org/10.1016/j.chroma.2017.08.044>
- Alexander, A.J., Hooker, T.F., Tomasella, F.P., 2012. Evaluation of mobile phase gradient supercritical fluid chromatography for impurity profiling of pharmaceutical compounds. *J. Pharm. Biomed. Anal.* 70, 77–86. <https://doi.org/10.1016/j.jpba.2012.05.025>
- Alexander, A.J., Zhang, L., Hooker, T.F., Tomasella, F.P., 2013. Comparison of supercritical fluid chromatography and reverse phase liquid chromatography for the impurity profiling of the antiretroviral drugs lamivudine/BMS-986001/efavirenz in a combination tablet. *J. Pharm. Biomed. Anal.* 78–79, 243–251. <https://doi.org/10.1016/j.jpba.2013.02.019>
- Aminot, Y., Fuster, L., Pardon, P., Le Menach, K., Budzinski, H., 2018. Suspended solids moderate the degradation and sorption of waste water-derived pharmaceuticals in estuarine waters. *Sci. Total Environ.* 612, 39–48. <https://doi.org/10.1016/j.scitotenv.2017.08.162>
- Aminot, Y., Le Menach, K., Pardon, P., Etcheber, H., Budzinski, H., 2016. Inputs and seasonal removal of pharmaceuticals in the estuarine Garonne River. *Mar. Chem.* 185, 3–11. <https://doi.org/10.1016/j.marchem.2016.05.010>
- Aminot, Y., Litrico, X., Chambolle, M., Arnaud, C., Pardon, P., Budzinski, H., 2015. Development and application of a multi-residue method for the determination of 53 pharmaceuticals in water, sediment, and suspended solids using liquid chromatography-tandem mass spectrometry. *Anal. Bioanal. Chem.* 407, 8585–8604. <https://doi.org/10.1007/s00216-015-9017-3>
- Andra, S.S., Austin, C., Patel, D., Dolios, G., Awawda, M., Arora, M., 2017. Trends in the application of high-resolution mass spectrometry for human biomonitoring: An analytical primer to studying the environmental chemical space of the human exposome. *Environ. Int.* 100, 32–61. <https://doi.org/10.1016/j.envint.2016.11.026>

- Andrade, C.H., de Freitas, L.M., de Oliveira, V., 2011. Twenty-six years of HIV science: An overview of anti-HIV drugs metabolism. *Brazilian J. Pharm. Sci.* 47, 209–230.  
<https://doi.org/10.1590/S1984-82502011000200003>
- Antignac, J.P., Le Bizec, B., Monteau, F., Andre, F., 2003. Validation of analytical methods based on mass spectrometric detection according to the “2002/657/EC” European decision: Guideline and application. *Anal. Chim. Acta* 483, 325–334. [https://doi.org/10.1016/S0003-2670\(02\)01379-X](https://doi.org/10.1016/S0003-2670(02)01379-X)
- Araujo, P., 2009. Key aspects of analytical method validation and linearity evaluation. *J. Chromatogr. B Anal. Technol. Biomed. Life Sci.* 877, 2224–2234.  
<https://doi.org/10.1016/j.jchromb.2008.09.030>
- Atinkpahoun, C.N.H., Le, N.D., Pontvianne, S., Poirot, H., Leclerc, J.P., Pons, M.N., Soclo, H.H., 2018. Population mobility and urban wastewater dynamics. *Sci. Total Environ.* 622–623, 1431–1437.  
<https://doi.org/10.1016/j.scitotenv.2017.12.087>
- Bade, R., Rousis, N.I., Bijlsma, L., Gracia-Lor, E., Castiglioni, S., Sancho, J. V., Hernandez, F., 2015. Screening of pharmaceuticals and illicit drugs in wastewater and surface waters of Spain and Italy by high resolution mass spectrometry using UHPLC-QTOF MS and LC-LTQ-Orbitrap MS. *Anal. Bioanal. Chem.* 407, 8979–8988. <https://doi.org/10.1007/s00216-015-9063-x>
- Banerjee, S., Mazumdar, S., 2012. Electrospray Ionization Mass Spectrometry: A Technique to Access the Information beyond the Molecular Weight of the Analyte. *Int. J. Anal. Chem.* 2012, 1–40.  
<https://doi.org/10.1155/2012/282574>
- Bateman, K.P., Castro-perez, J., Wrona, M., Shockcor, J.P., Yu, K., Oballa, R., Nicoll-griffith, D.A., 2007. MS<sup>E</sup> with mass defect filtering for in vitro and in vivo metabolite identification. *Rapid Commun. mass Spectrom.* 21, 1485–1496. <https://doi.org/10.1002/rcm>
- Bengtsson, M., Tillman, A.-M., 2004. Actors and interpretations in an environmental controversy: the Swedish debate on sewage sludge use in agriculture. *Resour. Conserv. Recycl.* 42, 65–82.  
<https://doi.org/10.1016/j.resconrec.2004.02.004>
- Bielicka-Daszkiwicz, K., Voelkel, A., 2009. Theoretical and experimental methods of determination of the breakthrough volume of SPE sorbents. *Talanta* 80, 614–621.  
<https://doi.org/10.1016/j.talanta.2009.07.037>
- Bielicka-Daszkiwicz, K., Voelkel, A., Rusińska-Roszak, D., Zarzycki, P.K., 2013. Estimation of the breakthrough volume of selected steroids for C-18 solid-phase extraction sorbent using retention data from micro-thin layer chromatography. *J. Sep. Sci.* 36, 1104–1111.  
<https://doi.org/10.1002/jssc.201200917>

- Borowska, E., Bourgin, M., Hollender, J., Kienle, C., McArdell, C.S., von Gunten, U., 2016. Oxidation of cetirizine, fexofenadine and hydrochlorothiazide during ozonation: Kinetics and transformation products. *Water Res.* 94, 350–362. <https://doi.org/10.1016/j.watres.2016.02.020>
- Boulard, L., Dierkes, G., Ternes, T., 2018. Utilization of large volume zwitterionic hydrophilic interaction liquid chromatography for the analysis of polar pharmaceuticals in aqueous environmental samples: Benefits and limitations. *J. Chromatogr. A* 1535, 27–43. <https://doi.org/10.1016/j.chroma.2017.12.023>
- Brown, R.J.C., Mustoe, C.L., 2014. Demonstration of a standard dilution technique for standard addition calibration. *Talanta* 122, 97–100. <https://doi.org/10.1016/j.talanta.2014.01.014>
- Busetti, F., Backe, W.J., Bendixen, N., Maier, U., Place, B., Giger, W., Field, J.A., 2012. Trace analysis of environmental matrices by large-volume injection and liquid chromatography-mass spectrometry. *Anal. Bioanal. Chem.* 402, 175–186. <https://doi.org/10.1007/s00216-011-5290-y>
- Busetti, F., Linge, K.L., Blythe, J.W., Heitz, A., 2008. Rapid analysis of iodinated X-ray contrast media in secondary and tertiary treated wastewater by direct injection liquid chromatography-tandem mass spectrometry. *J. Chromatogr. A* 1213, 200–208. <https://doi.org/10.1016/j.chroma.2008.10.021>
- Campuzano, I., Bush, M.F., Robinson, C. V., Beaumont, C., Richardson, K., Kim, H., Kim, H.I., 2012. Structural characterization of drug-like compounds by ion mobility mass spectrometry: Comparison of theoretical and experimentally derived nitrogen collision cross sections. *Anal. Chem.* 84, 1026–1033. <https://doi.org/10.1021/ac202625t>
- Castro-perez, J., Yu, K., Shockcor, J., Shion, H., Marsden-edwards, E., Goshawk, J., Corporation, 2009. Fast and sensitive in vitro metabolism study of rate and routes of clearance for Ritonavir using UPLC coupled with the xevo QTOF MS system. *Appl. Note Waters Corp. Milford, MA, USA* 3–9.
- Chiaia, A.C., Banta-Green, C., Field, J., 2008. Eliminating solid phase extraction with large-volume injection LC/MS/MS: Analysis of illicit and legal drugs and human urine indicators in US wastewaters. *Environ. Sci. Technol.* 42, 8841–8848. <https://doi.org/10.1021/es802309v>
- Choi, P.M., Tschärke, B.J., Donner, E., O'Brien, J.W., Grant, S.C., Kaserzon, S.L., Mackie, R., O'Malley, E., Crosbie, N.D., Thomas, K. V., Mueller, J.F., 2018. Wastewater-based epidemiology biomarkers: Past, present and future. *TrAC - Trends Anal. Chem.* 105, 453–469. <https://doi.org/10.1016/j.trac.2018.06.004>
- Cihlar, T., Ray, A.S., 2010. Nucleoside and nucleotide HIV reverse transcriptase inhibitors: 25 years after zidovudine. *Antiviral Res.* 85, 39–58. <https://doi.org/10.1016/j.antiviral.2009.09.014>

- Cimetiere, N., Soutrel, I., Lemasle, M., Laplanche, A., Crocq, A., 2013. Standard addition method for the determination of pharmaceutical residues in drinking water by SPE-LC-MS/MS. *Environ. Technol.* 34, 3031–41. <https://doi.org/10.1080/09593330.2013.800563>
- Colombo, S., Beguin, A., Telenti, A., Biollaz, J., Buclin, T., 2005. Intracellular measurements of anti-HIV drugs indinavir, amprenavir, saquinavir, ritonavir, nelfinavir, lopinavir, atazanavir, efavirenz and nevirapine in peripheral blood mononuclear cells by liquid chromatography coupled to tandem mass spectrometry. *J. Chromatogr. B* 819, 259–276. <https://doi.org/10.1016/j.jchromb.2005.02.010>
- Creaser, C.S., Griffiths, J.M.R., Bramwell, C.J., Noreen, S., Hill, C.A., Thomas, C.L.P., 2004. Ion mobility spectrometry: A review. Part 1. Structural analysis by mobility measurement. *Analyst* 129, 984–994. <https://doi.org/10.1039/b404531a>
- Cuyckens, F., Hurkmans, R., Castro-perez, J.M., Leclercq, L., Mortishire-smith, R.J., 2009. Extracting metabolite ions out of a matrix background by combined mass defect, neutral loss and isotope filtration. *Rapid Commun. Mass Spectrom.* 23, 327–332. <https://doi.org/10.1002/rcm>
- De Clercq, E., 2009. Anti-HIV drugs: 25 compounds approved within 25 years after the discovery of HIV. *Int. J. Antimicrob. Agents* 33, 307–320. <https://doi.org/10.1016/j.ijantimicag.2008.10.010>
- de Villiers, A., Lestremau, F., Szucs, R., Gélébart, S., David, F., Sandra, P., 2006. Evaluation of ultra performance liquid chromatography. *J. Chromatogr. A* 1127, 60–69. <https://doi.org/10.1016/j.chroma.2006.05.071>
- de Voogt, P., van der Wielen, F.W.M., Govers, H.A.J., 2000. Freeze-drying brings about errors in polychlorinated biphenyl recovery calculations. *TrAC - Trends Anal. Chem.* 19, 292–299. [https://doi.org/10.1016/S0165-9936\(99\)00216-2](https://doi.org/10.1016/S0165-9936(99)00216-2)
- Desfontaine, V., Guillaume, D., Francotte, E., Nováková, L., 2015. Supercritical fluid chromatography in pharmaceutical analysis. *J. Pharm. Biomed. Anal.* 113, 56–71. <https://doi.org/10.1016/j.jpba.2015.03.007>
- Dispas, A., Jambo, H., André, S., Tyteca, E., Hubert, P., 2018. Supercritical fluid chromatography: A promising alternative to current bioanalytical techniques. *Bioanalysis* 10, 107–124. <https://doi.org/10.4155/bio-2017-0211>
- Dodds, J.N., Baker, E.S., 2019. Ion Mobility Spectrometry: Fundamental Concepts, Instrumentation, Applications, and the Road Ahead. *J. Am. Soc. Mass Spectrom.* 30, 2185–2195. <https://doi.org/10.1007/s13361-019-02288-2>
- Evard, H., Krueve, A., Leito, I., 2016. Tutorial on estimating the limit of detection using LC-MS analysis,



- part II: Practical aspects. *Anal. Chim. Acta* 942, 40–49. <https://doi.org/10.1016/j.aca.2016.08.042>
- Falås, P., Wick, A., Castronovo, S., Habermacher, J., Ternes, T.A., Joss, A., 2016. Tracing the limits of organic micropollutant removal in biological wastewater treatment. *Water Res.* 95, 240–249. <https://doi.org/10.1016/j.watres.2016.03.009>
- Funke, J., Prasse, C., Ternes, T.A., 2016. Identification of transformation products of antiviral drugs formed during biological wastewater treatment and their occurrence in the urban water cycle. *Water Res.* 98, 75–83. <https://doi.org/10.1016/j.watres.2016.03.045>
- Garcia-Ac, A., Segura, P.A., Viglino, L., Gagnon, C., Sauve, S., 2011. Comparison of APPI, APCI and ESI for the LC-MS/MS analysis of bezafibrate, cyclophosphamide, enalapril, methotrexate and orlistat in municipal wastewater. *J. Mass Spectrom.* 46, 383–390. <https://doi.org/10.1002/jms.1904>
- Grand-Guillaume Perrenoud, A., Boccard, J., Veuthey, J.L., Guillarme, D., 2012a. Analysis of basic compounds by supercritical fluid chromatography: Attempts to improve peak shape and maintain mass spectrometry compatibility. *J. Chromatogr. A* 1262, 205–213. <https://doi.org/10.1016/j.chroma.2012.08.091>
- Grand-Guillaume Perrenoud, A., Veuthey, J.L., Guillarme, D., 2014. The use of columns packed with sub-2  $\mu\text{m}$  particles in supercritical fluid chromatography. *TrAC - Trends Anal. Chem.* 63, 44–54. <https://doi.org/10.1016/j.trac.2014.06.023>
- Grand-Guillaume Perrenoud, A., Veuthey, J.L., Guillarme, D., 2012b. Comparison of ultra-high performance supercritical fluid chromatography and ultra-high performance liquid chromatography for the analysis of pharmaceutical compounds. *J. Chromatogr. A* 1266, 158–167. <https://doi.org/10.1016/j.chroma.2012.10.005>
- Hernández, F., Ibáñez, M., Bade, R., Bijlsma, L., Sancho, J. V., 2014. Investigation of pharmaceuticals and illicit drugs in waters by liquid chromatography-high-resolution mass spectrometry. *TrAC - Trends Anal. Chem.* 63, 140–157. <https://doi.org/10.1016/j.trac.2014.08.003>
- Hernández, F., Ibáñez, M., Gracia-Lor, E., Sancho, J. V., 2011. Retrospective LC-QTOF-MS analysis searching for pharmaceutical metabolites in urban wastewater. *J. Sep. Sci.* 34, 3517–3526. <https://doi.org/10.1002/jssc.201100540>
- Hinnenkamp, V., Balsaa, P., Schmidt, T.C., 2019. Quantitative screening and prioritization based on UPLC-IM-Q-TOF-MS as an alternative water sample monitoring strategy. *Anal. Bioanal. Chem.* 411, 6101–6110. <https://doi.org/10.1007/s00216-019-01994-w>
- Howdle, M.D., Eckers, C., Laures, A.M.F., Creaser, C.S., 2009. The Use of Shift Reagents in Ion

- Mobility-Mass Spectrometry: Studies on the Complexation of an Active Pharmaceutical Ingredient with Polyethylene Glycol Excipients. *J. Am. Soc. Mass Spectrom.* 20, 1–9.  
<https://doi.org/10.1016/j.jasms.2008.10.002>
- IUPAC, 2000. Harmonised guidelines for the in-house validation of methods of analysis (technical report) 1–34.
- Jafari Horestani, A.R., Jafari, M.T., Jazan, E., Mossaddegh, M., 2018. Effect of halide ions on secondary electrospray ionization-ion mobility spectrometry for the determination of TNT extracted by dispersive liquid-liquid microextraction. *Int. J. Mass Spectrom.* 433, 19–24.  
<https://doi.org/10.1016/j.ijms.2018.08.006>
- K'oreje, K.O., Demeestere, K., De Wispelaere, P., Vergeynst, L., Dewulf, J., Van Langenhove, H., 2012. From multi-residue screening to target analysis of pharmaceuticals in water: development of a new approach based on magnetic sector mass spectrometry and application in the Nairobi River basin, Kenya. *Sci. Total Environ.* 437, 153–64.  
<https://doi.org/10.1016/j.scitotenv.2012.07.052>
- K'oreje, K.O., Kandie, F.J., Vergeynst, L., Abira, M.A., Van Langenhove, H., Okoth, M., Demeestere, K., 2018. Science of the Total Environment Occurrence, fate and removal of pharmaceuticals, personal care products and pesticides in wastewater stabilization ponds and receiving rivers in the Nzoia Basin, Kenya. *Sci. Total Environ.* 637–638, 336–348.  
<https://doi.org/10.1016/j.scitotenv.2018.04.331>
- K'oreje, K.O., Vergeynst, L., Ombaka, D., De Wispelaere, P., Okoth, M., Van Langenhove, H., Demeestere, K., 2016. Occurrence patterns of pharmaceutical residues in wastewater, surface water and groundwater of Nairobi and Kisumu city, Kenya. *Chemosphere* 149, 238–244.  
<https://doi.org/10.1016/j.chemosphere.2016.01.095>
- Kauppila, T.J., Kersten, H., Benter, T., 2014. The Ionization Mechanisms in Direct and Dopant-Assisted Atmospheric Pressure Photoionization and Atmospheric Pressure Laser Ionization. *J. Am. Soc. Mass Spectrom.* 25, 1870–1881. <https://doi.org/10.1007/s13361-014-0988-7>
- Kruve, A., Rebane, R., Kipper, K., Oldekop, M.-L., Evard, H., Herodes, K., Ravio, P., Leito, I., 2015. Tutorial review on validation of liquid chromatography–mass spectrometry methods: Part I. *Anal. Chim. Acta* 870, 29–44. <https://doi.org/10.1016/j.aca.2015.02.017>
- Kumar, G.N., Jayanti, V.K., Johnson, M.K., Uchic, J., Thomas, S., Lee, R.D., Grabowski, B.A., Sham, H.L., Kempf, D.J., Denissen, J.F., Marsh, K.C., Sun, E., Roberts, S.A., 2004. Metabolism and disposition of the HIV-1 protease inhibitor lopinavir (ABT-378) given in combination with ritonavir in rats, dogs, and humans. *Pharm. Res.* 21, 1622–30.

- Laaniste, A., Leito, I., Kruve, A., 2019. ESI outcompetes other ion sources in LC/MS trace analysis. *Anal. Bioanal. Chem.* 411, 3533–3542. <https://doi.org/10.1007/s00216-019-01832-z>
- Lanucara, F., Holman, S.W., Gray, C.J., Evers, C.E., 2014. The power of ion mobility-mass spectrometry for structural characterization and the study of conformational dynamics. *Nat. Chem.* 6, 281–294. <https://doi.org/10.1038/nchem.1889>
- Li, W., Liu, Y., Duan, J., Saint, C.P., Mulcahy, D., 2015. The role of methanol addition to water samples in reducing analyte adsorption and matrix effects in liquid chromatography-tandem mass spectrometry. *J. Chromatogr. A* 1389, 76–84. <https://doi.org/10.1016/j.chroma.2015.02.044>
- Lian, R., Zhang, F., Zhang, Y., Wu, Z., Ye, H., Ni, C., Lv, X., Guo, Y., 2018. Ion mobility derived collision cross section as an additional measure to support the rapid analysis of abused drugs and toxic compounds using electrospray ion mobility time-of-flight mass spectrometry. *Anal. Methods* 10, 749–756. <https://doi.org/10.1039/C7AY02808C>
- Little, J.N., Fallick, G.J., 1975. New considerations in detector-application relationships. *J. Chromatogr. A*, 112, 389–397. [https://doi.org/10.1016/S0021-9673\(00\)99971-0](https://doi.org/10.1016/S0021-9673(00)99971-0)
- Luo, Y., Guo, W., Ngo, H.H., Nghiem, L.D., Hai, F.I., Zhang, J., Liang, S., Wang, X.C., 2014. A review on the occurrence of micropollutants in the aquatic environment and their fate and removal during wastewater treatment. *Sci. Total Environ.* 473–474, 619–641. <https://doi.org/10.1016/j.scitotenv.2013.12.065>
- Luque De Castro, M.D., Izquierdo, A., 1990. Lyophilisation: a useful approach to the automation of analytical processes? *J. Automat. Chem.* 12, 267–279. <https://doi.org/10.1155/S1463924690000347>
- Madikizela, L.M., Ncube, S., Chimuka, L., 2020. Analysis, occurrence and removal of pharmaceuticals in African water resources: A current status. *J. Environ. Manage.* 253, 109741. <https://doi.org/10.1016/j.jenvman.2019.109741>
- Magnusson, O., 2014. *Eurachem Guide: The Fitness for Purpose of Analytical Methods – A Laboratory Guide to Method Validation and Related Topics*, Eurachem Guide.
- Martínez Bueno, M.J., Uclés, S., Hernando, M.D., Fernández-Alba, A.R., 2011. Development of a solvent-free method for the simultaneous identification/quantification of drugs of abuse and their metabolites in environmental water by LC-MS/MS. *Talanta* 85, 157–166. <https://doi.org/10.1016/j.talanta.2011.03.051>
- Martins, M.L., Rizzetti, T.M., Kemmerich, M., Saibt, N., Prestes, O.D., Adaime, M.B., Zanella, R., 2016. Dilution standard addition calibration: A practical calibration strategy for multiresidue

- organic compounds determination. *J. Chromatogr. A* 1460, 84–91.  
<https://doi.org/10.1016/j.chroma.2016.07.013>
- Mirochnick, M., Thomas, T., Capparelli, E., Zeh, C., Holland, D., Masaba, R., Odhiambo, P., Fowler, M.G., Weidle, P.J., Thigpen, M.C., 2009. Antiretroviral concentrations in breast-feeding infants of mothers receiving highly active antiretroviral therapy. *Antimicrob. Agents Chemother.* 53, 1170–1176. <https://doi.org/10.1128/AAC.01117-08>
- Mirzaei, A., Chen, Z., Haghghat, F., Yerushalmi, L., 2017. Removal of pharmaceuticals from water by homo/heterogeneous Fenton-type processes – A review. *Chemosphere* 174, 665–688.  
<https://doi.org/10.1016/j.chemosphere.2017.02.019>
- Mlunguza, Y.N., Ncube, S., Mahlambi, N.P., Chimuka, L., Madikizela, L.M., 2020. Determination of selected antiretroviral drugs in wastewater, surface water and aquatic plants using hollow fibre liquid phase microextraction and liquid chromatography - tandem mass spectrometry. *J. Hazard. Mater.* 382, 121067. <https://doi.org/10.1016/j.jhazmat.2019.121067>
- Moldoveanu, S., David, V., 2015. Solid-Phase Extraction. *Modern Sample Preparation for Chromatography*, Modern Sample Preparation for Chromatography. Elsevier  
<https://doi.org/10.1016/B978-0-444-54319-6.00007-4>
- Mosekiemang, T.T., Stander, M.A., de Villiers, A., 2019. Simultaneous quantification of commonly prescribed antiretroviral drugs and their selected metabolites in aqueous environmental samples by direct injection and solid phase extraction liquid chromatography - Tandem mass spectrometry. *Chemosphere* 220, 983–992. <https://doi.org/10.1016/j.chemosphere.2018.12.205>
- Mtolo, S.P., Mahlambi, P.N., Madikizela, L.M., 2019. Synthesis and application of a molecularly imprinted polymer in selective solid-phase extraction of efavirenz from water. *Water Sci. Technol.* 79, 1–10. <https://doi.org/10.2166/wst.2019.054>
- Muriuki, C., Kairigo, P., Home, P., Ngumba, E., Raude, J., Gachanja, A., Tuhkanen, T., 2020. Mass loading, distribution, and removal of antibiotics and antiretroviral drugs in selected wastewater treatment plants in Kenya. *Sci. Total Environ.* 743, 140655.  
<https://doi.org/10.1016/j.scitotenv.2020.140655>
- Mutlib, E., Chen, H., Nemeth, G.A., Markwalder, J. a, Seitz, S.P., Gan, L.S., Christ, D.D., 1999. Identification and characterization of efavirenz metabolites by liquid chromatography/mass spectrometry and high field NMR: species differences in the metabolism of efavirenz. *Drug Metab. Dispos.* 27, 1319–1333.
- Nannou, C., Ofrydopoulou, A., Evgenidou, E., Heath, D., Heath, E., Lambropoulou, D., 2020. Antiviral drugs in aquatic environment and wastewater treatment plants: A review on occurrence, fate,

- removal and ecotoxicity. *Sci. Total Environ.* <https://doi.org/10.1016/j.scitotenv.2019.134322>
- Nannou, C., Ofrydopoulou, A., Evgenidou, E., Heath, D., Heath, E., Lambropoulou, D., 2019. Analytical strategies for the determination of antiviral drugs in the aquatic environment. *Trends Environ. Anal. Chem.* 24, e00071. <https://doi.org/10.1016/j.teac.2019.e00071>
- Ncube, S., Madikizela, L.M., Chimuka, L., Nindi, M.M., 2018. Environmental fate and ecotoxicological effects of antiretrovirals: A current global status and future perspectives. *Water Res.* 145, 231–247. <https://doi.org/10.1016/j.watres.2018.08.017>
- Ng, K.T., Rapp-Wright, H., Egli, M., Hartmann, A., Steele, J.C., Sosa-Hernández, J.E., Melchor-Martínez, E.M., Jacobs, M., White, B., Regan, F., Parra-Saldivar, R., Couchman, L., Halden, R.U., Barron, L.P., 2020. High-throughput multi-residue quantification of contaminants of emerging concern in wastewaters enabled using direct injection liquid chromatography-tandem mass spectrometry. *J. Hazard. Mater.* 398, 122933. <https://doi.org/10.1016/j.jhazmat.2020.122933>
- Ngumba, E., 2018. Occurrence and Control of Selected Antibiotics and Antiretroviral Drugs in Urban Hydrological Cycles. PhD Thesis, Jyväskylä University Printing House, Jyväskylä.
- Ngumba, E., Gachanja, A., Tuhkanen, T., 2016a. Occurrence of selected antibiotics and antiretroviral drugs in Nairobi River Basin, Kenya. *Sci. Total Environ.* 539, 206–213. <https://doi.org/10.1016/j.scitotenv.2015.08.139>
- Ngumba, E., Kosunen, P., Gachanja, A., Tuhkanen, T., 2016b. A multiresidue analytical method for trace level determination of antibiotics and antiretroviral drugs in wastewater and surface water using SPE-LC-MS/MS and matrix-matched standards. *Anal. Methods* 8, 6720–6729. <https://doi.org/10.1039/c6ay01695b>
- Nováková, L., Grand-Guillaume Perrenoud, A., Francois, I., West, C., Lesellier, E., Guillarme, D., 2014. Modern analytical supercritical fluid chromatography using columns packed with sub-2 $\mu$ m particles: A tutorial. *Anal. Chim. Acta* 824, 18–35. <https://doi.org/10.1016/j.aca.2014.03.034>
- Ort, C., Lawrence, M.G., Reungoat, J., Mueller, J.F., 2010. Sampling for PPCPs in Wastewater Systems: Comparison of Different Sampling Modes and Optimization Strategies. *Environ. Sci. Technol.* 44, 6289–6296. <https://doi.org/10.1021/es100778d>
- Paglia, G., Angel, P., Williams, J.P., Richardson, K., Olivos, H.J., Thompson, J.W., Menikarachchi, L., Lai, S., Walsh, C., Moseley, A., Plumb, R.S., Grant, D.F., Palsson, B.O., Langridge, J., Geromanos, S., Astarita, G., 2015. Ion mobility-derived collision cross section as an additional measure for lipid fingerprinting and identification. *Anal. Chem.* 87, 1137–1144. <https://doi.org/10.1021/ac503715v>

- Paredes, L., Omil, F., Lema, J.M., Carballa, M., 2018. What happens with organic micropollutants during UV disinfection in WWTPs? A global perspective from laboratory to full-scale. *J. Hazard. Mater.* 342, 670–678. <https://doi.org/10.1016/j.jhazmat.2017.08.075>
- Parr, M.K., Wüst, B., Teubel, J., Joseph, J.F., 2018. Splitless hyphenation of SFC with MS by APCI, APPI, and ESI exemplified by steroids as model compounds. *J. Chromatogr. B Anal. Technol. Biomed. Life Sci.* 1091, 67–78. <https://doi.org/10.1016/j.jchromb.2018.05.017>
- Peng, X., Wang, C., Zhang, K., Wang, Z., Huang, Q., Yu, Y., Ou, W., 2014. Profile and behavior of antiviral drugs in aquatic environments of the Pearl River Delta, China. *Sci. Total Environ.* 466–467, 755–761. <https://doi.org/10.1016/j.scitotenv.2013.07.062>
- Petrovic, M., Farré, M., de Alda, M.L., Perez, S., Postigo, C., Köck, M., Radjenovic, J., Gros, M., Barcelo, D., 2010. Recent trends in the liquid chromatography–mass spectrometry analysis of organic contaminants in environmental samples. *J. Chromatogr. A* 1217, 4004–4017. <https://doi.org/10.1016/j.chroma.2010.02.059>
- Prasse, C., Schlusener, M.P., Schulz, R., Ternes, T.A., 2010. Antiviral drugs in wastewater and surface waters: a new pharmaceutical class of environmental relevance. *Environ. Sci. Technol.* 44, 1728–1735. <https://doi.org/10.1021/es903216p>
- Prichard, L., Barwick, V., 2003. Preparation of Calibration Curves: A Guide to Best Practice. Technical Report, LGC/VAM/2003/032. <https://doi.org/10.13140/RG.2.2.36338.76488>
- Ramirez, C.E., Bellmund, S., Gardinali, P.R., 2014. A simple method for routine monitoring of glyphosate and its main metabolite in surface waters using lyophilisation and LC-FLD + MS/MS. Case study: Canals with influence on Biscayne National Park. *Sci. Total Environ.* 496, 389–401. <https://doi.org/10.1016/j.scitotenv.2014.06.118>
- Rimayi, C., Chimuka, L., Gravell, A., Fones, G.R., Mills, G.A., 2019. Use of the Chemcatcher® passive sampler and time-of-flight mass spectrometry to screen for emerging pollutants in rivers in Gauteng Province of South Africa. *Environ. Monit. Assess.* 191. <https://doi.org/10.1007/s10661-019-7515-z>
- Rimayi, C., Odusanya, D., Weiss, J.M., de Boer, J., Chimuka, L., 2018. Contaminants of emerging concern in the Hartbeespoort Dam catchment and the uMngeni River estuary 2016 pollution incident, South Africa. *Sci. Total Environ.* 627, 1008–1017. <https://doi.org/10.1016/j.scitotenv.2018.01.263>
- Robb, D.B., Covey, T.R., Bruins, A.P., 2000. Atmospheric pressure photoionization: An ionization method for liquid chromatography-mass spectrometry. *Anal. Chem.* 72, 3653–3659. <https://doi.org/10.1021/ac0001636>

- Rochat, B., 2018. Quantitative and Qualitative LC-High-Resolution MS: The Technological and Biological Reasons for a Shift of Paradigm, in: *Recent Advances in Analytical Chemistry*. IntechOpen, London.
- Rochat, B., 2016. From targeted quantification to untargeted metabolomics: Why LC-high-resolution-MS will become a key instrument in clinical labs. *TrAC - Trends Anal. Chem.* 84, 151–164. <https://doi.org/10.1016/j.trac.2016.02.009>
- Romand, S., Rudaz, S., Guillarme, D., 2016. Separation of substrates and closely related glucuronide metabolites using various chromatographic modes. *J. Chromatogr. A* 1435, 54–65. <https://doi.org/10.1016/j.chroma.2016.01.033>
- Ross, M.S., Wong, C.S., 2010. Comparison of electrospray ionization, atmospheric pressure photoionization, and anion attachment atmospheric pressure photoionization for the analysis of hexabromocyclododecane enantiomers in environmental samples. *J. Chromatogr. A* 1217, 7855–7863. <https://doi.org/10.1016/j.chroma.2010.09.083>
- Rossmann, J., Gurke, R., Renner, L.D., Oertel, R., Kirch, W., 2015. Evaluation of the matrix effect of different sample matrices for 33 pharmaceuticals by post-column infusion. *J. Chromatogr. B* 1000, 84–94. <https://doi.org/10.1016/j.jchromb.2015.06.019>
- Russo, D., Siciliano, A., Guida, M., Andreozzi, R., Reis, N.M., 2018. Removal of antiretroviral drugs stavudine and zidovudine in water under UV 254 and UV 254 / H<sub>2</sub>O<sub>2</sub> processes : Quantum yields, kinetics and ecotoxicology assessment. *J. Hazard. Mater.* 349, 195–204. <https://doi.org/10.1016/j.jhazmat.2018.01.052>
- Salgot, M., Folch, M., Unit, S.S., 2018. Wastewater treatment and water reuse. *Curr. Opin. Environ. Sci. Heal.* 2, 64–74. <https://doi.org/10.1016/j.coesh.2018.03.005>
- SANTE 2015, 2015. Guidance document on analytical quality control and method validation procedures for pesticides residues analysis in food and feed. SANTE/11945/2015, Legal Deposit.
- Schoeman, C., Dlamini, M., Okonkwo, O.J., 2017. The impact of a Wastewater Treatment Works in Southern Gauteng, South Africa on efavirenz and nevirapine discharges into the aquatic environment. *Emerg. Contam.* 3, 95–106. <https://doi.org/10.1016/j.emcon.2017.09.001>
- Shaaban, H., Górecki, T., 2012. Fast ultrahigh performance liquid chromatographic method for the simultaneous determination of 25 emerging contaminants in surface water and wastewater samples using superficially porous sub-3 µm particles as an alternative to fully porous sub-2 µm partic. *Talanta* 100, 80–89. <https://doi.org/10.1016/j.talanta.2012.08.010>

- Stephan, S., Hippler, J., Kohler, T., Deeb, A.A., Schmidt, T.C., Schmitz, O.J., 2016. Contaminant screening of wastewater with HPLC-IM-qTOF-MS and LC+LC-IM-qTOF-MS using a CCS database. *Anal. Bioanal. Chem.* 408, 6545–6555. <https://doi.org/10.1007/s00216-016-9820-5>
- Sun, S., Baker, A., Chen, P. 2011. Profiling the indole alkaloids in yohimba bark with ultra-performance liquid chromatography couple with ion mobility quadrupole time-of-flight mass spectrometry. *Rapid Commun. Mass Spectrom.* 25, 2591-2602. <https://doi.org/10.1002/rcm.5158>
- Svan, A., Hedeland, M., Arvidsson, T., Pettersson, C.E., 2018. The differences in matrix effect between supercritical fluid chromatography and reversed phase liquid chromatography coupled to ESI/MS. *Anal. Chim. Acta* 1000, 163–171. <https://doi.org/10.1016/j.aca.2017.10.014>
- Syslová, K., Rambousek, L., Kuzma, M., Najmanová, V., Bubeníková-Valešová, V., Šlamberová, R., Kačer, P., 2011. Monitoring of dopamine and its metabolites in brain microdialysates: Method combining freeze-drying with liquid chromatography-tandem mass spectrometry. *J. Chromatogr. A* 1218, 3382–3391. <https://doi.org/10.1016/j.chroma.2011.02.006>
- Terzopoulou, Z., Papageorgiou, M., Kyzas, G.Z., Bikiaris, D.N., Lambropoulou, D.A., 2016. Preparation of molecularly imprinted solid-phase microextraction fiber for the selective removal and extraction of the antiviral drug abacavir in environmental and biological matrices. *Anal. Chim. Acta* 913, 63–75. <https://doi.org/10.1016/j.aca.2016.01.059>
- Tiller, P.R., Yu, S., Bateman, K.P., Castro-Perez, J., McIntosh, I.S., Kuo, Y., Baillie, T.A., 2008a. Fractional mass filtering as a means to assess circulating metabolites in early human clinical studies. *Rapid Commun. Mass Spectrom.* 22, 3510–3516. <https://doi.org/10.1002/rcm>
- Tiller, P.R., Yu, S., Castro-Perez, J., Fillgrove, K.L., Baillie, T., 2008b. High-throughput, accurate mass liquid chromatography/ tandem mass spectrometry on a quadrupole time-of-flight system as a ‘first-line’ approach for metabolite identification studies. *Rapid Commun. Mass Spectrom.* 22, 1053–1061. <https://doi.org/10.1002/rcm>
- US Environmental Protection Agency, 2012. Estimation Programs Interface Suite™ for Microsoft® Windows.
- Veal, G.J., Back, D.J., 1995. Metabolism of zidovudine. *Gen. Pharmacol.* 26, 1469–1475. [https://doi.org/10.1016/0306-3623\(95\)00047-X](https://doi.org/10.1016/0306-3623(95)00047-X)
- Vella, S., Schwartländer, B., Sow, S.P., Eholie, S.P., Murphy, R.L., 2012. The history of antiretroviral therapy and of its implementation in resource-limited areas of the world. *Aids* 26, 1231–1241. <https://doi.org/10.1097/QAD.0b013e3283552/a3>
- Vieno, N., Tuhkanen, T., Kronberg, L., 2007. Elimination of pharmaceuticals in sewage treatment



- plants in Finland. *Water Res.* 41, 1001–1012. <https://doi.org/10.1016/j.watres.2006.12.017>
- Wood, T.P., Basson, A.E., Duvenage, C., Rohwer, E.R., 2016. The chlorination behaviour and environmental fate of the antiretroviral drug nevirapine in South African surface water. *Water Res.* 104, 349–360. <https://doi.org/10.1016/j.watres.2016.08.038>
- Wood, T.P., Duvenage, C.S.J., Rohwer, E., 2015. The occurrence of anti-retroviral compounds used for HIV treatment in South African surface water. *Environ. Pollut.* 199, 235–243. <https://doi.org/10.1016/j.envpol.2015.01.030>
- Wooding, M., Rohwer, E.R., Naude, Y., 2017. Determination of endocrine disrupting chemicals and antiretroviral compounds in surface water: A disposable sorptive sampler with comprehensive gas chromatography -Time-of-flight mass spectrometry and large volume injection with ultra-high performance. *J. Chromatogr. A* 1496, 122–132. <https://doi.org/10.1016/j.chroma.2017.03.057>
- World Health Organization, UNICEF, UNAIDS, 2013. Global update on HIV treatment 2013 : Results, Impact and Opportunities, Global update on HIV treatment 2013: results, impact and opportunities. [https://doi.org/ISBN 978 92 4 150573 4](https://doi.org/ISBN%20978%2092%204%20150573%204)
- Zhang, H., Gonzales, G.B., Beloglazova, N. V., De Saeger, S., Shen, J., Zhang, S., Yang, S., Wang, Z., 2020. Development of a validated direct injection-liquid chromatographic tandem mass spectrometric method under negative electrospray ionization for quantitation of nine microcystins and nodularin-R in lake water. *J. Chromatogr. A* 1609, 460432. <https://doi.org/10.1016/j.chroma.2019.460432>
- Zhang, H., Zhang, D., Ray, K., 2003. A software filter to remove interference ions from drug metabolites in accurate mass liquid chromatography/mass spectrometric analyses. *J. Mass Spectrom.* 38, 1110–1112. <https://doi.org/10.1002/jms.521>
- Zhang, H., Zhang, D., Ray, K., Zhu, M., 2009a. Mass defect filter technique and its applications to drug metabolite identification by high-resolution mass spectrometry. *J. Mass Spectrom.* 44, 999–1016. <https://doi.org/10.1002/jms.1610>
- Zhang, H., Zhang, D., Ray, K., Zhu, M., 2009b. Mass defect filter technique and its applications to drug metabolite identification by high-resolution mass spectrometry. *J. Mass Spectrom.* 44, 999–1016. <https://doi.org/10.1002/jms.1610>
- Zhang, H., Zhu, M., Ray, K.L., Ma, L., Zhang, D., 2008. Mass defect profiles of biological matrices and the general applicability of mass defect filtering for metabolite detection. *Rapid Commun. Mass Spectrom.* 22, 2082–2088. <https://doi.org/10.1002/rcm.3585>

Declaration with signatures in possession of candidate and supervisor.

**Declaration by the candidate:**

Regarding **Chapter 3**, the nature and scope of my contribution were as follows:

Nature of contribution	Extent of contribution (%)
Performed the experiments, data analysis, co-wrote paper	60

The following co-authors have contributed to **Chapter 3**:

Name	E-mail address	Nature of contribution	Extent of contribution (%)
Maria A. Stander	<a href="mailto:lcms@sun.ac.za">lcms@sun.ac.za</a>	Assisted with experimental set-up and data manipulation; editorial input	15
André de Villiers	<a href="mailto:ajdevill@sun.ac.za">ajdevill@sun.ac.za</a>	Co-wrote paper	25



Signature of candidate:

Date: 28<sup>th</sup> February 2021

**Declaration by co-authors:**

The undersigned confirm that:

1. The declaration above accurately reflects the nature and extent of the contributions of the candidate and the co-authors to **Chapter 3**,
2. No other authors contributed to **Chapter 3** besides those specified above, and
3. Potential conflicts of interest have been revealed to all interested parties and that the necessary changes have been made to use the material in Chapter 3 of this dissertation.

Signature	Institutional affiliation	Date
	Stellenbosch University	1 October 2020
	Stellenbosch University	24 February 2021

## Chapter 3

---

**Simultaneous quantification of commonly prescribed antiretroviral drugs and their selected metabolites in aqueous environmental samples by direct injection and solid phase extraction liquid chromatography - tandem mass spectrometry<sup>#</sup>**

<sup>#</sup> This chapter has been published in Chemosphere 2019, 220, 983-992

## Abstract

The widespread implementation of antiretroviral therapy medication has made antiretroviral drugs (ARVDs) a significant pharmaceutical class in regions of high HIV infection rates. However, relatively little is known regarding the environmental occurrence of these emerging contaminants, and this is especially true for their metabolites. In this work, we report analytical methods to study the simultaneous occurrence of a range of common ARVDs and some of their known metabolites in surface water and wastewater. A novel direct injection liquid chromatography-tandem mass spectrometry (LC-MS/MS) method is reported for the analysis of ARVDs of different therapeutic classes and their selected metabolites in wastewater samples. In addition, a solid phase extraction (SPE) procedure was developed for pre-concentration of ARVs and metabolites from surface water samples. The respective methods proved suitable for the quantitative analysis of six parent ARVDs from three ARV classes, as well as three metabolites. Method validation showed average recoveries of 86% for the direct injection method, and 64% for the SPE method. With the exception of zidovudine and the metabolites of zidovudine and ritonavir, all target ARVDs were detected in wastewater samples from two wastewater treatment plants in the Western Cape, South Africa. Higher concentrations were generally measured in influent compared to effluent samples, in the dry compared to the wet season as well as in chlorinated compared to *uv*-irradiated effluents. This study contributes for the first-time quantitative data on the environmental occurrence of the known metabolites of nevirapine (12-hydroxy-nevirapine) and efavirenz (8,14-dihydroxy-efavirenz).

### 3.1. Introduction

The link between excretion of pharmaceutical compounds and their environmental occurrence has been well established (Funke *et al.*, 2016; Vieno *et al.*, 2005; Wood *et al.*, 2015). That is, after ingestion and by the end of within-body therapeutic processes, unaltered compounds and their metabolites are eliminated from the body via excreta and enter the sewer system. This suggests that wastewater may contain community-scale information on trends in pharmaceutical consumption, at least for compounds which are not excessively transformed and for which the metabolites are relatively stable (Brewer and Lunte, 2015). Wastewater analysis therefore potentially provides a non-invasive means, complementary to conventional methods, of obtaining community-level health information (Banta-Green *et al.*, 2016). Furthermore, information on the levels of pharmaceuticals and their metabolites entering the environment through wastewater effluent is essential to assess their potential health and environmental impacts.

Antiretroviral drugs (ARVDs) are an emerging class of environmental contaminants (Abafe *et al.*, 2018; K'oreje *et al.*, 2018, 2016, Ngumba *et al.*, 2016a, 2016b; Prasse *et al.*, 2010), the environmental impact of which is still relatively unknown, despite their high consumption rates in the past two decades (Andrade *et al.*, 2011). Until recently, analytical data for ARVDs were largely limited to human secretions such as plasma, saliva, meconium *etc.* (Himes *et al.*, 2013). Indeed, compared to more common pharmaceuticals, data on the occurrence of ARVDs in wastewater and environmental samples are still relatively limited (Funke *et al.*, 2016; K'oreje *et al.*, 2016, 2012; Ncube *et al.*, 2018; Ngumba *et al.*, 2016a, 2016b; Prasse *et al.*, 2010; Wood *et al.*, 2016, 2015). A standard dose of typical antiretroviral therapy (ART) medication contains active compounds in the range of 300-600 mg, which, taken two-three times daily implies approximately 600-1800 mg of the active compound(s) per patient per day (World Health Organization, 2015). If the number of patients on therapy is considered, it is reasonable to suspect that, despite some analyte loss due to their metabolism and transformation, ARVDs contribute significantly to the overall pharmaceutical load in wastewater.

Significantly, ART medication may contain constituents of one or more ARV classes, *i.e.* nucleoside reverse transcriptase inhibitors (NRTI), non-nucleoside reverse transcriptase inhibitors (*n*NRTI) and protease inhibitors (PI) (World Health Organization, 2015). For example, the ART formulation Trivenz® contains 600 mg efavirenz (*n*NRTI), 200 mg emtricitabine and 300 mg tenofovir disoproxil fumarate (both NRTIs). This emphasises the need for analytical methods capable of simultaneous detection of all the therapeutic classes of ARVDs. However, analytical methods used in previous studies were mostly focused on a few selected target analytes of specific ARV (K'oreje *et al.*, 2018, 2016, 2012; Ngumba *et al.*, 2016a, 2016b; Wood *et al.*, 2015), with some recent exceptions (Ncube *et al.*, 2018; Abafe *et al.*, 2018). In light of this, one of the goals of the present work was to develop a multi-residue direct injection method capable of the determination of multiclass ARVDs and selected of their metabolites in a single analysis.

Like other pharmaceuticals, NRTI and *n*NRTI ARVDs are metabolised via phase I and II metabolic processes, which entail hydroxylation and excretion, or further glucuronidation of hydroxylated metabolites prior to excretion (Aouri *et al.*, 2016; Deng *et al.*, 2015; Riska *et al.*, 1999). For instance, the NRTI zidovudine is mostly metabolised to zidovudine-glucuronide, which is found in human urine with the parent compound (Veal and Back, 1995). While nevirapine and efavirenz, both *n*NRTIs, are either excreted unchanged or metabolised into several hydroxylated metabolites, which may be further glucuronidated before excretion (Deng *et al.*, 2015; Riska *et al.*, 1999). In contrast, the PI class is typically metabolised to produce simpler fragments of the parent compounds (Andrade *et al.*, 2011). For example, ritonavir is metabolised into several non-glucuronide derivatives, of which the main metabolite is desthiazolylmethyloxycarbonyl ritonavir (Denissen *et al.*, 1997). To our knowledge, there are no documented data regarding the levels of ARV metabolites in wastewater. Inclusion of these human biomarkers in wastewater analysis will confirm human consumption as the source of ARV contamination, eliminating other potential sources such as disposal of unused drugs and inputs from industrial waste (Funke *et al.*, 2016). Expanding the scope of environmental analysis of ARVDs to include their metabolites is therefore relevant to supplement data reported in previous studies.

In addition to the scarcity of commercially available standards for ARVD metabolites, complicated method development for target analytes of diverse physico-chemical properties likely contributes to the limited data on the environmental occurrence of ARVDs and their metabolites. This is also true for liquid chromatography-tandem mass spectrometry (LC-MS/MS), the method of choice for such analyses. Sample preparation by solid phase extraction (SPE) is commonly used to overcome matrix effects for such analyses, although the selectivity of the technique can be a drawback when analysing of compounds with diverse properties (Backe and Field, 2012). For instance, NRTIs and their metabolites are relatively polar, and therefore poorly retained on reversed phase SPE beds, unlike PIs and some *n*NRTIs (Backe and Field, 2012). It is therefore challenging to devise methods for the simultaneous extraction of the diverse therapeutic classes of ARVDs in a single step (Wood *et al.*, 2015). Since ARVDs commonly occur at  $\mu\text{g/L}$  levels in wastewater samples (Abafe *et al.*, 2018; K'oreje *et al.*, 2018, 2012; Ngumba *et al.*, 2016a; Wood *et al.*, 2016) – well within the detection capabilities of modern LC-MS/MS instruments – SPE sample preparation may result in over-amplification of some analytes (Backe and Field, 2012), and poor recoveries for more polar compounds (K'oreje *et al.*, 2012). Large volume direct injection has successfully been applied for wastewater analysis, including for ARVDs (Funke *et al.*, 2016; Wooding *et al.*, 2017), although the success of this approach depends on the sensitivity and selectivity of the MS instrumentation and the requirement of minimising matrix effects.

Considering the above, the objective of this study was to develop two separate LC-MS/MS methods for the simultaneous analysis of commonly prescribed multiclass ARVDs and their metabolites in wastewater and surface water samples: a direct injection approach for wastewater samples, and a modified SPE pre-concentration method for the analysis of surface water. The applicability of the

developed methods is demonstrated for the analysis of non-sewage-impacted surface water and municipal wastewater samples.

## 3.2. Materials and methods

### 3.2.1 Reagents and chemicals

All analytical standards (**Figure S3.1, Supplementary Information (SI)**) were of  $\geq 99\%$  purity. Standards for efavirenz (EFZ), emtricitabine (FTC), lamivudine (3TC), nevirapine (NVP), ritonavir (RTV), zidovudine (ZDV) and zidovudine glucuronide (ZDVG) were purchased from ClearSynth (Mumbai, India), whereas 8,14-dihydroxy-efavirenz (EFVM), 12-hydroxy-nevirapine (NVPM), desthiazolylmethyloxycarbonyl ritonavir (RTVM) and nevirapine-D<sub>3</sub> (NVP-D<sub>3</sub>, the isotopically labelled internal standard (ILIS)) were purchased from Toronto Research Chemicals (Toronto, Canada). All solvents were of HPLC grade or better, and were obtained from ROMIL (Waterbeach, Cambridge). Deionised water was obtained from a Millipore Direct Q3 system (Millipore, Milford, MA, USA).

### 3.2.2 Sample collection

Samples were collected from two municipal wastewater treatment plants (WWTPs) with diverse demographic catchment areas and different treatment processes in the Western Cape province of South Africa (**Table S3.1**). Sampling was timed to coincide with high daily inflows (~14:30-15:30 pm) at each plant to maximise chances of acquiring representative samples of the respective catchment areas. For evaluation of seasonal effects on ARV mass loads, two sampling excursions were undertaken in April and July 2016 to coincide with the dry and wet seasons, respectively (**Section 3.6.1**). Samples from a third sampling excursion to both WWTPs in September 2016 were used to evaluate the efficiency of tertiary-stage treatment processes (chlorination versus *uv*-irradiation, **Table 3.1**). Finally, to evaluate the effect of the extreme drought experienced in the Western Cape in 2016-2018, a fourth set of samples were collected from the domestic WWTP (WWTP1, **Table S3.1**) during April 2018, at the peak of stern water restrictions.

For simplicity and viability reasons, grab sampling was used (Ort *et al.*, 2010). Since grab sampling does not provide samples representative of spatial-temporal trends, composite samples (500 mL) were collected at ~15 min time intervals over 2 h and pooled into a 5 L precleaned conical flask. The homogenised composite samples were then aliquoted into 500 mL amber bottles cleaned with hot water and methanol and heated ( $\pm 50^{\circ}\text{C}$ ) prior to sampling. Bottles were rinsed with the sampled water and filled with minimal headspace void. Raw wastewater samples were collected at the mixing reservoir after the grit removal stage, whereas tertiary stage-treated effluent samples (*i.e.* biologically or membrane bioreactor (MBR) treated, either chlorinated or *uv*-irradiated), were collected at appropriate sampling points or at the discharge spillway (**Figure S3.2**). The surface water sample was collected from a creek in the Western Cape, South Africa, at a remote point considered free from human activity.

All samples were transported to the lab in an insulated box where they were vacuum filtered using 2.7  $\mu\text{m}$  (47 mm) followed by 0.45  $\mu\text{m}$  (25 mm) GF/D glass microfibre filters (Whatman, Maidstone, England) and kept at  $-4^{\circ}\text{C}$  without addition of preservatives prior to processing within 24 h.

### 3.2.3 Instrumentation and experimental conditions

Analyses were performed on an ACQUITY™ ultra performance LC system, equipped with sample organizer, solvent manager and column oven modules (Waters, Milford, USA). Separations were performed using an HSS T3 (1.8  $\mu\text{m}$ , 150  $\times$  2.1 mm) column (Waters) thermostatted to  $35^{\circ}\text{C}$ . The mobile phase gradient started at 98% A (0.1% formic acid) and 2% B (acetonitrile), maintained for 0.2 min and increased to 98% B in 8 min, maintained for 0.5 min before returning to the initial conditions in 0.5 min for a 3 min re-equilibration period. The flow rate was 0.3 mL/min and the injection volume 2  $\mu\text{L}$ .

The LC was connected to a Xevo TQ-S triple-quadrupole MS equipped with an ESI source (Waters). MS settings were optimised to achieve the best sensitivity in both positive and negative ESI modes. The cone and desolvation gas ( $\text{N}_2$ ) flows were 150 and 800 L/h, respectively, while the collision gas (Ar) flow rate was 0.15 mL/min. The capillary and cone voltages were 3.7 kV and 30 V, respectively, and the source and desolvation temperatures  $150^{\circ}\text{C}$  and  $350^{\circ}\text{C}$ , respectively. Instrument control and data acquisition were performed using MassLynx v4.1, and data were processed using TargetLynx software (Waters). Multiple reaction monitoring (MRM) acquisition parameters were optimised based on intensities of two transitions for each analyte and are summarised in **Table S3.2**.

### 3.2.4 Quantitation and method validation

A working standard mixture of all standards at 20  $\mu\text{g}/\text{mL}$  was prepared by diluting 1 mL of 100  $\mu\text{g}/\text{mL}$  methanol-dissolved stock solutions to 5 mL with deionised water. A NVP-D<sub>3</sub> (ILIS) stock solution of 10  $\mu\text{g}/\text{mL}$  was prepared in acetonitrile, and a working solution (5 mL, 0.1  $\mu\text{g}/\text{mL}$ ) by 1:99 dilution with acetonitrile-water (2:98, v/v). Serial dilution of the working standard mixture (20  $\mu\text{g}/\text{mL}$ ) with equal proportions (v/v) of either deionised water or methanol-water (3:7, v/v) provided the predominantly aqueous and the methanol-water (3:7, v/v) batches of standards at 11 concentration levels between 1.220 and 1250 ng/mL. Calibration standards in the concentration range 0.610 – 625 ng/mL were prepared by dispensing 0.25 mL aliquots of each concentration level, 0.15 mL ILIS (0.1  $\mu\text{g}/\text{mL}$ ) and 0.1 mL diluent (deionised water or methanol-water (3:7, v/v)). These two sets of standards were used in the solubility experiments (**Figure S3.4**), while spiking and recovery experiments were performed using the methanol-water batch of the standards.

Method validation parameters evaluated include linearity, selectivity, sensitivity, matrix effects, accuracy and intermediate precision (Araujo, 2009). Calibration curves were constructed for 8 equidistant concentration levels (0.610-625 ng/mL), with 4 injection repetitions per calibration point.



Linearity and sensitivity were determined from the calibration graph (**Section 3.3.5.1**). Matrix effects and intermediate precision were determined from recovery experiments as outlined below. An overview of the experimental procedure followed for method validation is presented in **Figure S3.3**.

### 3.2.5 Direct injection LC-MS/MS: Procedure and evaluation of recovery and matrix effects

For samples and sample blank analyses, 1.3 mL filtered wastewater samples were spiked with 0.6 mL NVP-D<sub>3</sub> (0.1 µg/mL) and diluted to 2 mL (ILIS concentration 30 ng/mL). For recovery experiments, the ILIS-spiked raw and treated wastewater samples were either analysed as is (blank) or spiked with 0.06 mL of 0.1, 1 or 10 µg/mL methanol-water standard mixtures prior to dilution; dilution to 2 mL with the sample matrix provided final concentrations of the standards of 3, 30 and 300 ng/mL, respectively. Recoveries were calculated from the blank-subtracted measured concentrations relative to the nominal concentration at each spiking level. Matrix effects (% ME) were calculated according to Eq. (1) (Stahnke *et al.*, 2012).

$$\% \text{ ME} = \left[ \left( \frac{\text{Conc.}(\text{spiking level}) - \text{Blank}(\text{Matrix})}{\text{Nominal Conc.}} \right) - 1 \right] \times 100 \quad (3.1)$$

### 3.2.6 SPE-LC-MS/MS: Procedure and evaluation of recovery and matrix effects

SPE was only used for surface water samples and was performed using Strata SDB-L cartridges (200 mg/6 mL, Phenomenex, Torrance, CA, USA). Prior to SPE, the pH of a ~49 mL aliquot was adjusted to 7 with 5% NH<sub>4</sub>OH or 5% HCOOH (v/v) before adding 0.3 mL of the 0.1 µg/mL NVP-D<sub>3</sub> working solution and diluting to 50.0 mL with the sample to provide the sample blank (final ILIS concentration 0.6 ng/mL). For pre-extraction spiked samples, 0.03 mL of 0.1, 1 or 10 µg/mL of the methanol-water (3:7, v/v) analyte standard mixture was added to the ILIS-spiked samples prior to final dilution (final standard concentrations of 0.06, 0.6 and 6 ng/mL, respectively). Post-extraction spiked samples were prepared by adding 0.03 mL of 0.1, 1 and 10 µg/mL standard mixtures to the dried residue obtained from SPE (see below) and diluting to 1 mL with methanol-water (3:7, (v/v)). Recoveries were calculated by dividing the blank-subtracted pre-extraction concentration by the blank-subtracted post extraction concentration (Araujo, 2009). Matrix effects (ME) were estimated using Eq. (3.2) (Stahnke *et al.*, 2012).

$$\% \text{ ME} = \left[ \left( \frac{\text{Conc.}(\text{post extracted}) - \text{Blank}(\text{Matrix})}{\text{Conc.}(\text{neat standard})} \right) - 1 \right] \times 100 \quad (3.2)$$

A 24-port vacuum extraction SPE manifold (Restek, Bellefonte, PA, USA) was used with the following optimised procedure: cartridges were conditioned sequentially with 4 mL each of acetonitrile, methanol and deionised water (pH 7). Surface water samples (50 mL) were loaded at ~1 mL/min. Cartridges were then dried under a stream of nitrogen and eluted with 4 mL methanol/dichloromethane/formic acid (49:49:2, v/v/v). The eluate was dried under stream of nitrogen, and sample blanks and pre-extraction spiked samples were reconstituted to 1 mL with 3:7 methanol-water (v/v).

### 3.3 Results and discussion

#### 3.3.1 Solubility profiling of the target analytes

For RP-LC separation, samples should ideally be dissolved in predominantly aqueous solvents to facilitate on-column focussing (Araujo, 2009). This is easily achieved for direct injection of aqueous samples, and when using SPE sample clean-up by evaporating the elution solvent and redissolving the residue in an aqueous matrix (Ngumba *et al.*, 2016a, 2016b). However, previous studies on ARVDs in aqueous samples have focused on selected target analytes only, whereas in the present work a range of ARVDs of different chemical classes and metabolites spanning a wide range of polarities were targeted. The poor solubility of the most hydrophobic analytes ( $\log K_{ow} > 4$ , EFZ, RTV and RTVM) in aqueous media was confirmed by much lower response factors for these compounds measured for standard solutions prepared in predominantly aqueous matrix (**Figure S3.4**). This could be partially circumvented by preparing standard solutions in ~30% methanol, a solution previously reported for hydrophobic analytes (Li *et al.*, 2015) and essential for the analysis of multiclass ARVDs in a single run. For this reason, methanol-water (3:7, *v/v*) was used for the preparation of all standard solutions and samples analysed in this study. However, even under these conditions, RTVM ( $K_{ow} = 4.74$ ) showed poor reproducibility and linearity. This is likely due to its adsorption in the injector flow path since carry-over was also observed for this compound. This could not be avoided by adapting the injector rinsing conditions using 90% methanol as strong needle wash. This metabolite was therefore excluded in subsequent experiments due to poor reproducibility.

#### 3.3.2 Chromatographic performance

For the separation of the target analytes, an HSS T3 C18 column was chosen due to the good performance of this column for analytes of a wide range of polarities (K'oreje *et al.*, 2012). A column of 15 cm in length and packed with 1.8  $\mu\text{m}$  particles was selected to provide good chromatographic efficiency. This separation performance proved essential for the direct injection of wastewater samples, where potential interferences were resolved from the target analytes (see below). Furthermore, a gradient spanning a wide range of organic modifier content (2-98%) was used to exploit focussing of especially the polar analytes (3TC, FTC and ZDVG) and to separate all compounds within 8 minutes. A typical total ion chromatogram (TIC) obtained for the analysis of a treated wastewater sample spiked at 30 ng/L is presented in **Figure 3.1**. All analytes were sufficiently resolved and spread evenly over the chromatographic space (except for the partial co-elution of NVP and NVP-D<sub>3</sub>, a desirable attribute). Peak symmetry was relatively good for all analytes (peak asymmetry factors (*A<sub>s</sub>*) at 5% peak height,  $\sim 1.15 \pm 0.10$ ), which also showed commensurate responses across two ionisation modes (ESI- for ZDVG and EFVM, ESI+ for the remainder of the target analytes). Analyte elution was generally in the order of therapeutic classes, with NRTIs eluting first, followed by *n*NRTIs. The PIs RTV and its metabolite

RTVM eluted before the most hydrophobic *n*NRTIs (EFZ and EFVM) though. In all cases, metabolites eluted before their parent compounds.

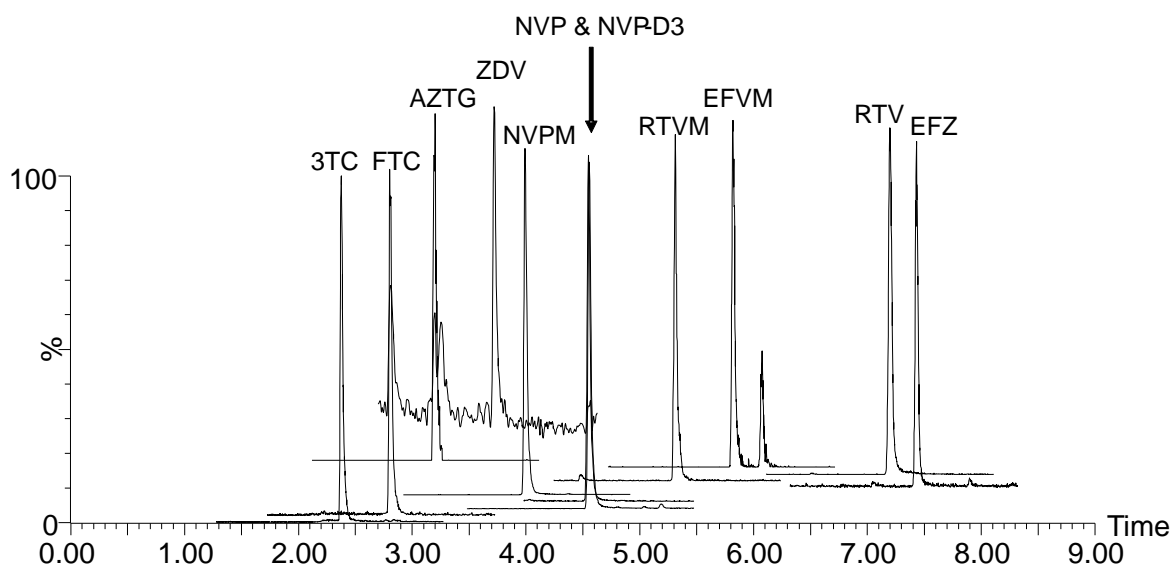


**Figure 3.1:** Exemplary total ion chromatograms (TICs) obtained for the LC-MS/MS analysis of the target ARVDs and metabolites in a treated wastewater sample spiked at 30 ng/mL. For experimental conditions, refer to **Section 3.2.3**. The chromatograms are offset in the y-dimension to improve the clarity of the figure.

### 3.3.3 Evaluation of direct injection LC-MS/MS for the analysis of wastewater samples

The reasons for selecting direct injection LC-MS/MS for the current application were two-fold. In the first instance, the sensitivity of modern triple quadrupole instruments in MRM mode is sufficient for the analysis of pharmaceuticals in wastewater (Backe and Field, 2012; Brewer and Lunte, 2015), as indeed confirmed by the validation results reported below. Secondly, because the target analytes spanned a wide range of polarities, conventional sample clean-up methods like SPE are unsuitable for all analytes (as confirmed here also, **Section 3.3.4**). Indeed, compared to previously reported LC-MS/MS methods utilising SPE sample clean-up (Ngumba *et al.*, 2016b; Peng *et al.*, 2014), the current method using direct injection extended the range of analytes in terms of both compound classes and the inclusion of ARVD metabolites. The obvious drawback of direct injection is the risk of matrix effects, which may result in inaccurate quantification; this places more importance on the chromatographic separation step.

Indeed, even using restricted MRM settings, potential interferents were detected in raw and treated wastewater samples, although in all cases these were resolved chromatographically from the target analytes. The chromatograms in **Figure S3.5** show the presence of a compound in treated wastewater eluting at  $t_R$  6.06 min and displaying the same ion transitions as 8,14-dihydroxy-efavirenz (EFVM,  $t_R$  5.81 min). EFVM is to our knowledge the only known dihydroxylated metabolite of EFZ, although the

monohydroxylated derivatives 7- and 8-hydroxy EFZ have been isolated from human urine (Deng *et al.*, 2015). The additional peak is therefore likely a positional dihydroxylated isomer. To verify this hypothesis, retrospective LC-quadrupole-time-of-flight (Q-TOF) analysis was performed (**Section S3.2, SI**). High resolution MS data and the fragmentation behaviour of the compound eluting at 6.06 min ( $m/z$  346.0094,  $C_{14}H_8NO_4ClF_3 \leq 5$  ppm, daughter ions at  $m/z$  262 and 241, **Figure S3.6**) indicate that it is closely related to EFVM, and likely a positional isomer such as 7,14-dihydroxy-efavirenz (considering the monohydroxylated derivatives previously reported (Deng *et al.*, 2015), although this could not be unambiguously confirmed. Another interferent is shown in **Figure S3.5d**, where a compound with the same quantifier transition as NVPM (12-hydroxy-nevirapine) was detected eluting close to the standard in raw wastewater. This compound did not provide a response for the quantifier ion transition and is therefore likely an isobaric rather an isomeric derivative. Since it was successfully separated chromatographically, accurate quantification of NVPM was not affected.

#### 3.3.4 Optimisation and evaluation of SPE sample preparation for surface water samples

For surface water samples, where the target analytes are expected at much lower concentrations, an SPE method was developed for the pre-concentration of the analytes of interest in the current study. Considering the poor recoveries reported in the literature for ARVDs of the *n*NRTI class (Abafe *et al.*, 2018; Prasse *et al.*, 2010; Wood *et al.*, 2015), a reversed phase (RP) polystyrene-divinylbenzene phase (Strata SDB-L) suitable for the extraction of organic analytes of diverse polarities and stable over a wide pH range was used (K'oreje *et al.*, 2012). SPE optimisation focused on ascertaining analyte losses due to either breakthrough during sample loading or incomplete elution using spiked surface water samples. The results, summarised in **Table S3.4**, confirm the poor retention (confirmed by analysis of the wash solvent) and recovery of the nucleosides ZDVG, 3TC and FTC, in accordance with previous work (Abafe *et al.*, 2018; Prasse *et al.*, 2010; Wood *et al.*, 2015). No losses due to incomplete desorption were found for an elution solvent of methanol/dichloromethane/formic acid (49:49:2, *v/v/v*). Recoveries for NVP and EFZ were generally good and consistent with past studies (Ngumba *et al.*, 2016b; Schoeman *et al.*, 2017; Wood *et al.*, 2016). This is to our knowledge the first SPE method reported for the pre-concentration of ARVD metabolites (NVPM and EFVM) from surface water samples. It is clear that RP-SPE is only suitable for the extraction of a selected range of ARVDs, primarily those of the *n*NRTI and PI classes. For the analysis of polar NRTIs and polar ARV metabolites, poor recoveries preclude the use of RP-SPE. (Note that the data reported here were obtained for relatively small sample loading volumes, while much larger volumes often used in literature reports would result in worse recoveries). Considering the success of the direct injection approach for wastewater samples, it would be interesting to explore the use of much larger injection volumes (50-100  $\mu$ L) for surface water samples, as previously reported for ARVDs (Funke *et al.*, 2016; Wooding *et al.*, 2017) to similarly avoid the limitations of SPE for these samples; this was not explored in the present work.

### 3.3.5 Method validation

#### 3.3.5.1 Calibration and method selectivity

A summary of calibration data and method selectivity criteria is presented in **Table S3.3**. Internal standard calibration was performed using Nevirapine-D<sub>3</sub> as ILIS. Calibration curves generally showed good linearity, with coefficients of determination higher than 0.99 for all the compounds over three orders of magnitude (0.610 - 625 ng/mL) and no heteroscedasticity. Sensitivity for the reported methods was determined in terms of limits of detection (LODs) and quantification (LOQs) for the direct injection method (three and ten times the standard error of the y-intercepts divided by the slope, respectively (Araujo, 2009), and method detection limits (MDLs) and method quantification limits (MQLs) for the SPE method (LOD and LOQ values of each analyte divided by the SPE pre-concentration factor and recovery data reported for surface water in **Table S3.4** (Vega-Morales *et al.*, 2010). The lowest and highest LOD values were recorded for NVP and ZDV, respectively. Apart from ZDV, LOD and MDL values obtained were comparable to past studies (Ngumba *et al.*, 2016b; Wood *et al.*, 2015). From the perspective of using direct injection LC-MS/MS, it is important to point out that LOQ values for all compounds, except for ZDV and ZDVG, are in the range (0.43 – 0.92 ng/mL) where ARVDs are commonly detected in wastewater samples. To minimise the risk of false positive detection, method selectivity criteria were based on the ratio of the quantifier (Q) to qualifier (q) ion transitions, set at a tolerance of  $\pm 30\%$ , and retention time, set at  $\pm 0.05$  min (SANTE, 2015). Both retention times and transition ion ratios were within acceptable tolerances for all analytes independent of the matrix (**Table S3.3**).

#### 3.3.5.2 Accuracy, intermediate precision and matrix effects

The accuracy of the direct injection LC-MS/MS method was fair to good, as confirmed by the relatively high analyte recoveries independent of ARV class (**Table S3.4**). Partial exceptions are the hydrophobic ARVDs EFZ (and to a lesser extent its metabolite, EFVM) and RTV, for which recoveries were ~35-80%. Although recovery experiments were performed using samples prepared in methanol-water (3:7, *v/v*) to minimise solubility issues, it seems likely that a combination of poor solubility and matrix effects associated with co-eluting matrix components at the end of the RP-LC gradient are responsible for the lower recoveries of EFZ and RTV. Recoveries for RTV were slightly higher in raw wastewater, suggesting that the matrix of these samples may sustain this compound in solution (Alade *et al.*, 2011). Despite their lower recoveries and considering their low LODs (**Table S3.4**), quantification of these compounds at the sub-ng/mL level is feasible by the direct injection method.

In contrast, SPE recoveries were generally ordered according to analyte polarity (NRTIs < nNRTIs), except for the PI RTV. For example, ZDVG was not detected at any of the studied concentrations following SPE sample clean-up, while significant losses were measured for the NRTIs 3TC and FTC; recoveries were close to 100% for these compounds by direct injection. The low sensitivity for ZDVG

and its poor retention in SPE meant that recoveries for this compound could not be determined in the studied range. Furthermore, recoveries for RTV were low at all spiking levels. This may be attributed to the low solubility of this compound in aqueous matrices (**Figure S3.4(i)**), which may have resulted in losses during SPE spiking experiments where aqueous standard solutions were used (**Section 3.2.6**), as well as matrix effects due to its elution at the end of the gradient. This may be why this compound was not detected in a previous study (Wood *et al.*, 2015). Overall, the data reported in **Table S3.4** provide clear motivation for the use direct injection as an appropriate technique for the generic screening of ARVDs and their metabolites in wastewater samples, as a means of avoiding inevitable losses associated with SPE for compounds spanning such a range of polarities.

The overall precision data (**Table S3.5**) for both direct injection and SPE methods exhibited low and random errors across the three studied matrices and were not biased towards any class of ARVDs. As expected, intra-day repeatability was better than inter-day reproducibility, and generally acceptable. Matrix effects for the direct injection of wastewater samples showed that ion suppression was more prevalent than ion enhancement (**Table S3.6**). This is not unexpected in light of the known vulnerability of ESI to ion suppression (Stahnke *et al.*, 2012). Generally, the effect was more pronounced for the hydrophobic compounds EFZ, EVM and RTV. This is likely a consequence of the fact that these compounds elute at the end of the gradient, where co-eluting hydrophobic matrix constituents may be responsible for ionisation suppression. The results further reveal that matrix effects are more prevalent for the direct injection of wastewater samples compared to surface water samples subjected to SPE clean-up, as would be expected (**Table S3.6**).

### *3.3.6 Occurrence of ARVDs and selected metabolites in wastewater samples from two wastewater plants in South Africa*

Despite the effective pre-concentration of most of the target analytes by the developed SPE method (**Table S3.4**), none of these were detected in the surface water samples analysed in this work. This is not surprising considering their origin (a mountain stream with minimal exposure to human activity) (Vieno *et al.*, 2005). In contrast, all target compounds except for ZDV and ZDVG were detected in samples from two WWTPs in the Western Cape using the direct injection LC-MS/MS method. The relatively high LODs for ZDV and ZDVG are likely responsible for the failure to detect these compounds in the present work. Quantitative data obtained for the target analytes in wastewater samples are summarised in **Table 3.1**.

The most prevalent compounds were found to be the NRTIs 3TC and FTC, and the *n*NRTIs NVP, NVPM, EFZ and EFVM. It is clear from **Table 3.1** that WWTP 1 processed higher concentrations of ARVDs compared to WWTP 2. This is in accordance with the different influent types of the two sites: WWTP 1 received predominantly domestic waste, compared to WWTP 2 which mainly processes industrial wastewater (**Table S3.1**). The ARVD detected at the highest concentrations in samples from both treatment plants was FTC, which was measured at much higher concentrations than other

compounds (172 and 31 ng/mL in raw domestic and industrial inflows, respectively). Among the quantified analytes, NVP and its metabolite NVPM were present at the lowest concentrations. Especially noteworthy is that the two metabolites (NVPM and EFVM) quantified in this work occurred at roughly the same concentrations as their respective parent compounds in influent streams (**Table 3.1**). This seemingly contradicts pharmacokinetic data indicating that these metabolites account for a small proportion of the total ARV content in the body effluent (Riska *et al.*, 1999). Based on the good chromatographic separation obtained using the present method (**Figures 3.1** and **S3.5**) and the method selectivity criteria, it is unlikely that co-elution of isomeric metabolites is responsible for this observation. A possible explanation may be that in-pipe losses in the sewage system are more pronounced for the parent compounds, which are more hydrophobic than their respective metabolites. As expected, analyte concentrations were generally much higher in influent compared to effluent samples, indicating the relatively successful removal of ARVDs by established WWTP procedures. Three distinct groups could be distinguished based on removal efficiencies (**Table S3.7**), (Botero-Coy *et al.*, 2018): virtually complete removal was observed for the polar compounds FTC, 3TC, NVPM and EFVM, whereas EFZ levels were significantly reduced in effluent streams, and for NVP little change in concentration was observed between influent and effluent streams of WWTP 1. The removal efficiencies should however be considered in light of the transformation products formed during wastewater treatment. For example, Funke *et al.* (2016) have shown that FTC and especially 3TC are transformed to the respective carboxylic acid derivatives, which may be present in effluent streams at comparable concentrations as their parent compounds in the influent streams. Overall, biological treatment was more effective compared to membrane bioreactor (MBR) treatment. Furthermore, advanced stage treatment by *uv*-irradiation appears to be more effective compared to chlorination (**Table 3.1**). The inefficiency of chlorination in the removal of ARVDs, as well the observed increases in concentration in effluent streams in some cases have been reported before, particularly for NVP and EFZ (Schoeman *et al.*, 2017; Wood *et al.*, 2016). The latter observation may be due to reconversion of the metabolites to their respective parent compounds during the treatment process (Schoeman *et al.*, 2017; Wood *et al.*, 2016), while sub-optimal WWTP operational conditions may also lead to post-treatment increments of mass loads (Schoeman *et al.*, 2017).

**Table 3.1:** Levels of occurrence (ng/mL) of ARVDs and selected metabolites in raw, treated and tertiary stage treated effluent for samples collected in September 2016. Numbers in parenthesis represent %RSD for sample replicates ( $n = 5$ ).

Analytes	WWTP 1				WWTP 2				
	Influent (A) <sup>a</sup>	Biological (B) <sup>a</sup>	Effluent MBR <sup>b</sup> (C) <sup>a</sup>	Accumulated Chlorinated effluent (D) <sup>a</sup>	Influent (1) <sup>a</sup>	Biological		Effluent	
						Non <i>uv</i> irradiated (2) <sup>a</sup>	<i>uv</i> irradiated (4) <sup>a</sup>	Non <i>uv</i> irradiated (3) <sup>a</sup>	<i>uv</i> irradiated (5) <sup>a</sup>
ZDVG	n.d. <sup>c</sup>	n.d.	n.d.	n.d.	n.d.	n.d.	n.d.	n.d.	n.d.
ZDV	n.d.	n.d.	n.d.	n.d.	n.d.	n.d.	n.d.	n.d.	n.d.
3TC	20.9 (19)	<LOQ	<LOQ	<LOQ	3.67 (8)	<LOQ	<LOQ	<LOQ	<LOQ
FTC	172 (5)	4.23 (6)	4.60 (6)	41.7 (7)	31.3 (3)	<LOQ	<LOQ	0.721 (4)	4.06 (10)
NVPM	0.519 (7)	<LOQ	<LOQ	<LOQ	<LOQ	<LOQ	<LOQ	<LOQ	<LOQ
NVP	0.681 (2)	0.764 (9)	0.710 (7)	0.658 (8)	<LOQ	<LOQ	<LOQ	<LOQ	<LOQ
EFZ	15.4 (2)	1.93 (9)	4.27 (4)	9.15 (2)	1.42 (9)	1.22 (2)	0.982 (8)	18.1 (5)	1.97 (7)
EFVM	12.4 (6)	<LOQ	<LOQ	8.04 (2)	1.48 (6)	<LOQ	<LOQ	<LOQ	<LOQ
RTV	<LOQ <sup>d</sup>	<LOQ	<LOQ	<LOQ	<LOQ	<LOQ	<LOQ	<LOQ	<LOQ

<sup>a</sup> Numbers and letters in parenthesis refer to the sampling sites in the respective WWTPs (**Figure S2**).

<sup>b</sup> Membrane bioreactor.

<sup>c</sup> Not detected.

<sup>d</sup> below limit of quantification



Our data further show increases in concentrations of FTC and EFZ in the accumulated chlorinated effluent collected after biological and MBR treatment, whereas NVP levels remain constant throughout the treatment process (in agreement with Wood *et al.*, 2016). The reasons for this observation are unclear and are likely due to the complex interplay between several factors. Insufficient dosing of the oxidant may be one possible cause, since chlorine has a strong affinity for dissolved organic matter, which limits its availability for the oxidation of residual pharmaceuticals (Acero *et al.*, 2010). Related to this, the accumulation of effluent before discharge also implies that fluctuations in influent analyte concentrations prior to effluent sampling will affect the levels detected in the chlorinated effluent. The observed increase in the level of EFZ may also partially be attributed to its high  $K_{ow}$  and affinity for the solid phase, which shields it from interaction with the aqueous oxidant (Schoeman *et al.*, 2017).

#### 3.3.6.1 Seasonal patterns of occurrence of ARVDs and their metabolites

Unlike other pharmaceuticals whose consumption is linked to weather-related ailments, dispensation of ARVDs is not subject to seasonal variations. However, seasonal variations may impact on the levels of occurrence of ARVDs in numerous complex ways. For example, dilution during precipitation events may lead to significantly lower analyte concentrations; severe drought periods often lead to higher concentrations because of lower dilution due to less rainfall and/or reduced water usage. On the other hand, increased inflows due to excessive run-off may promote delivery of compound-bearing sewage water to the WWTP, thereby elevating analyte concentrations. Furthermore, wastewater treatment processes are affected by biodegradation and sludge-water partitioning, both of which are temperature dependent (Vieno *et al.*, 2005). A comparison of the levels of the target analytes in the studied WWTPs in wet and dry seasons for samples collected in April and July 2016 is presented in **Figure 3.2**, together with data obtained from a third sampling excursion in April 2018 at the end of an exceptional drought in the Western Cape province (**Section 3.2.2**). The relevant quantitative data are summarised in **Tables S3.8** and **S3.9**.

For the 2016 samples, a significant reduction in the measured levels of most ARVDs was observed in the wet compared to the dry season for both WWTPs. Generally, the reduction in detected levels was more significant for WWTP 2, likely due to differences in inflow volumes and composition between the WWTPs, regarding which no information was available. Somewhat surprisingly, an increase in concentration was observed for EFZ and its metabolite in the wet compared to the dry season for WWTP 1. This may be a consequence of the low inflows in the dry season, which promote in-pipe settling of compound-bearing solids, as opposed to the wet season where high flow rates facilitate suspension and transmission of compound-bearing solids to WWTPs (Peng *et al.*, 2014; Schoeman *et al.*, 2017). The fact that the most hydrophobic compounds (**Figure S3.4**) display this unique behaviour seems to support this hypothesis. As expected, samples collected in April 2018 from WWTP 1 during severe

water usage restrictions following an extreme drought show much higher levels of the target analytes, suggesting substantially reduced dilution. Despite these higher concentrations, there is a notable similarity in the relative prevalence of the respective compounds between 2016 and 2018. The same generally applies for the relative removal efficiencies for the respective compounds in the drought period (compare **Tables 3.1** and **S3.9**).

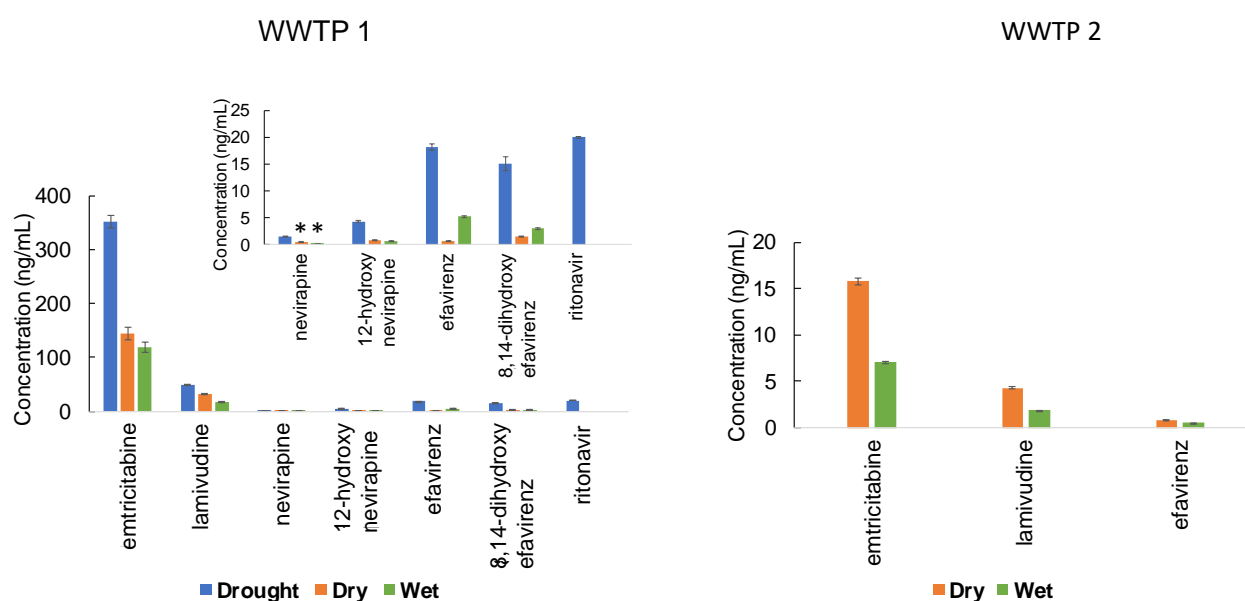


**Figure 3.2:** Comparison of seasonal effects on the occurrence of ARVDs and their metabolites in raw wastewater in the dry and wet seasons for samples collected in April and July 2016 (orange and green) and at the end of a severe drought (April 2018, blue). Error bars represent standard deviations for sample replicates ( $n = 5$ ). Quantitative data are summarised in **Tables S3.8** and **S3.9**. \*denotes measurement below the LOQ.

### 3.3.6.2 Comparison of quantitative data for ARVDs with previous studies

Several previous studies have investigated the occurrence of ARVDs in aqueous environmental matrices (K'oreje *et al.*, 2016, 2012, Ngumba *et al.*, 2016a, 2016b; Prasse *et al.*, 2010; Wood *et al.*, 2016, 2015; Wooding *et al.*, 2017), although the target analytes vary considerably between these. The selection of target analytes can largely be ascribed to prescription preferences in the relevant location, as well as to some extent to the availability of standards and the suitability of analytical methods. An abridged comparison of the results obtained in the current work with previous literature reports for environmental water samples in Africa is presented in **Table 3.2**. Previous studies mainly focussed on the NRTI and *n*NRTI therapeutic classes, with 3TC, ZDV and NVP being by far the most studied compounds. In South Africa, Wood *et al.*, 2015 recorded the lowest concentrations for these compounds, mostly for surface water samples. The highest level of 3TC (49 ng/mL) was measured in this study in influent samples, while Abafe *et al.*, 2018 recorded the highest concentration of ZDV (53 ng/mL) in influent

samples from the Gauteng province of South Africa, comparable to values reported in Finland by Ngumba *et al.* (2016b) (22-62 ng/L). K'oreje *et al.*, 2016 reported very high values for 3TC (167 ng/mL) in river water samples in the vicinity of high density low-income dwellings in Kenya; their values for raw and treated effluent wastewater samples were comparable to the present study. Similar levels (20-55 ng/L) were measured in wastewater samples in Finland (Ngumba *et al.*, 2016b). Levels of NVP found in the present study were of the same order of magnitude as those reported by Schoeman *et al.*, 2017 for WWTPs in Gauteng and Wood *et al.*, 2015 in surface and WWTP samples from across South Africa. Comparatively, higher concentrations for NVP (2.80 ng/mL) were reported by Abafe *et al.*, 2018 in influent/effluent samples from the Gauteng province of South Africa (much higher concentrations were measured in Finland – 8-19 ng/L (Ngumba *et al.*, 2016b). ZDV was not detected in any of the samples investigated in the present study, in contrast to significant concentrations measured in surface- and wastewater sample from Kenya (K'oreje *et al.*, 2016; Ngumba *et al.*, 2016a) and South Africa (Wood *et al.*, 2015). Considering the levels reported in these studies, the fact that ZDV was not detected in the present work is due to the high LOD for this compound. FTC has previously been reported in German WWTP samples (Funke *et al.*, 2016). To the best of our knowledge, this is the first report of the presence of FTC in African wastewater samples; this compound was indeed the major ARV detected in the present study. Bischel *et al.*, 2015 reported a similar concentration (100 ng/mL) in source-separated urine from a bucket toilet system, which implies that the compound is excreted in significant amounts in human urine and would therefore be expected in wastewater samples. Abafe *et al.*, 2018 recorded slightly higher concentration of EFZ (35 ng/mL) in wastewater samples from Gauteng than those measured in the present work. This compound was detected at concentrations below the LOQ in South African river water samples by Wood *et al.*, 2015. EFZ has also been quantified at µg/mL levels in South African wastewater samples (Schoeman *et al.*, 2017) and at lower levels in surface water samples (Wooding *et al.*, 2017) using one- and two-dimensional gas chromatography. Similar to the findings of Wood *et al.*, 2015 for predominantly river water samples, RTV was detected, but could not be quantified in the 2016 wastewater samples in the present work. However, relatively high concentrations of this compound (20 ng/mL) were detected in the samples collected in the drought period (**Section 3.2.2**). Concentrations up to 3.20 ng/mL were recently reported for wastewater samples from Gauteng (Abafe *et al.*, 2018).

This is the first report of the levels of the ARVD metabolites NVPM and EFVM in wastewater samples. Our findings show that similar levels of these compounds compared to their respective parent drugs were present in the wastewater streams, indicating that future work should certainly include metabolites in order to assess their environmental impact. Generally, the prevalence of ARVDs in aquatic systems evident from this and other studies reflect the widespread and sustained utilisation of these drugs, which may warrant further investigation into the health implications of pre-exposure to these compounds.

**Table 3.2:** Comparison of ARVD and selected metabolite levels in surface and wastewater samples between the present and previous studies in South Africa and across Africa. Values from the present study are for all samples analysed (**Section 3.2.2**).

Analyte	Concentration (ng/mL)		
	Present study*	In South Africa	Elsewhere in Africa
ZDVG	n.d.	Not reported	Not reported
ZDV	n.d.	6.9-53 <sup>b*</sup> , 0.09-0.50 <sup>c*</sup> (Abafe <i>et al.</i> , 2018); <LOD-0.97 <sup>b,e*</sup> (Wood <i>et al.</i> , 2015)	12-20 <sup>b*</sup> , 0.09-0.11 <sup>c*</sup> , 0.04-17 <sup>e*</sup> (K'oreje <i>et al.</i> , 2016); ~2-9 <sup>e*</sup> (K'oreje <i>et al.</i> , 2012); <LOQ-7.7 <sup>c,e*</sup> (Ngumba <i>et al.</i> , 2016a)
3TC	3.67-48.7	0.84-2.2 <sup>b*</sup> , <LOD-0.13 <sup>c*</sup> (Abafe <i>et al.</i> , 2018); <LOD-0.24 <sup>b,e*</sup> (Wood <i>et al.</i> , 2015)	30-61 <sup>b*</sup> , 20-31 <sup>c*</sup> , <LOD-167 <sup>e*</sup> (K'oreje <i>et al.</i> , 2016); ~0.6-1.5 <sup>e*</sup> (K'oreje <i>et al.</i> , 2012); <LOQ-5.4 <sup>c,e*</sup> (Ngumba <i>et al.</i> , 2016a)
FTC	0.721-352	Not reported	Not reported
NVPM	0.519-4.30	Not reported	Not reported
NVP	0.658-1.43	0.67-2.8 <sup>b*</sup> , 0.54-1.9 <sup>c*</sup> (Abafe <i>et al.</i> , 2018); ~0.05-0.20 <sup>b**</sup> , ~0.10-0.20 <sup>**</sup> , ~0.10-0.45 <sup>d**</sup> (Schoeman <i>et al.</i> , 2017); <LOQ-1.5 <sup>b,e*</sup> (Wood <i>et al.</i> , 2015); <LOQ-0.23 <sup>e***</sup> (Wooding <i>et al.</i> , 2017a)	0.85-3.3 <sup>b*</sup> , 1.0-2.1 <sup>c*</sup> , 0.03-5.6 <sup>e*</sup> (K'oreje <i>et al.</i> , 2016); ~0.5-2 <sup>e*</sup> (K'oreje <i>et al.</i> , 2012); <LOQ-4.9 <sup>c,e*</sup> (Ngumba <i>et al.</i> , 2016a)
EFZ	0.982-18.2	24-34 <sup>b*</sup> , 20-34 <sup>c*</sup> (Abafe <i>et al.</i> , 2018); ~5.6-13 <sup>b**</sup> , ~3.8-7.6 <sup>c**</sup> , ~3.9-4.0 <sup>d**</sup> (Schoeman <i>et al.</i> , 2017); <LOQ <sup>b,e*</sup> (Wood <i>et al.</i> , 2015); <LOD-0.15 <sup>e***</sup> (Wooding <i>et al.</i> , 2017a)	0.46-1.0 <sup>b*</sup> , 0.01 <sup>c*</sup> , <LOD-0.56 <sup>e*</sup> (K'oreje <i>et al.</i> , 2016)
EFVM	1.48-15.2	Not reported	Not reported
RTV	0.787-20.0	1.6-3.2 <sup>b*</sup> , 0.46-1.5 <sup>c*</sup> (Abafe <i>et al.</i> , 2018); <LOQ <sup>b,e*</sup> (Wood <i>et al.</i> , 2015)	Not reported

<sup>a</sup> not detected.

<sup>b</sup> influent, <sup>c</sup> effluent and <sup>d</sup> tertiary treated effluent; <sup>e</sup> surface water.

\* denotes analysis by LC-MS/MS, \*\* analysis by GC-TOFMS, \*\*\* analysis by GC×GC-TOFMS

### 3.4 Conclusions

This study has demonstrated the suitability of direct injection LC-ESI-MS/MS for the simultaneous quantification of all three major therapeutic classes of ARVDs and selected metabolites in aqueous

matrices. This is the first reported method for the simultaneous analysis of *n*NRTI, NRTI and PI ARVDs and metabolites by direct injection. For the investigation of such a wide range of analytes, RP-SPE sample clean-up was found to suffer from significant losses of polar targets, whereas the performance of the latest generation triple quadrupole instruments was found to be sufficient for the detection of ARVDs in wastewater samples following direct injection. The direct injection method demonstrated sufficient selectivity, sensitivity and quantitative performance for the quantification of the target analytes. Except for the polar NRTIs ZDV and ZDVG, all target analytes belonging to NRTI, *n*NRTI and PI classes were detected in raw and treated wastewater, while none of the target compounds was detected in surface water. This is the first report of the presence of ARVD metabolites in wastewater streams. Known metabolites of nevirapine (12-hydroxy-nevirapine) and efavirenz (8,14-dihydroxy-efavirenz) were detected at roughly similar concentrations as the parent drugs, while our data point to the possible occurrence of additional metabolites in these samples. Generally, concentrations of compounds were higher in raw compared to treated wastewater, in domestic compared industrial wastewater as well as in dry compared to wet seasons (the latter especially evident during a severe drought period in the sampling area). Removal efficiency of ARVDs varied from complete elimination for some compounds (lamivudine, 8,14-dihydroxy-efavirenz) to close to zero for others (nevirapine). Tertiary stage treatment efficiency was higher in biologically compared to MBR treated waste with subsequent *uv*-irradiation in the WWTPs studied here.

### 3.5 References

- Abafe, O.A., Späth, J., Fick, J., Jansson, S., Buckley, C., Stark, A., Pietruschka, B., Martincigh, B.S., 2018. LC-MS/MS determination of antiretroviral drugs in influents and effluents from wastewater treatment plants in KwaZulu-Natal, South Africa. *Chemosphere* 200, 660–670. doi:10.1016/j.chemosphere.2018.02.105
- Acero, J.L., Benitez, F.J., Real, F.J., Roldan, G., 2010. Kinetics of aqueous chlorination of some pharmaceuticals and their elimination from water matrices. *Water Res.* 44, 4158–4170. doi:10.1016/j.watres.2010.05.012
- Alade, A.O., Jameel, A.T., Muyubi, S.A., Karim, M.I.A., Alam, M.Z., 2011. Removal of Oil and Grease As Emerging Pollutants of Concern ( Epc ) in Wastewater Stream. *IIUM Eng. J.* 12, 161–169.
- Andrade, C.H., de Freitas, L.M., de Oliveira, V., 2011. Twenty-six years of HIV science: An overview of anti-HIV drugs metabolism. *Brazilian J. Pharm. Sci.* 47, 209–230. doi:10.1590/S1984-82502011000200003
- Aouri, M., Barcelo, C., Ternon, B., Cavassini, M., Anagnostopoulos, A., Yerly, S., Hugues, H., Vernazza, P., Günthard, H.F., Buclin, T., Telenti, A., Rotger, M., Decosterd, L.A., Aubert, V., Battegay, M., Bernasconi, E., Böni, J., Braun, D.L., Bucher, H.C., Burton-Jeangros, C., Calmy, A., Cavassini, M., Dollenmaier, G., Egger, M., Elzi, L., Fehr, J., Fellay, J., Furrer, H., Fux, C.A., Gorgievski, M., Günthard, H., Haerry, D., Hasse, B., Hirsch, H.H., Hoffmann, M., Hösli, I., Kahlert, C., Kaiser, L., Keiser, O., Klimkait, T., Kouyos, R., Kovari, H., Ledergerber, B., Martinetti, G., Martinez De Tejada, B., Marzolini, C., Metzner, K., Müller, N., Nadal, D., Nicca, D., Pantaleo, G., Rauch, A., Regenass, S., Rudin, C., Schöni-Affolter, F., Schmid, P., Speck, R., Stöckle, M., Tarr, P., Trkola, A., Vernazza, P., Weber, R., Yerly, S., 2016. In vivo profiling and distribution of known and novel phase I and phase II metabolites of efavirenz in plasma, urine, and cerebrospinal fluid. *Drug Metab. Dispos.* 44, 151–161. doi:10.1124/dmd.115.065839
- Araujo, P., 2009. Key aspects of analytical method validation and linearity evaluation. *J. Chromatogr. B Anal. Technol. Biomed. Life Sci.* 877, 2224–2234. doi:10.1016/j.jchromb.2008.09.030
- Backe, W.J., Field, J.A., 2012. Is SPE necessary for environmental analysis? A quantitative comparison of matrix effects from large-volume injection and solid-phase extraction based methods. *Environ. Sci. Technol.* 46, 6750–6758. doi:10.1021/es300235z
- Banta-Green, C.J., Brewer, A.J., Ort, C., Helsel, D.R., Williams, J.R., Field, J.A., 2016. Using wastewater-based epidemiology to estimate drug consumption—Statistical analyses and data presentation. *Sci. Total Environ.* 568, 856–863. doi:10.1016/j.scitotenv.2016.06.052
- Bischel, H.N., Özel Duygan, B.D., Strande, L., Mc Ardell, C.S., Udert, K.M., Kohn, T., 2015. Pathogens and pharmaceuticals in source-separated urine in eThekweni, South Africa. *Water Res.* 85, 57–65. doi:10.1016/j.watres.2015.08.022
- Botero-Coy, A.M., Martínez-Pachón, D., Boix, C., Rincón, R.J., Castillo, N., Arias-Marín, L.P.,

- Manrique-Losada, L., Torres-Palma, R., Moncayo-Lasso, A., Hernández, F., 2018. An investigation into the occurrence and removal of pharmaceuticals in Colombian wastewater. *Sci. Total Environ.* 642, 842–853. doi:10.1016/j.scitotenv.2018.06.088
- Brewer, A.J., Lunte, C., 2015. Analysis of Nucleosides in Municipal Wastewater by Large-Volume Liquid Chromatography Tandem Mass Spectrometry. *Anal. Methods* 7, 5504–5510. doi:10.1039/C5AY00929D
- Deng, Y., Liu, R., Ping, Y., Liang, J., 2015. Rapid identification of efavirenz metabolites in rats and humans by ultra high performance liquid chromatography combined with quadrupole time-of-flight tandem mass spectrometry. *J. Sep. Sci.* 38, 1529–1536. doi:10.1002/jssc.201401120
- Denissen, J.F., Grabowski, B.A., Johnson, M.K., Buko, A.M., Kempf, D.J., Thomas, S.B., Surber, B.W., 1997. Metabolism and disposition of the HIV-1 protease inhibitor ritonavir (ABT-538) in rats, dogs, and humans. *Drug Metab. Dispos.* 25, 489–501.
- Funke, J., Prasse, C., Ternes, T.A., 2016. Identification of transformation products of antiviral drugs formed during biological wastewater treatment and their occurrence in the urban water cycle. *Water Res.* 98, 75–83. doi:10.1016/j.watres.2016.03.045
- Himes, S.K., Scheidweiler, K.B., Tassiopoulos, K., Kacanek, D., Hazra, R., Rich, K., Huestis, M.A., Pediatric, H.I.V.A.C.S., 2013. Development and validation of the first liquid chromatography-tandem mass spectrometry assay for simultaneous quantification of multiple antiretrovirals in meconium. *Anal. Chem.* 85, 1896–1904. doi:10.1021/ac303188j
- K'oreje, K.O., Demeestere, K., De Wispelaere, P., Vergeynst, L., Dewulf, J., Van Langenhove, H., 2012. From multi-residue screening to target analysis of pharmaceuticals in water: development of a new approach based on magnetic sector mass spectrometry and application in the Nairobi River basin, Kenya. *Sci. Total Environ.* 437, 153–64. doi:10.1016/j.scitotenv.2012.07.052
- K'oreje, K.O., Kandie, F.J., Vergeynst, L., Abira, M.A., Van Langenhove, H., Okoth, M., Demeestere, K., 2018. Science of the Total Environment Occurrence, fate and removal of pharmaceuticals, personal care products and pesticides in wastewater stabilization ponds and receiving rivers in the Nzoia Basin, Kenya. *Sci. Total Environ.* 637–638, 336–348. doi:10.1016/j.scitotenv.2018.04.331
- K'oreje, K.O., Vergeynst, L., Ombaka, D., De Wispelaere, P., Okoth, M., Van Langenhove, H., Demeestere, K., 2016. Occurrence patterns of pharmaceutical residues in wastewater, surface water and groundwater of Nairobi and Kisumu city, Kenya. *Chemosphere* 149, 238–244. doi:10.1016/j.chemosphere.2016.01.095
- Li, W., Liu, Y., Duan, J., Saint, C.P., Mulcahy, D., 2015. The role of methanol addition to water samples in reducing analyte adsorption and matrix effects in liquid chromatography-tandem mass spectrometry. *J. Chromatogr. A* 1389, 76–84. doi:10.1016/j.chroma.2015.02.044
- Ncube, S., Madikizela, L.M., Chimuka, L., Nindi, M.M., 2018. Environmental fate and ecotoxicological effects of antiretrovirals: A current global status and future perspectives. *Water Res.* 145, 231–247. doi:10.1016/j.watres.2018.08.017

- Ngumba, E., Gachanja, A., Tuhkanen, T., 2016a. Occurrence of selected antibiotics and antiretroviral drugs in Nairobi River Basin, Kenya. *Sci. Total Environ.* 539, 206–213.  
doi:10.1016/j.scitotenv.2015.08.139
- Ngumba, E., Kosunen, P., Gachanja, A., Tuhkanen, T., 2016b. A multiresidue analytical method for trace level determination of antibiotics and antiretroviral drugs in wastewater and surface water using SPE-LC-MS/MS and matrix-matched standards. *Anal. Methods* 8, 6720–6729.  
doi:10.1039/C6AY01695B
- Ort, C., Lawrence, M.G., Reungoat, J., Mueller, J.F., 2010. Sampling for PPCPs in Wastewater Systems: Comparison of Different Sampling Modes and Optimization Strategies. *Environ. Sci. Technol.* 44, 6289–6296. doi:10.1021/es100778d
- Peng, X., Wang, C., Zhang, K., Wang, Z., Huang, Q., Yu, Y., Ou, W., 2014. Profile and behavior of antiviral drugs in aquatic environments of the Pearl River Delta, China. *Sci. Total Environ.* 466–467, 755–761. doi:10.1016/j.scitotenv.2013.07.062
- Prasse, C., Schlüsener, M.P., Schulz, R., Ternes, T.A., 2010. Antiviral drugs in wastewater and surface waters: A new pharmaceutical class of environmental relevance? *Environ. Sci. Technol.* 44, 1728–1735. doi:10.1021/es903216p
- Riska, P., Lamson, M., Macgregor, T., Sabo, J., Hattox, S., Pav, J., Keirns, J., 1999. Disposition and biotransformation of the antiretroviral drug nevirapine in humans. *Drug Metab. Dispos.* 27, 895–901.
- SANTE 2015, 2015. Guidance document on analytical quality control and method validation procedures for pesticides residues analysis in food and feed. SANTE/11945/2015, Legal Deposit.
- Schoeman, C., Dlamini, M., Okonkwo, O.J., 2017. The impact of a Wastewater Treatment Works in Southern Gauteng, South Africa on efavirenz and nevirapine discharges into the aquatic environment. *Emerg. Contam.* 3, 95–106. doi:10.1016/j.emcon.2017.09.001
- Stahnke, H., Kittlaus, S., Kempe, G., Hemmerling, C., Alder, L., 2012. The influence of electrospray ion source design on matrix effects. *J. Mass Spectrom.* 47, 875–884. doi:10.1002/jms.3047
- Veal, G.J., Back, D.J., 1995. Metabolism of zidovudine. *Gen. Pharmacol.* 26, 1469–1475.  
doi:10.1016/0306-3623(95)00047-X
- Vega-Morales, T., Sosa-Ferrera, Z., Santana-Rodriguez, J., 2010. Determination of alkylphenol polyethoxylates, bisphenol-A, 17  $\alpha$ -ethynylestradiol and 17  $\beta$ -estradiol and its metabolites in sewage samples by SPE and LC/MS/MS. *J. Hazard. Mater.* 183, 701–711.  
doi:10.1016/j.jhazmat.2010.07.083
- Vieno, N.M., Tuhkanen, T., Kronberg, L., 2005. Seasonal variation in the occurrence of pharmaceuticals in effluents from a sewage treatment plant and in the recipient water. *Environ. Sci. Technol.* 39, 8220–8226. doi:10.1021/es051124k
- Wood, T.P., Basson, A.E., Duvenage, C., Rohwer, E.R., 2016. The chlorination behaviour and environmental fate of the antiretroviral drug nevirapine in South African surface water. *Water*



Res. 104, 349–360. doi:10.1016/j.watres.2016.08.038

Wood, T.P., Duvenage, C.S.J., Rohwer, E., 2015. The occurrence of anti-retroviral compounds used for HIV treatment in South African surface water. *Environ. Pollut.* 199, 235–243.

doi:10.1016/j.envpol.2015.01.030

Wooding, M., Rohwer, E.R., Naude, Y., 2017. Determination of endocrine disrupting chemicals and antiretroviral compounds in surface water: A disposable sorptive sampler with comprehensive gas chromatography -Time-of-flight mass spectrometry and large volume injection with ultra-high performance. *J. Chromatogr. A* 1496, 122–132. doi:10.1016/j.chroma.2017.03.057

World Health Organization, 2015. Guidelines Guideline on When To Start Antiretroviral Therapy and on Pre-Exposure Prophylaxis for Hiv. *World Heal. Organ.* 78. doi:978 92 4 150956 5

## Chapter 3

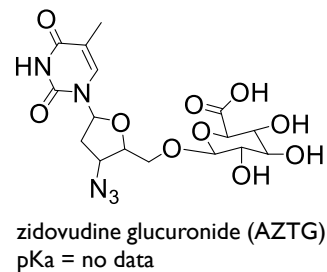
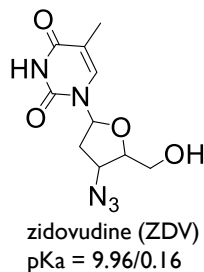
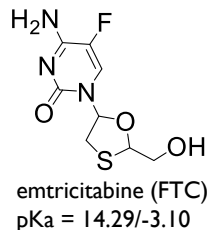
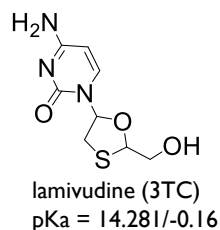
---

**Supplementary information for:**

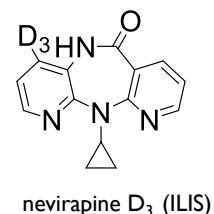
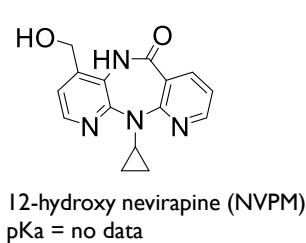
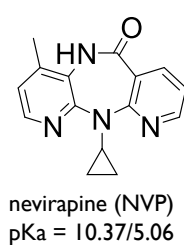
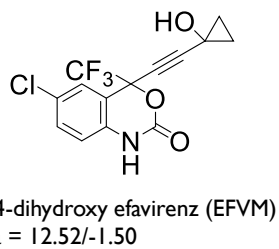
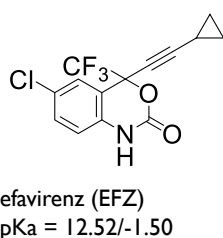
**Simultaneous quantification of commonly prescribed antiretroviral drugs and their selected metabolites in aqueous environmental samples by direct injection and solid phase extraction liquid chromatography - tandem mass spectrometry**

## Section S3.1

## Nucleoside reverse transcriptase inhibitors (NRTIs)



## Non-nucleoside reverse transcriptase inhibitors (nNRTIs)



## Protease inhibitors

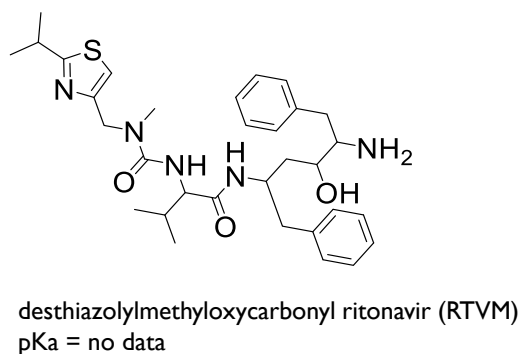
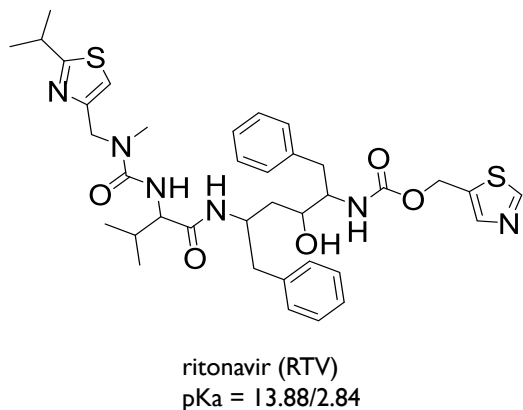


**Figure S3.1:** Structures of the target analytes with their known pK<sub>a</sub> values (strongest acid/strongest base) (K'oreje *et al.*, 2016; Prasse *et al.*, 2010; Wood *et al.*, 2015)

## Study area

Raw and treated wastewater samples were collected from two WWTPs in the Western Cape province, South Africa. Both plants predominantly use biological treatment processes (primary stage-grit removal, and secondary stages using activated sludge and aeration tanks) and both operated a small-scale membrane bioreactor treatment process. However, the main difference between the two plants is the advanced treatment process, where WWTP 1 uses chlorination and WWTP 2 *uv*-irradiation (**Table S3.1, Figure S3.2**). Surface water was at an isolated point - deemed free from anthropogenic impact - along a perennial creek originating from a natural spring in the mountains in the Western Cape province.

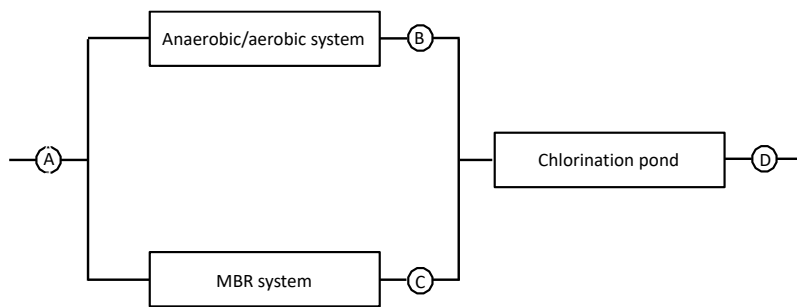
**Table S3.1:** Information on the sampling sites used in this study. Refer to **Figure S3.2** for further details on the treatment processes and sampling sites at each WWTP.

Location	Influent type	Catchment demography	Capacity (ML/day)	Treatment process
WWTP 1	95% Domestic	High density low income	55	Activated sludge / MBR <sup>a</sup> / chlorination
WWTP 2	80% Industrial	Mixed income and predominantly industrial	46	Activated sludge / MBR / <i>uv</i> -irradiation
Spring water		Protected environmental physical feature	Perennial	Unaltered natural flowing water

<sup>a</sup> MBR – Membrane bioreactor

**Sampling sites**

(a) WWTP 1



(b) WWTP 2

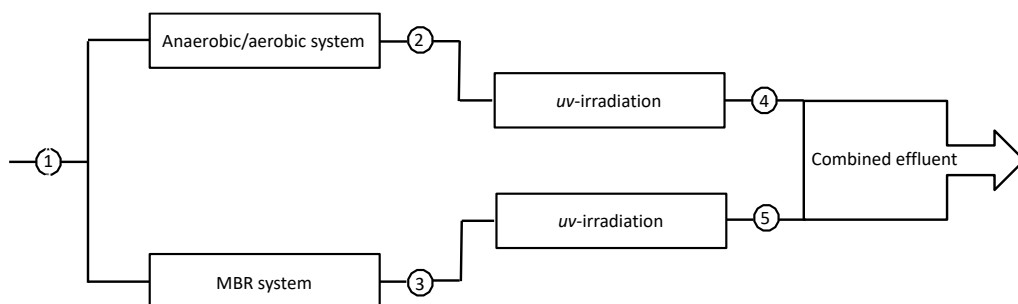


**Figure S3.2:** Schematic diagrams of the treatment processes used at WWTPs 1 and 2 where samples were obtained for the study. Circled numbers and letters indicate the sampling points at each WWTP.

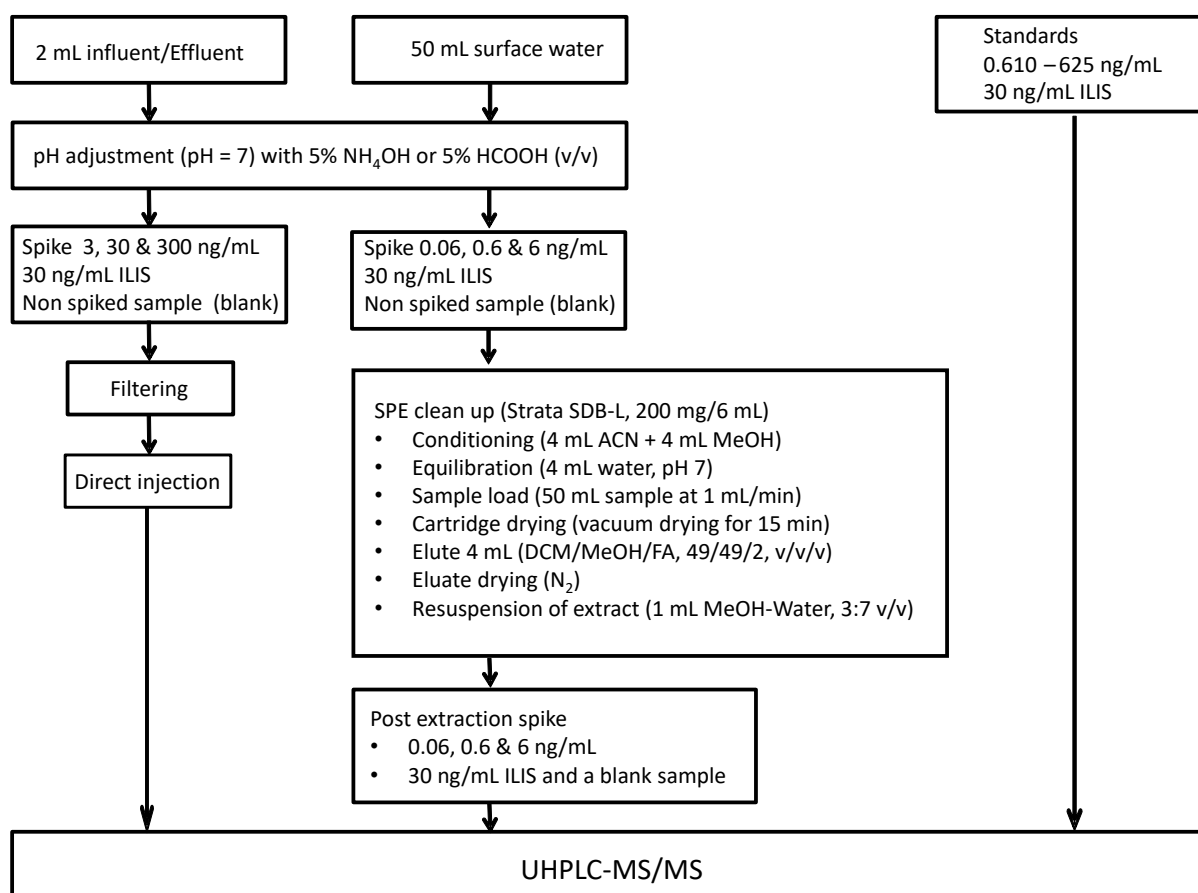


**Figure S3.3:** A workflow scheme representing the procedure used for method validation.

Abbreviations: Acetonitrile (ACN), isotopically labelled internal standard (ILIS), formic acid (FA), dichloromethane (DCM), methanol (MeOH).

**Table S3.2:** Optimised LC-ESI-MS/MS MRM conditions used for the analysis of the target ARVs and their metabolites.

Analyte	MW (g/mol.)	ESI(±)	Quantifier transition	CV/CE <sup>a</sup> (V/eV)	Qualifier transition	CV/CE <sup>a</sup> (V/eV)
zidovudine glucuronide (ZDVG)	443.4	-	442.0 > 125.0	20/20	442.0 > 113.0	20/20
zidovudine (ZDV)	267.2	+	268.0 > 127.0	20/20	268.0 > 110.0	20/20
lamivudine (3TC)	229.3	+	230.0 > 226.1	30/15	230.0 > 95.1	30/25
emtricitabine (FTC)	247.3	+	248.0 > 130.6	15/15	248.0 > 113.5	15/30
12-hydroxy-nevirapine (NVPM)	282.3	+	283.2 > 223.0	20/25	283.2 > 196.1	20/30
nevirapine (NVP)	266.3	+	267.3 > 226.1	20/30	267.3 > 107.1	20/15
efavirenz (EFZ)	315.7	+	316.1 > 168.0	20/30	316.1 > 244.1	20/25
8,14-dihydroxy-efavirenz (EFVM)	347.7	-	346.0 > 261.8	20/15	346.0 > 241.8	20/20
ritonavir (RTV)	720.9	+	721.5 > 296.1	15/15	721.5 > 426.5	15/15
desthiazolylmethyloxycarbonyl ritonavir (RTVM)	579.8	+	580.1 > 268.1	20/25	580.1 > 410.1	20/25

<sup>a</sup> CV: Cone voltage (V), CE: collision energy (eV).

**Table S3.3:** Summary of calibration data and method selectivity criteria for both direct injection and SPE LC-MS/MS methods.

Analyte	Range (ng/mL)	R <sup>2</sup>	LOD <sup>a</sup> (ng/mL)	MDL <sup>b</sup> (ng/mL)	t <sub>R</sub> <sup>c</sup> (min.)	q/Q <sup>d</sup>
ZDVG	0.72 - 625	0.999	0.727	0.015	3.12±0.040	0.36±0.03
ZDV	11.2 - 625	0.998	11.2	0.224	3.72±0.001	0.05±0.01
3TC	0.198 - 625	0.995	0.198	0.004	2.38±0.005	0.04±0.01
FTC	0.276 - 625	0.995	0.276	0.006	2.81±0.004	0.11±0.01
NVPM	0.191 - 625	0.997	0.191	0.004	4.00±0.004	0.75±0.04
NVP	0.128 - 625	0.998	0.128	0.003	4.49±0.001	0.42±0.04
EFZ	0.179 - 625	0.996	0.179	0.004	7.40±0.003	0.57±0.05
EFVM	0.238 - 625	0.998	0.238	0.005	5.80±0.003	0.47±0.06
RTV	0.236 - 625	0.992	0.236	0.005	7.20±0.004	0.33±0.04
RTVM	16.34 - 625	0.966	16.34	n.q. <sup>e</sup>	5.27±0.001	0.14±0.01

<sup>a</sup> Limit of detection for the direct injection method.

<sup>b</sup> Method detection limit for the SPE method.

<sup>c</sup> Average t<sub>R</sub> ± standard deviation for the calibration standards, fortified and real samples ( $n \leq 64$ ), except for ZDV and ZDVG where the standard deviation was calculated for calibration standards and fortified samples ( $n = 44$ ).

<sup>d</sup> Ratio of qualifier (q) to quantifier (Q) ion transitions ± standard deviation for standards, fortified and real samples ( $n \leq 64$ ), except for ZDV and ZDVG ( $n = 44$ ).

<sup>e</sup> not quantified due to lack of recovery data.

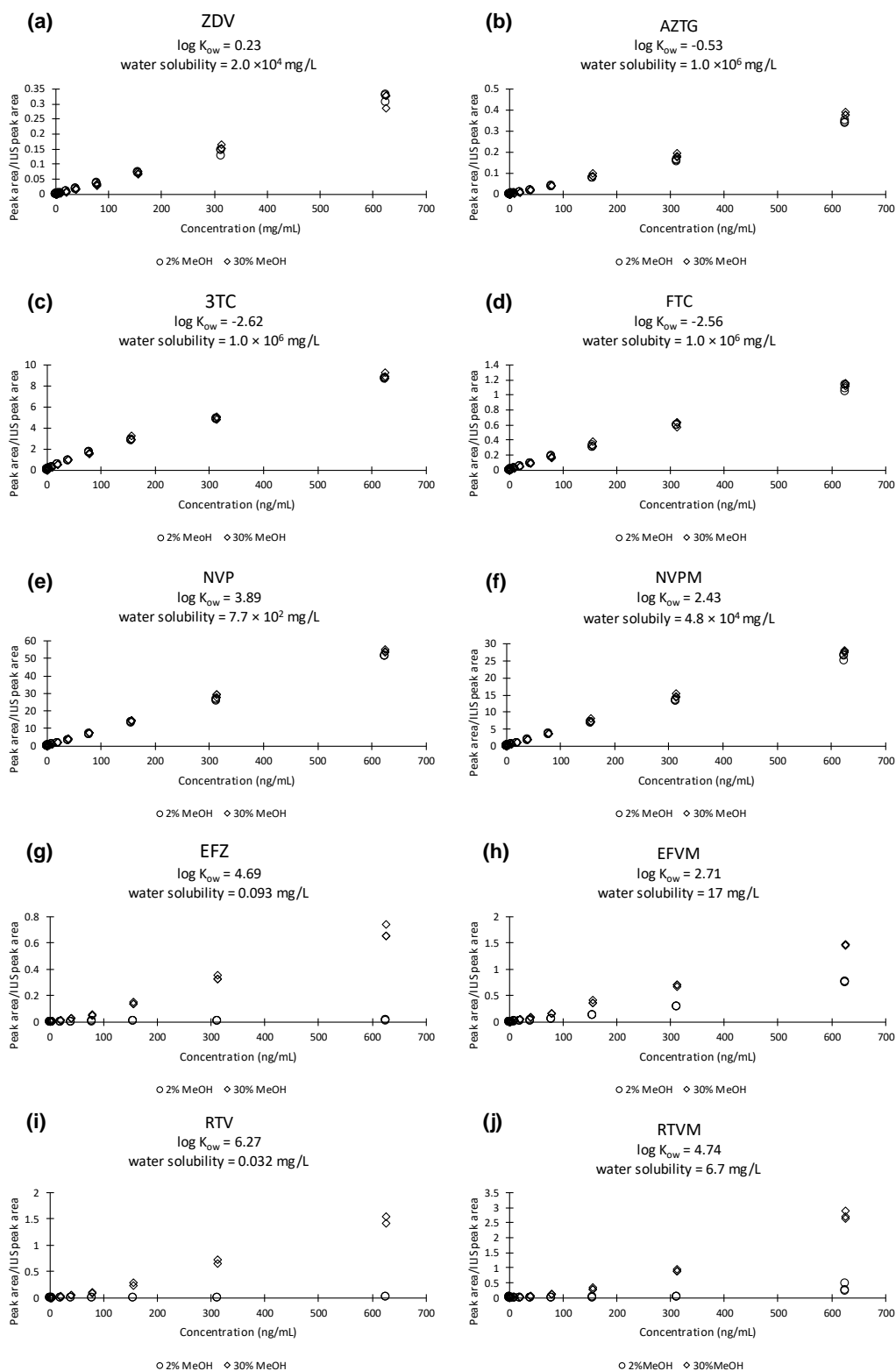


**Figure S3.4:** Comparison of calibration curves obtained for the target ARVs and metabolites for standard solutions prepared in predominantly aqueous medium (○) and (◇) 3:7 methanol-water (v/v). Replicate injections are displayed as individual data points. Log  $K_{ow}$  and water solubility values reported were estimated using EPI Suite™ (US Environmental Protection Agency, 2012).



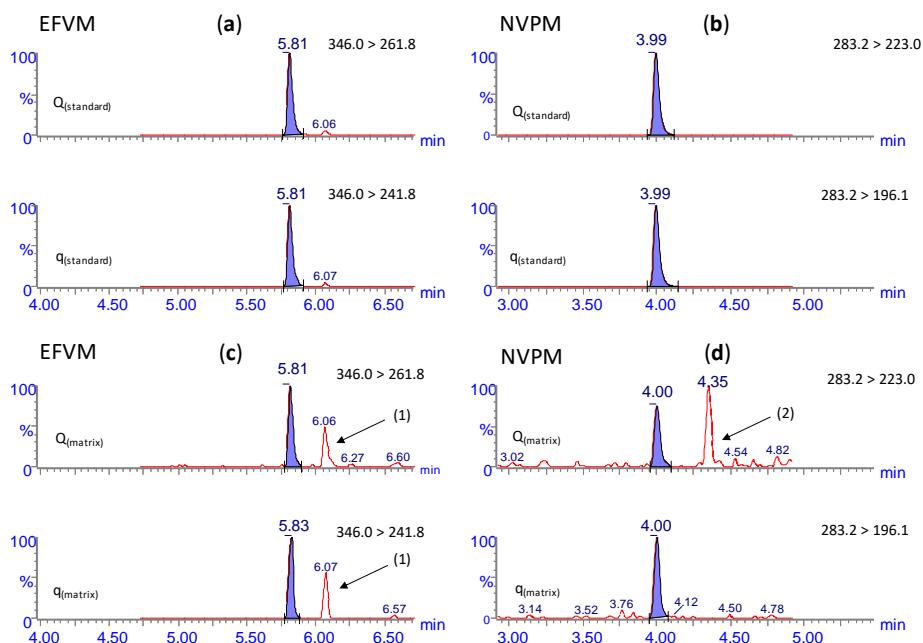


**Figure S3.5:** Typical total ion chromatograms obtained for the LC-MS/MS analysis of EFVM (a) and NVPM (b) standards (9.765 ng/mL in methanol-water, 3:7, v/v), and the same transitions obtained for treated (c) and raw (d) wastewater samples by direct injection. The top chromatogram in each panel represents the quantifier (Q) and the bottom the qualifier (q) ion transitions. The peak labelled (1) in (b) is an isomer of EFVM detected in a treated wastewater sample (refer to **Section S3.2** and **Figure S3.6** for further details), while the peak labelled (2) in (d) is a likely isobaric derivative of NVPM.

## Section S3.2: LC-Q-TOF analysis of potential interferents detected in wastewater samples

### Experimental

An ACQUITY™ ultra performance LC system as described in **Section 3.2.3** was interfaced to a Waters Synapt G2 Q-TOF mass spectrometer. Separation was achieved using the same column and solvents as discussed in **Section 3.2.3**, with the exception that the flow rate was 0.25 mL/min and the following longer gradient was used: 0 – 28% B (0 - 22 min), 28 – 40% B (22 - 2.5 min), 40 – 80% B (22.50 – 40 min), 80 – 100% B (40 – 42 min), 100 – 0% B (42 – 43 min), followed by re-equilibration (43 – 45 min).

The mass spectrometer was operated in the negative ionisation mode. Capillary and cone voltages were set at 3.0 kV and 25 V, respectively. The source and desolvation temperatures were 120° and 275°C, and nebulisation desolvation and cone gas flows were 650 L/h and 50 L/h, respectively. Data were acquired using two functions: a low collision energy (LE) function with a trap collision energy of 6 eV and a scan range of 120 – 2000 Da, and a high collision energy (HE) MS<sup>E</sup> function with a collision ramp of 20 – 60 eV and a scan range 40 – 2000 Da. The mass spectrometer was calibrated using sodium formate over the mass range 50 – 1200 Da, and leucine-enkephalin was used as lockmass reference (deprotonated ion at m/z 554.2615) infused during the analysis.

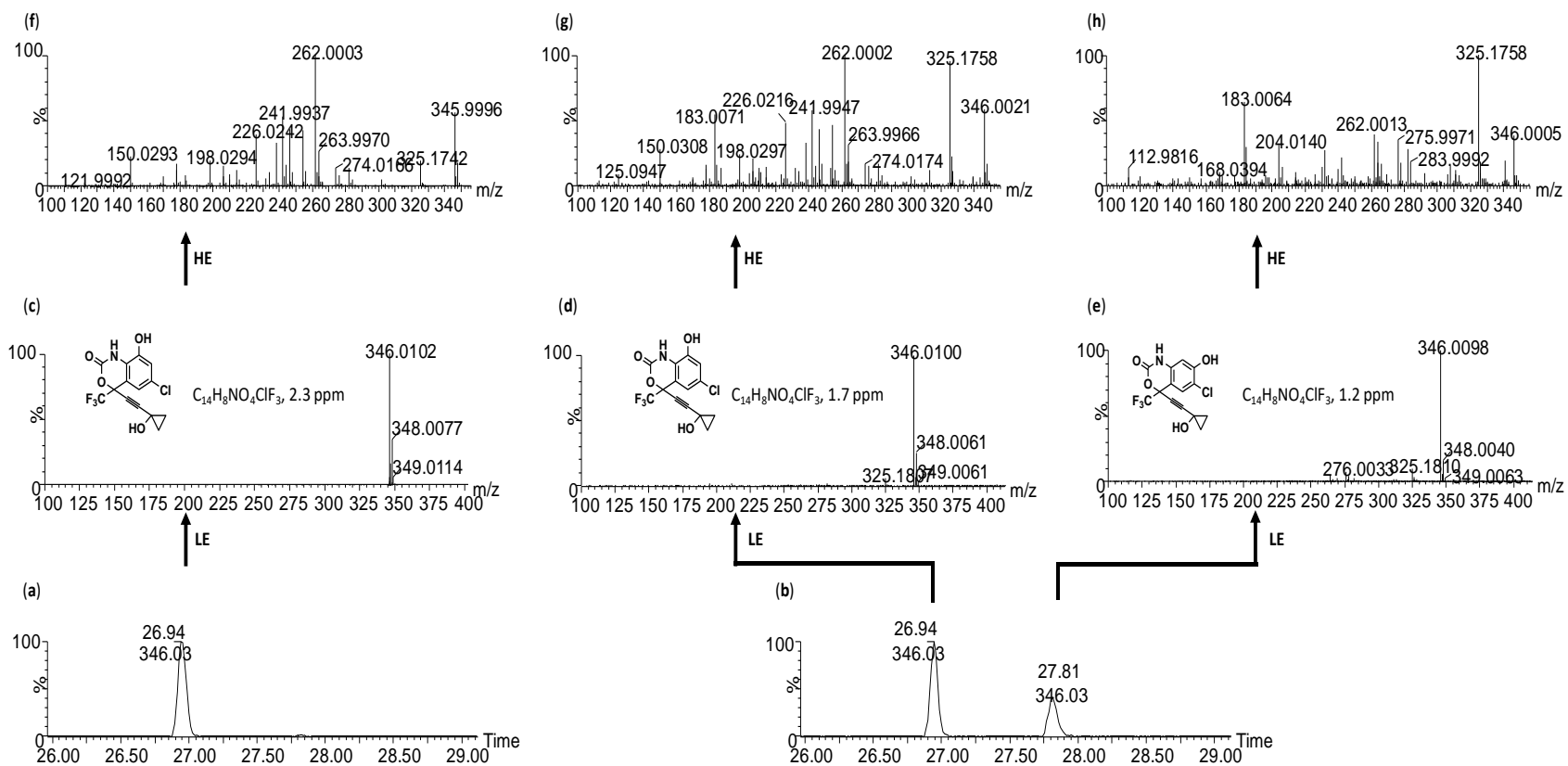


**Figure S3.6:** Extracted ion chromatograms obtained for the LC-Q-TOFMS analysis of **(a)** a 8,14-dihydroxy-Efavirenz (EFVM) standard at 10  $\mu$ g/mL, and **(b)** SPE-processed raw wastewater sample. Low energy (LE) spectra for the standard **(c)**, EFVM in the sample ( $t_R$  26.94 min) **(d)** and a suspected positional isomer of EFVM **(e)** as well as high collision energy (HE) spectra for the sample compounds are compared.

**Section S3.3: Validation and quantitation data****Table S3.4:** Summary of recovery data obtained for the target analytes in raw and treated wastewater (spiked at 3, 30 and 300 ng/mL,  $n = 12$ ) analysed by direct injection LC-MS/MS and SPE pre-concentrated surface water samples (spiked at 0.06, 0.6 and 6 ng/mL,  $n = 9$ ). Numbers in parentheses represent %RSDs for inter-day precision.

Analytes	% recoveries for direct injection samples						% recoveries for SPE-processed samples				
	LOQ (ng/mL)	Influent (ng/mL)			Effluent (ng/mL)			MQL (ng/mL)	Surface water (ng/mL)		
		3	30	300	3	30	300		0.06	0.6	6
ZDVG	2.42	n.d. <sup>a</sup>	91.7 (5)	95.2(8)	n.d.	101 (9)	96.4 (7)	n.q. <sup>b</sup>	n.d.	n.d.	n.d.
ZDV	37.5	n.d.	107 (10)	112 (9)	n.d.	97.7 (6)	113 (8)	0.86	n.d.	74.7 (7)	100 (2)
3TC	0.661	99.6 (9)	100 (4)	106 (8)	108 (1)	106 (4)	107 (1)	0.03	48.9 (3)	32.6 (8)	42.5 (3)
FTC	0.919	90.0 (3)	105 (4)	95.6 (4)	85.5 (9)	62.7 (2)	103 (3)	0.04	58.1 (10)	43.3 (7)	50.1 (4)
NVPM	0.638	80.5 (5)	105 (6)	107 (9)	78.3 (6)	101 (4)	102 (3)	0.02	91.3 (6)	66.8 (3)	77.6 (2)
NVP	0.425	110 (3)	102 (5)	101 (1)	110 (3)	97.0 (5)	98.9 (2)	0.01	94.7 (3)	67.9 (3)	77.8 (2)
EFZ	0.596	57.1 (2)	50.3 (6)	46.5 (5)	77.8 (5)	59.9 (4)	59.1 (10)	0.02	87.4 (8)	64.4 (8)	74.9 (5)
EFVM	0.794	105 (3)	82.9 (9)	77.1 (2)	103 (9)	75.2 (6)	76.8 (6)	0.02	67.9 (5)	61.4 (5)	77.8 (9)
RTV	0.787	41.1 (4)	48.3 (11)	52.8 (9)	41.7 (1)	35.6 (2)	63.9 (7)	0.06	17.2 (3)	19.3 (4)	39.2 (5)

<sup>a</sup> Not detected.<sup>b</sup> Not quantified due poor recovery by SPE.

**Table S3.5:** Precision data (%RSD)<sup>a</sup> obtained for the fortified samples ( $n = 9$ ) of surface water by SPE-LC-MS/MS and effluent and influent wastewater samples by direct injection LC-MS/MS.

Precision	Analytes								
	ZDVG	ZDV	3TC	FTC	NVP	NVPM	EFZ	EFVM	RTV
<b>Intra-day</b>									
3 ng/mL	-	-	<i>2/2/6</i>	<i>5/6/3</i>	<i>4/3/5</i>	<i>3/7/5</i>	<i>5/5/2</i>	<i>2/5/4</i>	<i>3/1/5</i>
30 ng/mL	<i>-/7/8</i>	<i>7/6/3</i>	<i>9/2/3</i>	<i>5/2/8</i>	<i>4/1/2</i>	<i>4/1/1</i>	<i>6/2/8</i>	<i>6/2/4</i>	<i>10/3/1</i>
300 ng/mL	<i>-/1/2</i>	<i>2/8/7</i>	<i>2/2/2</i>	<i>5/4/5</i>	<i>1/2/1</i>	<i>2/2/1</i>	<i>7/5/3</i>	<i>2/3/2</i>	<i>10/3/3</i>
<b>Inter-day</b>									
3 ng/mL	-	-	<i>3/1/9</i>	<i>10/9/3</i>	<i>3/3/3</i>	<i>6/6/5</i>	<i>8/5/2</i>	<i>5/9/3</i>	<i>3/1/4</i>
30 ng/mL	<i>-/9/5</i>	<i>7/6/10</i>	<i>8/4/4</i>	<i>7/2/4</i>	<i>3/5/5</i>	<i>3/4/6</i>	<i>8/4/6</i>	<i>5/6/9</i>	<i>4/2/11</i>
300 ng/mL	<i>-/7/8</i>	<i>2/8/9</i>	<i>3/1/8</i>	<i>4/3/4</i>	<i>2/2/1</i>	<i>2/3/9</i>	<i>5/10/5</i>	<i>9/6/2</i>	<i>5/7/9</i>

<sup>a</sup> Values are displayed in *italic font*/**bold font**/normal font for *surface water*/**effluent**/influent samples, respectively.

**Table S3.6:** Matrix effects (%)<sup>a</sup> measured for fortified samples<sup>b</sup> ( $n = 9$ ) of surface water by SPE-LC-MS/MS and effluent and influent wastewater samples by direct injection LC-MS/MS. Data were calculated using Equations (1) and (2) (Experimental Section) for direct injection and SPE methods, respectively.

Matrix effect	Analyte								
	ZDVG	ZDV	3TC	FTC	NVP	NVPM	EFZ	EFVM	RTV
Low <sup>b</sup>	-	-	<i>-2/8/0</i>	<i>9/-15/-10</i>	<i>-3/10/10</i>	<i>-0.4/-22/-20</i>	<i>-7/-22/-43</i>	<i>-39/3/5</i>	<i>21/-58/-59</i>
Mid <sup>b</sup>	<i>-/1/-8</i>	<i>-0.2/-2/7</i>	<i>-6/6/0</i>	<i>-5/-37/5</i>	<i>-2/-3/2</i>	<i>-22/1/5</i>	<i>-10/-40/-50</i>	<i>-39/-25/-17</i>	<i>1/-64/-52</i>
High <sup>b</sup>	<i>-/-4/-5</i>	<i>12/13/12</i>	<i>0.9/7/6</i>	<i>6/3/-4</i>	<i>-0.1/-1/1</i>	<i>18/2/7</i>	<i>-2/-41/-53</i>	<i>-20/-23/-23</i>	<i>13/-36/-47</i>

<sup>a</sup> Values are displayed in *italic font*/**bold font**/normal font for *surface water*/**effluent**/influent samples, respectively.

<sup>b</sup> spiking levels: Low = 3 and 0.06 ng/mL, Mid = 30 and 0.6 ng/mL, High = 300 and 6 ng/mL, for direct injection and SPE methods, respectively.

**Table S3.7:** Estimated removal efficiencies (%) for ARVDs and their metabolites in WWTPs 1 and 2. Data represent average values determined for samples collected in April, July and September 2016.

Effluent type	Removal efficiency (%)								
	ZDVG	ZDV	3TC	FTC	NVPM	NVP	EFZ	EFVM	RTV
Chlorinated	n.d.	n.d.	100	76	100	3	40	33	n.d.
uv-MBR	n.d.	n.d.	100	98	100	100	-38	100	n.d.
uv-Biological	n.d.	n.d.	100	100	100	100	31	100	n.d.

Removal efficiencies (%) were calculated according to Botero-Coy *et al.*, (2018) using equation S1:

$$\text{Removal efficiency (\%)} = 100 \times \left(1 - \frac{C_{\text{effluent}}}{C_{\text{influent}}}\right) \quad (\text{Eq. S3.1})$$

**Table S3.8:** Levels of occurrence (ng/mL) of ARVs and selected metabolites in raw wastewater for samples collected in April and July 2016 (wet and dry seasons, respectively). Numbers in parenthesis represent %RSD for sample replicates (n = 5).

Season and sampling sites	Analytes								
	ZDVG	ZDV	3TC	FTC	NVP	NVPM	EFZ	EFVM	RTV
Dry <sup>a</sup> (WWTP 1)	n.d. <sup>c</sup>	n.d.	31.6 (3)	144 (7)	<LOQ <sup>d</sup>	0.749 (8)	0.646 (2)	1.41 (6)	n.d.
Wet <sup>b</sup> (WWTP 1)	n.d.	n.d.	16.2 (4)	119 (3)	<LOQ	0.607 (8)	5.23 (4)	3.00 (6)	n.d.
Dry <sup>a</sup> (WWTP 2)	n.d.	n.d.	4.29 (3)	15.8 (3)	<LOQ	<LOQ	0.793 (4)	n.d.	n.d.
Wet <sup>b</sup> (WWTP 2)	n.d.	n.d.	1.87 (1)	7.05 (1)	<LOQ	<LOQ	<LOQ	n.d.	n.d.

<sup>a</sup> refers to samples collected in April 2016

<sup>b</sup> refers to samples collected in July 2016

<sup>c</sup> not detected

<sup>d</sup> below limit of quantification

**Table S3.9:** Levels of occurrence of ARVs and their metabolites in raw and tertiary treated effluent (ng/mL) for samples collected in April 2018 during a severe drought. Values in parenthesis are %RSD for sample replicates ( $n = 5$ ).

Analytes	Influent (A) <sup>a</sup>	Effluent		
		Biological (B) <sup>a</sup>	MBR <sup>b</sup> (C) <sup>a</sup>	Accumulated chlorinated effluent (D) <sup>a</sup>
ZDVG	n.d. <sup>c</sup>	n.d.	n.d.	n.d.
ZDV	n.d.	n.d.	n.d.	n.d.
3TC	48.7 (3)	n.d.	n.d.	n.d.
FTC	352 (3)	75.2 (3)	n.d.	56.0 (2)
NVPM	4.30 (0.2)	3.23 (4)	n.d.	2.38 (2)
NVP	1.43 (6)	1.94 (2)	1.64 (2)	1.49 (4)
EFZ	18.2 (4)	45.6 (3)	17.3 (5)	15.6 (5)
EFVM	15.2 (8)	19.0 (7)	n.d.	n.d.
RTV	20.0 (0.6)	20.6 (0.5)	18.9 (0.1)	19.2 (0.2)

<sup>a</sup> Numbers and letters in parenthesis refer to the sampling sites in the respective WWTPs (**Figure S2**).

<sup>b</sup> Membrane bioreactor.

<sup>c</sup> Not detected.

## References

- Botero-Coy, A.M., Martínez-Pachón, D., Boix, C., Rincón, R.J., Castillo, N., Arias-Marín, L.P., Manrique-Losada, L., Torres-Palma, R., Moncayo-Lasso, A., Hernández, F., 2018. An investigation into the occurrence and removal of pharmaceuticals in Colombian wastewater. *Sci. Total Environ.* 642, 842–853. doi:10.1016/j.scitotenv.2018.06.088
- K'oreje, K.O., Vergeynst, L., Ombaka, D., De Wispelaere, P., Okoth, M., Van Langenhove, H., Demeestere, K., 2016. Occurrence patterns of pharmaceutical residues in wastewater, surface water and groundwater of Nairobi and Kisumu city, Kenya. *Chemosphere* 149, 238–244. doi:10.1016/j.chemosphere.2016.01.095
- Prasse, C., Schlüsener, M.P., Schulz, R., Ternes, T.A., 2010. Antiviral drugs in wastewater and surface waters: A new pharmaceutical class of environmental relevance? *Environ. Sci. Technol.* 44, 1728–1735. doi:10.1021/es903216p
- US Environmental Protection Agency, 2012. Estimation Programs Interface Suite™ for Microsoft® Windows.
- Wood, T.P., Duvenage, C.S.J., Rohwer, E., 2015. The occurrence of anti-retroviral compounds used for HIV treatment in South African surface water. *Environ. Pollut.* 199, 235–243. doi:10.1016/j.envpol.2015.01.030



Declaration with signatures in possession of candidate and supervisor.


**Declaration by the candidate:**

Regarding **Chapter 4**, the nature and scope of my contribution were as follows:

Nature of contribution	Extent of contribution (%)
Performed the experiments, data analysis, co-wrote paper	65

The following co-authors have contributed to **Chapter 4**:

Name	E-mail address	Nature of contribution	Extent of contribution (%)
Maria A. Stander	<a href="mailto:lcms@sun.ac.za">lcms@sun.ac.za</a>	Assisted with experimental set-up and data manipulation; editorial input	15
André de Villiers	<a href="mailto:ajdevill@sun.ac.za">ajdevill@sun.ac.za</a>	Co-wrote paper	20

Signature of candidate: 

Date: 28<sup>th</sup> February 2021

**Declaration by co-authors:**

The undersigned confirm that:

1. The declaration above accurately reflects the nature and extent of the contributions of the candidate and the co-authors to **Chapter 4**,
2. No other authors contributed to **Chapter 4** besides those specified above, and
3. Potential conflicts of interest have been revealed to all interested parties and that the necessary changes have been made to use the material in Chapter 3 of this dissertation.

Signature	Institutional affiliation	Date
	Stellenbosch University	1 October 2020
	Stellenbosch University	24 February 2021

## **Chapter 4**

---

**Evaluation of supercritical fluid chromatography-tandem mass spectrometry (SFC-MS/MS) for the analysis antiretrovirals and their selected metabolites in wastewater**

## Abstract

Supercritical fluid chromatography (SFC) is increasingly being used in pharmaceutical analysis, where it has demonstrated a wide application range. The technique has however found relatively limited application in the determination of pharmaceuticals in environmental samples. Here we report an evaluation of the potential of SFC-MS/MS as an alternative to UHPLC-MS/MS for the analysis of antiretroviral drugs (ARVs) and selected metabolites in wastewater samples. A range of stationary phases were screened for the separation of six commonly prescribed ARVs and three known metabolites. An optimised method suitable for the analysis of all target parent drugs and a known metabolite of nevirapine was developed on an Acquity UPC<sup>2</sup> BEH column using a gradient of up to 60% methanol as modifier. In addition, lyophilisation was evaluated as sample pre-treatment step for the pre-concentration of the target analytes from wastewater samples. This method was validated, and its performance compared to a recent UHPLC-MS/MS method utilising direct injection and SPE sample clean-up reported for the same application. The SFC-MS/MS method provided good chromatographic performance and acceptable peak shapes and sensitivity, with the exception of two ARV metabolites, which could not be detected using positive electrospray ionisation. Limits of detection were generally higher than measured by direct injection UHPLC-MS/MS, and linear ranges were narrower, although in combination with lyophilisation method detection limits were sufficient for the trace-level detection of the target analytes in wastewater samples. Significantly improved recoveries for the polar nucleoside ARVs lamivudine and emtricitabine were obtained by lyophilisation compared to SPE samples clean-up, whereas recovery data for the hydrophobic analytes were comparable for both methods. Matrix effects measured for influent and effluent wastewater samples revealed severe ion suppression for lamivudine in lyophilised samples. Finally, analysis of a wastewater samples confirmed excellent agreement between quantitative data obtained by SFC- and UHPLC-MS/MS. Overall, SFC is shown to be a viable complementary alternative to LC for the analysis ARVs in environmental samples.

## 4.1 Introduction

The deterioration of aquatic ecosystems as a result of the sustained discharge of toxic and environmentally-persistent contaminants into rivers and streams has become an important environmental problem (Fatta-Kassinos *et al.*, 2011). The environmental release of pharmaceuticals is of particular concern, due to ecosystem alterations that may result from the presence of these compounds (Oller *et al.*, 2011; Pal *et al.*, 2014). Recent research has confirmed the emergence of a more complex class of pollutants in the form of human-excreted remnants of pharmaceuticals and their metabolites (Brown and Wong, 2015; Camacho-Muñoz and Kasprzyk-Hordern, 2015). Antiretrovirals (ARVs) represent a class of emerging pharmaceutical contaminants which have received significant attention in recent years (Mlunguza *et al.*, 2020; Peng *et al.*, 2014; Prasse *et al.*, 2010; Wood *et al.*, 2015). The development of analytical methods targeting ARV drugs and their metabolites is therefore important in order to complement the ongoing surveillance and biomonitoring of pharmaceutical pollutants in aquatic ecosystems.

Currently, liquid chromatography-tandem mass spectrometry (LC-MS/MS) is the mainstream technique for the detection of emerging trace-level environmental pollutants (Abafe *et al.*, 2018; Ngumba *et al.*, 2016). However, the diversity in physicochemical characteristics of the main ARV classes – nucleoside reverse transcriptase inhibitors (NRTIs), non-nucleoside reverse transcriptase inhibitors (*n*NRTIs) and protease inhibitors (PIs) – means that most LC-MS/MS methods are mainly suitable for selected target ARVs (Mosekiemang *et al.*, 2019). This is exacerbated by the common use of reversed-phase (RP) solid phase extraction (SPE) for sample clean-up (Brown and Wong, 2015), which limits the scope of current validated methods.

Supercritical fluid chromatography (SFC) offers an alternative to HPLC for the analysis of pharmaceutical compounds (Alexander *et al.*, 2012, 2013; Desfontaine *et al.*, 2016; Desfontaine and Guillaume, 2015; Grand-Guillaume Perrenoud *et al.*, 2012a; Nováková *et al.*, 2014; Romand *et al.*, 2016). Although not historically considered suitable for this purpose – SFC is prone to peak broadening, especially for polar, basic compounds (Desfontaine *et al.*, 2016; Grand-Guillaume Perrenoud *et al.*, 2012b, 2012a) – the re-emergence of packed-column SFC and the availability of improved instrumentation have highlighted the potential of the technique for pharmaceutical analysis (Alexander *et al.*, 2013, 2012; Desfontaine and Guillaume, 2015; Grand-Guillaume Perrenoud *et al.*, 2012b; Nováková *et al.*, 2014). SFC offers several potential benefits compared to HPLC, including faster analyses and lower pressures (due to increased diffusion and lower viscosity, respectively), lower organic solvent consumption (Alexander *et al.*, 2013; Desfontaine *et al.*, 2016, 2015; Desfontaine and Guillaume, 2015; Dispas *et al.*, 2016; Grand-Guillaume Perrenoud *et al.*, 2012a; Lemasson *et al.*, 2015; Tarafder, 2018) and alternative selectivity (Ashraf-Khorassani and Taylor, 2010; Grand-Guillaume Perrenoud *et al.*, 2012a). The technique is also compatible with ESI-MS detection, and therefore

suitable for trace-level environmental analyses. Although SFC is increasingly being used in pharmaceutical analysis (Alexander *et al.*, 2012; Desfontaine *et al.*, 2015; Grand-Guillaume Perrenoud *et al.*, 2012a), including ARVs (Akbal and Hopfgartner, 2017; Alexander *et al.*, 2013), the technique has to date found limited application in the analysis of pharmaceutical contaminants in environmental samples (Camacho-Muñoz and Kasprzyk-Hordern, 2015; Svan *et al.*, 2018).

For the analysis of multi-class ARVs in environmental samples, there is a need for a more universal mode of sample preparation (Backe and Field, 2012; Brewer and Lunte, 2015; Ngumba *et al.*, 2016). SPE is widely used for this purpose, but recoveries are analyte-dependant (Ngumba *et al.*, 2016; Prasse *et al.*, 2010). For example, polar NRTIs such as lamivudine (3TC) and emtricitabine (FTC) are not effectively retained on RP SPE cartridges, resulting in poor recoveries. Lyophilisation offers a relatively unexplored, simple and inexpensive alternative to SPE (Hu *et al.*, 2014; Narayan *et al.*, 2011). The technique has found limited application in the enrichment of diverse compounds from aqueous environmental samples to date (de Voogt *et al.*, 2000; Hirsch *et al.*, 1998; Hu *et al.*, 2014; Ramirez *et al.*, 2014), including for the analysis of some ARVs by HILIC-MS/MS (Boulard *et al.*, 2018). Lyophilisation offers several potential benefits, including its low cost and high throughput, but most importantly it offers an environmentally benign form of sample preparation (Hu *et al.*, 2014). On the other hand, potential drawbacks of the technique include loss of volatile analytes (de Voogt *et al.*, 2000), potential irreproducible recoveries due to operational errors (Hirsch *et al.*, 1998; Ramirez *et al.*, 2014) and the fact that it is not suitable for sample clean-up and may co-concentrate interferents along with the analytes of interest.

In this work, we report an evaluation of the combination of lyophilisation and SFC-MS/MS as a novel and environmentally friendly alternative analytical approach to SPE-LC-MS/MS for the analysis of multi-class ARVs in municipal wastewaters. Quantitative data obtained for six ARV compounds belonging to all three therapeutic classes, and two ARV metabolites, are compared to those obtained by a validated UHPLC-MS/MS method recently reported (Mosekiemang *et al.*, 2019), and the potential benefits and limitations of the proposed methodology are discussed.

## 4.2 Experimental

### 4.2.1 Chemicals and reagents

Analytical standards (>98% purity) for 12-hydroxy nevirapine (NVPM), efavirenz (EFZ), emtricitabine (FTC), lamivudine (3TC), nevirapine (NVP), ritonavir (RTV) and zidovudine (ZDV) were obtained from Clearsynth (Mumbai, India), while 8,14 dihydroxy efavirenz (EFVM), deuterated nevirapine (NVP-D<sub>3</sub>), desthiazolylmethyloxycarbonyl ritonavir (RTVM), and zidovudine glucuronide (ZDVG) (>98% purity) were obtained from Toronto Research Chemicals (Toronto, Canada) (**Figure 4.1**). All reagents used in this study were LC-MS grade or better. Methanol (MeOH) was supplied by Romil Ltd.

(Waterbeach, Cambridge, GB). Formic acid (FA) and ammonium hydroxide (NH<sub>4</sub>OH) were supplied by Merck Millipore (Cape Town, South Africa). Laboratory water was prepared in-house using a Millipore Direct Q3 system.

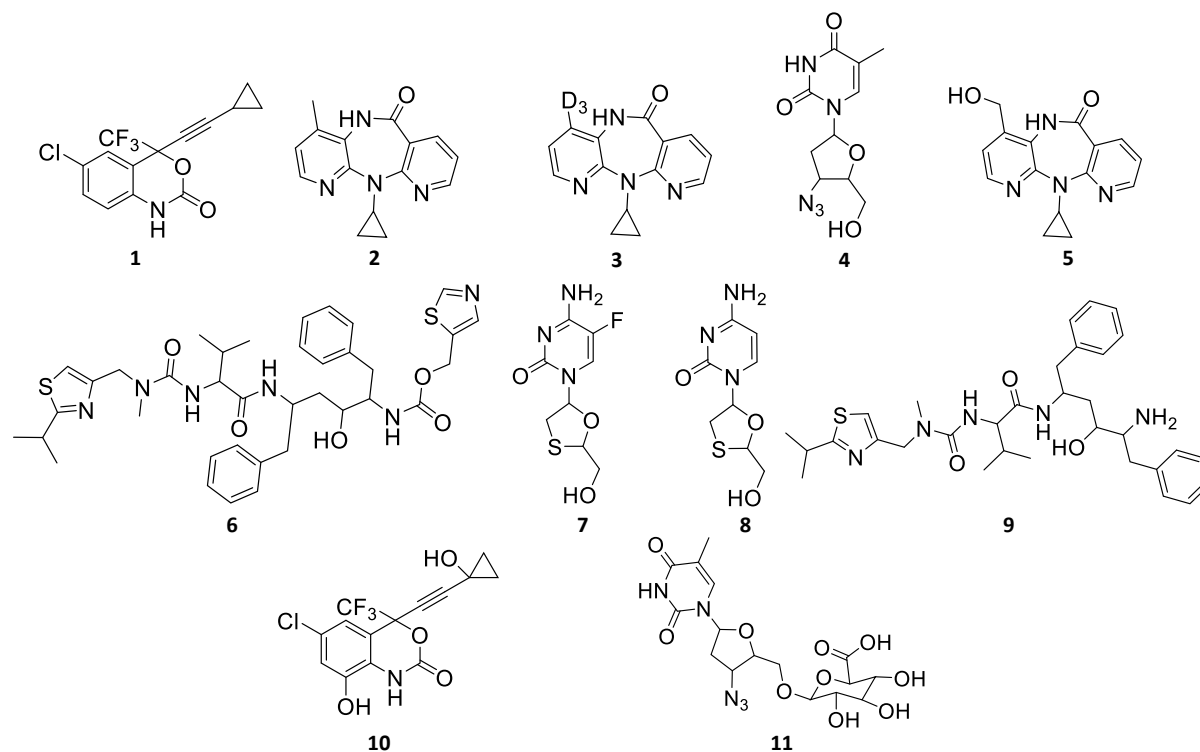


**Figure 4.1:** Molecular structures of the ARVs and their metabolites evaluated in the current study: **1)** EFZ, **2)** NVP, **3)** NVP-D<sub>3</sub>, **4)** ZDV, **5)** NVPM, **6)** RTV, **7)** FTC, **8)** 3TC, **9)** RTVM, **10)** EFVM, **11)** ZDVG. For full names of compounds, refer to **Section 4.2.1**.

#### 4.2.2 SFC experimental conditions and column evaluation

The Acquity UPC<sup>2</sup> system used in this work comprised a binary solvent pump, column compartment, convergence manager controlling the automatic back pressure regulator (ABPR), and a sample manager module (Waters, Milford, MA). The mobile phases were CO<sub>2</sub> and MeOH, while the ABPR was set at 1700 psi. The sample compartment was maintained at room temperature and the injection volume was 2 μL. Five SFC columns with different ligand chemistries (Acquity UPC<sup>2</sup> BEH 2-EP (2-ethylpyridine), Acquity UPC<sup>2</sup> Torus-1 AA (1-aminoanthracene), Acquity UPC<sup>2</sup> Torus-2 PIC (2-picolylamine), Acquity UPC<sup>2</sup> BEH (ethylene bridged hybrid), and Acquity HSS (high strength silica) C18) SB and the same dimensions (100 × 3.0 mm, 1.7 μm particle size) were evaluated using the same gradient conditions described below.

The optimised method used an Acquity UPC<sup>2</sup> BEH column (100 × 3.0 mm, 1.7 µm particle size) maintained at 60°C. The gradient was performed at 1 mL/min as follows: 98% CO<sub>2</sub> (0–0.2 min), 98–77.7% CO<sub>2</sub> (0.2–5 min), 77.7–40% CO<sub>2</sub> (5–7 min), 40% CO<sub>2</sub> (7–7.2 min), 40–98% CO<sub>2</sub> (7.20–9 min), 98% CO<sub>2</sub> (9–11 min).

#### 4.2.3 Mass spectrometric optimisation

A Xevo TQ-S triple quadrupole mass spectrometer was used (Waters). An auxiliary pump (Waters 515) was connected post-column with a zero-dead-volume T-piece in a ‘pre-BPR splitter with sheath pump interface’ configuration (Guillarme *et al.*, 2018) to deliver 1% FA in MeOH at a flow rate of 0.2 mL/min prior to the MS. The source and desolvation temperatures were set at 150°C and 350°C, respectively, with N<sub>2</sub> desolvation and cone gas flows of 900 and 150 L/h, respectively. The capillary and cone voltages were set at 3.8 kV and 20 V.

Detection was performed using electrospray ionisation and multiple reaction monitoring (MRM) scanning mode. Initial scouting experiments were performed in both positive and negative ionisation modes, with the final method using positive ionisation. ZDVG and EFVM could not be detected in negative mode using polarity-switching (Mosekiemang *et al.*, 2019), likely due to the 1% FA in MeOH make-up flow used in the present work. MRM settings were determined based on preliminary precursor ion and fragment ion scan experiments performed by infusion of individual standards (52 ng/mL) in MeOH. Precursor ion acquisition was performed at cone voltages (CVs) of 15–30 V to determine the optimum CV, and these values were used to optimise collision energies (CEs) in the range 15–30 eV in subsequent fragment ion scan experiments. For these experiments, the dwell and cycle times ( $t_{\text{dwell}}$ ,  $t_{\text{cycle}}$ ) were automatically set (MassLynx version 4.1), and the number of data points per peak was set to 10. For quantification, the most intense fragment ion was assigned as the quantifier ion (Q), and the second most intense fragment ion as the qualifier ion (q). The optimised experimental conditions as well as transition ion ratios are listed in **Table S4.1 (Supplementary Information, SI)**.

#### 4.2.4 Preparation of calibration standard solutions

A series of working standard solutions were prepared by dilution of a 20 µg/mL MeOH stock solution containing all analytes to the following concentrations: 0.610, 1.22, 2.44, 4.88, 9.77, 19.5, 39.1, 78.1, 156, 312 ng/mL. Calibration samples comprising ten levels were prepared by diluting 2 mL of each working standard solution and 0.9 mL of isotopically labelled internal standard solution (ILIS, NVP-D<sub>3</sub>, 100 ng/mL in MeOH) to 3 mL with MeOH. The calibration concentration range was therefore 0.407–208 ng/mL, with a constant ILIS concentration of 30 ng/mL.

#### 4.2.5 Sample collection and preparation

Samples were collected from two wastewater treatment plants (WWTPs) as recently described (Mosekiemang *et al.*, 2019). For comparison of quantitative data obtained using the present SFC-MS/MS method and a recently reported direct injection UHPLC-MS/MS method (Mosekiemang *et al.*, 2019), a raw wastewater sample collected during a severe drought period (April 2018) was used, given the likelihood of detection of most compounds at significant concentrations. Sample preparation entailed filtering to remove suspended solids and adjusting the pH to 7 using either 5% NH<sub>4</sub>OH or 5% FA. Prior to enrichment, 300 µL of ILIS (100 ng/mL) was added to each sample before diluting with the sample matrix to 50 mL (ILIS concentration 0.6 ng/mL). For the recovery samples, 75 µL of either 0.02, 0.2 and 2 µg/mL standard solution was also spiked prior to dilution to 50 mL with the sample matrix (spiking levels at 0.03, 0.3 and 3 ng/mL, each containing 0.6 ng/mL ILIS, **Figure S4.1, Phase 1, SI**).

##### 4.2.5.1 Lyophilisation

Sample aliquots (50 mL) were transferred to 100 mL round-bottom flasks and frozen in a liquid nitrogen bath for 10–15 minutes. Frozen samples were mounted on a Beta 1-8 LD plus Freeze drier (Christ, Germany) operated at 0.03 mbar and -20°C for 24 hours or until completely dry. Desiccated residues were re-suspended with 4 mL FA/MeOH (5/95, v/v) and vortexed for 5 min. The reconstituted solutions were dispensed into 10 mL polytop vials and evaporated to dryness under a gentle stream of N<sub>2</sub> (**Figure S4.1, Phase 2, SI**).

##### 4.2.5.2 Solid phase extraction

Strata-SDB-L cartridges (200 mg/6 mL, Phenomenex, Torrance, USA) were used with a 24-port vacuum extraction SPE manifold (Restek, Bellefonte, USA). Cartridges were conditioned sequentially with 4 mL acetonitrile (ACN), MeOH and equilibrated with 4 mL pH-adjusted water (pH = 7). Sample aliquots (50 mL) were loaded, and the cartridges were rinsed with 4 mL pH 7 water at ~1 mL/min. The cartridges were dried under vacuum for 15 min, before elution with 4 mL FA/MeOH (5/95, v/v). The collected fractions were dried under a gentle stream of N<sub>2</sub> (**Figure S4.1, Phase 2, SI**).

#### 4.2.6 Reconstitution of dried extracts

Resuspension of lyophilised and SPE extracts followed the same procedure. Briefly, the N<sub>2</sub>-dried extracts for pre-extraction fortified samples and method blanks were reconstituted with 1 mL MeOH. All samples therefore contained 30 ng/mL ILIS after enrichment, and the fortified samples 1.5, 15 or 150 ng/mL standards. Post-enrichment fortification samples were prepared by spiking N<sub>2</sub>-dried blanks with 75 µL of either 0.02, 0.2 or 2 µg/mL standard solutions prior to dilution to 1 mL with MeOH, to



give post-extraction fortification concentrations of 1.5, 15 or 150 ng/mL, respectively. The same spiked concentrations were prepared in MeOH (**Figure S4.2, SI**).

#### 4.2.7 Evaluation of method performance

Method performance was evaluated using conventional method validation parameters, including linearity, linear range, selectivity, limit of detection (LOD), limit of quantification (LOQ), method detection limit (MDL), method quantification limit (MQL), repeatability and reproducibility (Evard *et al.*, 2016a, 2016b; SANTE, 2015).

The linearity of the standard curves (10-point internal standard calibration curve, 4 repetitions/point) was studied in the range LOD–104 ng/mL for NVP and NVPM and MQL–208 ng/mL for the rest of the compounds. The reduced linear range for NVP and NVPM is a result of saturation of the detector at the highest calibration level; as a consequence, recoveries and matrix effects (%) could not be calculated at the highest spiking level (150 ng/mL) for these compounds. Linearity was assessed using the coefficient of determination ( $R^2$ ) for each calibration curve. LODs and LOQs were determined from the calibration curve, as 3.3 and 10 times, respectively, the standard error of the intercept divided by the slope (**Equations S4.1 & S4.2, SI**) (Evard *et al.*, 2016b). MDL and MQL values were determined from LOD and LOQ values taking into account recoveries (%) and pre-concentration factors (50×) for lyophilisation and SPE, respectively (**Equations S4.3 & S4.4, SI**). Recovery (%) was estimated by dividing the blank-subtracted pre-extraction concentration by the blank-subtracted post-extraction concentration, expressed as a percentage (**Equation S4.5**), while matrix effects (%) were calculated by dividing blank-subtracted post-extraction fortified concentrations by neat solvent concentrations (**Equation S4.6, SI**) (Kruve *et al.*, 2015a, 2015b). Precision is expressed as %RSD of mean recoveries (%) at three spiking levels, calculated for within-day (repeatability) and between-days runs (reproducibility) over three consecutive days.

### 4.3 Results and Discussion

#### 4.3.1 Optimisation of SFC-MS/MS conditions

The MS detection parameters were previously optimised (Mosekiemang *et al.*, 2019) for LC separation on the same triple quadrupole instrument (Xevo TQ-S, **Section 4.2.3**). In the present study, re-optimisation using the SFC mobile phase and make-up flow was performed. The optimised MRM transitions, transition ratios, cone voltages and collision energies (**Section 4.2.3**) are listed in **Table S4.1 (SI)**, and example MRM chromatograms are presented in **Figure S4.4**. ZDVG and EFVM, detected in negative ionisation mode using polarity switching in our previous study (Mosekiemang *et al.*, 2019), were not detected in positive ionisation mode in the present study, likely due to the post-column addition of 1% FA in MeOH, and were therefore not included in further experiments.

For the separation of the target analytes, comprising six ARVs of three therapeutic classes as well as several of their metabolites (**Figure 4.1**), column screening experiments were performed to identify a phase providing acceptable retention and peak shapes for most compounds, considering the importance of peak symmetry in quantitative chromatography. Five common SFC phases were evaluated in this study (**Figure S4.3, SI**), and peak asymmetry ( $A_s$ ) factors (Snyder and Kirkland, 1979) for the compounds of interest were considered for column evaluation.

In the interpretation of our findings, extensive previous work on SFC column classification by linear solvation energy relationships (LSER) (Khater *et al.*, 2013; West *et al.*, 2016; West and Lesellier, 2008, 2006) and experimental data for basic compounds on the same stationary phases (Desfontaine *et al.*, 2016) are taken into account.

Generally, the elution order of the ARVs in SFC on all columns resembled that of normal phase (**Figure 4.2**), with apolar compounds (EFZ, NVP,  $\log K_{O/W} \geq 2$ ) showing lower retention than polar compounds (3TC, FTC,  $\log K_{O/W} \leq 0$ ). Exceptions are RTV and RTVM ( $\log K_{O/W} \geq 5$ ), both of which eluted relatively late on all columns, likely due to extensive ionic interactions (see below). Approximately gaussian peaks were observed for the early-eluting peaks (EFZ, NVP, NVPM), while tailing was observed for RTV, and especially FTC, 3TC and RTVM (**Table S4.2, SI**). The latter compounds showed extensive tailing on the 2-PIC and 2-EP columns, and some evidence of fronting on the HSS-C18 SB and BEH columns. The reason for the stark differences in peak symmetry observed for RTV and its metabolite RTVM is not clear, since these two compounds are structurally similar, but may be related to additional  $\pi$ - $\pi$  and silanol interactions. ZDV showed extensive fronting on the 2-PIC column. Some selectivity differences were also observed, with 3TC and FTC eluting earlier on the HSS-C18 SB and BEH columns, and ZDV eluting noticeably earlier on the HSS-C18 column (**Figure 4.2D & E**).

Also noteworthy is that the high retention observed for some of the target analytes necessitated the use of high contents of MeOH (up to 60%) in the mobile phase. Under these conditions, the mobile phase is no longer supercritical, and the separation can be more accurately described as ‘enhanced fluidity’ chromatography (Cui and Olesik, 1991; Pereira *et al.*, 2011). Nevertheless, the benefits of the CO<sub>2</sub>-based mobile phase remain valid, and enhanced fluidity chromatography is beneficial in the context of extending the applicable range of SFC to highly polar analytes (West, 2015).

The stationary phases evaluated in the present study for ARV analysis can broadly be grouped into polar bonded (1-AA, 2-PIC, BEH-2EP), polar unbonded (BEH) and apolar aliphatic phases (HSS C18 SB) with some polar character, since this phase is not end capped) (West and Lesellier, 2006). At the estimated pH of the CO<sub>2</sub>/MeOH mobile phase (~4-5(Desfontaine *et al.*, 2016)), the target ARV’s are expected to be positively charged as a consequence of their high pK<sub>a</sub>’s (~10-13.7) (Mosekiemang *et al.*, 2019).

On the polar bonded 1-AA, 2-PIC and 2-EP phases, similar elution orders were observed. On these phases, interaction of the is mainly governed by dipole interactions and hydrogen bonding with bases (West and Lesellier, 2006), whereas additional electrostatic repulsion as a result of protonation of the basic bonded ligands prevents secondary ionic interaction of the target analytes with residual silanols (Desfontaine *et al.*, 2016, 2015). This phenomenon may partially be responsible for the generally good peak shapes observed on these columns. Between these columns, the 1-AA phase shows slightly higher retention. A similar observation for basic drugs has been ascribed to either the lower basic  $pK_a$  of this ligand, resulting in reduced repulsion, or additional  $\pi$ - $\pi$  interactions with the target analytes (Desfontaine *et al.*, 2016).

Regarding the unbonded BEH phase, it has been established that the retention mechanisms for this column are entirely governed by the uniformly distributed silanols which are predominantly negatively charged (Desfontaine *et al.*, 2016; Hirose *et al.*, 2019). The ethylene bridge in the BEH silica matrix is said to be instrumental in providing symmetrical peaks compared to the old generation of silica material (Desfontaine *et al.*, 2016). Similar interactions to those listed for the polar bonded phases are involved in the retention of basic compounds, with stronger hydrogen bonding and electrostatic interactions with the silanols being more influential on this phase (West and Lesellier, 2006). All target analytes were detected with acceptable peak shapes using this column.

The relatively similar elution order observed on the HSS C18 SB phase (**Figure 4.2D**) implies that, in addition to hydrophobic dispersion interactions of the aliphatic  $C_{18}$  backbone, additional interaction of the basic analytes with the more acidic silanol functional groups of this non end capped phase also plays an important role in retention (West and Lesellier, 2006). This may explain the tailing observed for the most retained analytes (FTC, 3TC and RTVM). Partial exceptions are the relatively polar ( $\log K_{ow}$ 's close to 0) ZDV and FTC, which elute relatively much earlier on this phase.

In summary, the apolar ARVs showed relatively good peak shapes, whereas noticeable peak deformation was observed for 3TC, FTC and RTVM on all test columns (**Figure 4.2**) due to slow secondary interactions. Overall, peak symmetry was worse than is the case for the RP-LC separation of the same compounds (Mosekiemang *et al.*, 2019), as expected considering the nature of SFC. Further improvement in peak shapes may be obtained by the addition of suitable additives to the mobile phase and/or the injection solvent (Bennett *et al.*, 2019; Desfontaine *et al.*, 2016; Grand-Guillaume Perrenoud *et al.*, 2012a; Lemasson *et al.*, 2015), although this was not attempted in the present study since the chromatographic performance was sufficient to allow separation and quantification of the target analytes.

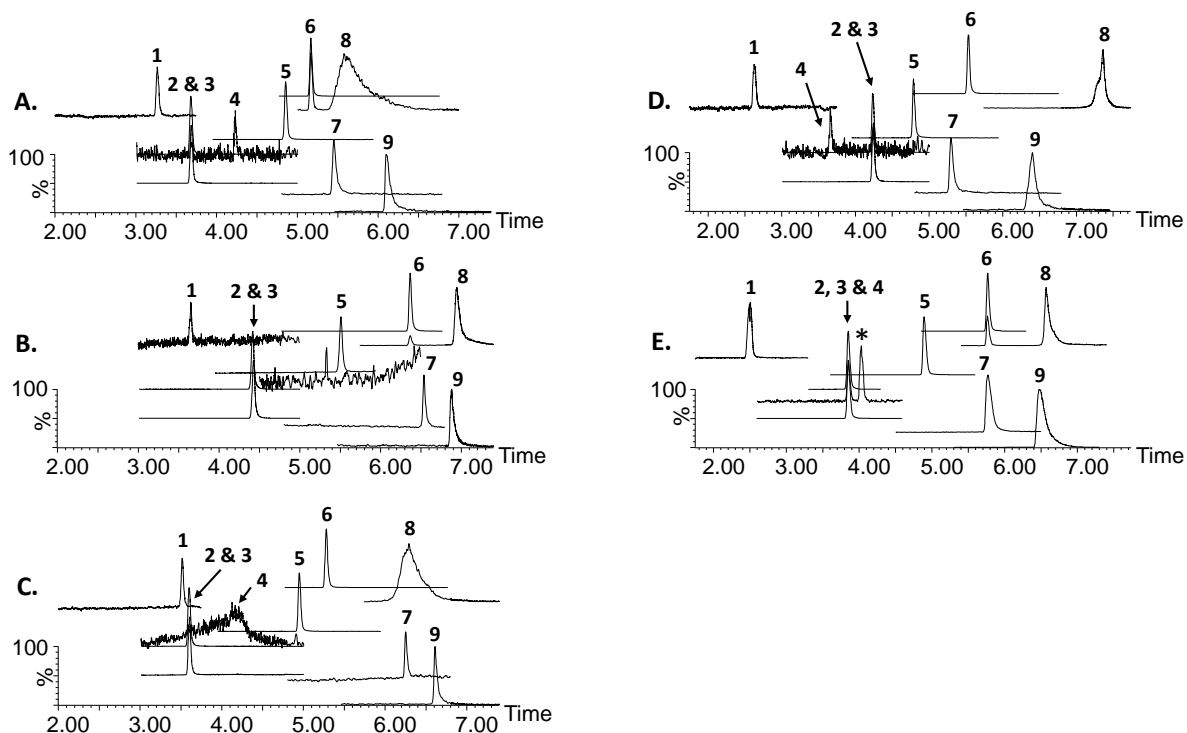


**Figure 4.2:** Representative total ion chromatograms (TICs) obtained for the SFC-MS/MS analysis of the target ARV compounds in a 52.1 ng/mL MeOH standard: (1) EFZ, (2) NVP, (3) NVP-D<sub>3</sub>, (4) ZDV, (5) NVPM, (6) RTV, (7) FTC, (8) RTVM and (9) 3TC on (A) BEH 2-EP, (B) Torus 1-AA, (C) Torus 2-PIC, (D) HSS C18 SB and (E) BEH columns. The peak denoted by an asterisk in (E) is a background signal. SFC-MS/MS conditions are described in **Section 4.2.2**. Compound abbreviations are defined in **Section 2.1** and **Figure 1**.

Considering the above, the BEH column was selected in the present study based on its ability to elute all target compounds with acceptable peak shapes. Most compounds were also sufficiently resolved, with the exception of the partial co-elution of NVP/NVP-D<sub>3</sub> and ZDV, as well as RTV and FTC. These analyte pairs were successfully differentiated based on their unique mass-to-charge ratios used in the relevant MRM ion transition pairs. The inter-channel delay time and other critical MRM parameters ( $t_{\text{dwell}}$ ,  $t_{\text{cycle}}$ ) (Hermes *et al.*, 2018) were optimised using the instrument software to provide sufficient data points across each peak. **Figure 4.3** demonstrates as example the successful differentiation of the Q and q transitions for the closely eluting NVP and ZDV peaks in a fortified wastewater sample.

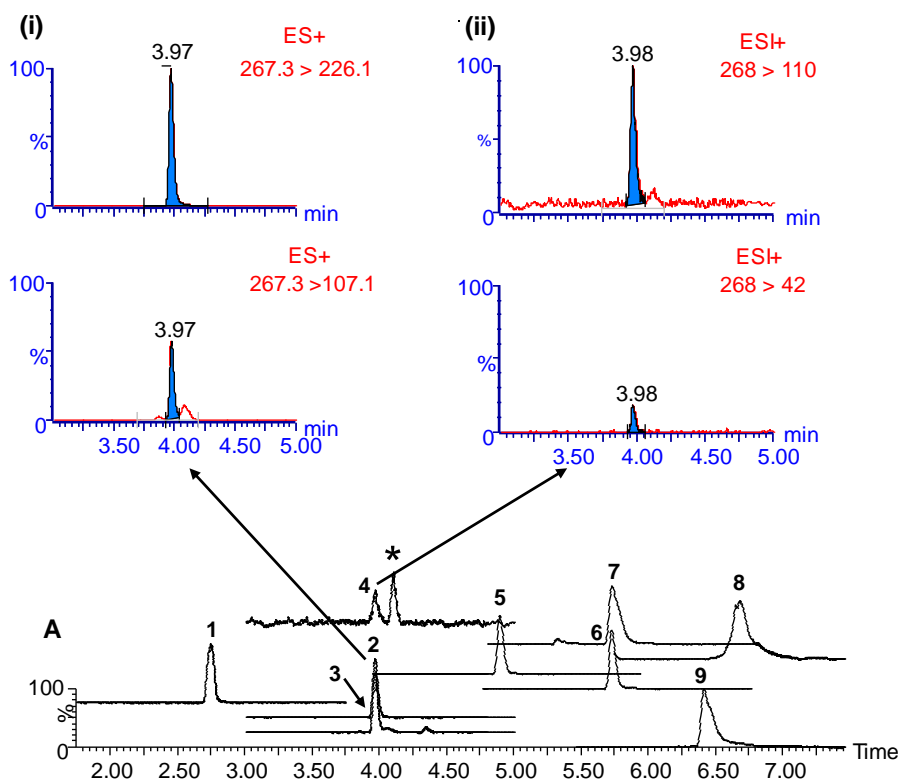


**Figure 4.3:** (A) Representative TICs obtained for the SFC-MS/MS analysis of the target ARV compounds in a fortified wastewater sample (52.1 ng/mL) processed by lyophilisation. Target compounds are: (1) EFZ, (2) NVP, (3) NVP-D<sub>3</sub>, (4) ZDV, (5) NVPM, (6) RTV, (7) FTC, (8) RTVM and (9) 3TC separated using the Acquity UPC<sup>2</sup> BEH column. Integrated chromatograms for the partially co-eluting (i) NVP and (ii) ZDV are shown to illustrate the selectivity of the MRM transitions. \* denotes a background signal. SFC conditions are described in **Section 4.2.2**. Compound abbreviations are defined in **Section 4.2.1** and **Figure 4.1**.

#### 4.3.2 Comparison of SPE and lyophilisation for sample preparation

In a recent study, we found relatively poor recoveries for the NRTI ARVs (ZDVG, ZDV, FTC and 3TC) from wastewater samples using RP-SPE (Mosekiemang *et al.*, 2019). This prompted us in the present work to investigate lyophilisation as a potentially simpler, more universal and solventless alternative to SPE (Hu *et al.*, 2014; Welch *et al.*, 2010) for wastewater analysis. For this work, an isotopically labelled internal standard (NVP-D<sub>3</sub>, ILIS) was added prior to extraction to compensate for sample handling variations. The extraction efficiencies of both lyophilisation and SPE were then compared in terms of both relative (i.e., ILIS-corrected) and absolute (non-ILIS-corrected) recoveries (**Table 4.1**). Detailed summaries of the recovery data measured at the three studied levels (0.03, 0.3 and 3 ng/mL) are presented in **Tables S4.3-4.5, SI**.

The relative recoveries obtained by lyophilisation for wastewater effluent samples were adequate (63–99%) across the spiking levels for all compounds. The exception is RTVM, which could not be accurately quantified, either due to adsorption in the chromatographic system (previously hypothesised (Mosekiemang *et al.*, 2019)) or losses during freeze-drying (de Voogt *et al.*, 2000). The same trend was manifested in influent samples, albeit with slightly higher recoveries in the range of 68–108%. In contrast, recoveries by SPE were good for apolar compounds of the *n*NRTI and PI classes (NVP, NVPM, RTV, EFZ, as well as RTVM), and poor for the NRTIs 3TC and FTC (10–63%). These findings are in accordance with previous literature reports (Mosekiemang *et al.*, 2019; Prasse *et al.*, 2010; Wood *et al.*, 2015). Notably, lyophilisation offered significantly better recoveries for the polar target analytes, again in agreement with previous reports (Boulard *et al.*, 2018). Indeed, the results for the recovery study indicate the suitability of this form of sample preparation for the analysis of the target analytes spanning a relatively wide range of polarities. The technique therefore offers a potentially complementary sample preparation route to RP-SPE, which suffer from poor recoveries for polar analytes (Nannou *et al.*, 2019), and an alternative to direct injection (Mosekiemang *et al.*, 2019) when matrix effects or sensitivity are a concern, although care should be exercised to avoid analyte losses (de Voogt *et al.*, 2000; Stahnke *et al.*, 2012).

In addition, absolute recoveries (*i.e.* not corrected by the ILIS) were also measured. These values are informative in the context of providing a measure of the true analyte extraction efficiencies not corrected for sample handling or ionization variations (Kruve *et al.*, 2015a, 2015b). Overall, there were few notable differences between relative and absolute recoveries for the respective methods, suggesting that minimal analyte losses were incurred during sample preparation. The worse absolute recoveries for 3TC and FTC by SPE could be ascribed to partial compensation of analyte losses by the ILIS (partial because of structural differences between the ILIS and analytes), although matrix effects related to different retention times may also play a role (Furey *et al.*, 2013). Satisfactory absolute recoveries (*i.e.* 53–118%) were obtained for all target analytes in influent and effluent samples across spiking levels by lyophilisation.

**Table 4.1:** A summary of analyte recoveries determined by SFC-MS/MS for lyophilisation and SPE sample preparation of spiked wastewater samples. Values reported as a recovery range determined at 0.03, 0.3 and 3 ng/mL. For further details, refer to **Tables S4.3-S4.5**.

Matrix	Recovery (%)	Analytes							
		EFZ	NVP	ZDV	NVPM	RTV	FTC	3TC	RTVM
Effluent	ILIS-corrected								
	a) Lyophilisation	82.4–95.9	71.7–73.0 <sup>a</sup>	81.0 <sup>b</sup>	74.5–77.4 <sup>a</sup>	62.9–84.4	65.5–75.6	73.1–98.9	n.q. <sup>d</sup>
	b) SPE	87.2–97.0	99.1–103 <sup>a</sup>	114 <sup>b</sup>	98.6–101 <sup>a</sup>	77.4–88.5	21.8–41.7	24.0–41.2	56.2–58.7
	Non-ILIS-corrected								
	a) Lyophilisation	53.2–118	77.2–89.2 <sup>a</sup>	84.8 <sup>b</sup>	79.8–86.4 <sup>a</sup>	73.6–86.3	56.7–88.0	65.1–82.4 <sup>c</sup>	n.q.
	b) SPE	49.3–98.2	89.5–101 <sup>a</sup>	89.3 <sup>b</sup>	89.4–103 <sup>a</sup>	72.4–87.1	23.2–40.4	19.1–30.5	34.1–57.3
Influent	ILIS-corrected								
	a) Lyophilisation	100–108	94.8–94.8 <sup>a</sup>	98.0 <sup>b</sup>	86.8–96.7 <sup>a</sup>	84.8–89.7	67.6–104	99.6–103	n.q.
	b) SPE	63.6–101	99.7–107 <sup>a</sup>	106 <sup>b</sup>	101–111 <sup>a</sup>	87.7–95.5	23.0–63.3	19.3–50.7	78.1–90.1
	Non-ILIS-corrected								
	a) Lyophilisation	65.3–112	85.8–88.5 <sup>a</sup>	95.8 <sup>b</sup>	85.5–91.3 <sup>a</sup>	70.1–90.2	67.0–81.7	91.5–101	n.q.
	b) SPE	70.9–97.7	89.6–105 <sup>a</sup>	114 <sup>b</sup>	84.7–105 <sup>a</sup>	78.1–99.5	13.7–34.9	10.2–21.5	72.9–80.3

<sup>a</sup> measured at 0.03 and 0.3 ng/mL.

<sup>b</sup> measured 3 ng/mL.

<sup>c</sup> measured at 0.3 and 3 ng/mL.

<sup>d</sup> n.q. – not quantified.

#### 4.3.3 Method evaluation and validation

*Linearity, sensitivity, repeatability and reproducibility.* A summary of the lyophilisation-SFC-MS/MS method performance is presented in **Table 4.2**. For all compounds, linearities for the calibration curves displayed coefficients of determination ( $R^2$ ) of 0.996 or better, with residual errors of  $\leq 20\%$ . Linear ranges were from LOD–208 ng/mL, with the exception of NVP and NVPM, for which the linear ranges were between MDL and 104 ng/mL due to the detector saturation (**Figure S4.4**). Superior linearity was obtained by SFC-MS/MS compared to our previous study using LC-MS/MS (Mosekiemang *et al.*, 2019). The MDLs were in the range 30–37 ng/L, with exception of ZDV which measured 113 ng/L, while MQLs were in the range 103–132 ng/L; sufficiently low to enable detection of ARVs at levels expected for these compounds in wastewater samples (Mosekiemang *et al.*, 2019; Ngumba *et al.*, 2016; Prasse *et al.*, 2010). The intra-day precision, a measure of instrumental repeatability, was  $\leq 9\%$  RSD at the three spiking levels (ZDV was not detected at the lower spiking levels, but nevertheless showed good repeatability). The precision values for instrumental reproducibility (inter-day precision) were slightly higher, in the ranges 2–14% and 2–15% RSD in effluent and influent samples, respectively. The overall intermediate precision values are within acceptable ranges (Kruve *et al.*, 2015a, 2015b).



**Table 4.2:** Summary of the performance attributes of the developed lyophilisation-SFC-MS/MS method.

Analyte s	$t_R^a$ (min)	Range (ng/mL)	$R^2$	LOD (ng/mL)	MDL (ng/mL)	MQL (ng/mL)	$As^b$	Precision (% RSD) <sup>c</sup>			
								Effluent		Influent	
								Intra-day	Inter-day	Intra-day	Inter-day
EFZ	2.76 ( $\pm$ 0.01)	1.48–208	0.999	1.48	0.0307	0.104	1.00 ( $\pm$ 0.4)	3 / 1 / <b>3</b>	6 / 4 / <b>4</b>	3 / 3 / <b>7</b>	5 / 6 / <b>7</b>
NVP	3.97 ( $\pm$ 0.004)	44.1–104	0.999	1.79	0.0377	0.126	1.05 ( $\pm$ 0.5)	3 / 7 / <b>5</b>	10 / 7 / <b>5</b>	3 / 1 / <b>3</b>	11 / 2 / <b>3</b>
ZDV	3.98 ( $\pm$ 0.02)	5.72–208	0.998	5.52	0.113	0.368	1.00 ( $\pm$ 0.3)	- / - / <b>3</b>	- / - / <b>2</b>	- / - / <b>4</b>	- / - / <b>4</b>
NVPM	5.04 ( $\pm$ 0.01)	1.48–104	0.998	1.48	0.0395	0.132	1.05 ( $\pm$ 0.2)	3 / 5 / <b>5</b>	6 / 4 / <b>5</b>	5 / 1 / <b>5</b>	5 / 15 / <b>6</b>
RTV	5.85 ( $\pm$ 0.004)	1.63–208	0.996	1.63	0.0342	0.126	1.05 ( $\pm$ 0.1)	3 / 8 / <b>6</b>	7 / 12 / <b>14</b>	9 / 4 / <b>7</b>	9 / 7 / <b>7</b>
FTC	5.87 ( $\pm$ 0.01)	1.24–208	0.997	1.24	0.0319	0.106	1.15 ( $\pm$ 0.1)	6 / 7 / <b>6</b>	8 / 13 / <b>5</b>	9 / 2 / <b>2</b>	7 / 6 / <b>9</b>
3TC	6.55 ( $\pm$ 0.01)	1.53–208	0.999	1.53	0.0308	0.103	1.20 ( $\pm$ 0.9)	3 / 8 / <b>1</b>	2 / 3 / <b>5</b>	8 / 6 / <b>6</b>	5 / 5 / <b>7</b>
RTVM	6.64 ( $\pm$ 0.01)	1.48–208	0.999	1.48	0.0328	0.109	1.20 ( $\pm$ 0.4)	- / - / <b>9</b>	- / - / <b>6</b>	- / - / <b>5</b>	- / - / <b>5</b>

<sup>a</sup> retention time  $\pm$  standard deviation for analytes in the neat solvent, effluent and influent samples (n = 15)

<sup>b</sup> Peak asymmetry,  $As = b/a$  where  $a$  and  $b$  are the distances from the peak leading edge to peak maximum and from the maximum to the peak trailing edge at 10% height, respectively. Average  $\pm$  standard deviation for peaks measured in neat solvent, influent and effluent matrices (n = 15).

<sup>c</sup> precision was calculated as % RSD for the intra-day % recoveries at three spiking levels (low / *mid* / **high**, n = 8).

*Matrix effects (MEs)*. Despite the sensitivity of ESI-SFC-MS/MS, the electrospray ionisation process is susceptible to matrix effects, especially when dealing with a complex sample matrix such as wastewater (Stahnke *et al.*, 2012; Svan *et al.*, 2018; Van De Steene and Lambert, 2008). Co-elution of non-target matrix constituents may result in ionisation suppression or enhancement (Hewavitharana *et al.*, 2018), and indeed is a common occurrence in the LC-ESI-MS/MS analysis of wastewater samples (Van De Steene and Lambert, 2008). Due to the different mobile phases used in SFC, which has been shown to play a role in matrix effects (Hirose *et al.*, 2019; Svan and Hedeland, 2018), it was considered relevant to assess the extent of matrix effects for the proposed method. Matrix effects (MEs) were assessed using **Equation S4.6 (SI)** (Svan and Hedeland, 2018). Evaluation of ME may be hampered by several other factors, including the possibility of CO<sub>2</sub> decompression at the SFC-MS interface leading to analyte precipitation (Akbal and Hopfgartner, 2020) and poor t<sub>R</sub> repeatability (Hirose *et al.*, 2019). No evidence of t<sub>R</sub> fluctuations were observed in the present study (**Table 4.2**).

The results are summarised in **Table 4.3**, which provides an overview of matrix effects for effluent and influent samples processed by both SPE and lyophilisation. Generally, ion enhancement was more common in effluent samples, whereas ion suppression was more prevalent in influent samples. Effluent samples prepared by lyophilisation showed slightly higher ion enhancement compared to SPE, except for 3TC, which, despite high absolute recoveries, suffered severe ion suppression (~95%) in lyophilised samples. This is not entirely surprising, since lyophilisation is in essence not a sample clean-up method that suffers from poor selectivity for non-volatile analytes and may potentially enrich interferents together with the target analytes. On the other hand, the selectivity associated with the stationary phase chemistry and washing and elution solvents in SPE play an important role in reducing matrix effects.

Furthermore, ion suppression was slightly more enhanced for most compounds in the lyophilised influent samples (with the exception of 3TC, where this effect was much more pronounced, especially at higher concentrations). RTVM, which was not quantified by lyophilisation method, exhibited severe ion enhancement (up to 59%) in SPE processed samples. Overall, the proposed lyophilisation method yielded acceptable recoveries (53–118%) and relatively low matrix effects (57–129%), with the exception of 3TC and RTVM.

**Table 4.3:** Summary of ILIS-corrected matrix effects determined for the target analytes in effluent and influent wastewater samples processed by lyophilisation and SPE at 0.03, 0.3 and 3 ng/mL spiking levels (n= 5, standard deviations are specified in brackets).

Matrix	Spiking level	Analytes							
		EFZ	NVP	ZDV	NVPM	RTV	FTC	3TC	RTVM
Effluent	0.03 ng/mL								
	a) Lyophilisation	112 ( $\pm$ 9)	126 ( $\pm$ 4)	n.d. <sup>a</sup>	114 ( $\pm$ 8)	129 ( $\pm$ 4)	98.2 ( $\pm$ 4)	5.8 ( $\pm$ 1)	n.q. <sup>b</sup>
	b) SPE	74.4 ( $\pm$ 3)	104 ( $\pm$ 5)	n.d.	89.0 ( $\pm$ 1)	103 ( $\pm$ 2)	97.8 ( $\pm$ 7)	109 ( $\pm$ 1)	110 ( $\pm$ 4)
	0.3 ng/mL								
	(a) Lyophilisation	109 ( $\pm$ 7)	129 ( $\pm$ 7)	n.d.	128 ( $\pm$ 5)	129 ( $\pm$ 8)	112 ( $\pm$ 6)	4.7 ( $\pm$ 1)	n.q.
	(b) SPE	112 ( $\pm$ 13)	127 ( $\pm$ 2)	n.d.	103 ( $\pm$ 4)	114.0 ( $\pm$ 3)	93.7 ( $\pm$ 7)	99.4 ( $\pm$ 4)	119 ( $\pm$ 8)
	3 ng/mL								
	(a) Lyophilisation	105 ( $\pm$ 7)	121 ( $\pm$ 3)	119 ( $\pm$ 5)	123 ( $\pm$ 3)	105 ( $\pm$ 7)	116 ( $\pm$ 1)	4.7 ( $\pm$ 1)	n.q.
	(b) SPE	104.0 ( $\pm$ 5)	108 ( $\pm$ 1)	95.6 ( $\pm$ 2)	106 ( $\pm$ 1)	104.0 ( $\pm$ 5)	106 ( $\pm$ 8)	93.7 ( $\pm$ 5)	110 ( $\pm$ 8)
	Influent	0.03 ng/mL							
(a) Lyophilisation		84.8 ( $\pm$ 2)	114 ( $\pm$ 2)	n.d.	82.2 ( $\pm$ 5)	84.8 ( $\pm$ 2)	56.5 ( $\pm$ 1)	59.7 ( $\pm$ 1)	n.q.
(b) SPE		96.4 ( $\pm$ 3)	109 ( $\pm$ 10)	n.d.	114 ( $\pm$ 4)	96.4 ( $\pm$ 3)	78.3 ( $\pm$ 4)	92.4 ( $\pm$ 17)	138 ( $\pm$ 5)
0.3 ng/mL									
(a) Lyophilisation		106 ( $\pm$ 6)	103 ( $\pm$ 3)	n.d.	64.1 ( $\pm$ 6)	106 ( $\pm$ 6)	95.2 ( $\pm$ 5)	95.2 ( $\pm$ 5)	n.q.
(b) SPE		101 ( $\pm$ 8)	137.8 ( $\pm$ 4)	n.d.	105 ( $\pm$ 2)	100 ( $\pm$ 8)	94.6 ( $\pm$ 9)	94.6 ( $\pm$ 9)	159 ( $\pm$ 12)
3 ng/L									
(a) Lyophilisation		n.q.	101 ( $\pm$ 4)	117 ( $\pm$ 4)	68.3 ( $\pm$ 6)	89.6 ( $\pm$ 3)	89.6 ( $\pm$ 3)	2.4 ( $\pm$ 1)	n.q.
(b) SPE		159 ( $\pm$ 2)	106 ( $\pm$ 2)	98.5 ( $\pm$ 3)	95.7 ( $\pm$ 5)	93.9 ( $\pm$ 7)	93.9 ( $\pm$ 7)	99.2 ( $\pm$ 5)	159 ( $\pm$ 2)

<sup>a</sup> n.d. – not detected.<sup>b</sup> n.q. – not quantified.

#### 4.3.4 Comparison of quantitative results: SFC-MS/MS and UHPLC-MS/MS

In order to validate the quantitative performance of the SFC method for the target ARVs in wastewater samples, a wastewater sample was analysed and the quantitative data were compared to those obtained by a previously reported direct injection UHPLC-MS/MS method (Mosekiemang *et al.*, 2019). For this purpose, a raw wastewater sample collected during a severe drought period (April 2018) was used, given the likelihood of detection of most compounds at significant concentrations. ZDV and RTVM were not detected in this sample using either method, whereas EFZ and EFVM were only quantified using the UHPLC-MS/MS method. For those compounds quantified using both methods, remarkable agreement was obtained, with differences in mean values of less than 3.5% between the two data sets (Table 4.4). A paired t-test comparison between the two data sets confirmed that differences between the methods are statistically insignificant (i.e.  $p > 0.05$ ).

**Table 4.4:** Comparison of quantitation data obtained by lyophilisation-SFC-MS/MS and direct injection UHPLC-MS/MS for a raw wastewater samples obtained from a largely domestic water-receiving WWTP during a drought.

Instrument	Analytes (ng/mL)							
	EFZ	NVP	ZDV	NVPM	RTV	3TC	FTC	RTV M
UHPLC	18.2 (4)	1.43 ( $\pm 6.3$ )	n.d.	4.30 ( $\pm 4.6$ )	20.0 ( $\pm 0.6$ )	48.7 ( $\pm 3.2$ )	352 ( $\pm 3.2$ )	n.d.
SFC	n.d.	1.42 ( $\pm 6.2$ )	n.d.	4.15 ( $\pm 3.1$ )	19.4 ( $\pm 1.3$ )	49.7 ( $\pm 1.8$ )	343 ( $\pm 3.0$ )	n.d.
% Difference	–	1.0	–	3.5	3.2	-2.0	2.7	–
p-value (paired t-test)	–	0.83	–	0.19	0.07	0.24	0.17	–

<sup>a</sup> denotes average concentrations of six measurements with standard deviations in parenthesis.

#### 4.3.5 Overall method performance

Comparison of the SFC-MS/MS method developed in the present study to a previously optimised LC-MS/MS method (Mosekiemang *et al.*, 2019) for the analysis ARVs and their metabolites in wastewater illustrates the advantages and limitations of each method. First, regarding the scope of the methods, all target compounds were successfully analysed using the LC-MS/MS method, with the exception of RTVM which showed poor reproducibility and linearity. Although this metabolite showed good linearity and sensitivity by SFC, it could not be quantified using the lyophilisation SFC-MS/MS method. Furthermore, the ARV metabolites EFVM and ZDVG, detected in the negative ion mode in the LC

method, could not be analysed in positive ion mode nor could they be detected in negative mode under the conditions used for the SFC method.

Superior linearities ( $>0.996$ ) were obtained by SFC-MS/MS for all analytes, albeit for a smaller linear range, especially for NVP and NVPM. Generally, LC-MS/MS offered better sensitivity than SFC-MS/MS for the majority of target compounds, especially NVP and NVPM. The exceptions are ZDV and RTVM, for which lower detection limits were measured by SFC-MS/MS.

#### 4.4 Conclusions

SFC is increasingly being used in the analysis of pharmaceutical compounds. Despite this, the technique has to date found limited application in the analysis of pharmaceuticals in environmental samples. In this work we demonstrate the applicability of SFC-tandem MS as a complementary alternative to LC-MS/MS for the determination of selected ARVs and their metabolites in wastewater samples. SFC separation performed on an Acquity UPC<sup>2</sup> BEH column using a mobile phase gradient of up to 60% MeOH provided comparatively fast separation of six commonly prescribed ARV drugs and a known nevirapine metabolite in wastewater samples. Two further ARV metabolites, ZDVG and EFVM could not successfully be analysed by SFC-MS/MS, an indication that further method development work, particularly in terms of the organic solvent make-up (flow rate and composition) and addition of modifiers, should be performed to extend the application range of the method. ESI-MS/MS detection in MRM mode provided sufficient sensitivity for trace-level analysis of the target compounds in pre-concentrated environmental samples. Combined with lyophilisation for sample preparation, the method can be considered more environmentally friendly than conventional SPE-RP-LC-MS/MS methods. Analyte enrichment by lyophilisation provided comparable recoveries for apolar compounds to SPE and offered improved recoveries for polar compounds. Although samples prepared by lyophilisation showed higher matrix effects compared to SPE samples, notably severe ion suppression (~95%) for 3TC, these were generally within an acceptable range. Following successful validation of the proposed lyophilisation-SFC-MS/MS method, excellent agreement was obtained for the quantitation of several ARVs and their metabolites in wastewater samples compared to SPE-LC-MS/MS. Our findings indicate, to our knowledge for the first time, the suitability of SFC for the analysis of trace-levels of ARVs in environmental samples. Clearly, no single analytical method provides ideal performance for the determination all ARVs and their metabolites. In this context, SFC-MS/MS can be considered a useful complementary method to LC-MS/MS to monitor the environmental fate of these emerging contaminants.

## 4.5 References

- Abafe, O.A., Späth, J., Fick, J., Jansson, S., Buckley, C., Stark, A., Pietruschka, B., Martincigh, B.S., 2018. LC-MS/MS determination of antiretroviral drugs in influents and effluents from wastewater treatment plants in KwaZulu-Natal, South Africa. *Chemosphere* 200, 660–670. <https://doi.org/10.1016/j.chemosphere.2018.02.105>
- Akbal, L., Hopfgartner, G., 2020. Hyphenation of packed column supercritical fluid chromatography with mass spectrometry: where are we and what are the remaining challenges? *Anal. Bioanal. Chem.* 412, 6667–6677. <https://doi.org/10.1007/s00216-020-02715-4>
- Akbal, L., Hopfgartner, G., 2017. Effects of liquid post-column addition in electrospray ionization performance in supercritical fluid chromatography – mass spectrometry. *J. Chromatogr. A* 1517, 176–184. <https://doi.org/10.1016/j.chroma.2017.08.044>
- Alexander, A.J., Hooker, T.F., Tomasella, F.P., 2012. Evaluation of mobile phase gradient supercritical fluid chromatography for impurity profiling of pharmaceutical compounds. *J. Pharm. Biomed. Anal.* 70, 77–86. <https://doi.org/10.1016/j.jpba.2012.05.025>
- Alexander, A.J., Zhang, L., Hooker, T.F., Tomasella, F.P., 2013. Comparison of supercritical fluid chromatography and reverse phase liquid chromatography for the impurity profiling of the antiretroviral drugs lamivudine/BMS-986001/efavirenz in a combination tablet. *J. Pharm. Biomed. Anal.* 78–79, 243–251.
- Ashraf-Khorassani, M., Taylor, L.T., 2010. Subcritical fluid chromatography of water soluble nucleobases on various polar stationary phases facilitated with alcohol-modified CO<sub>2</sub> and water as the polar additive. *J. Sep. Sci.* 33, 1682–1691. <https://doi.org/10.1002/jssc.201000047>
- Backe, W.J., Field, J.A., 2012. Is SPE necessary for environmental analysis? A quantitative comparison of matrix effects from large-volume injection and solid-phase extraction based methods. *Environ. Sci. Technol.* 46, 6750–6758. <https://doi.org/10.1021/es300235z>
- Bennett, R., Biba, M., Liu, J., Ahmad, I.A.H., Hicks, M.B., Regalado, E.L., 2019. Enhanced fluidity liquid chromatography: A guide to scaling up from analytical to preparative separations. *J. Chromatogr. A* 1595, 190–198. <https://doi.org/10.1016/j.chroma.2019.02.017>
- Boulard, L., Dierkes, G., Ternes, T., 2018. Utilization of large volume zwitterionic hydrophilic interaction liquid chromatography for the analysis of polar pharmaceuticals in aqueous environmental samples: Benefits and limitations. *J. Chromatogr. A* 1535, 27–43. <https://doi.org/10.1016/j.chroma.2017.12.023>
- Brewer, A.J., Lunte, C., 2015. Analysis of nucleosides in municipal wastewater by large-volume liquid

- chromatography tandem mass spectrometry. *Anal. Methods* 7, 5504–5510.  
<https://doi.org/10.1039/C5AY00929D>
- Brown, A.K., Wong, C.S., 2015. Current trends in environmental analysis of human metabolite conjugates of pharmaceuticals. *Trends Environ. Anal. Chem.* 5, 8–17.  
<https://doi.org/10.1016/j.teac.2015.01.002>
- Camacho-Muñoz, D., Kasprzyk-Hordern, B., 2015. Multi-residue enantiomeric analysis of human and veterinary pharmaceuticals and their metabolites in environmental samples by chiral liquid chromatography coupled with tandem mass spectrometry detection. *Anal. Bioanal. Chem.* 407, 9085–9104. <https://doi.org/10.1007/s00216-015-9075-6>
- Cui, Y., Olesik, S. V., 1991. High-Performance Liquid Chromatography Using Mobile Phases with Enhanced Fluidity. *Anal. Chem.* 63, 1812–1819. <https://doi.org/10.1021/ac00017a028>
- de Voogt, P., van der Wielen, F.W.M., Govers, H.A.J., 2000. Freeze-drying brings about errors in polychlorinated biphenyl recovery calculations. *Trends Anal. Chem.* 19, 292–299.
- Desfontaine, V., Guillarme, D., 2015. SFC – MS versus RPLC – MS for drug analysis in biological samples. *Bioanalysis* 7, 1193–1195.
- Desfontaine, V., Guillarme, D., Francotte, E., Nováková, L., 2015. Supercritical fluid chromatography in pharmaceutical analysis. *J. Pharm. Biomed. Anal.* 113, 56–71.  
<https://doi.org/10.1016/j.jpba.2015.03.007>
- Desfontaine, V., Veuthey, J.L., Guillarme, D., 2016. Evaluation of innovative stationary phase ligand chemistries and analytical conditions for the analysis of basic drugs by supercritical fluid chromatography. *J. Chromatogr. A* 1438, 244–253. <https://doi.org/10.1016/j.chroma.2016.02.029>
- Dispas, A., Lebrun, P., Sacré, P., Hubert, P., 2016. Screening study of SFC critical method parameters for the determination of pharmaceutical compounds. *J. Pharm. Biomed. Anal.* 125, 339–354.  
<https://doi.org/10.1016/j.jpba.2016.04.005>
- Evard, H., Kruve, A., Leito, I., 2016a. Tutorial on estimating the limit of detection using LC-MS analysis, part I: Theoretical review. *Anal. Chim. Acta* 942, 23–39.  
<https://doi.org/10.1016/j.aca.2016.08.043>
- Evard, H., Kruve, A., Leito, I., 2016b. Tutorial on estimating the limit of detection using LC-MS analysis, part II: Practical aspects. *Anal. Chim. Acta* 942, 40–49.  
<https://doi.org/10.1016/j.aca.2016.08.042>
- Fatta-Kassinos, D., Meric, S., Nikolaou, A., 2011. Pharmaceutical residues in environmental waters and wastewater: Current state of knowledge and future research. *Anal. Bioanal. Chem.* 399, 251–275.

<https://doi.org/10.1007/s00216-010-4300-9>

Furey, A., Moriarty, M., Bane, V., Kinsella, B., Lehane, M., 2013. Ion suppression; A critical review on causes, evaluation, prevention and applications. *Talanta* 115, 104–122.

<https://doi.org/10.1016/j.talanta.2013.03.048>

Grand-Guillaume Perrenoud, A., Boccard, J., Veuthey, J.L., Guillarme, D., 2012a. Analysis of basic compounds by supercritical fluid chromatography: Attempts to improve peak shape and maintain mass spectrometry compatibility. *J. Chromatogr. A* 1262, 205–213.

<https://doi.org/10.1016/j.chroma.2012.08.091>

Grand-Guillaume Perrenoud, A., Veuthey, J.L., Guillarme, D., 2012b. Comparison of ultra-high performance supercritical fluid chromatography and ultra-high performance liquid chromatography for the analysis of pharmaceutical compounds. *J. Chromatogr. A* 1266, 158–167.

<https://doi.org/10.1016/j.chroma.2012.10.005>

Guillarme, D., Desfontaine, V., Heinisch, S., Veuthey, J., 2018. What are the current solutions for interfacing supercritical fluid chromatography and mass spectrometry? *J. Chromatogr. B* 1083, 160–170. <https://doi.org/10.1016/j.jchromb.2018.03.010>

Hermes, N., Jewell, K.S., Wick, A., Ternes, T.A., 2018. Quantification of more than 150 micropollutants including transformation products in aqueous samples by liquid chromatography-tandem mass spectrometry using scheduled multiple reaction monitoring. *J. Chromatogr. A* 1531, 64–73. <https://doi.org/10.1016/j.chroma.2017.11.020>

Hewavitharana, A.K., Sofiah, N., Kassim, A., Shaw, P.N., 2018. Standard addition with internal standardisation as an alternative to using stable isotope labelled internal standards to correct for matrix effects — Comparison and validation using liquid chromatography-tandem mass spectrometric assay of vitamin D. *J. Chromatogr. A* 1553, 101–107.

<https://doi.org/10.1016/j.chroma.2018.04.026>

Hirose, T., Keck, D., Izumi, Y., 2019. Comparison of Retention Behavior between Chromatography with Various Stationary Phases. *Molecules* 24, 2425–2438.

Hirsch, R., Ternes, T.A., Haberer, K., Mehlich, A., Ballwanz, F., Kratz, K.L., 1998. Determination of antibiotics in different water compartments via liquid chromatography-electrospray tandem mass spectrometry. *J. Chromatogr. A* 815, 213–223. [https://doi.org/10.1016/S0021-9673\(98\)00335-5](https://doi.org/10.1016/S0021-9673(98)00335-5)

Hu, F.Y., He, L.M., Yang, J.W., Bian, K., Wang, Z.N., Yang, H.C., Liu, Y.H., 2014. Determination of 26 veterinary antibiotics residues in water matrices by lyophilisation in combination with LC-MS/MS. *J. Chromatogr. B Anal. Technol. Biomed. Life Sci.* 949–950, 79–86. <https://doi.org/10.1016/j.jchromb.2014.01.008>



- Khater, S., West, C., Lesellier, E., 2013. Characterization of five chemistries and three particle sizes of stationary phases used in supercritical fluid chromatography. *J. Chromatogr. A* 1319, 148–159. <https://doi.org/10.1016/j.chroma.2013.10.037>
- Kruve, A., Rebane, R., Kipper, K., Oldekop, M.L., Evard, H., Herodes, K., Ravio, P., Leito, I., 2015a. Tutorial review on validation of liquid chromatography-mass spectrometry methods: Part I. *Anal. Chim. Acta* 870, 29–44. <https://doi.org/10.1016/j.aca.2015.02.017>
- Kruve, A., Rebane, R., Kipper, K., Oldekop, M.L., Evard, H., Herodes, K., Ravio, P., Leito, I., 2015b. Tutorial review on validation of liquid chromatography-mass spectrometry methods: Part II. *Anal. Chim. Acta* 870, 8–28. <https://doi.org/10.1016/j.aca.2015.02.016>
- Lemasson, E., Bertin, S., Hennig, P., Boiteux, H., Westa, E.L., 2015. Development of an achiral supercritical fluid chromatography method with ultraviolet absorbance and mass spectrometric detection for impurity profiling of drug candidates. Part I: Optimization of mobile phase composition. *J. Chromatogr. A* 1408, 217–226. <https://doi.org/10.1016/j.chroma.2015.07.037>
- Mlunguza, N.Y., Ncube, S., Mahlambi, P.N., Chimuka, L., Madikizela, L.M., 2020. Determination of selected antiretroviral drugs in wastewater, surface water and aquatic plants using hollow fibre liquid phase microextraction and liquid chromatography - tandem mass spectrometry. *J. Hazard. Mater.* 382, 121067. <https://doi.org/10.1016/j.jhazmat.2019.121067>
- Mosekiemang, T.T., Stander, M.A., de Villiers, A., 2019. Simultaneous quantification of commonly prescribed antiretroviral drugs and their selected metabolites in aqueous environmental samples by direct injection and solid phase extraction liquid chromatography - Tandem mass spectrometry. *Chemosphere* 220, 983–992. <https://doi.org/10.1016/j.chemosphere.2018.12.205>
- Nannou, C., Ofrydopoulou, A., Evgenidou, E., Heath, D., Heath, E., Lambropoulou, D., 2019. Analytical strategies for the determination of antiviral drugs in the aquatic environment. *Trends Environ. Anal. Chem.* 24, e00071. <https://doi.org/10.1016/j.teac.2019.e00071>
- Narayan, S., Vasudev, K., Vardhana, M.V., Odetokun, M., 2011. Quantification of organophosphate insecticides in drinking water in urban areas using lyophilisation and high-performance liquid chromatography – electrospray ionization-mass spectrometry techniques. *Int. J. Mass Spectrom.* 300, 12–20. <https://doi.org/10.1016/j.ijms.2010.11.006>
- Ngumba, E., Kosunen, P., Gachanja, A., Tuhkanen, T., 2016. A multiresidue analytical method for trace level determination of antibiotics and antiretroviral drugs in wastewater and surface water using SPE-LC-MS/MS and matrix-matched standards. *Anal. Methods* 8, 6720–6729. <https://doi.org/10.1039/c6ay01695b>
- Nováková, L., Grand-Guillaume Perrenoud, A., Francois, I., West, C., Lesellier, E., Guillarme, D.,

2014. Modern analytical supercritical fluid chromatography using columns packed with sub-2 $\mu$ m particles: A tutorial. *Anal. Chim. Acta* 824, 18–35. <https://doi.org/10.1016/j.aca.2014.03.034>
- Oller, I., Malato, S., Sánchez-Pérez, J.A., 2011. Combination of Advanced Oxidation Processes and biological treatments for wastewater decontamination-A review. *Sci. Total Environ.* 409, 4141–4166. <https://doi.org/10.1016/j.scitotenv.2010.08.061>
- Pal, A., He, Y., Jekel, M., Reinhard, M., Gin, K.Y.-H., 2014. Emerging contaminants of public health significance as water quality indicator compounds in the urban water cycle. *Environ. Int.* 71, 46–62. <https://doi.org/10.1016/j.envint.2014.05.025>
- Peng, X., Wang, C., Zhang, K., Wang, Z., Huang, Q., Yu, Y., Ou, W., 2014. Profile and behavior of antiviral drugs in aquatic environments of the Pearl River Delta, China. *Sci. Total Environ.* 466–467, 755–761. <https://doi.org/10.1016/j.scitotenv.2013.07.062>
- Pereirra, A., David, F., Vanhoenacker, G., Brunelli, C., Sandra, P., 2011. A simple instrumental approach for “supercritical” fluid chromatography in drug discovery and its consequences for coupling with mass spectrometric and light scattering detection. *LCGC North Am.* 29, 1006–1016.
- Prasse, C., Schlüsener, M.P., Schulz, R., Ternes, T.A., 2010. Antiviral drugs in wastewater and surface waters: A new pharmaceutical class of environmental relevance? *Environ. Sci. Technol.* 44, 1728–1735. <https://doi.org/10.1021/es903216p>
- Ramirez, C.E., Bellmund, S., Gardinali, P.R., 2014. A simple method for routine monitoring of glyphosate and its main metabolite in surface waters using lyophilisation and LC-FLD + MS/MS. Case study: Canals with influence on Biscayne National Park. *Sci. Total Environ.* 496, 389–401. <https://doi.org/10.1016/j.scitotenv.2014.06.118>
- Romand, S., Rudaz, S., Guillarme, D., 2016. Separation of substrates and closely related glucuronide metabolites using various chromatographic modes. *J. Chromatogr. A* 1435, 54–65. <https://doi.org/10.1016/j.chroma.2016.01.033>
- SANTE, 2015. Guidance document on analytical quality control and method validation procedures for pesticides residues analysis in food and feed. SANTE/11945/2015, Legal Deposit.
- Snyder, L.R., Kirkland, J.J. (Eds.), 1979. *Introduction to modern liquid chromatography*. Wiley, New York, NY.
- Stahnke, H., Kittlaus, S., Kempe, G., Hemmerling, C., Alder, L., 2012. The influence of electrospray ion source design on matrix effects. *J. Mass Spectrom.* 47, 875–884. <https://doi.org/10.1002/jms.3047>
- Svan, A., Hedeland, M., 2018. The differences in matrix effect between supercritical fluid

- chromatography and reversed phase liquid chromatography coupled to ESI / MS. *Anal. Chim. Acta* 1000, 163–171. <https://doi.org/10.1016/j.aca.2017.10.014>
- Svan, A., Hedeland, M., Arvidsson, T., Pettersson, C.E., 2018. The differences in matrix effect between supercritical fluid chromatography and reversed phase liquid chromatography coupled to ESI/MS. *Anal. Chim. Acta* 1000, 163–171. <https://doi.org/10.1016/j.aca.2017.10.014>
- Tarafder, A., 2018. Designs and methods for interfacing SFC with MS. *J. Chromatogr. B* 1091, 1–13. <https://doi.org/10.1016/j.jchromb.2018.05.003>
- Van De Steene, J.C., Lambert, W.E., 2008. Comparison of Matrix Effects in HPLC-MS/MS and UPLC-MS/MS Analysis of Nine Basic Pharmaceuticals in Surface Waters. *J. Am. Soc. Mass Spectrom.* 19, 713–718. <https://doi.org/10.1016/j.jasms.2008.01.013>
- Welch, C.J., Wu, N., Biba, M., Hartman, R., Brkovic, T., Gong, X., Helmy, R., Schafer, W., Cuff, J., Pirzada, Z., Zhou, L., 2010. Greening analytical chromatography. *TrAC - Trends Anal. Chem.* 29, 667–680. <https://doi.org/10.1016/j.trac.2010.03.008>
- West, C., 2015. The new face of supercritical fluid chromatography: why analysts should take another look. *LC GC North Am.* 33, 522–523.
- West, C., Lemasson, E., Bertin, S., Hennig, P., Lesellier, E., 2016. An improved classification of stationary phases for ultra-high performance supercritical fluid chromatography. *J. Chromatogr. A* 1440, 212–228. <https://doi.org/10.1016/j.chroma.2016.02.052>
- West, C., Lesellier, E., 2008. A unified classification of stationary phases for packed column supercritical fluid chromatography. *J. Chromatogr. A* 1191, 21–39. <https://doi.org/10.1016/j.chroma.2008.02.108>
- West, C., Lesellier, E., 2006. Characterisation of stationary phases in subcritical fluid chromatography with the solvation parameter model III . Polar stationary phases. *J. Chromatogr. A* 1110, 200–213. <https://doi.org/10.1016/j.chroma.2006.01.109>
- Wood, T.P., Duvenage, C.S.J., Rohwer, E., 2015. The occurrence of anti-retroviral compounds used for HIV treatment in South African surface water. *Environ. Pollut.* 199, 235–243. <https://doi.org/10.1016/j.envpol.2015.01.030>

## Chapter 4

---

**Supplementary information for:**

**Evaluation of supercritical fluid chromatography-tandem mass spectrometry (SFC-MS/MS) for the analysis antiretrovirals and their selected metabolites using SFC-MS/MS**

#### **S4.1 Sample collection**

A raw wastewater sample was collected during a severe drought episode (April 2018) in the Western Cape region of South Africa (following the detailed sample collection protocol described in (Mosekiemang *et al.*, 2019)). For this purpose, grab samples were collected from a wholly domestic wastewater-receiving treatment plant. Several 500 mL samples were collected at ~15 minutes intervals over 2 hours and pooled into a 5 L pre-cleaned volumetric flask for homogenisation. The sampling expedition was timed to coincide with high daily inflows (~14:30–15:30) into the plant to maximise chances of obtaining a representative sample. The homogenised sample was then aliquoted into several 500 mL pre-cleaned amber bottles without addition of preservatives, placed in an insulated box containing ice packs and transported to the lab where it was processed within 24 h.

## S4.2 Sample preparation

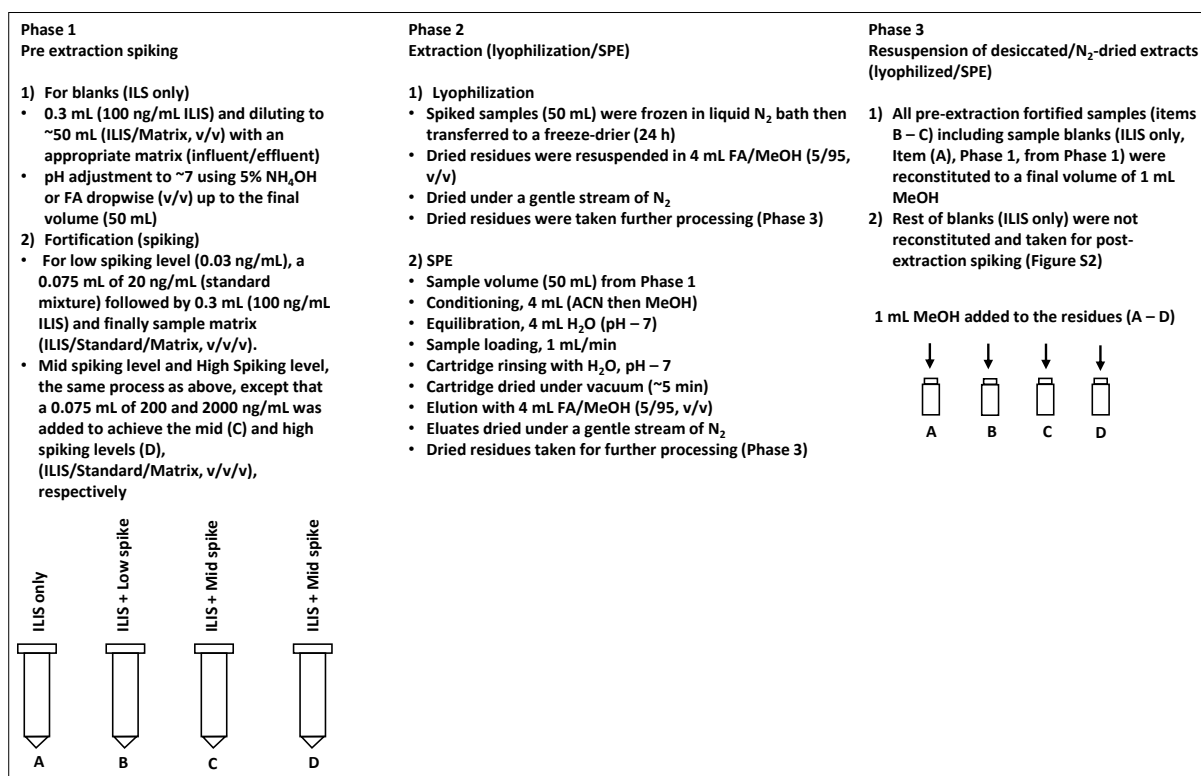


**Figure S1:** Illustrative scheme of the procedure used for analyte spiking prior to extraction by lyophilisation and SPE (pre-extraction spiked samples).

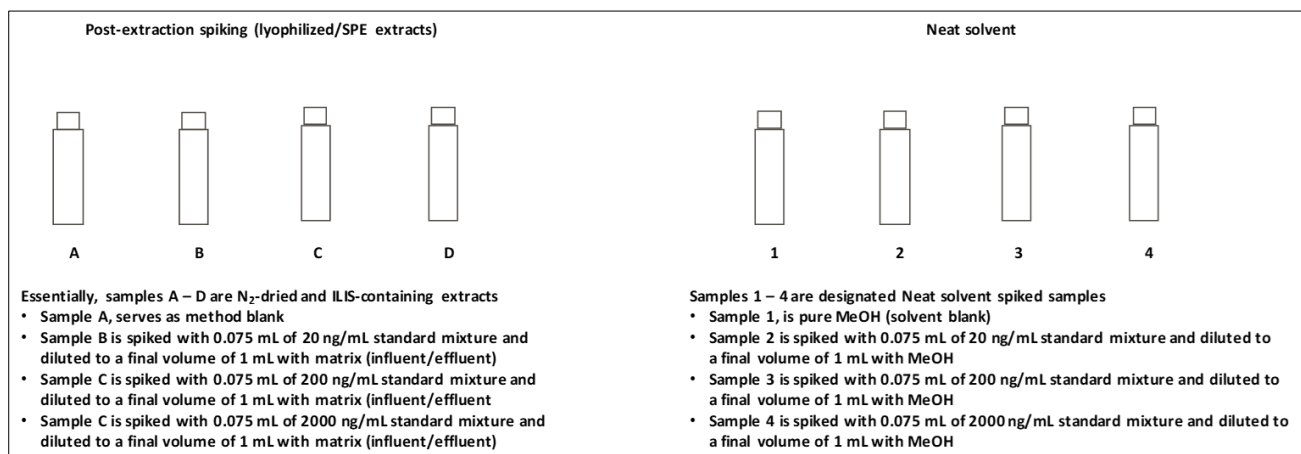


**Figure S4.2:** Illustrative scheme of the procedure used for post-extraction analyte spiking for samples obtained by both lyophilisation and SPE, and for the preparation of neat solvent spiked samples.

### S3. Method optimisation and validation

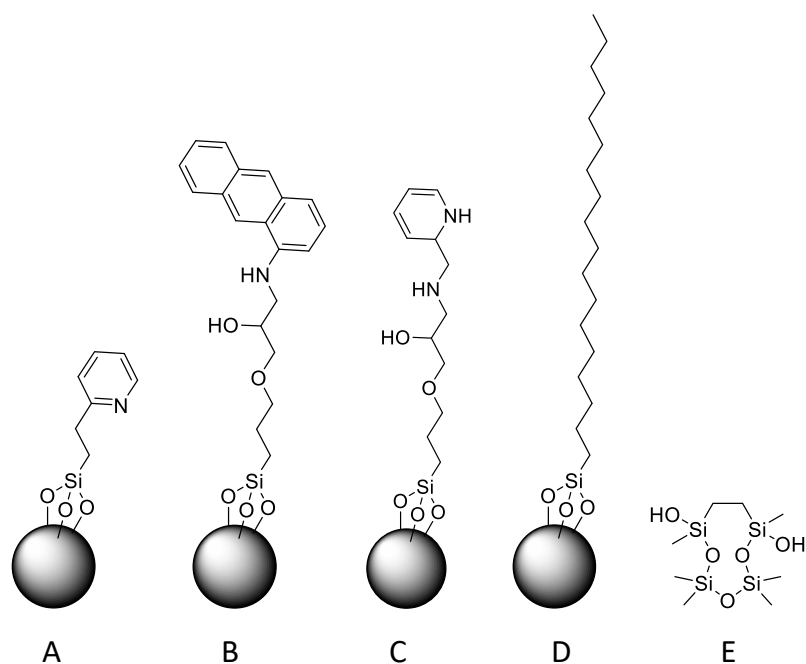


**Figure S4.3:** Stationary phase chemistries for the five columns evaluated in the present study: (A) 2-ethylpyridine (2-EP), 1-aminoanthracene (1-AA), 2-picolylamine (2-PIC), high strength silica octadecyl (HSS C18), and ethylene bridged hybrid (BEH) silica. BEH silica is employed as base material for 2-EP, 1-AA and 2-PIC phases.

**Table S4.1:** Optimised SFC-ESI-MS/MS MRM conditions used for the analysis of the target ARVs and their metabolites.

Compound	MW (gmol <sup>-1</sup> )	t <sub>R</sub> (±SD)	Q ion transition (t <sub>dwell</sub> , sec)	CV/CE (V/eV)	Q ion transition (t <sub>dwell</sub> , sec)	CV/CE (V/eV)	q/Q (±SD)
efavirenz	315.7	2.76 (±0.01)	316.1 > 168.0 (0.018)	20/30	316.1 > 244.1 (0.018)	20/25	0.41 (±0.1)
nevirapine	266.3	3.97 (±0.004)	267.3 > 226.1 (0.003)	20/25	267.3 > 107.1 (0.003)	20/30	0.67 (±0.1)
nevirapine-D <sub>3</sub>	269.0	3.97 (±0.002)	270.0 > 110.0 (0.003)	20/25	a <sub>-</sub>	a <sub>-</sub>	a <sub>-</sub>
zidovudine	267.2	3.98 (±0.02)	268.0 > 110.0 (0.003)	20/20	268.0 > 42.0 (0.003)	20/30	0.29 (±0.04)
12-hydroxy nevirapine	282.3	5.04 (±0.01)	283.2 > 223.0 (0.003)	20/25	283.2 > 196.1 (0.003)	20/30	0.77 (±0.1)
ritonavir	720.9	5.85 (±0.004)	721.5 > 296.1 (0.003)	15/15	721.5 > 426.5 (0.003)	15/15	0.26 (±0.03)
emtricitabine	247.3	5.87 (±0.01)	248.0 > 130.6 (0.046)	15/15	248.0 > 113.5 (0.046)	15/30	0.13 (±0.02)
lamivudine	229.3	6.55 (±0.01)	230.0 > 112.2 (0.003)	30/15	230.0 > 95.1 (0.003)	30/25	0.04 (±0.1)
desthiazolylmethyloxycarbonyl ritonavir	579.8	6.64 (±0.01)	580.1 > 268.1 (0.003)	20/25	580.1 > 410.1 (0.003)	20/25	0.11 (±0.02)
8,14 dihydroxy efavirenz	347.7	b <sub>-</sub>	346.0 > 261.8 (0.003)	20/15	346.0 > 241.8 (0.003)	20/15	b <sub>-</sub>
zidovudine glucuronide	443.4	c <sub>-</sub>	442.0 > 125.0 (0.003)	20/20	442.0 > 113.0 (0.003)	20/20	c <sub>-</sub>

<sup>a</sup> The qualifier ion for nevirapine-D<sub>3</sub> was not measured.

<sup>b</sup> & <sup>c</sup> The SFC-MS/MS was not suitable for the analysis of zidovudine glucuronide and 8,14-dihydroxy efavirenz.

<sup>c</sup> Values in parenthesis denote the standard deviations measured for the ion ratios (q/Q) (n = 9).



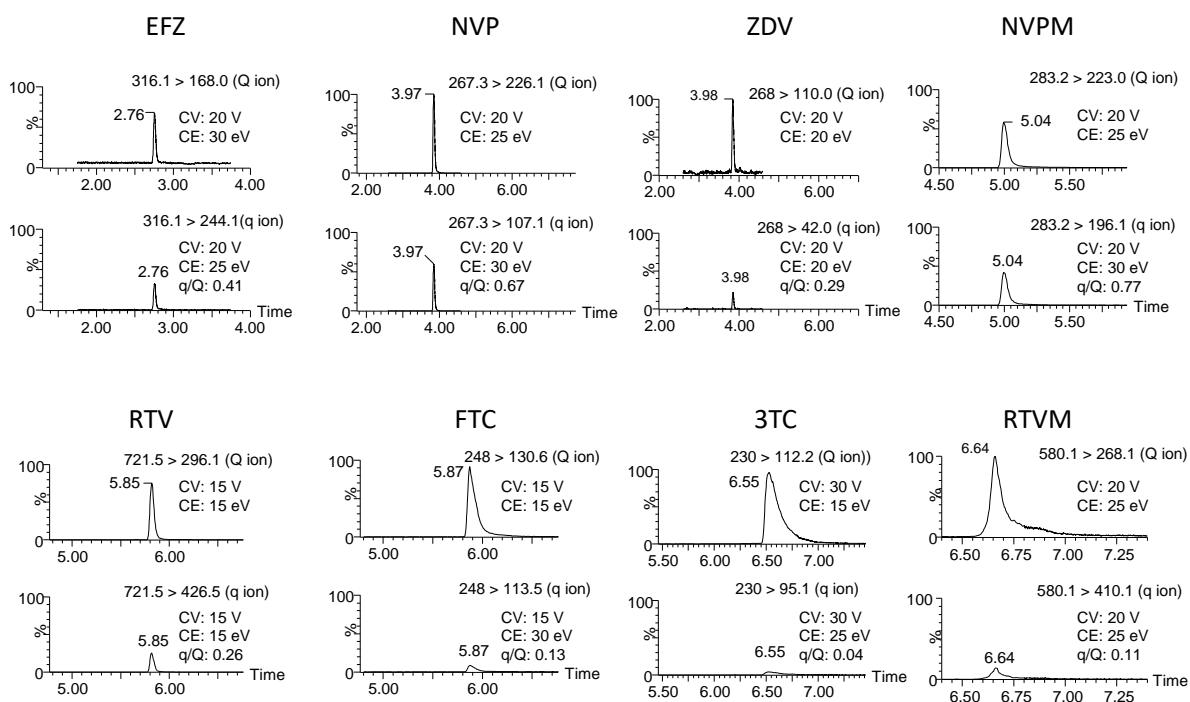


**Figure S4.4:** Typical integrated MRM chromatograms obtained for the target analyte standards at 52.1 ng/mL illustrating the optimised MS/MS acquisition conditions. Experimental conditions as specified in Section 4.2.2 and Table S4.1.

**Table S4.2:** Asymmetry factors at 10% peak height for the test analytes on the columns evaluated for this study (Snyder and Kirkland, 1979)

Columns	Test compounds								
	EFZ	NVP	NVP-D3	ZDV	NVPM	RTV	FTC	3TC	RTVM
BEH 2-EP	1.00	1.10	1.00	1.05	1.00	1.05	1.67	1.67	1.80
1-AA	1.00	1.13	1.05	<sup>a</sup> —	1.05	1.10	1.20	1.50	1.55
2-PIC	1.05	1.00	1.00	0.80	1.05	1.00	1.05	1.15	1.60
HSS C18	1.05	1.10	1.05	1.05	1.10	1.05	1.10	1.20	1.20
SB									
BEH	1.00	1.05	1.00	1.00	1.05	1.05	1.15	1.20	1.20

<sup>a</sup> ZDV peak below signal-to-noise ratio

### Method validation procedures

Limits of detection (LODs) and limits of quantification (LOQs) were calculated according to Eq.'s S4.1 and S4.2 (Evard *et al.*, 2016b, 2016a):

$$\text{a) } \text{LOD} = 3.3 \times \frac{S_y}{b} \quad \text{Equation S4.1}$$

$$\text{b) } \text{LOQ} = 10 \times \frac{S_y}{b} \quad \text{Equation S4.2}$$

Where  $S_y$  is the standard error of the calibration curve intercept, and  $b$  the calibration curve slope. Method detection limits (MDLs) and method quantification limits (MQLs) were calculated according to Eq.'s S3 and S4 (Camacho-Muñoz and Kasprzyk-Hordern, 2015; Fatta-Kassinos *et al.*, 2011; Ngumba *et al.*, 2016):

$$\text{a) } MDL = \frac{LOD \times 100}{Rec \times PF} \quad \text{Equation S4.3}$$

$$\text{b) } MQL = \frac{LOQ \times 100}{Rec \times PF} \quad \text{Equation S4.4}$$

where Rec is the analyte recovery and PF the pre-concentration factor. Recoveries (%) and matrix effects (%) for fortified samples (lyophilisation/SPE) were calculated according to Eq.'s S4.5 and S4.6 (Matuszewski and Constanzer, 2003; Ngumba *et al.*, 2016; Prasse *et al.*, 2010)

$$\text{a) } \text{Recovery (\%)} = \frac{\text{blank subtracted pre-extraction spike concentration}}{\text{blank-subtracted post-extracted spike concentration}} \times 100 \quad \text{Equation S4.5}$$

$$\text{b) } \text{Matrix effects (\%)} = \frac{\text{blank subtracted post-extraction spike concentration}}{\text{neat standard concentration}} \times 100 \quad \text{Equation S4.6}$$

**Table S4.3:** Relative and absolute recoveries measured for the target analytes in wastewater effluent and influent samples at the 0.03 ng/mL.

Matrix	Sample preparation method	Analytes <sup>a</sup>							
		EFZ	NVP	ZDV	NVPM	RTV	FTC	3TC	RTVM
Effluent	ILIS-corrected								
	a) Lyophilisation	95.9 (±6)	73.0 (±7)	n.d. <sup>b</sup>	77.4 (±5)	62.9 (±5)	73.1 (±6)	98.9 (±3)	n.q. <sup>c</sup>
	b) SPE	92.7 (±10)	103 (±5)	n.d.	98.6 (±2)	77.4 (±4)	21.8 (±2)	41.2 (±1)	56.3 (±6)
	Non-ILIS-corrected								
	a) Lyophilisation	53.2 (±5)	89.2 (±3)	n.d.	79.8 (±2)	73.6 (±6)	88.0 (±6)	n.d.	n.q.
	b) SPE	49.3 (±8)	89.5 (±2)	n.d.	89.4 (±5)	72.4 (±7)	23.2 (±5)	20.3 (±1)	34.1 (±4)
Influent	ILIS-corrected								
	a) Lyophilisation	108 (±6)	94.8 (±10)	n.d.	86.8 (±4)	84.8 (±2)	104 (±9)	103 (±8)	n.q.
	b) SPE	72.0 (±1)	107 (±11)	n.d.	111 (±3)	87.7 (±3)	63.3 (±3)	50.7 (±3)	34.1 (±4)
	Non-ILIS-corrected								
	a) Lyophilisation	112 (±3)	85.8 (±7)	n.d.	85.5 (±6)	70.1 (±4)	67.0 (±9)	101 (±2)	n.d.
	b) SPE	70.9 (±2)	89.6 (±16)	n.d.	84.7 (±2)	78.1 (±3)	13.7 (±1)	10.2 (±1)	72.9 (±2)

<sup>a</sup> mean value ( $n = 4$ ), with standard deviation in parenthesis.<sup>b</sup> n.d. – not detected.<sup>c</sup> n.q. – not quantified.

**Table S4.4:** Relative and absolute recoveries measured for the target analytes in wastewater effluent and influent samples at the 0.3 ng/mL.

Matrix	Sample preparation method	Analytes <sup>a</sup>							
		EFV	NVP	ZDV	NVPM	RTV	FTC	3TC	RTVM
Effluent	ILIS-corrected								
	a) Lyophilisation	90.7 (±4)	71.7 (±5)	n.d. <sup>b</sup>	74.5 (±3)	81.0 (±9)	65.5 (±8)	83.0 (±7)	n.q. <sup>c</sup>
	b) SPE	87.2 (±5)	99.1 (±1)	n.d.	101 (±4)	80.7 (±3)	31.4 (±2)	24.0 (±1)	58.7 (±2)
	Non-ILIS-corrected								
	a) Lyophilisation	118 (±9)	77.2 (±1)	n.d.	86.4 (±1)	86.3 (±14)	56.7 (±2)	65.1 (±1)	n.q.
	b) SPE	91.0 (±6)	101 (±1)	n.d.	103 (±5)	80.7 (±1)	30.3 (±3)	19.1 (±1)	57.3 (±1)
Influent	ILIS-corrected								
	a) Lyophilisation	103 (±6)	94.8 (±2)	n.d.	96.7 (±14)	89.7 (±7)	100.5 (±2)	99.6 (±6)	n.q.
	b) SPE	63.6 (±1)	99.7 (±1)	n.d.	101 (±6)	95.5 (±4)	54.3 (±3)	19.3 (±1)	78.1 (±2)
	Non-ILIS-corrected								
	a) Lyophilisation	65.3 (±12)	88.5 (±16)	n.d.	91.3 (±11)	86.1 (±9)	71.7 (±11)	91.5 (±1)	n.q.
	b) SPE	94.9 (±8)	105 (±3)	n.d.	105 (±2)	95.9 (±3)	29.6 (±5)	20.0 (±1)	80.0 (±2)

<sup>a</sup> mean value ( $n = 4$ ), with standard deviation in parenthesis.

<sup>b</sup> n.d. – not detected.

<sup>c</sup> n.q. – not quantified.

**Table S4.5:** Relative and absolute recoveries measured for the target analytes in wastewater effluent and influent samples at the 3 ng/mL.

Matrix	Sample preparation method	Analytes <sup>a</sup>							
		EFZ	NVP	ZDV	NVPM	RTV	FTC	3TC	RTVM
Effluent	ILIS-corrected								
	a) Lyophilisation	82.4 (±4)	n.q. <sup>b</sup>	81.0 (±2)	n.q.	84.4 (±12)	75.6 (±4)	73.1 (±1)	n.q. <sup>c</sup>
	b) SPE	97.0 (±6)	n.q.	114 (±5)	n.q.	88.5 (±5)	41.7 (±4)	31.3 (±1)	56.2 (±2)
	Non-ILIS-corrected								
	a) Lyophilisation	90.8 (±10)	n.q.	84.8 (±6)	n.q.	78.0 (±5)	80.4 (±4)	82.4 (±1)	n.q.
	b) SPE	98.2 (±5)	n.q.	89.3 (±7)	n.q.	87.1 (±1)	40.4 (±2)	30.5 (±1)	56.2 (±1)
Influent	ILIS-corrected								
	a) Lyophilisation	100 (±7)	n.q.	98.0 (±6)	n.q.	88.0 (±6)	67.6 (±1)	99.6 (±6)	n.q.
	b) SPE	101 (±3)	n.q.	106 (±4)	n.q.	91.7 (±1)	23.0 (±7)	19.6 (±1)	79.0 (±6)
	Non-ILIS-corrected								
	a) Lyophilisation	94.7 (±9)	n.q.	95.8 (±8)	n.q.	90.2 (±2)	81.7 (±9)	96.9 (±6)	n.q.
	b) SPE	97.7 (±1)	n.q.	114 (±9)	n.q.	99.5 (±1)	34.9 (±1)	21.5 (±1)	80.3 (±1)

<sup>a</sup> mean value ( $n = 4$ ), with standard deviation in parenthesis.

<sup>b</sup> not quantified due to detector saturation.

<sup>c</sup> not quantified.

## References

- Camacho-Muñoz, D., Kasprzyk-Hordern, B., 2015. Multi-residue enantiomeric analysis of human and veterinary pharmaceuticals and their metabolites in environmental samples by chiral liquid chromatography coupled with tandem mass spectrometry detection. *Anal. Bioanal. Chem.* 407, 9085–9104. <https://doi.org/10.1007/s00216-015-9075-6>
- Evard, H., Krueve, A., Leito, I., 2016a. Tutorial on estimating the limit of detection using LC-MS analysis, part I: Theoretical review. *Anal. Chim. Acta* 942, 23–39. <https://doi.org/10.1016/j.aca.2016.08.043>
- Evard, H., Krueve, A., Leito, I., 2016b. Tutorial on estimating the limit of detection using LC-MS analysis, part II: Practical aspects. *Anal. Chim. Acta* 942, 40–49. <https://doi.org/10.1016/j.aca.2016.08.042>
- Fatta-Kassinos, D., Meric, S., Nikolaou, A., 2011. Pharmaceutical residues in environmental waters and wastewater: Current state of knowledge and future research. *Anal. Bioanal. Chem.* 399, 251–275. <https://doi.org/10.1007/s00216-010-4300-9>
- Matuszewski, B.K., Constanzer, M.L., 2003. Strategies for the Assessment of Matrix Effect in Quantitative Bioanalytical Methods Based on HPLC - MS / MS. *Anal Chem* 75, 3019–3030. <https://doi.org/10.1021/ac020361s>
- Mosekiemang, T.T., Stander, M.A., de Villiers, A., 2019. Simultaneous quantification of commonly prescribed antiretroviral drugs and their selected metabolites in aqueous environmental samples by direct injection and solid phase extraction liquid chromatography - Tandem mass spectrometry. *Chemosphere* 220, 983–992. <https://doi.org/10.1016/j.chemosphere.2018.12.205>
- Ngumba, E., Gachanja, A., Tuhkanen, T., 2016. Occurrence of selected antibiotics and antiretroviral drugs in Nairobi River Basin, Kenya. *Sci. Total Environ.* 539, 206–213. <https://doi.org/10.1016/j.scitotenv.2015.08.139>
- Prasse, C., Schlüsener, M.P., Schulz, R., Ternes, T.A., 2010. Antiviral drugs in wastewater and surface waters: A new pharmaceutical class of environmental relevance? *Environ. Sci. Technol.* 44, 1728–1735. <https://doi.org/10.1021/es903216p>
- Snyder, L.R., Kirkland, J.J. (Eds.), 1979. *Introduction to modern liquid chromatography*. Wiley, New York, NY.

Declaration with signatures in possession of candidate and supervisor.

**Declaration by the candidate:**

Regarding **Chapter 5**, the nature and scope of my contribution were as follows:

<b>Nature of contribution</b>	<b>Extent of contribution (%)</b>
Performed the experiments, data analysis, co-wrote paper	65

The following co-authors have contributed to **Chapter 5**:

<b>Name</b>	<b>E-mail address</b>	<b>Nature of contribution</b>	<b>Extent of contribution (%)</b>
Maria A. Stander	_____	Assisted with experimental set-up and data manipulation; editorial input	15
André de Villiers	_____	Co-wrote paper	20

Signature of candidate:

Date: 28<sup>th</sup> February 2021

**Declaration by co-authors:**

The undersigned confirm that:

1. The declaration above accurately reflects the nature and extent of the contributions of the candidate and the co-authors to **Chapter 5**,
2. No other authors contributed to **Chapter 5** besides those specified above, and
3. Potential conflicts of interest have been revealed to all interested parties and that the necessary changes have been made to use the material in Chapter 3 of this dissertation.

<b>Signature</b>	<b>Institutional affiliation</b>	<b>Date</b>
	Stellenbosch University	1 October 2020
	Stellenbosch University	24 February 2021

## Chapter 5

---

**Ultra high pressure liquid chromatography coupled to travelling wave ion mobility-time of flight mass spectrometry for the screening of pharmaceutical metabolites in wastewater samples: application to antiretrovirals.**



## Abstract

The presence of pharmaceutical compounds in the aquatic environment is a significant environmental health concern, which is exacerbated by recent evidence of the contribution of drug metabolites to the overall pharmaceutical load. In light of a recent report of the occurrence of metabolites of antiretroviral drugs (ARVDs) in wastewater, we investigate in the present work the occurrence of further ARVD metabolites in samples obtained from a domestic wastewater treatment plant in the Western Cape, South Africa. ARVDs are extensively metabolized in the human body and their parent forms have been frequently detected in wastewater samples, suggesting partial elimination during treatment. Pharmacokinetic data indicate that ARVDs are biotransformed into several positional isomeric metabolites, only two of which have been reported wastewater samples. Given the challenges associated with the separation and identification of isomeric species in complex wastewater samples, a method based on liquid chromatography hyphenated to ion mobility spectrometry – high resolution mass spectrometry (LC-IMS-HR-MS) was implemented. Gradient LC separation was achieved on a sub-2  $\mu\text{m}$  reversed phase column, while the quadrupole-time-of-flight MS was operated in the data independent acquisition (DIA) mode  $\text{MS}^E$  to increase spectral coverage of detected features. A mass defect filter (MDF) template was implemented to detect ARVD metabolites with known phase I and phase II mass shifts and fractional mass differences and to filter out potential interferents. IMS proved particularly useful in filtering the MS data for co-eluting species according to drift time to provide cleaner mass spectra. This approach allowed us to confirm the presence of two known hydroxylated efavirenz (EFZ) and nevirapine (NVP) metabolites using authentic standards, and to tentatively identify a carboxylate metabolite of abacavir (ABC) previously reported in literature. Furthermore, three hydroxylated-, two sulphated and one glucuronidated metabolite of EFZ, two hydroxylated metabolites of NVP and one hydroxylated metabolite of ritonavir (RTV) were either tentatively or putatively identified in wastewater samples for the first time. Assignment of the metabolites is discussed in terms of high resolution fragmentation data and mass defect values, while collisional cross section (CCS) values measured for the detected analytes are reported to facilitate further work in this area. All metabolites provided fractional mass defect values consistent with literature.

## 5.1 Introduction

Despite the advances in wastewater treatment technology, it has become apparent that the process is still relatively ineffective in the removal of organic micropollutants from wastewater. This is especially true for pharmaceutical compounds (Botero-Coy *et al.*, 2018; Paíga *et al.*, 2016). Recent literature shows an increasing trend in the detection of pharmaceutical compounds in treated effluent and effluent-impacted surface water samples, which can at least in part be ascribed to heightened research interest in water quality and the availability and performance of state-of-the-art mass spectrometry instrumentation (Nannou *et al.*, 2020, 2019).

In addition to the parent drug molecules, however, it has in recent years become increasingly evident that their metabolites also contribute to the environmental impact (Celiz *et al.*, 2009). During wastewater treatment, drug metabolites may be reduced to their parent forms, resulting in augmented concentrations of the parent drug (Bahlmann *et al.*, 2014; Brown and Wong, 2015). In some instances, metabolites are excreted at concentrations equal to or rivalling those of their parent compounds, indicating that metabolites may represent a hidden and understudied component of the overall pharmaceutical load in wastewater (Brown and Wong, 2018, 2016, 2015). Qualitative data regarding the occurrence of pharmaceutical metabolites in the aquatic environment is still fragmentary (Funke *et al.*, 2016; Verlicchi and Zambello, 2016). Several reasons may explain this scenario. Metabolites for many pharmaceuticals are unknown, especially those that cannot be predicted via the known enzymatic reactions (phase I and phase II metabolic processes) (Funke *et al.*, 2016). In addition, analytical methods used for detection for metabolites are most often targeted at known parent and metabolite molecules and may not be suitable for unknown metabolites of different properties (including potential in-sewer transformation products) (Nannou *et al.*, 2019); this is a typical challenge encountered for targeted multi-residue methods using tandem mass spectrometry (Funke *et al.*, 2016).

Antiretroviral drugs (ARVDs) represent an important class of pharmaceutical contaminants, which have the focus of significant attention in recent years (Madikizela *et al.*, 2020; Nannou *et al.*, 2020, 2019; Ncube *et al.*, 2018). However, much less is known about the occurrence of ARVD metabolites in the aquatic environment (Madikizela *et al.*, 2020; Mosekiemang *et al.*, 2019; Nannou *et al.*, 2020, 2019), with the first confirmation of known metabolites of nevirapine and efavirenz in wastewater only recently reported (Mosekiemang *et al.*, 2019; Richardson *et al.*, 2021).

The metabolism and high body clearance potential of ARVDs are already known (Andrade *et al.*, 2011; Aouri *et al.*, 2016; Bélanger *et al.*, 2009; Harjivan *et al.*, 2014; Ren *et al.*, 2010; Riska *et al.*, 1999). For example, cytochrome P450 (CYP) enzymes are involved in phase I metabolism of non-nucleoside reverse transcriptase inhibitor (*n*NRTI) ARVDs. In the case of efavirenz (EFZ), several hydroxylated metabolites are produced (**Figure S1**), with the CYP2A6 and CYP2B6 isoforms responsible for the formation of 7- and 8-hydroxy EFZ (7-/8-OH-EFZ), respectively. CYP2B6 is also involved in the

formation of 8,14-dihydroxy efavirenz (8,14-diOH-EFZ), a secondary metabolite for 8-OH-EFZ (Harjivan *et al.*, 2014; Mutlib *et al.*, 1999; Ogburn *et al.*, 2010). UDP-glucuronosyltransferase and sulfotransferase enzymes are subsequently involved in the formation of glucuronic acid and sulphate phase II conjugates such as 7- and 8-hydroxy efavirenz glucuronide (7-, 8- and *N*-OH-EFZ-Glu) and 7- and 8-hydroxy Efavirenz sulphate (7- and 8-OH-EFZ-sulphate) (Bélanger *et al.*, 2009; Ogburn *et al.*, 2010). Similarly, nevirapine (NVP) is biotransformed by the same enzymes to several hydroxylated metabolites (**Figure S5.2**), including 2-, 3-, 8-, 12-hydroxy (2-, 3-, 8- and 12-OHNVP) and 4-carboxy nevirapine (4-COOHNVP), which together with their glucuronide conjugates (2-, 3-, 8- and 12-OHNVP-Glu) have been identified in human urine (Fan-Havard *et al.*, 2013; Riska *et al.*, 1999). Nucleoside reverse transcriptase inhibitors (NRTIs) such as abacavir undergo hepatic metabolism via the alcohol dehydrogenase and uridine diphosphate glucuronyl transferase pathways to form abacavir-5'-carboxylate and abacavir-5'-glucuronide, respectively. These two metabolites are the main clearance routes for abacavir, constituting ~30–36% of the dose through renal excretion, while fecal excretion of mostly unchanged drug accounts for ~16% of the dose (Yuen *et al.*, 2008). Similarly, hepatic metabolism of the protease inhibitor ritonavir produces several oxidative excretory metabolites at low levels compared to the parent drug, which is mostly excreted unchanged in fecal matter. The main metabolite for this drug is the isopropylthiazolyl ritonavir, which accounts for ~30% of the dose in excreta (Denissen *et al.*, 1997). These drugs and their metabolites are partially removed during wastewater treatment processes (Funke *et al.*, 2016; Richardson *et al.*, 2021; Schoeman *et al.*, 2017; Wood *et al.*, 2016).

The method of choice for the analysis of pharmaceuticals and their transformation products in wastewater is liquid chromatography hyphenated to tandem quadrupole MS (LC-MS/MS), typically operated in multiple reaction monitoring (MRM) mode (Mosekiemang *et al.*, 2019; Ncube *et al.*, 2018). While the selectivity and sensitivity of this approach is unsurpassed, the technique is less suitable for untargeted screening analyses, such as required for the determination of unknown metabolites. For such analyses, LC-high resolution MS (HR-MS) offers a powerful alternative analytical approach (Andra *et al.*, 2017). For complex samples such as wastewater, however, several challenges remain.

Processing full-scan HR-MS data to confidently distinguish small compound-related signals from complex matrix background can be challenging, and typical manual data analysis workflows are time consuming and labour intensive (Andra *et al.*, 2017; Mortishire-smith *et al.*, 2005). A number of data analysis strategies have been developed to facilitate processing of complex total ion chromatograms (TICs). One such approach is to use mass defect filters (MDFs) to remove interferences to simplify the identification of target compound classes (Bateman *et al.*, 2007; Zhang *et al.*, 2007). Phase I and II metabolites exhibit distinct mass shifts (Da) and fractional mass differences ( $\Delta$ FM, mDa) relative to their parent drugs (*e.g.* M+16 Da and  $\Delta$ FM -5.1 mDa for hydroxylated metabolites), suggesting the

possibility of implementing suitable MDF templates to look for such metabolites in complex samples (Zhang *et al.*, 2007, 2008).

A further development of relevance is the incorporation of ion mobility spectrometry (IMS) into LC-HR-MS workflows. In IMS, gaseous ions are separated as they traverse a buffer gas filled chamber under the influence of a weak electric field (D'Atri *et al.*, 2018; Lanucara *et al.*, 2014; May *et al.*, 2017). The additional separation step offered by IMS suggests that the technique can compensate for the limited selectivity typical of data independent acquisition modes (DIA) such as MS<sup>E</sup> - often used in screening analyses - where low- and high collision energy spectra are obtained for all co-eluting species. Using IMS, mass spectral data can be filtered according to the arrival time ( $t_A$ ) of particular ions to improve spectral interpretation (Castro-Perez *et al.*, 2007), while  $t_A$ -alignment of co-eluting precursors with their respective fragment ions can be used to enhance selectivity and improve spectral quality (Zandkarimi *et al.*, 2013). In addition, an ion's arrival time can be converted to its gas phase averaged collision cross section (CCS,  $\Omega$ ), which provides an additional identification criterion complementary to the retention time ( $t_R$ ) and mass-to-charge ratio ( $m/z$ ) data (Gabelica *et al.*, 2019; May *et al.*, 2017; May and McLean, 2015). The use of CCS values as an additional identification point is promising due to the extremely high precision of these values (Regueiro *et al.*, 2016; Stow *et al.*, 2017). This approach is however limited to compounds for which reliable experimental CCS values are available, which precludes its use for ARVD metabolites. In such cases, predicted CCS values may be used to support assignments (Bijlsma *et al.*, 2017; Ross *et al.*, 2020).

Against this background, the aim of the present study was to apply an untargeted screening approach based on LC-IMS-HR-MS operated in DIA mode to investigate the potential occurrence of ARVD metabolites in wastewater samples. We report the first evidence confirming the presence of several human metabolites of the ARVDs abacavir, efavirenz, nevirapine and ritonavir in influent and effluent samples.

## 5.2 Experimental

### 5.2.1 Chemicals

All solvents were LC-MS grade or better. Acetonitrile (ACN) and methanol (MeOH) were supplied by Romil Ltd. (Waterbeach, Cambridge, GB). Poly-DL-alanine (PolyAla) was supplied by Sigma-Aldrich, (St. Louis, MO, USA) while Formic acid (FA) and Ammonium Hydroxide (NH<sub>4</sub>OH) were supplied by Merck Millipore (Cape Town, South Africa). Laboratory water was obtained inhouse using a Millipore, Direct Q3 system. efavirenz (EFZ), emtricitabine (FTC), lamivudine (3TC), nevirapine (NVP) and ritonavir (RTV) were supplied by ClearSynth (Mumbai, India). 8,14-dihydroxy efavirenz (8,14-diOH-EFZ) and 12-hydroxy nevirapine (12OHNVP) were purchased from Toronto Research Chemicals Inc.

(North York, ON, Canada). Carbamazepine (CBZ), caffeine (CAF), and diclofenac (DIC) were obtained from Sigma-Aldrich.

### 5.2.2 Sample preparation

Wastewater samples were collected at a wastewater treatment plant receiving predominantly domestic sewage water, in Western Cape, South Africa. The samples were collected in April 2018 during a severe drought (2016-2018). Grab sampling was used to obtain several 500 mL sub-samples at 10-15 min intervals over 2h, which were pooled into a homogenised composite sample in a precleaned 5 L borosilicate glass conical flask. The composite sample was aliquoted into new and precleaned 500 mL amber bottles and transported to the lab where they were refrigerated at 4°C without preservative additives until processing within 24h. The raw wastewater samples were collected at an influent accumulation pond after the grit removal facility, while the biologically or membrane bioreactor (MBR) treated effluent samples were collected at designated sampling points before and after the chlorination pond. Prior to sample preparation, samples were sequentially filtered through 2.7 µm (47 mm) and 0.45 µm (25 mm) glass microfibre filters (Whatman, Maidstone, England). Samples were pre-concentrated either by solid phase extraction (SPE) using Strata SDB-L cartridges (200 mg/6 mL, Phenomenex, Torrance, CA, USA) or by lyophilisation (the latter for the analysis of polar metabolites that are poorly retained by SPE).

A generic SPE procedure was used, which entailed conditioning sequentially with ACN followed by MeOH (1 × 4 mL), equilibration with pH-adjusted (pH 7) deionised water (1 × 4 mL), sample loading (100 mL sample at ~1 mL/min), bed rinsing (pH-adjusted deionised water), vacuum drying for 10 min and elution using 4 mL FA/MeOH (5/95, v/v). The eluate was dried under N<sub>2</sub> and reconstituted in MeOH/water (3/7, v/v). For lyophilisation, 100 mL sample aliquots were dispensed into 250 mL volumetric flasks and frozen in a liquid N<sub>2</sub> bath. Frozen samples were mounted on a Beta 1-8 LD plus freeze-drier (Christ, Germany) for 24 h or until completely dry. Residues were re-suspended in 4 mL FA/MeOH (5/95, v/v), dried under N<sub>2</sub> and reconstituted in MeOH/water (3/7, v/v).

### 5.2.3 UHPLC settings

A Waters Acquity UPLC (Waters, Milford, USA) instrument was used, with separation performed using an Acquity HSS T3 column (1.8 µm, 2.1 × 150 mm) maintained at 45°C. The inlet method was a gradient programme set to deliver the mobile phases (0.1% FA, solvent A and ACN, solvent B) at 0.25 mL/min as follows: 100% A (0-1 min), 100-72% A (1-22 min), 72-60% A (22-22.5 min), 60-20% A (22.5-40 min), 20-0% A (40-42 min), 0-100% A (42-43 min) before re-equilibration. The injection volume was 2 µL.

#### 5.2.4 TWIMS-Q-TOF settings

High resolution ion mobility data was acquired using a Waters Synapt G2 quadrupole time-of-flight (Q-TOF) mass spectrometer equipped with an electrospray ionisation (ESI) source and an inline travelling wave ion mobility spectrometer (TWIMS). The instrument was operated in DIA ( $MS^E$ ) mode, where low and high collision energy data are acquired alternately. For the low collision energy (LE) function, a collision energy of 4 V was applied to scan for precursor or adduct ions in the mass range 100-2000 amu, whereas high collision energy (HE) data were acquired using a collision energy ramp of 20-50 V to scan for fragment ions over the mass range 50-2000 amu. Ultra-pure Argon (Ar) was used as a collision-induced dissociation gas. Separate analyses were performed using positive and negative ESI. The ESI conditions were as follows: cone and capillary voltages 15 V and 2.5 kV, respectively, and source and desolvation temperatures 120 and 275°C, respectively. The flow rates for the cone and desolvation gas ( $N_2$ ) flows were 50 and 650 L/h, respectively.

For IM separations, the T-wave trap and transfer devices were operated at a wave height and velocity of 6 V and 311 m/s, respectively. In the mobility cell, flow rates for helium (He) in the He-chamber and  $N_2$ -drift gas in the T-wave IMS cell were set at 180 and 90 mL/min, respectively.

Prior to operation, the QTOF was externally calibrated using sodium formate solution, and leucine enkephalin (reference masses  $m/z$  556.2771 and 554.2615 for ESI $_{\pm}$ , respectively) was used as lockspray mass. TWIMS calibration was performed in both ionisation modes using poly-DL-alanine as calibrant ( $z = 1$ ,  $m/z$  230.1–798.4, CCS 150.0–264.8 Å). All experimental CCS values reported were therefore obtained using TWIMS and nitrogen as drift gas ( $^{TWIMS}CCS_{N_2}$ ). IMS data were viewed and manipulated using DriftScope™ v2.9 software (Waters) and extracted ion data were exported to MassLynx™ v4.1 (Waters) for conversion into  $t_D$  mobilograms.

MetaboLynx™ (Waters) was used to search for expected metabolites by processing full scan accurate mass data (Mortishire-smith *et al.*, 2005; Tiller *et al.*, 2008). Metabolites of a single parent compound were searched using accurate mass filters (tolerance  $\pm 5$  ppm), with the phase I and II metabolites as targets using the predicted mass shifts relative to the target parent compound (e.g. parent + (OH,  $2 \times$  OH for phase I and  $C_6H_8O_8$ ,  $SO_3$  for phase II). Retention time filters were not applied to allow for a complete search of the entire chromatographic space. The resulting extracted range chromatograms (XRC) were further refined by implementing a fractional mass defect filter set at -50 and +50 mDa around a detected metabolite ion (Zhang *et al.*, 2009).

### 5.3 Results and discussion

#### 5.3.1 Analytical procedure for the untargeted screening of ARVD metabolites in wastewater samples.

The untargeted screening for ARVD metabolites in wastewater samples was achieved using UHPLC separation in combination with TWIMS-HR-MS detection (**Section 5.2.4**). For high efficiency

separations, a 150 mm Acquity HSS T3 column (1.8  $\mu\text{m}$ ,  $d_p$ ) was selected based on the capability of this phase to retain polar analytes as well as its compatibility with aqueous-rich mobile phases. A relatively long gradient was used for maximum chromatographic resolution (**Section 5.2.4**). For sample pre-treatment, both reversed phase SPE and lyophilisation were used, the latter to improve the detection of the polar nucleoside ARVDs (emtricitabine and lamivudine), which show poor retention on reversed phase (RP) SPE phases (Backe and Field, 2012; Mosekiemang *et al.*, 2019). Further details on the compounds detected in sample prepared by SPE and lyophilisation are presented in **Table S5.1**.

As expected, the total ion chromatograms obtained for the wastewater samples were highly complex, with incomplete resolution of the many detected features (**Figure S5.3**). In order to improve the identification of compounds, two approaches were used. First, all mass spectral data were filtered according to TWIMS arrival time, which improved spectral quality for co-eluting compounds. Secondly, full scan MS data was subjected to a mass defect filtering algorithm to eliminate matrix-related interferences. A typical output summary obtained using the Metabolyx platform is shown in **Figure S5.4**, which illustrates a list of expected metabolites for ritonavir ( $\text{C}_{37}\text{H}_{48}\text{N}_6\text{O}_5\text{S}_2$ ,  $\Delta m/z$  -2.2 ppm), and an hydroxylated ritonavir metabolite detected at  $t_R$  28.71 min ( $\text{C}_{37}\text{H}_{48}\text{N}_6\text{O}_6\text{S}_2$ ,  $\Delta m/z$  -2.8 ppm).

Using this screening method, several pharmaceuticals of different classes (*i.e.* anticonvulsants, analgesics, beta blockers, etc.) were detected in wastewater samples. For instance, the sedative methaqualone, a constituent of Mandrax whose illicit use is well-documented among adolescents in Cape Town (Parry *et al.*, 2004), was tentatively identified, as well as the opiates codeine and tramadol and the antibiotic trimethoprim. The anticonvulsant carbamazepine, the anti-inflammatory drug diclofenac and caffeine were identified using authentic standards. Furthermore, polyethylene glycols (PEGs) of chain lengths ranging from 7-17 ethoxy groups ( $m/z$  327–784 and CCS 173.0–268.9  $\text{\AA}^2$ ) were also detected in the positive mode as  $[\text{M}+\text{NH}_4]^+$  or  $[\text{M}+\text{H}]^+$  adduct ions in raw wastewater samples only. The presence of PEG may originate from medical formulations where they serve as vehicles for drug delivery or excipients (Howdle *et al.*, 2009), or from plastic labware (Rardin, 2018), although this is unlikely as they were only detected in raw wastewater samples.

A further benefit of incorporating IMS into the analytical workflows is that tentative identification can be strengthened by comparing experimentally determined CCS values ( $\text{CCS}_{\text{exp}}$ ) to literature ( $\text{CCS}_{\text{lit}}$ ) values (e.g. codeine, methaqualone, PEGs, tramadol and trimethoprim in **Table 1**). Generally, good agreement with measured CCS values from literature was obtained for most compounds, with  $\Delta\text{CCS}$  values in the range  $\pm 0.1$ –3.1% (an acceptable deviation considering that this is essentially an interlaboratory reproducibility assessment, where an acceptability threshold is set at  $< 2\%$  (Regueiro *et al.*, 2016)). Higher  $\Delta\text{CCS}$  values measured for especially low molecular weight MW compounds ( $m/z \leq 180$ ) can be ascribed to the limitations of the calibrant (poly-DL-alanine) in this region (Masike *et al.*, 2021; Richardson *et al.*, 2019). Note that for most of the ARVD metabolites identified in the present

work, experimentally determined CCS values are reported here for the first time. In such cases,  $CCS_{lit}$  values were predicted using the approach of Ross *et al.*(2020) for comparison purposes.

The above results confirm the suitability of the UHPLC-IMS-HR-MS method for the screening analysis of pharmaceutical compounds in wastewater samples. Despite this, zidovudine and its glucuronide were not detected in this work, possibly due to poor recovery from SPE and lyophilisation.



**Table 5.1:** Summary of the pharmaceutical compounds and metabolites detected in wastewater samples by LC-IMS-HR-MS.

<i>Non ARVD pharmaceuticals and their metabolites</i>											
$t_R$ (min)	Compound	Class	Elemental formula	Detected ion	Observed $m/z$	$\Delta m/z$ (ppm)	$^{TWIMS}CCS_{N_2}$ ( $\text{\AA}^2$ )			Observed MS/MS ions	****Reference
							$^{\S}Exp.$	$^{\S\S}Lit.$	$^{\S\S\S}\Delta CCS$ (%)		
10.59	codeine	Opiate	C <sub>18</sub> H <sub>22</sub> NO <sub>3</sub>	[M+H] <sup>+</sup>	300.1604	0.4	166.6	168.2 <sup>d</sup>	-0.9	243.1032, 225.0943, 215.1098	(Qu <i>et al.</i> , 2016)
12.82	caffeine	Methylxanthine	C <sub>8</sub> H <sub>11</sub> N <sub>4</sub> O <sub>2</sub>	[M+H] <sup>+</sup>	195.0875	-3.6	134.0	136.9 <sup>e</sup>	-2.1	138.0661, 110.0715	Standard
12.90	<i>O</i> -desmethyltramadol	Opioid metabolite	C <sub>15</sub> H <sub>24</sub> NO <sub>2</sub>	[M+H] <sup>+</sup>	250.1793	-5.5	155.6	157.4 <sup>e</sup>	-1.1	214.9307, 191.1119, 149.0310	(Mollerup <i>et al.</i> , 2018)
13.23	trimethoprim	Antibiotic	C <sub>14</sub> H <sub>19</sub> N <sub>4</sub> O <sub>3</sub>	[M+H] <sup>+</sup>	291.1457	0.0	169.2	170.8 <sup>e</sup>	-0.9	275.1123, 261.0981, 230.1135, 123.0632	(Jewell <i>et al.</i> , 2016)
16.92	tramadol	Opiate	C <sub>16</sub> H <sub>26</sub> NO <sub>2</sub>	[M+H] <sup>+</sup>	264.1964	-3.0	157.8	160.4 <sup>d</sup>	-1.7	214.9243, 132.0895, 119.019	(Mollerup <i>et al.</i> , 2018)
25.52	carbamazepine	Anticonvulsant	C <sub>15</sub> H <sub>13</sub> N <sub>2</sub> O	[M+H] <sup>+</sup>	237.1026	-0.8	145.7	150.3 <sup>e</sup>	-3.1	220.0759, 194.0964, 167.0856	Standard
26.68	methaqualone	Sedative	C <sub>16</sub> H <sub>15</sub> N <sub>2</sub> O	[M+H] <sup>+</sup>	251.1186	0.8	150.2	155.0 <sup>e</sup>	-3.1	132.0832, 120.0598, 91.0496	(Oliveira <i>et al.</i> , 2015)
31.89	diclofenac	NSAID	C <sub>14</sub> H <sub>12</sub> NO <sub>2</sub> Cl <sub>2</sub>	[M+H] <sup>+</sup>	296.0235	-3.4	161.2	161.1 <sup>d</sup>	0.1	214.0423, 179.0716, 151.0533	Standard
<i>ARVD pharmaceuticals and their metabolites</i>											
$t_R$ (min)	Compound	Class	Elemental formula	Detected ion	Observed $m/z$	$\Delta m/z$ (ppm)	$^{TWIMS}CCS_{N_2}$ ( $\text{\AA}^2$ )			Observed MS/MS ions	****Reference
							$^{\S}Exp.$	$^{\S\S}Lit.$	$^{\S\S\S}\Delta CCS$ (%)		
2.91	lamivudine	ARVD	C <sub>8</sub> H <sub>12</sub> N <sub>3</sub> O <sub>3</sub> S	[M+H] <sup>+</sup>	230.0590	-3.9	140.8	146.8 <sup>a</sup>	-0.6	230.0594, 95.0237	Standard
4.33	emtricitabine	ARVD	C <sub>8</sub> H <sub>11</sub> N <sub>3</sub> O <sub>3</sub> SF	[M+H] <sup>+</sup>	248.0499	-2.4	145.3	149.4 <sup>a</sup>	-2.7	248.0500, 130.0406	Standard
11.96	abacavir	ARVD	C <sub>14</sub> H <sub>19</sub> N <sub>6</sub> O	[M+H] <sup>+</sup>	287.1615	-3.5	162.1	167.2 <sup>a</sup>	-3.0	191.1014, 150.0631, 134.0437	(Funke <i>et al.</i> , 2016)
12.21	abacavir-5'-carboxylate	ARVD Metabolite	C <sub>14</sub> H <sub>17</sub> N <sub>6</sub> O <sub>2</sub>	[M+H] <sup>+</sup>	301.1410	-1.0	168.9	169.9 <sup>a</sup>	-0.6	191.1040, 174.0767, 150.0627, 134.0469	(Funke <i>et al.</i> , 2016)
15.91	2-hydroxy efavirenz	ARVD Metabolite	C <sub>15</sub> H <sub>15</sub> N <sub>4</sub> O <sub>2</sub>	[M+H] <sup>+</sup>	283.1193	-0.7	159.8	167.0 <sup>a</sup>	-4.3	242.0819, 214.0879, 161.0720, 123.0490	(Ren <i>et al.</i> , 2010)
16.92	12-hydroxy nevirapine	ARVD Metabolite	C <sub>15</sub> H <sub>15</sub> N <sub>4</sub> O <sub>2</sub>	[M+H] <sup>+</sup>	283.1190	-1.8	164.7	167.0 <sup>a</sup>	-1.4	265.1089, 237.1139, 223.1101, 196.0748	Standard
17.58	3-hydroxy nevirapine	ARVD Metabolite	C <sub>15</sub> H <sub>15</sub> N <sub>4</sub> O <sub>2</sub>	[M+H] <sup>+</sup>	283.1182	-4.6	159.8	167.0 <sup>a</sup>	-4.3	242.0823, 214.0881, 161.0724, 123.0477	(Ren <i>et al.</i> , 2010)

19.94	nevirapine	ARVD	C <sub>15</sub> H <sub>15</sub> N <sub>4</sub> O	[M+H] <sup>+</sup>	267.1245	-0.4	162.7	163.8 <sup>a</sup>	-0.7	227.0926, 226.0854, 107.0605	Standard
26.95	8,14-dihydroxy efavirenz	ARVD Metabolite	C <sub>14</sub> H <sub>8</sub> NO <sub>4</sub> F <sub>3</sub> Cl	[M-H] <sup>-</sup>	346.0105	3.2	188.4	181.2 <sup>a</sup>	4.0	262.0003, 241.9937, 226.0342	Standard
27.20	N-hydroxy efavirenz glucuronide	ARVD Metabolite	C <sub>20</sub> H <sub>16</sub> NO <sub>8</sub> F <sub>3</sub> Cl	[M-H] <sup>-</sup>	490.0527	2.0	220.4	218.6 <sup>a</sup>	0.8	314.0201, 244.0200	(Deng <i>et al.</i> , 2015)
27.24	atazanavir	ARVD	C <sub>38</sub> H <sub>53</sub> N <sub>6</sub> O <sub>7</sub>	[M+H] <sup>+</sup>	705.3968	-1.1	265.3	263.6 <sup>b</sup>	-0.1	563.3292, 534.3036, 335.1921, 168.0810	(Alelyunas <i>et al.</i> , 2017)
27.81	7,14-dihydroxy efavirenz	ARVD Metabolite	C <sub>14</sub> H <sub>8</sub> NO <sub>4</sub> F <sub>3</sub> Cl	[M-H] <sup>-</sup>	346.0106	3.5	183.0	181.2 <sup>a</sup>	1.0	262.0013, 204.0140, 183.0064	(Deng <i>et al.</i> , 2015)
27.91	8,14-dihydroxy efavirenz sulphate	ARVD Metabolite	C <sub>14</sub> H <sub>8</sub> NO <sub>7</sub> F <sub>3</sub> ClS	[M-H] <sup>-</sup>	425.9662	1.4	195.1	197.5 <sup>a</sup>	-1.2	325.1932, 302.0269, 282.0211, 262.0147	(Deng <i>et al.</i> , 2015)
28.69	hydroxy ritonavir	ARVD Metabolite	C <sub>37</sub> H <sub>49</sub> N <sub>6</sub> O <sub>6</sub> S <sub>2</sub>	[M+H] <sup>+</sup>	737.3148	0.9	260.9	260.1 <sup>a</sup>	0.3	312.1306, 284.1354, 187.1017	(Gangl <i>et al.</i> , 2002)
30.93	7- and/or 8-hydroxy efavirenz	ARVD Metabolite	C <sub>14</sub> H <sub>8</sub> NO <sub>3</sub> F <sub>3</sub> Cl	[M-H] <sup>-</sup>	330.0157	3.6	186.6	187.6 <sup>a</sup>	-0.5	286.0240, 257.9933, 250.0481, 210.0355	(Deng <i>et al.</i> , 2015)
31.72	N-hydroxy efavirenz	ARVD Metabolite	C <sub>14</sub> H <sub>8</sub> NO <sub>3</sub> F <sub>3</sub> Cl	[M-H] <sup>-</sup>	330.0160	4.5	186.6	187.6 <sup>a</sup>	-0.5	263.9684, 260.0119	(Deng <i>et al.</i> , 2015)
32.62	8-hydroxy efavirenz sulphate	ARVD Metabolite	C <sub>14</sub> H <sub>8</sub> NO <sub>6</sub> F <sub>3</sub> ClS	[M-H] <sup>-</sup>	409.9717	1.0	201.1	203.9 <sup>a</sup>	-1.4	330.0149, 286.0246, 257.9940, 210.0364	(Deng <i>et al.</i> , 2015)
32.87	ritonavir	ARVD	C <sub>37</sub> H <sub>49</sub> N <sub>6</sub> O <sub>5</sub> S <sub>2</sub>	[M+H] <sup>+</sup>	721.9198	-1.1	262.4	255.7 <sup>a</sup>	2.6	426.2375, 268.1511, 197.0759, 171.0978	Standard
33.19	efavirenz	ARVD	C <sub>14</sub> H <sub>8</sub> NO <sub>2</sub> F <sub>3</sub> Cl	[M-H] <sup>-</sup>	314.0208	3.8	184.8	187.8 <sup>a</sup>	-1.6	250.0266, 244.0175, 183.0108	Standard
33.69	lopinavir	ARVD	C <sub>37</sub> H <sub>49</sub> N <sub>4</sub> O <sub>5</sub>	[M+H] <sup>+</sup>	629.3732	4.6	257.6	256.7 <sup>a</sup>	0.3	447.3050, 429.2880, 310.2079, 183.1264	(Marzinke <i>et al.</i> , 2014)

*Synthetic polymers*

t <sub>R</sub> (min)	Compound	Class	Elemental formula	Detected ion	Observed m/z	Δ m/z (ppm)	TWIMSCCSN <sub>2</sub> (Å <sup>2</sup> )			Observed MS/MS ions	****Reference
							§Exp.	§§Lit.	§§§ΔCCS (%)		
13.31	PEG <sup>#</sup> (n = 7)	Surfactant	C <sub>14</sub> H <sub>30</sub> O <sub>8</sub>	[M+H] <sup>+</sup>	327.2019	0.9	173.0	178.0 <sup>e</sup>	-2.8	–	(Fiebig and Laux, 2016)
14.53	PEG (n = 8)	Surfactant	C <sub>16</sub> H <sub>34</sub> O <sub>9</sub>	[M+NH <sub>4</sub> ] <sup>+</sup>	388.2547	-1.5	182.5	183.0 <sup>e</sup>	-0.3	–	(Fiebig and Laux, 2016)
15.62	PEG (n = 9)	Surfactant	C <sub>18</sub> H <sub>38</sub> O <sub>10</sub>	[M+NH <sub>4</sub> ] <sup>+</sup>	432.2805	-0.9	192.1	191.0 <sup>e</sup>	0.6	–	(Fiebig and Laux, 2016)
16.60	PEG (n = 10)	Surfactant	C <sub>20</sub> H <sub>42</sub> O <sub>11</sub>	[M+NH <sub>4</sub> ] <sup>+</sup>	476.3071	-2.5	199.1	200.0 <sup>e</sup>	-0.5	–	(Fiebig and Laux, 2016)
17.49	PEG (n = 11)	Surfactant	C <sub>22</sub> H <sub>46</sub> O <sub>12</sub>	[M+NH <sub>4</sub> ] <sup>+</sup>	520.3333	-0.5	209.7	209.0 <sup>e</sup>	-0.5	–	(Fiebig and Laux, 2016)
18.31	PEG (n = 12)	Surfactant	C <sub>24</sub> H <sub>50</sub> O <sub>13</sub>	[M+NH <sub>4</sub> ] <sup>+</sup>	564.3595	-1.1	219.5	219.0 <sup>e</sup>	0.2	–	(Fiebig and Laux, 2016)
19.05	PEG (n = 13)	Surfactant	C <sub>26</sub> H <sub>54</sub> O <sub>14</sub>	[M+NH <sub>4</sub> ] <sup>+</sup>	608.3857	-2.0	230.5	230.0 <sup>e</sup>	0.2	–	(Fiebig and Laux, 2016)
19.74	PEG (n = 14)	Surfactant	C <sub>28</sub> H <sub>58</sub> O <sub>15</sub>	[M+NH <sub>4</sub> ] <sup>+</sup>	652.4119	-1.2	241.2	240.0 <sup>e</sup>	0.5	–	(Fiebig and Laux, 2016)
20.37	PEG (n = 15)	Surfactant	C <sub>30</sub> H <sub>62</sub> O <sub>16</sub>	[M+NH <sub>4</sub> ] <sup>+</sup>	696.4382	1.6	249.8	251.0 <sup>e</sup>	-0.5	–	(Fiebig and Laux, 2016)
24.08	PEG (n = 16)	Surfactant	C <sub>32</sub> H <sub>66</sub> O <sub>17</sub>	[M+NH <sub>4</sub> ] <sup>+</sup>	740.4644	0.5	259.4	261.0 <sup>e</sup>	-0.6	–	(Fiebig and Laux, 2016)
24.08	PEG (n = 17)	Surfactant	C <sub>34</sub> H <sub>70</sub> O <sub>18</sub>	[M+NH <sub>4</sub> ] <sup>+</sup>	784.4877	-3.7	268.9	271.0 <sup>e</sup>	-0.8	–	(Fiebig and Laux, 2016)

<sup>#</sup>Monomer/chain length.

<sup>§</sup>Experimental CCS values, <sup>§§</sup>CCS obtained from literature, or where none was available, the CCS value predicted according to Ross *et al.* (2020), <sup>§§§</sup>Error between experimental CCS values and those obtained from literature or by prediction, <sup>§§§§</sup>References used for comparison of MS/MS data.

<sup>a</sup>(Ross *et al.*, 2020), <sup>b</sup>(Alelyunas *et al.* 2017), <sup>c</sup>(Hines *et al.*, 2017), <sup>d</sup>(Bijlsma *et al.*, 2017), <sup>e</sup>(Fiebig and Laux, 2016),

The goal of this work was however to investigate the potential occurrence of ARVD metabolites using the proposed analytical screening methodology (**Figure S5.5**). Indeed, eight ARVDs were detected in the analysed wastewater samples (**Table 5.1**), belonging to nucleoside reverse transcriptase inhibitors (NRTI, abacavir, emtricitabine and lamivudine), non-nucleoside reverse transcriptase inhibitors (*n*NRTI, efavirenz and nevirapine) and protease inhibitors (PI, atazanavir, ritonavir and lopinavir) classes. Of these, efavirenz, emtricitabine, lamivudine, nevirapine and ritonavir were identified using standards, whereas abacavir, atazanavir and lopinavir were tentatively assigned based on HR-MS data and experimental CCS values. Furthermore, two ARV metabolites recently reported in wastewater samples (Mosekiemang *et al.*, 2019), namely 8,14-dihydroxy-efavirenz and 12-hydroxy-nevirapine, were identified using reference standards. Interestingly, several additional chromatographic peaks were found to potentially correspond to further metabolites of abacavir, efavirenz, nevirapine and ritonavir based on HR-MS and IMS data. The tentative or putative assignments of these are discussed in detail below.

### 5.3.2 Identification of ARVD metabolites

#### 5.3.2.1 Efavirenz metabolites

A total ion current (TIC) chromatogram illustrating the retention window where efavirenz (EFZ) metabolites were detected is presented in **Figure 1**. The parent compound EFZ was detected in both raw and treated wastewater samples processed by both SPE and lyophilisation and confirmed using a reference standard, with good agreement between  $CCS_{exp}$  ( $CCS\ 184.8\ \text{\AA}^2$ ) and  $CCS_{lit}$  values ( $\Delta CCS - 1.6\%$ ). EFZ eluted later ( $t_R\ 33.19\ \text{min}$ ) than its metabolites in RP-LC, as expected based on its larger hydrophobicity.

##### 5.3.2.1.1 Monohydroxylated metabolites of efavirenz

Three monohydroxylated metabolites of EFZ have previously been identified in human urine samples obtained from clinical subjects undergoing EFZ-based therapy (Ogburn *et al.*, 2010), namely 7-, 8- and *N*-hydroxy-efavirenz (7-, 8- and *N*-OH-EFZ), while 8-OH-EFZ was recently detected in river water in the UK (Richardson *et al.*, 2021). These are relatively easily identified by the distinctive  $^{37}\text{Cl}$  isotope peak ( $m/z\ 332$ ) of the deprotonated molecular ions at  $m/z\ 330$  ( $\text{C}_{14}\text{H}_8\text{NO}_3\text{F}_3\text{Cl}$ ), 16 Da higher than that of the parent drug ( $m/z\ 314$   $[\text{M}-\text{H}]^-$ ,  $\text{C}_{14}\text{H}_8\text{NO}_2\text{F}_3\text{Cl}$ ) (**Figure 5.2 B&C**). However, the extracted ion chromatogram (XIC) for  $m/z\ 330$  provided only two well-separated peaks in wastewater samples, at  $t_R\ 30.93$  and  $31.72\ \text{min}$  (**Figure 5.2A**).

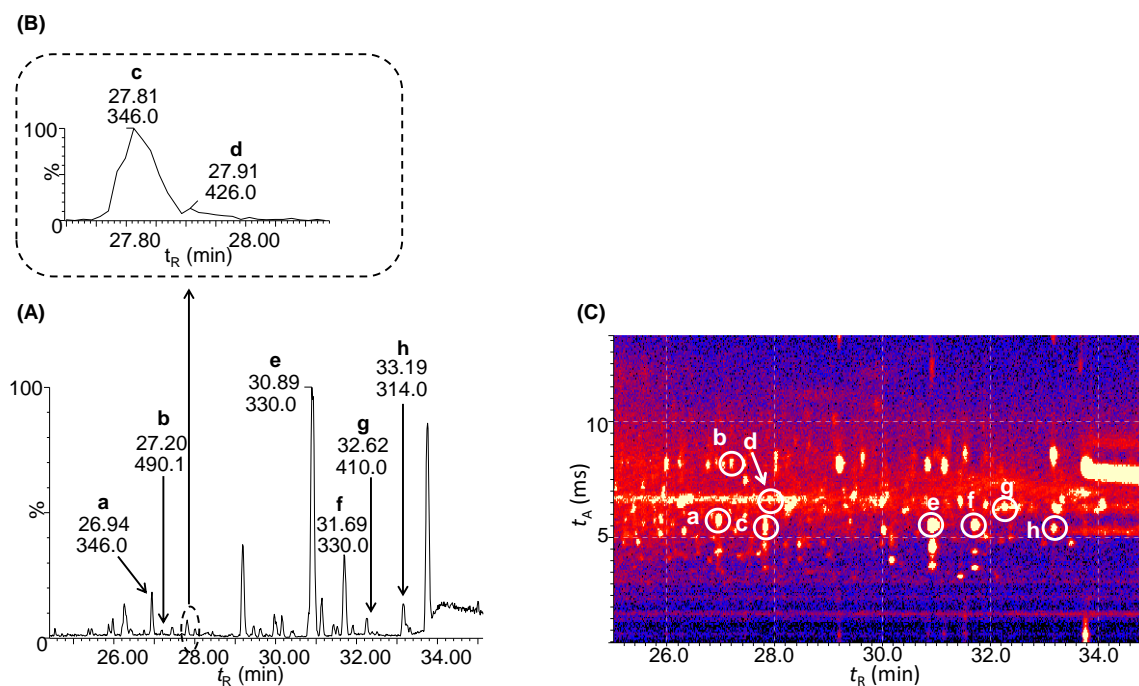


**Figure 5.1:** (A) Region of the total ion current (TIC) chromatogram where EFZ and its metabolites were detected in a raw wastewater sample processed by SPE. Data obtained using negative ESI. (B) shows a close-up of the partial separation of **c** and **d**, and (C) presents the relevant region in contour plot format (retention time vs. IMS arrival time). Peak annotation: (a) 8,14-dihydroxy-efavirenz, (b) *N*-hydroxy efavirenz-glucuronide, (c) 7,14-dihydroxy-efavirenz, (d) 8,14-dihydroxy-efavirenz-sulphate, (e) 7- and/or 8-hydroxy-efavirenz (refer to text), (f) *N*-hydroxy-efavirenz, (g) 8-hydroxy-efavirenz-sulphate, and (h) efavirenz.

Further information can be obtained from the  $MS^E$  data, where the high collision energy (HE) spectrum for the two peaks differ significantly. The earlier eluting peak showed diagnostic ions at  $m/z$  286.0242 ( $C_{13}H_8NOF_3Cl$ ,  $\Delta m/z$  -1.7 ppm), 257.9936 ( $C_{11}H_4NOF_3Cl$ ,  $\Delta m/z$  0.8 ppm), 250.0482 ( $C_{13}H_7NOF_3$ ,  $\Delta m/z$  0.8 ppm) and 210 ( $C_{10}H_6NO_2F_2$ ,  $\Delta m/z$  -5.2 ppm), which agree remarkably well with the fragmentation behaviour reported for both 7- and 8-OH-EFZ (Deng *et al.*, 2015), also reported for the same compounds in human urine (Mutlib *et al.*, 1999; Ogburn *et al.*, 2010). These fragment ions allowed differentiation of the compound from *N*-OH-EFZ (see below). Because 7- and 8-OH-EFZ show similar HR-MS behaviour, and both compounds elute before *N*-OH-EFZ (Aouri *et al.*, 2016; Deng *et al.*, 2015; Ogburn *et al.*, 2010) the peak eluting at 30.93 min was tentatively assigned as 7- or 8-OH-EFZ, or indeed could correspond to both species co-eluting. Note that IMS could not be used to assign this compound, since the experimental CCS values for both peaks were identical ( $t_A$  5.45 ms, and CCS 186.6 Å<sup>2</sup>, respectively) (Figure S5.6), as indeed confirmed by the CCS prediction based on the SMILES structures for monohydroxylated EFZ species according to Ross *et al.* (2020) (Table 5.1).

The peak eluting at  $t_r$  31.72 min was tentatively assigned to *N*-OH-EFZ based on its higher retention and on the unique fragmentation of this compound, including assignment of characteristic fragment ions (**Figure 5.2E**), both of which are in agreement with the previous studies (Deng *et al.*, 2015; Mutlib *et al.*, 1999). Unlike the fragmentation spectra for 7- and 8-OH-EFZ, which are essentially similar, the base peak ion for *N*-OH-EFZ is observed at  $m/z$  263 ( $C_9H_2NO_3F_3Cl$ ,  $\Delta m/z$  4.5 ppm), likely formed due to the loss of an ethynylcyclopropane ( $C_5H_6$ ) fragment from the deprotonated molecular ion according to (Deng *et al.*, 2015). The presence of this ion confirms that the hydroxyl is not situated on the cyclopropyl side chain, while the distinct fragmentation pathways for this molecule implies that neither is it situated on the aromatic ring. A second characteristic ion was observed at  $m/z$  260 ( $C_{13}H_7NO_3Cl$ ,  $\Delta m/z$  1.9 ppm), which is produced by the loss of a  $CHF_3$  moiety; this is followed by the loss of carbon monoxide (CO) to produce the fragment ion at  $m/z$  232 ( $C_{12}H_7NO_2Cl$ ,  $\Delta m/z$  3.9 ppm).

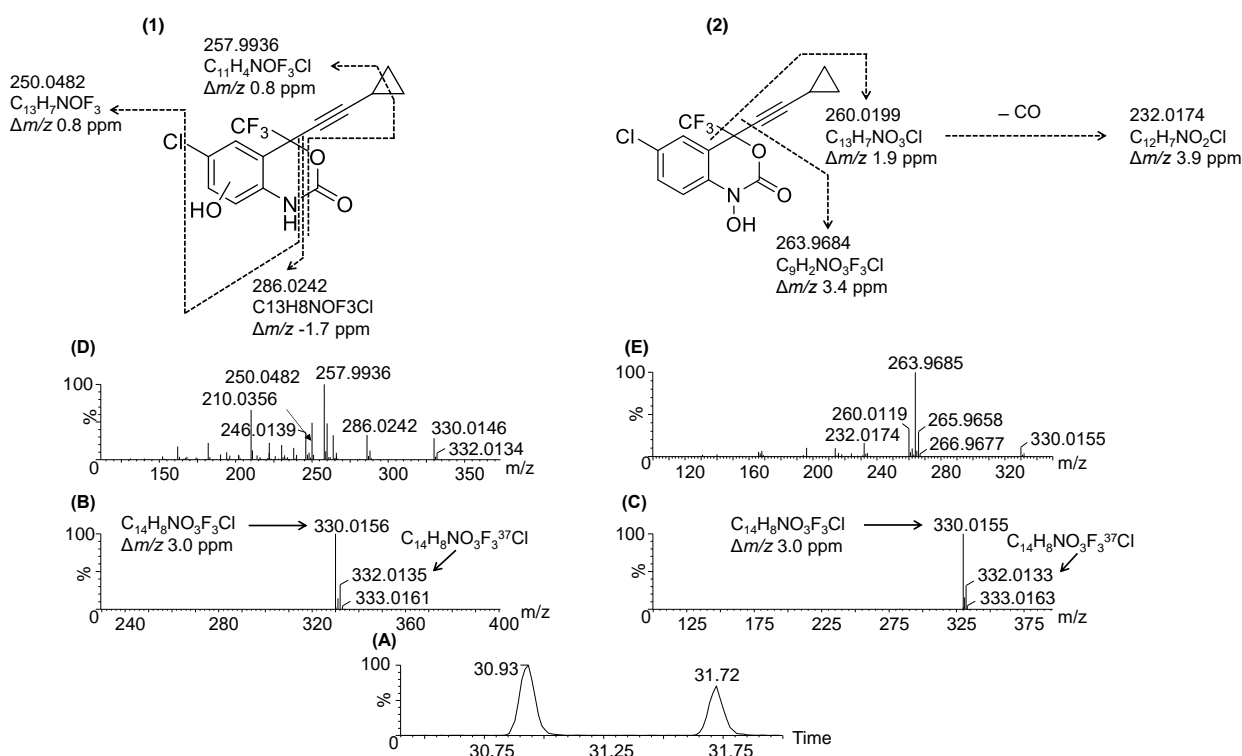


**Figure 5.2:** (A) Extracted ion chromatogram (XIC) at  $m/z$  330 showing the monohydroxylated EFZ metabolites 7- and/or 8-OH-EFZ (1) and *N*-OH-EFZ (2) detected in a treated wastewater sample. Also shown are the low collision energy (B and C) and high collision energy ( $MS^E$ ) (D and E) spectra for the two isomeric metabolites.

### 5.3.2.1.2 Dihydroxylated metabolites of efavirenz

Two dihydroxylated EFZ metabolites have been reported in pharmacokinetic studies using clinical samples (Mutlib *et al.*, 1999; Ogburn *et al.*, 2010). Both, 7,14- and 8,14-dihydroxy-efavirenz (7,14-diOH-EFZ and 8,14-diOH-EFZ), were also detected in influent and effluent wastewater samples, albeit at low signal intensities (**Figure S5.7**). Mass defects values are in accordance with expectations for dihydroxy metabolites (Zhang *et al.*, 2007, 2009, 2008). These metabolites show a deprotonated molecular ion at  $m/z$  346 ( $C_{14}H_8NO_4F_3Cl$ ), and the XIC for this mass (**Figure 5.3A**) shows two well separated isomers. The peak at  $t_R$  26.95 min was conclusively confirmed as 8,14-diOH-EFZ using a reference standard (Ross *et al.*, 2020). Accordingly, the later eluting peak at  $t_R$  27.81 min was tentatively assigned to 7,14-OH-EFZ. This is fully supported by the high collision energy spectrum of this compound, where the molecular formulae for fragment ions confirm the relevant fragmentation pathways (**Figure 5.3B-D**). The characteristic ion at  $m/z$  302 ( $C_{13}H_8NO_2F_3Cl$ , only visible in the spectrum for the reference compound) is formed by the loss of a  $CO_2$  from the molecular ion. Thereafter, the sequential losses of HF (20 Da) from this and subsequent ions produce fragment ions at  $m/z$  282.0131 ( $C_{13}H_7NO_2F_2Cl$ ,  $\Delta m/z$  -0.7 ppm), 262.0073 ( $C_{13}H_6NO_2FCl$ ,  $\Delta m/z$  -0.8 ppm) and 242.0016 ( $C_{13}H_5NO_2Cl$ ,  $\Delta m/z$  2.9 ppm), while the loss of HCl from  $m/z$  262 produces the fragment ion at  $m/z$  226.0309 ( $C_{13}H_5NO_2F$ ,  $\Delta m/z$  2.2 ppm).

IMS data shows that these two positional isomers were well separated according to arrival time ( $t_D$  5.38, CCS 183.0 Å and 5.73 ms, CCS 188.4 Å<sup>2</sup> for 7,14- and 8,14-diOH-EFZ, respectively), indicating that IMS could be used to identify them. This is in contrast to the CCS values predicted based on SMILES structures according to Ross *et al.* (2020), which provides identical and much smaller CCS values for these isomers (**Table 5.1**).

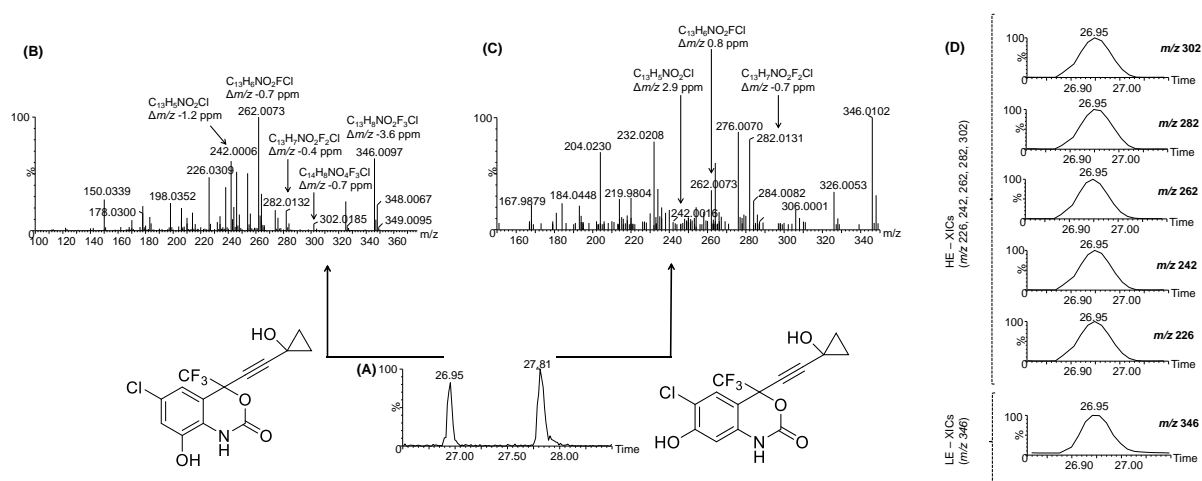


**Figure 5.3:** (A) Extracted ion chromatogram (XIC) for  $m/z$  346 obtained for a treated wastewater sample showing well separated peaks for 8,14-diOH-EFZ,  $t_R$  26.95 min, confirmed using a reference standard, and 7,14-diOH-EFZ,  $t_R$  27.81 min. MS<sup>E</sup> fragmentation spectra for both compounds are shown

in **(B)** and **(C)**, respectively. Confirmation of the origin of common fragment ions  $m/z$  226, 242, 262, 282, 302 is shown in their  $t_R$ -aligned XICs generated from the reference standard **(D)**.

#### 5.3.2.1.3 Phase II metabolites of efavirenz

##### *Glucuronide metabolite*

The only glucuronide metabolite of EFZ detected in this work is efavirenz-*N*-glucuronide (*N*-EFZ-glu,  $m/z$  490.0539,  $C_{20}H_{16}NO_8F_3Cl$ ,  $\Delta m/z$  2.7 ppm,  $CCS_{exp}$  220.4 Å<sup>2</sup>), with a mass defect relative to EFZ of 32 mDa in accordance with expectation for a glucuronide metabolite (Zhang *et al.*, 2007, 2009, 2008). This compound eluted at  $t_R$  27.20 min and provided fragment ions at  $m/z$  314.0209 ( $C_{14}H_8NO_2F_3Cl$ ,  $\Delta m/z$  4.1 ppm), corresponding to the EFZ aglycone following the neutral loss of a glucuronic acid moiety, and  $m/z$  244.0159 ( $C_{13}H_7NO_2Cl$ ,  $\Delta m/z$  -2.5 ppm), produced by the subsequent loss of trifluoromethane (CHF<sub>3</sub>) from the aglycone (Bélanger *et al.*, 2009; Mutlib *et al.*, 1999). This metabolite was detected only in raw wastewater samples, and not in treated samples. This suggests that *N*-EFZ-glu may either be effectively removed, or, more likely, may be reduced to EFZ during the treatment process, which may explain observations of elevated concentrations of EFZ in treated compared to raw wastewater (Abafe *et al.*, 2018; Schoeman *et al.*, 2017).

One of the primary benefits of incorporating IMS in untargeted LC-MS workflows is that it provides the option of filtering MS data according to arrival time, thereby improving the quality of mass spectra for co-eluting species. This is illustrated in **Figure 5.4**, where the low- and high energy mass spectra obtained for *N*-EFZ-glu with and without IMS filtering are compared. Because of the relatively low levels of these compounds, and the fact that they elute in a portion of the chromatogram where severe matrix background is observed (**Figure S5.7**), interpretation of especially their high collision energy spectra is greatly facilitated by arrival time filtering. The measured CCS for this compound is relatively large at 220.4 Å<sup>2</sup>, in agreement with the predicted CCS (**Table 5.1**).



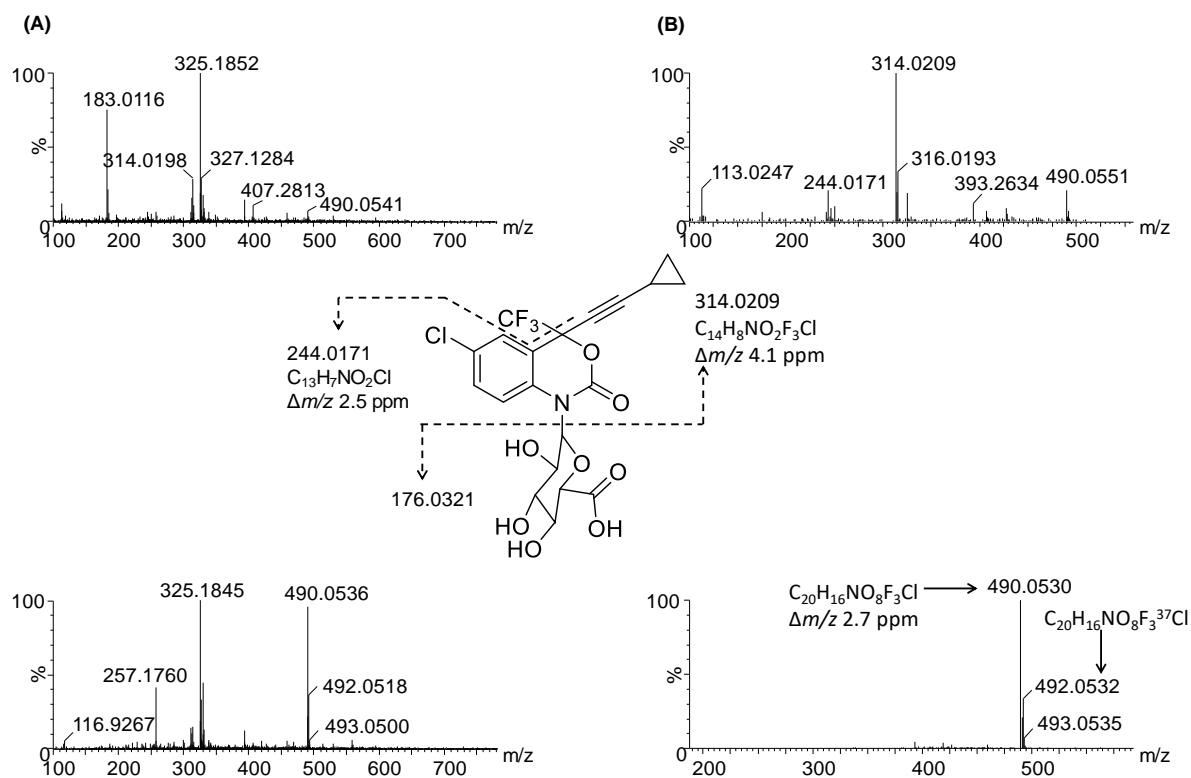


**Figure 5.4:** Mass spectra obtained for efavirenz-*N*-glucuronide (*N*-EFZ-glu) in a wastewater influent sample processed by SPE without (A) and with (B) prior filtering according to IMS arrival time. Low energy spectra are presented at the bottom, and high energy MS<sup>E</sup> spectra on top.

### Sulphated metabolites

One mono-hydroxy-sulphate EFZ metabolite (C<sub>14</sub>H<sub>8</sub>NO<sub>6</sub>F<sub>3</sub>SCl) as well as a dihydroxy-sulphate EFZ metabolites (C<sub>14</sub>H<sub>8</sub>NO<sub>7</sub>F<sub>3</sub>SCl) were also detected in raw and treated wastewater samples. In their respective XICs - *m/z* 409.9717 and 425.9662 for deprotonated molecular ions of the mono- and dihydroxy-sulphate derivatives - these ions are represented by peaks at *t<sub>R</sub>* 32.62 min and 27.91 (Figure S5.7). Both these compounds showed the neutral loss of sulphate groups (-80 Da) in their HE MS<sup>E</sup> spectra.

The monohydroxy-sulphate metabolite was tentatively identified as 8-OH-EFZ-sulphate based on its fragmentation spectrum that revealed the distinguishing aglycone fragment ion at *m/z* 330.0152 (C<sub>14</sub>H<sub>8</sub>NO<sub>3</sub>F<sub>3</sub>Cl, Δ*m/z* -2.5 ppm) - this ion is not observed in the fragmentation of 7-OH-EFZ-sulphate (Aouri *et al.*, 2016; Mutlib *et al.*, 1999). Subsequent losses of CO<sub>2</sub> and CO<sub>2</sub> + C<sub>2</sub>H<sub>4</sub> from the cyclopropyl group produced fragment ions at *m/z* 286.0246 and 257.9940, respectively (Figure 5.5). Sulphotransferase reactions involving EFZ have been hypothesised to predominantly occur at C-8 due to steric hindrance effects caused by the proximity of the Cl atom to C-7 (Deng *et al.*, 2015).

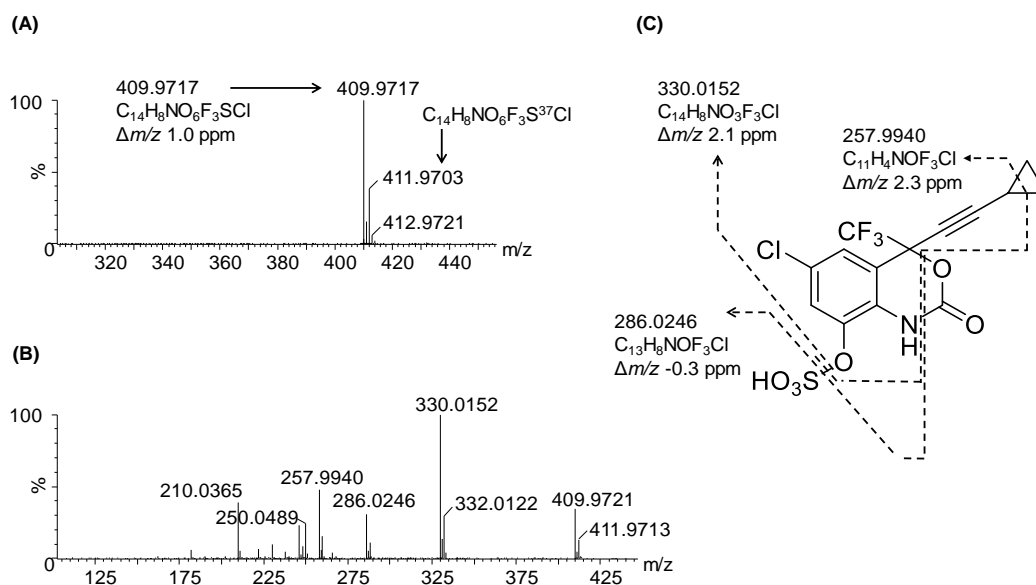


**Figure 5.5:** (A) Low and (B) high collision energy mass spectra of obtained for 8-OH-EFZ-sulfate in a treated wastewater sample. The proposed fragmentation pathways (C) are in accordance with literature (Mutlib *et al.*, 1999).

The dihydroxy-sulphate EFZ conjugate detected at  $t_R$  27.91 min partially co-eluted with 7,14-diOH-EFZ at  $t_R$  27.84 min (**Figure 5.6A**). Furthermore, the desulphated fragment ion of the dihydroxy-sulphate EFZ species provides a high intensity base peak ion at  $m/z$  346 corresponding to the dihydroxylated EFZ species. Fortunately, in addition to the partial chromatographic separation, these species were differentiated by IMS (**Figure 5.6B** and **C**), with the dihydroxy-sulphate EFZ metabolite showing a higher arrival time (6.35 ms) compared to 7,14-diOH-EFZ ( $t_A$  5.38 ms), as expected for the bulkier former ion. Accordingly, MS data could be filtered according to arrival time to obtain better quality spectra. This is demonstrated by the low collision energy MS spectrum of the dihydroxy-sulphate EFZ peak (**Figure 5.6D**), which did not reveal any ions belonging to the co-eluting compound. Based on the high collision energy MS<sup>E</sup> spectrum of the dihydroxy-sulphate peak similarly filtered according to drift time (**Figure 5.6E**), which displays remarkably similar fragment ions to those discussed above (**Figure 5.3**) for 8,14-diOH-EFZ, this compound was tentatively assigned as 8,14-diOH-EFZ-sulphate. Specifically, the ions at  $m/z$  262 and 226, the origin of which has been discussed for 8,14-diOH-EFZ, as well as the base peak ion corresponding to the aglycone ( $m/z$  346) have been shown to enable differentiation between 8,14-diOH-EFZ-sulphate and the isomeric 7,14-diOH-EFZ-sulphate not detected in the present work.

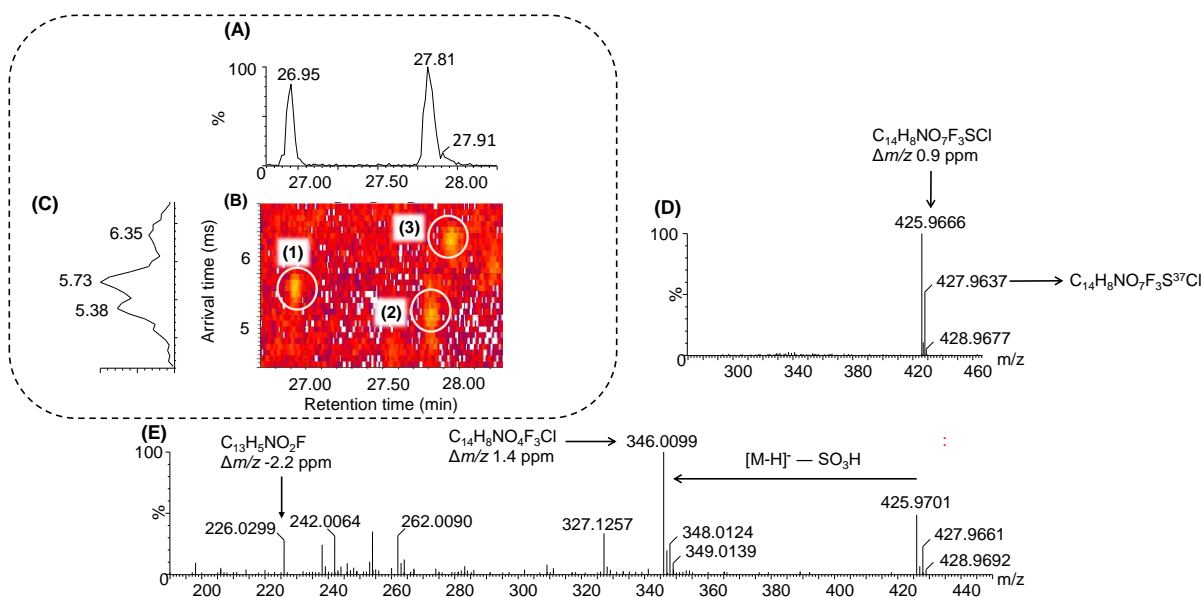


**Figure 5.6:** (A) Extracted ion chromatogram (XIC) for  $m/z$  425.9 and 346 illustrating the separation of (1) 8,14-diOH-EFZ, (2) 7,14-diOH-EFZ and (3) 8,14-diOH-EFZ-sulphate (refer to heatmap for labels) in a treated wastewater sample. (B) shows the corresponding  $t_A \times t_R$  contour plot, and (C) the extracted ion mobiligram for  $m/z$  425.9 and 346 illustrating the IMS separation of the three species. Arrival time-filtered low- (D) and high collision energy (E) mass spectra allowed tentative identification of 8,14-diOH-EFZ-sulphate based on characteristic fragment ions at  $m/z$  262 and 226.

### 5.3.2.2 Nevirapine metabolites

Nevirapine is amongst the preferred drugs in first line antiretroviral therapy (ART) due to its long half-life and high bioavailability, leading to significant excretory by-products that are mostly unresponsive to wastewater treatment processes (Wood *et al.*, 2016). Like other ARVDs of the *n*NRTI class, NVP is metabolised to produce hydroxylated and glucuronidated metabolites prior to body clearance. The presence of 12-hydroxy-Nevirapine (12-OH-NVP) in raw wastewater samples, at levels comparable to the parent drug, was recently reported (Mosekiemang *et al.*, 2019). In the present work, we therefore attempted to identify further NVP metabolites in wastewater samples using the non-targeted screening method.

Indeed, in addition to the parent drug NVP and 12-OH-NVP identified using reference standards, two further hydroxylated (phase 1) metabolites were also detected in raw and treated wastewater samples processed by SPE and lyophilisation (**Table S5.1**). Mass defect values for these metabolites were -10 mDa. No phase II glucuronide metabolites were detected. The three regioisomeric hydroxylated metabolites were well separated, as illustrated in the XIC for  $m/z$  283 ( $C_{15}H_{15}N_4O_2$ ) in **Figure 5.7**. The peak eluting at  $t_R$  16.92 min was conclusively identified as 12-OH-NVP using a reference standard

(CCS 164.7 Å<sup>2</sup>) and showed the characteristic dehydrated fragment ion of this compound previously reported (Ren *et al.*, 2010) at  $m/z$  265 (C<sub>15</sub>H<sub>13</sub>N<sub>4</sub>O,  $\Delta m/z$  2.6 ppm), which is unique to this hydroxylated NVP metabolite. The remaining two hydroxylated NVP metabolites may therefore be 2-, 3- or 8-hydroxy-Nevirapine. To distinguish between these options, both the RP-LC elution order and high collision energy MS<sup>E</sup> spectra were compared with previous studies. In general, the elution order for the hydroxylated metabolites of NVP is in the sequence, 2-OH-NVP < 8-OH-NVP~12-OH-NVP < 3-OH-NVP (Ren *et al.*, 2010; Riska *et al.*, 1999), which suggests, albeit inconclusively, that the early and late eluting peaks detected here likely correspond to 2- and 3-OH-NVP, respectively. More informative are the fragmentation spectra of these compounds. It is known that 2- and 3-OH-NVP produce very similar fragmentation spectra, which differ slightly from that of 8-OH-NVP. Fragment ions common to all three metabolites include  $m/z$  242, 214, 161 and 123. The ion at  $m/z$  242 (C<sub>12</sub>H<sub>10</sub>N<sub>4</sub>O<sub>2</sub><sup>+</sup>,  $\Delta m/z$  -6.2 ppm) is formed by a loss of the cyclopropyl group from the protonated molecular ion (this fragmentation pathway is also applicable to NVP, where it produces the fragment ion at  $m/z$  226). This ion is more stable in 8-OH-NVP and is often the base peak ion in fragmentation spectra for this compound. Subsequent loss of CO (28 Da) from  $m/z$  242, which involves contraction of seven-to-six-membered ring (Ren *et al.*, 2010), produces the fragment ion at  $m/z$  214 C<sub>11</sub>H<sub>10</sub>N<sub>4</sub>O<sup>+</sup>,  $\Delta m/z$  11.2 ppm). The fragment ion at  $m/z$  161.0720 (C<sub>9</sub>H<sub>9</sub>N<sub>2</sub>O,  $\Delta m/z$  3.1 ppm) has been proposed (Ren *et al.*, 2010) to originate from the molecular ion protonated at the carbonyl group, leading to the elimination of a bicyclic group. Importantly, this is a major fragment ion in the case of 2- and 3-OH-NVP, but in the case of 8-OH-NVP the position of the hydroxyl group means that it is retained in this fragment, which is therefore detected at  $m/z$  177. Taking into account the absence of the  $m/z$  177 fragment, the relatively low abundance of the  $m/z$  242 fragment and the similarity of the fragmentation spectra of the early and late eluting hydroxylated NVP metabolites detected here, these were therefore putatively identified as 2- and 3-OH-NVP, respectively. Furthermore, considering the relative retention of the three detected metabolites, the first eluting derivative was assigned as 2-OH-NVP, and the last eluting one as 3-OH-NVP, in accordance with literature (Ren *et al.*, 2010; Riska *et al.*, 1999) (**Figure 5.7**).

Both 2- and 3-OH-NVP have similar gas phase properties as evidenced by identical arrival times (2.48 ms) and CCS values (159.8 Å<sup>2</sup>) in IMS. In contrast, 12-OH-NVP was characterised by a higher arrival time (2.55 ms) and larger CCS value of 164.7 Å<sup>2</sup> (in contrast to predicted CCS values, **Table 5.1**). IMS data may therefore be used to differentiate that latter metabolite from its positional isomers.

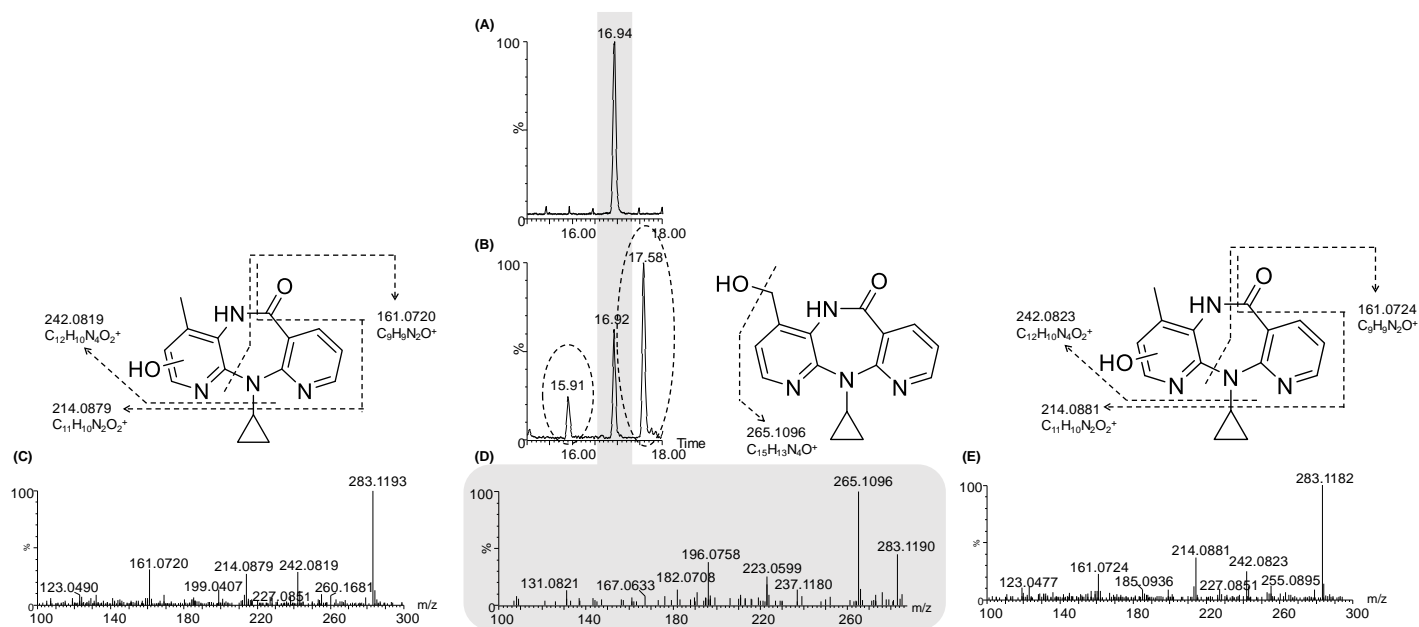


**Figure 5.7:** Extracted ion chromatograms (XICs) for  $m/z$  283 for (A) a reference standard of 12-OH-NVP, and (B) a treated wastewater sample processed by SPE. The peaks at  $t_R$  15.91 min and  $t_R$  17.58 min were tentatively identified as 2- and 3-OH-NVP, respectively, based on elution order and high collision energy MS<sup>E</sup> spectra, which are shown for 2-OH-NVP (C), 12-OH-NVP (D) and 3-OH-NVP (E), as discussed in the text.

### 5.3.2.3 Ritonavir metabolite

Ritonavir is biotransformed into several hydroxylated metabolites (Denissen *et al.*, 1997; Gangl *et al.*, 2002) and demethylated species such as desthiazolylmethyloxycarbonyl ritonavir which was recently detected in wastewater (Mosekiemang *et al.*, 2019). The workflow for the identification of ritonavir metabolites entailed post-acquisition processing of MS<sup>E</sup> raw data using MetaboLynx. The elemental composition of the parent (C<sub>37</sub>H<sub>48</sub>N<sub>6</sub>O<sub>5</sub>S<sub>2</sub>) was used to assign mass shifts for phase I (hydroxylation, 2 × hydroxylation, methylation, *etc.*) and II (sulfation, glucuronidation) metabolites, which were searched in the full-scan MS data (**Figure S5.4A**). After filtering out peaks not conforming to the specified accurate masses, the resultant extracted range chromatogram remained with fewer peaks, possibly metabolites and other isobaric species (**Figure S5.4B**). A fractional mass filter of 50 mDa around the exact mass of the parent was then applied to provide an XIC containing two peaks for the parent at  $t_R$  32.87 min ( $\Delta m/z$  -2.2 ppm) and a hydroxylated metabolite at  $t_R$  28.72 min (C<sub>37</sub>H<sub>49</sub>N<sub>6</sub>O<sub>6</sub>S<sub>2</sub>,  $\Delta m/z$  -2.8 ppm and  $\Delta FM$  -5.6 mDa) (**Figure S5.4C**). This assignment is supported by good agreement between the measured and predicted CCS values (**Table 5.1**). Due to low abundance of the signal, we were unable to obtain clean MS<sup>E</sup> spectra to allow further identification of the hydroxylated metabolite, except to confirm the presence of fragment ions at  $m/z$  426, 312, 284 and 213, which are consistent with hydroxylation on the isopropylmethylthiazole moiety (Gangl *et al.*, 2002).

### 5.3.2.4 Abacavir metabolite

The ions for abacavir ( $t_R$  14.25 min, C<sub>14</sub>H<sub>19</sub>N<sub>6</sub>O,  $\Delta m/z$  -3.5) and abacavir-5'-carboxylate ( $t_R$  12.21 min, C<sub>14</sub>H<sub>19</sub>N<sub>6</sub>O<sub>2</sub>,  $\Delta m/z$  -1.0) were clearly visible on the base peak ion chromatogram of the full scan MS data for raw wastewater processed by SPE. These compounds were previously identified in wastewater using authentic standards (Funke *et al.*, 2016). Low and high collision energy HR-MS data for both compounds are in accordance with (Funke *et al.*, 2016), and the experimental CCS values for both reported here for the first time are in agreement with predicted values (**Table 5.1**).

### 5.3.3 Occurrence of the ARVD metabolites

**Table S5.1** provides a summary of the compounds detected in the present work in wastewater influent and effluent samples. Interesting to note is that, apart from *N*-OH-EFZ-glu, which was not detected in effluent samples, all the remaining ARVD metabolites were detected in both influent and effluent samples. This points to the inefficiency of the wastewater treatment processes in removing ARVD metabolites, broadly supporting previous findings in literature (Brown and Wong, 2018, 2015; Ibáñez *et al.*, 2021). However, the present work reports the presence of several ARVD metabolites in wastewater for the first time. Of the ARVD metabolites identified here, 12-OH-NVP and 8,14-diOH-EFZ were previously detected in South African wastewater (Mosekiemang *et al.*, 2019), while 8-OH-EFZ was recently detected in river water in the United Kingdom (Richardson *et al.*, 2021). By

implication, the total load of ARVDs and their metabolites in environmental water samples may be significantly higher than previously considered.

Although quantification was not performed in the present work, the chromatographic and MS data reported herein for ARVD metabolites should prove useful in establishing targeted LC-MS/MS methods for the quantification of these compounds, which will ultimately shed further light on their occurrence, and potential impact, in the environment.

#### 5.4 Conclusions

A screening method employing LC separation with IMS-HR-MS detection was successfully applied to detect several metabolites of the ARVDs abacavir, efavirenz, nevirapine and ritonavir in wastewater samples for the first time. Published pharmacokinetic data for the parent drugs and a metabolite prediction software were used as basis to search for ARVD metabolites using the untargeted analytical method. In this manner, 8- and *N*-hydroxy-efavirenz, 7,14-dihydroxy-efavirenz, 8-hydroxy-efavirenz sulphate, 8,14-dihydroxy-efavirenz sulphate and *N*-hydroxy-efavirenz glucuronide were tentatively or putatively identified, while the presence of efavirenz and 8,14-dihydroxy-efavirenz was confirmed using reference standards. Similarly, nevirapine, 12-hydroxy-nevirapine and ritonavir were confirmed using standards, while 2- and 3-hydroxy-nevirapine, abacavir, abacavir-5'-carboxylate and hydroxy Ritonavir were putatively identified. Apart from *N*-hydroxy-efavirenz glucuronide, which was only detected in influent wastewater samples, the remainder of the metabolites were detected in effluent samples also, implying that these compounds may have potential environmental impact.

IMS proved a useful addition to the analytical method in providing better quality MS data for the complex wastewater samples and allowed us to report experimental CCS values for these compounds, which may be used for confirmation in future studies. Our findings provide the basis for further work on the identification of ARVD metabolites in environmental samples, including the development of targeted methods for quantitative analysis of these compounds.

## 5.5 References

- Abafe, O.A., Späth, J., Fick, J., Jansson, S., Buckley, C., Stark, A., Pietruschka, B., Martincigh, B.S., 2018. LC-MS/MS determination of antiretroviral drugs in influents and effluents from wastewater treatment plants in KwaZulu-Natal, South Africa. *Chemosphere* 200, 660–670.  
<https://doi.org/10.1016/j.chemosphere.2018.02.105>
- Alelyunas, Y.W., Smith, K., Cleland, G., Mortishire-smith, R., Wrona, M.D., 2017. Building a Collision Cross Section Library of Pharmaceutical Drugs Using the Vion IMS QToF Platform : Verification of System Performance , Precision and Deviation of CCS Measurements [APPLICATION NOTE]. Waters Corporation, Milford, MA, USA.
- Andra, S.S., Austin, C., Patel, D., Dolios, G., Awawda, M., Arora, M., 2017. Trends in the application of high-resolution mass spectrometry for human biomonitoring: An analytical primer to studying the environmental chemical space of the human exposome. *Environ. Int.* 100, 32–61.  
<https://doi.org/10.1016/j.envint.2016.11.026>
- Andrade, C.H., de Freitas, L.M., de Oliveira, V., 2011. Twenty-six years of HIV science: An overview of anti-HIV drugs metabolism. *Brazilian J. Pharm. Sci.* 47, 209–230.  
<https://doi.org/10.1590/S1984-82502011000200003>
- Aouri, M., Barcelo, C., Ternon, B., Cavassini, Matthias, Anagnostopoulos, A., Yerly, Sabine, Hugues, H., Vernazza, Pietro, Günthard, H.F., Buclin, T., Telenti, A., Rotger, M., Decosterd, L.A., Aubert, V., Battegay, M., Bernasconi, E., Böni, J., Braun, D.L., Bucher, H.C., Burton-Jeangros, C., Calmy, A., Cavassini, M., Dollenmaier, G., Egger, M., Elzi, L., Fehr, J., Fellay, J., Furrer, H., Fux, C.A., Gorgievski, M., Günthard, H., Haerry, D., Hasse, B., Hirsch, H.H., Hoffmann, M., Hösli, I., Kahlert, C., Kaiser, L., Keiser, O., Klimkait, T., Kouyos, R., Kovari, H., Ledergerber, B., Martinetti, G., Martinez De Tejada, B., Marzolini, C., Metzner, K., Müller, N., Nadal, D., Nicca, D., Pantaleo, G., Rauch, A., Regenass, S., Rudin, C., Schöni-Affolter, F., Schmid, P., Speck, R., Stöckle, M., Tarr, P., Trkola, A., Vernazza, P., Weber, R., Yerly, S., 2016. In vivo profiling and distribution of known and novel phase I and phase II metabolites of efavirenz in plasma, urine, and cerebrospinal fluid. *Drug Metab. Dispos.* 44, 151–161.  
<https://doi.org/10.1124/dmd.115.065839>
- Backe, W.J., Field, J.A., 2012. Is SPE Necessary for Environmental Analysis? A Quantitative Comparison of Matrix Effects from Large-Volume Injection and Solid-Phase Extraction Based Methods I. <https://doi.org/10.1021/es300235z>
- Bahlmann, A., Brack, W., Schneider, R.J., Krauss, M., 2014. Carbamazepine and its metabolites in wastewater: Analytical pitfalls and occurrence in Germany and Portugal. *Water Res.* 57, 104–114.



<https://doi.org/10.1016/j.watres.2014.03.022>

- Bateman, K.P., Castro-perez, J., Wrona, M., Shockcor, J.P., Yu, K., Oballa, R., Nicoll-griffith, D.A., 2007. MS E with mass defect filtering for in vitro and in vivo metabolite identification. *Rapid Commun. mass Spectrom.* 21, 1485–1496. <https://doi.org/10.1002/rcm>
- Bélanger, A.S., Caron, P., Harvey, M., Zimmerman, P. a., Mehlotra, R.K., Guillemette, C., 2009. Glucuronidation of the antiretroviral drug efavirenz by UGT2B7 and an in vitro investigation of drug-drug interaction with zidovudine. *Drug Metab. Dispos.* 37, 1793–1796. <https://doi.org/10.1124/DMD.109.0277606>
- Bijlsma, L., Bade, R., Celma, A., Mullin, L., Cleland, G., Stead, S., Hernandez, F., Sancho, J. V., 2017. Prediction of Collision Cross-Section Values for Small Molecules: Application to Pesticide Residue Analysis. *Anal. Chem.* 89. <https://doi.org/10.1021/acs.analchem.7b00741>
- Botero-Coy, A.M., Martínez-Pachón, D., Boix, C., Rincón, R.J., Castillo, N., Arias-Marín, L.P., Manrique-Losada, L., Torres-Palma, R., Moncayo-Lasso, A., Hernández, F., 2018. An investigation into the occurrence and removal of pharmaceuticals in Colombian wastewater. *Sci. Total Environ.* 642, 842–853. <https://doi.org/10.1016/j.scitotenv.2018.06.088>
- Brown, A.K., Wong, C.S., 2018. Distribution and fate of pharmaceuticals and their metabolite conjugates in a municipal wastewater treatment plant. *Water Res.* 144, 774–783. <https://doi.org/10.1016/j.watres.2018.08.034>
- Brown, A.K., Wong, C.S., 2016. Simultaneous quantification of propranolol and sulfamethoxazole and major human metabolite conjugates 4-hydroxy-propranolol sulfate and sulfamethoxazole- $\beta$ -glucuronide in municipal wastewater—A framework for multiple classes of drugs and conjugates. *J. Chromatogr. A* 1471, 34–44. <https://doi.org/10.1016/j.chroma.2016.10.011>
- Brown, A.K., Wong, C.S., 2015. Current trends in environmental analysis of human metabolite conjugates of pharmaceuticals. *Trends Environ. Anal. Chem.* 5, 8–17. <https://doi.org/10.1016/j.teac.2015.01.002>
- Castro-Perez, J., Yu, K., Shockcor, J., 2007. Removal of Interferences and Easier Metabolite Detection by Ion Mobility Mass Spectrometry. *Nat. Methods | Appl. Notes* 32–34. <https://doi.org/10.1038/an2658>
- Celiz, M.D., Tso, J., Aga, D.S., 2009. Pharmaceutical metabolites in the environment: Analytical challenges and ecological risks. *Environ. Toxicol. Chem.* 28, 2473–2484. <https://doi.org/10.1897/09-173.1>
- D’Atri, V., Causon, T., Hernandez-Alba, O., Mutabazi, A., Veuthey, J.L., Cianferani, S., Guillarme, D.,

2018. Adding a new separation dimension to MS and LC–MS: What is the utility of ion mobility spectrometry? *J. Sep. Sci.* 41, 20–67. <https://doi.org/10.1002/jssc.201700919>
- Deng, Y., Liu, R., Ping, Y., Liang, J., 2015. Rapid identification of efavirenz metabolites in rats and humans by ultra high performance liquid chromatography combined with quadrupole time-of-flight tandem mass spectrometry. *J. Sep. Sci.* 38, 1529–1536. <https://doi.org/10.1002/jssc.201401120>
- Denissen, J.F., Grabowski, B.A., Johnson, M.K., Buko, A.M., Kempf, D.J., Thomas, S.B., Surber, B.W., 1997. Metabolism and disposition of the HIV-1 protease inhibitor ritonavir (ABT-538) in rats, dogs, and humans. *Drug Metab. Dispos.* 25, 489–501.
- Fan-Havard, P., Liu, Z., Chou, M., Ling, Y., Barrail-Tran, A., Haas, D.W., Taburet, A.M., 2013. Pharmacokinetics of phase I nevirapine metabolites following a single dose and at steady state. *Antimicrob. Agents Chemother.* 57, 2154–2160. <https://doi.org/10.1128/AAC.02294-12>
- Fiebig, L., Laux, R., 2016. A collision cross section and exact ion mass database of the formulation constituents polyethylene glycol 400 and polysorbate 80. *Int. J. Ion Mobil. Spectrom.* 19, 131–137. <https://doi.org/10.1007/s12127-016-0195-2>
- Funke, J., Prasse, C., Ternes, T.A., 2016. Identification of transformation products of antiviral drugs formed during biological wastewater treatment and their occurrence in the urban water cycle. *Water Res.* 98, 75–83. <https://doi.org/10.1016/j.watres.2016.03.045>
- Gabelica, V., Shvartsburg, A.A., Afonso, C., Barran, P., Benesch, J.L.P., Bleiholder, C., Bowers, M.T., Bilbao, A., Bush, M.F., Campbell, J.L., Campuzano, I.D.G., Causon, T., Clowers, B.H., Creaser, C.S., De Pauw, E., Far, J., Fernandez-Lima, F., Fjeldsted, J.C., Giles, K., Groessl, M., Hogan, C.J., Hann, S., Kim, H.I., Kurulugama, R.T., May, J.C., McLean, J.A., Pagel, K., Richardson, K., Ridgeway, M.E., Rosu, F., Sobott, F., Thalassinos, K., Valentine, S.J., Wyttenbach, T., 2019. Recommendations for reporting ion mobility Mass Spectrometry measurements. *Mass Spectrom. Rev.* 38, 291–320. <https://doi.org/10.1002/mas.21585>
- Gangl, E., Utkin, I., Gerber, N., Vouros, P., 2002. Structural elucidation of metabolites of ritonavir and indinavir by liquid chromatography – mass spectrometry. *J. Chromatogr. A* 974, 91–101.
- Harjivan, S.G., Wanke, R., Ferreira Da Silva, J.L., Marques, M.M., Antunes, A.M.M., 2014. The phenolic metabolites of the anti-HIV drug efavirenz: Evidence for distinct reactivities upon oxidation with Frémy's salt. *Eur. J. Med. Chem.* 74, 7–11. <https://doi.org/10.1016/j.ejmech.2013.12.022>
- Hines, K.M., Ross, D.H., Davidson, K.L., Bush, M.F., Xu, L., 2017. Large-Scale Structural Characterization of Drug and Drug-Like Compounds by High-Throughput Ion Mobility-Mass

- Spectrometry. *Anal. Chem.* 89, 9023–9030. <https://doi.org/10.1021/acs.analchem.7b01709>
- Howdle, M.D., Eckers, C., Laures, A.M.F., Creaser, C.S., 2009. The Use of Shift Reagents in Ion Mobility-Mass Spectrometry: Studies on the Complexation of an Active Pharmaceutical Ingredient with Polyethylene Glycol Excipients. *J. Am. Soc. Mass Spectrom.* 20, 1–9. <https://doi.org/10.1016/j.jasms.2008.10.002>
- Ibáñez, M., Bijlsma, L., Pitarch, E., López, F.J., Hernández, F., 2021. Occurrence of pharmaceutical metabolites and transformation products in the aquatic environment of the Mediterranean area. *Trends Environ. Anal. Chem.* 29, e00118. <https://doi.org/10.1016/j.teac.2021.e00118>
- Jewell, K.S., Castronovo, S., Wick, A., Falås, P., Joss, A., Ternes, T.A., 2016. New insights into the transformation of trimethoprim during biological wastewater treatment. *Water Res.* 88, 550–557. <https://doi.org/10.1016/j.watres.2015.10.026>
- Lanucara, F., Holman, S.W., Gray, C.J., Eyers, C.E., 2014. The power of ion mobility-mass spectrometry for structural characterization and the study of conformational dynamics. *Nat. Chem.* 6, 281–294. <https://doi.org/10.1038/nchem.1889>
- Madikizela, L.M., Ncube, S., Chimuka, L., 2020. Analysis, occurrence and removal of pharmaceuticals in African water resources: A current status. *J. Environ. Manage.* 253, 109741. <https://doi.org/10.1016/j.jenvman.2019.109741>
- Marzinke, M.A., Breaud, A., Parsons, T.L., Cohen, M.S., Piwowar-Manning, E., Eshleman, S.H., Clarke, W., 2014. The development and validation of a method using high-resolution mass spectrometry (HRMS) for the qualitative detection of antiretroviral agents in human blood. *Clin. Chim. Acta* 433, 157–168. <https://doi.org/10.1016/j.cca.2014.03.016>
- Masike, K., Stander, M.A., de Villiers, A., 2021. Recent applications of ion mobility spectrometry in natural product research. *J. Pharm. Biomed. Anal.* 195. <https://doi.org/10.1016/j.jpba.2020.113846>
- May, J.C., McLean, J.A., 2015. Ion mobility-mass spectrometry: Time-dispersive instrumentation. *Anal. Chem.* 87, 1422–1436. <https://doi.org/10.1021/ac504720m>
- May, J.C., Morris, C.B., McLean, J.A., 2017. Ion mobility collision cross section compendium. *Anal. Chem.* 89, 1032–1044. <https://doi.org/10.1021/acs.analchem.6b04905>
- Mollerup, C.B., Mardal, M., Dalsgaard, P.W., Linnet, K., Barron, L.P., 2018. Prediction of collision cross section and retention time for broad scope screening in gradient reversed-phase liquid chromatography-ion mobility-high resolution accurate mass spectrometry. *J. Chromatogr. A* 1542, 82–88. <https://doi.org/10.1016/j.chroma.2018.02.025>

- Mortishire-smith, R.J., Connor, D.O., Castro-perez, J.M., Kirby, J., 2005. Accelerated throughput metabolic route screening in early drug discovery using high-resolution liquid chromatography / quadrupole time-of-flight mass spectrometry and automated data analysis. *Rapid Commun. Mass Spectrom.* 19, 2659–2670. <https://doi.org/10.1002/rcm.2111>
- Mosekiemang, T.T., Stander, M.A., de Villiers, A., 2019. Simultaneous quantification of commonly prescribed antiretroviral drugs and their selected metabolites in aqueous environmental samples by direct injection and solid phase extraction liquid chromatography - Tandem mass spectrometry. *Chemosphere* 220, 983–992. <https://doi.org/10.1016/j.chemosphere.2018.12.205>
- Mutlib, E., Chen, H., Nemeth, G. a, Markwalder, J. a, Seitz, S.P., Gan, L.S., Christ, D.D., 1999. Identification and characterization of efavirenz metabolites by liquid chromatography/mass spectrometry and high field NMR: species differences in the metabolism of efavirenz. *Drug Metab. Dispos.* 27, 1319–1333.
- Nannou, C., Ofrydopoulou, A., Evgenidou, E., Heath, D., Heath, E., Lambropoulou, D., 2020. Science of the Total Environment Antiviral drugs in aquatic environment and wastewater treatment plants : A review on occurrence , fate , removal and ecotoxicity. *Sci. Total Environ.* 699, 134322. <https://doi.org/10.1016/j.scitotenv.2019.134322>
- Nannou, C., Ofrydopoulou, A., Evgenidou, E., Heath, D., Heath, E., Lambropoulou, D., 2019. Analytical strategies for the determination of antiviral drugs in the aquatic environment. *Trends Environ. Anal. Chem.* 24, e00071. <https://doi.org/10.1016/j.teac.2019.e00071>
- Ncube, S., Madikizela, L.M., Chimuka, L., Nindi, M.M., 2018. Environmental fate and ecotoxicological effects of antiretrovirals : A current global status and future perspectives. *Water Res.* 145, 231–247. <https://doi.org/10.1016/j.watres.2018.08.017>
- Ogburn, E.T., Jones, D.R., Masters, A.R., Xu, C., Guo, Y., 2010. Efavirenz Primary and Secondary Metabolism In Vitro and In Vivo : Identification of Novel Metabolic Pathways and Cytochrome P450 2A6 as the Principal Catalyst of Efavirenz 7-Hydroxylation. *Drug Metab. Dispos.* 1218–1229.
- Oliveira, T.S., Murphy, M., Mendola, N., Wong, V., Carlson, D., Waring, L., 2015. Characterization of Pharmaceuticals and Personal Care products in hospital effluent and waste water influent/effluent by direct-injection LC-MS-MS. *Sci. Total Environ.* 518–519, 459–478. <https://doi.org/10.1016/j.scitotenv.2015.02.104>
- Paíga, P., Santos, L.H.M.L.M., Ramos, S., Jorge, S., Silva, J.G., Delerue-Matos, C., 2016. Presence of pharmaceuticals in the Lis river (Portugal): Sources, fate and seasonal variation. *Sci. Total Environ.* 573, 164–177. <https://doi.org/10.1016/j.scitotenv.2016.08.089>

- Parry, C.D.H., Myers, B., Morojele, N.K., Flisher, A.J., Bhana, A., Donson, H., Plüddemann, A., 2004. Trends in adolescent alcohol and other drug use: Findings from three sentinel sites in South Africa (1997-2001). *J. Adolesc.* 27, 429–440. <https://doi.org/10.1016/j.adolescence.2003.11.013>
- Qu, L., Fan, Y., Wang, W., Ma, K., Yin, Z., 2016. Development, validation and clinical application of an online-SPE-LC-HRMS/MS for simultaneous quantification of phenobarbital, phenytoin, carbamazepine, and its active metabolite carbamazepine 10,11-epoxide. *Talanta* 158, 77–88. <https://doi.org/10.1016/j.talanta.2016.05.036>
- Rardin, M.J., 2018. Rapid Assessment of Contaminants and Interferences in Mass Spectrometry Data Using Skyline. *J. Am. Soc. Mass Spectrom.* 29, 1327–1330. <https://doi.org/10.1007/s13361-018-1940-z>
- Regueiro, J., Negreira, N., Berntssen, M.H.G., 2016. Ion-mobility-derived collision cross section as an additional identification point for multiresidue screening of pesticides in fish feed. *Anal. Chem.* 88, 11169–11177. <https://doi.org/10.1021/acs.analchem.6b03381>
- Ren, C., Fan-havard, P., Schlabritz-loutsevitch, N., 2010. A sensitive and specific liquid chromatography / tandem mass spectrometry method for quantification of nevirapine and its five metabolites and their pharmacokinetics in baboons 2009, 717–726. <https://doi.org/10.1002/bmc.1353>
- Richardson, A.K., Chadha, M., Rapp-Wright, H., Mills, G.A., Fones, G.R., Gravell, A., Stürzenbaum, S., Cowan, D.A., Neep, D.J., Barron, L.P., 2021. Rapid direct analysis of river water and machine learning assisted suspect screening of emerging contaminants in passive sampler extracts. *Anal. Methods*. <https://doi.org/10.1039/d0ay02013c>
- Richardson, K., Langridge, D., Giles, K., Dixit, S., Ujma, J., Ruotolo, B., 2019. AN IMPROVED CALIBRATION APPROACH FOR TRAVELLING WAVE ION MOBILITY SPECTROMETRY: ROBUST, HIGH - PRECISION COLLISION CROSS SECTIONS, in: *Proceedings of the 67th Annual Conference of the ASMS*. Atlanta, GA. June 2-6.
- Riska, P., Lamson, M., Macgregor, T., Sabo, J., Hattox, S., Pav, J., Keirns, J., 1999. Disposition and biotransformation of the antiretroviral drug nevirapine in humans. *Drug Metab. Dispos.* 27, 895–901.
- Ross, D.H., Cho, J.H., Xu, L., 2020. Breaking down Structural Diversity for Comprehensive Prediction of Ion-Neutral Collision Cross Sections. *Anal. Chem.* 92, 4548–4557. <https://doi.org/10.1021/acs.analchem.9b05772>
- Schoeman, C., Dlamini, M., Okonkwo, O.J., 2017. The impact of a Wastewater Treatment Works in Southern Gauteng, South Africa on efavirenz and nevirapine discharges into the aquatic

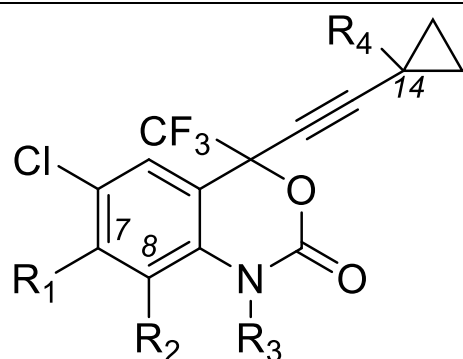
- environment. *Emerg. Contam.* 3, 95–106.  
<https://doi.org/10.1016/j.emcon.2017.09.001>
- Stow, S.M., Causon, T.J., Zheng, X., Kurulugama, R.T., Mairinger, T., May, J.C., Rennie, E.E., Baker, E.S., Smith, R.D., McLean, J.A., Hann, S., Fjeldsted, J.C., 2017. An Interlaboratory Evaluation of Drift Tube Ion Mobility-Mass Spectrometry Collision Cross Section Measurements. *Anal. Chem.* 89, 9048–9055. <https://doi.org/10.1021/acs.analchem.7b01729>
- Tiller, P.R., Yu, S., Bateman, K.P., Castro-Perez, J., Mcintosh, I.S., Kuo, Y., Baillie, T.A., 2008. Fractional mass filtering as a means to assess circulating metabolites in early human clinical studies. *Rapid Commun. Mass Spectrom.* 22, 3510–3516. <https://doi.org/10.1002/rcm>
- Verlicchi, P., Zambello, E., 2016. Predicted and measured concentrations of pharmaceuticals in hospital effluents. Examination of the strengths and weaknesses of the two approaches through the analysis of a case study. *Sci. Total Environ.* 565, 82–94. <https://doi.org/10.1016/j.scitotenv.2016.04.165>
- Wood, T.P., Basson, A.E., Duvenage, C., Rohwer, E.R., 2016. The chlorination behaviour and environmental fate of the antiretroviral drug nevirapine in South African surface water. *Water Res.* 104, 349–360. <https://doi.org/10.1016/j.watres.2016.08.038>
- Yuen, G.J., Weller, S., Pakes, G.E., 2008. A review of the pharmacokinetics of abacavir. *Clin. Pharmacokinet.* 47, 351–371. <https://doi.org/10.2165/00003088-200847060-00001>
- Zandkarimi, F., Wickramasekara, S., Morre, J., Stevens, J.F., Maier, C.S., 2013. 50 Years of Phytochemistry Research, in: Gang, D.R. (Ed.), 50 Years of Phytochemistry Research. Springer, Switzerland, pp. 21–31. <https://doi.org/10.1007/978-3-319-00581-2>
- Zhang, D., Cheng, P.T., Zhang, H., 2007. Mass Defect Filtering on High Resolution LC/MS Data as a Methodology for Detecting Metabolites with Unpredictable Structures: Identification of Oxazole-Ring Opened Metabolites of Muraglitazar, *Drug Metabolism Letters*.
- Zhang, H., Zhang, D., Ray, K., Zhu, M., 2009. Mass defect filter technique and its applications to drug metabolite identification by high-resolution mass spectrometry. *J. Mass Spectrom.* <https://doi.org/10.1002/jms.1610>
- Zhang, H., Zhu, M., Ray, K.L., Ma, L., Zhang, D., 2008. Mass defect profiles of biological matrices and the general applicability of mass defect filtering for metabolite detection. *Rapid Commun. Mass Spectrom.* 22, 2082–2088. <https://doi.org/10.1002/rcm.3585>

## Chapter 5

---

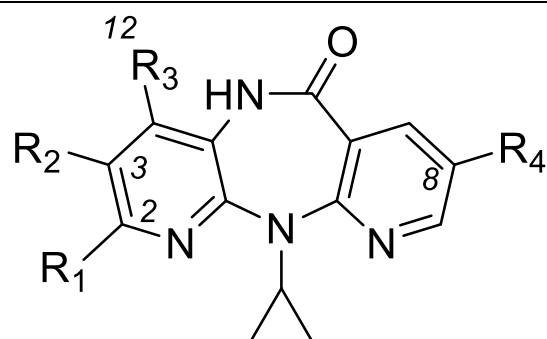
**Supplementary information for:**

**Ultra high pressure liquid chromatography coupled to travelling wave ion mobility-time of flight mass spectrometry for the screening of pharmaceutical metabolites in wastewater samples: application to antiretrovirals.**



Metabolites	Phase I				Phase II			
	R <sub>1</sub>	R <sub>2</sub>	R <sub>3</sub>	R <sub>4</sub>	R <sub>1</sub>	R <sub>2</sub>	R <sub>3</sub>	R <sub>4</sub>
efavirenz	H	H	H	H	-	-	-	-
7-hydroxy efavirenz	OH	H	H	H	-	-	-	-
8-hydroxy efavirenz	H	OH	H	H	-	-	-	-
7,14-dihydroxy efavirenz	OH	H	H	OH	-	-	-	-
8,14-dihydroxy efavirenz	H	OH	H	OH	-	-	-	-
<i>N</i> -hydroxy efavirenz*	H	H	OH	H	-	-	-	-
7-hydroxy efavirenz-glucuronide	-	-	-	-	<i>O</i> -glucuronide	H	H	H
8-hydroxy efavirenz-glucuronide	-	-	-	-	H	<i>O</i> -glucuronide	H	H
<i>N</i> -hydroxy efavirenz-glucuronide	-	-	-	-	H	H	<i>O</i> -glucuronide	H
8-hydroxy efavirenz-sulphate	-	-	-	-	H	-OSO <sub>3</sub> H	H	H
8,14-dihydroxy efavirenz-sulphate	-	-	-	-	H	-OSO <sub>3</sub> H	H	OH

**Figure S5.1:** Molecular structures of efavirenz and its phase I and II metabolites (refer to Mutlib *et al.* (1999) for molecular structure numbering).



Metabolites	Phase I				Phase II			
	R <sub>1</sub>	R <sub>2</sub>	R <sub>3</sub>	R <sub>4</sub>	R <sub>1</sub>	R <sub>2</sub>	R <sub>3</sub>	R <sub>4</sub>
nevirapine	H	H	CH <sub>3</sub>	H	-	-	-	-
2-hydroxy nevirapine	OH	H	CH <sub>3</sub>	H	-	-	-	-
3-hydroxy nevirapine	H	OH	CH <sub>3</sub>	H	-	-	-	-
8-hydroxy nevirapine	H	H	CH <sub>3</sub>	OH	-	-	-	-
12-hydroxy nevirapine	H	H	CH <sub>2</sub> OH	H	-	-	-	-
12-carboxy nevirapine	H	H	COOH	H	-	-	-	-
2-hydroxy nevirapine glucuronide	-	-	-	-	<i>O</i> -glu <sup>a</sup>	H	CH <sub>3</sub>	H
3-hydroxy nevirapine glucuronide	-	-	-	-	H	<i>O</i> -glu	CH <sub>3</sub>	H
8-hydroxy nevirapine glucuronide	-	-	-	-	H	H	-	<i>O</i> -glu
12-hydroxy nevirapine glucuronide	-	-	-	-	H	H	CH <sub>2</sub> - <i>O</i> -glu	H

<sup>a</sup> denotes *O*-glucuronide

**Figure S5.2:** Molecular structure of nevirapine and its phase I and II metabolites (Riska *et al.* (1999)).



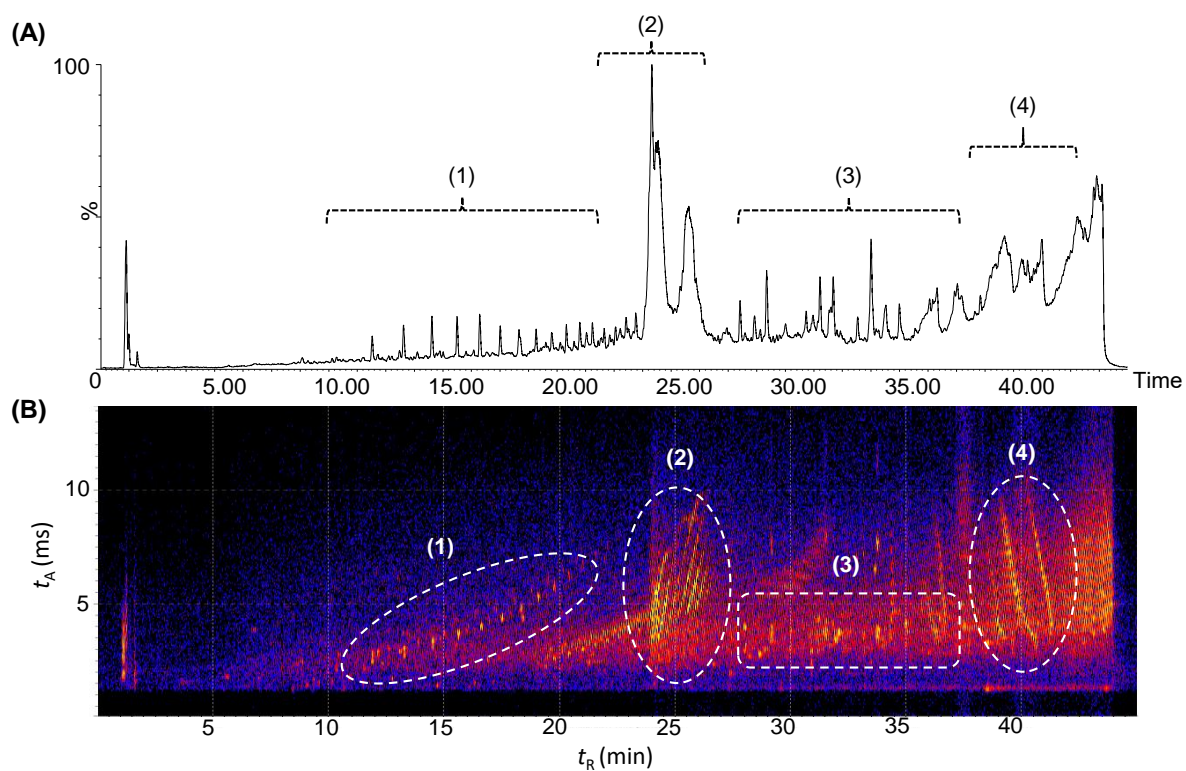


**Figure S5.3:** (A) A typical low energy TIC obtained for the analysis of raw wastewater sample processed by SPE, and (B) the corresponding  $t_R \times t_A$  DriftScope™ heat map view of the same data. Regions shown by dotted ovals represent (1) single charged PEGs, (2) multiply charged PEGs, (3) the region where ARVDs and their metabolites were detected, and (4) multiply charged unidentified species.

Status	Mass	Metabolite Name	Formula	Mass Difference	$m/z$ Found	mDa	$\Delta m/z$	Peak ID	Time
×	706.2971	Demethylation	C <sub>36</sub> H <sub>46</sub> N <sub>6</sub> O <sub>5</sub> S <sub>2</sub>	–	–	–	–	–	–
×	784.3284	Methylation	C <sub>38</sub> H <sub>50</sub> N <sub>6</sub> O <sub>5</sub> S <sub>2</sub>	–	–	–	–	–	–
×	752.3026	2× Hydroxylation	C <sub>37</sub> H <sub>48</sub> N <sub>6</sub> O <sub>7</sub> S <sub>2</sub>	–	–	–	–	–	–
×	896.3449	Glucuronidation	C <sub>43</sub> H <sub>56</sub> N <sub>6</sub> O <sub>11</sub> S <sub>2</sub>	–	–	–	–	–	–
✓	720.3128	Parent	C <sub>37</sub> H <sub>48</sub> N <sub>6</sub> O <sub>5</sub> S <sub>2</sub>	-0.0010	721.3190	-1.6	-2.2	7	32.87
✓	736.3077	Hydroxylation	C <sub>37</sub> H <sub>48</sub> N <sub>6</sub> O <sub>6</sub> S <sub>2</sub>	15.9905	737.3134	-2.1	-2.8	2	28.72

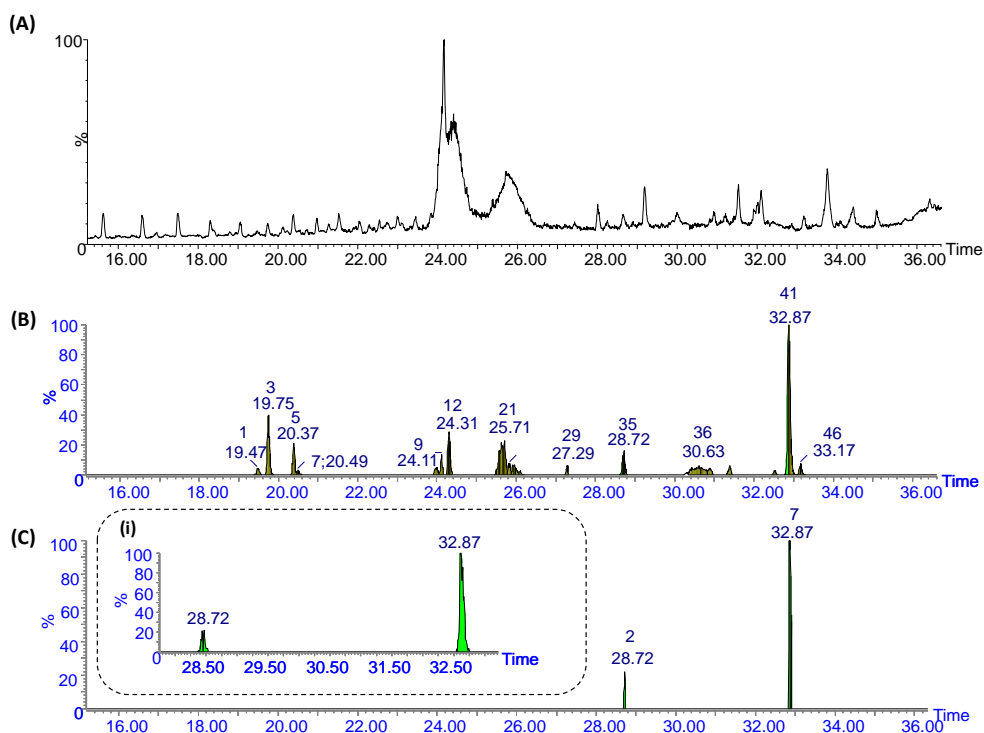


**Figure S5.4:** Post acquisition processing of full-scan MS data by MetaboLynx application manager: (A) ESI (+) base peak ion chromatogram for a raw wastewater sample processed by SPE, (B) extracted range chromatogram for hydroxylated metabolites and other isobaric species, (C) extracted range chromatogram after filtering out interferences by a fractional mass defect filter ( $\pm 50$  mDa) around the parent compound. The insert (i) is an enlarged elution region for RTV and OH-RTV. Refer to **Section 5.2.5** for MetaboLynx settings.

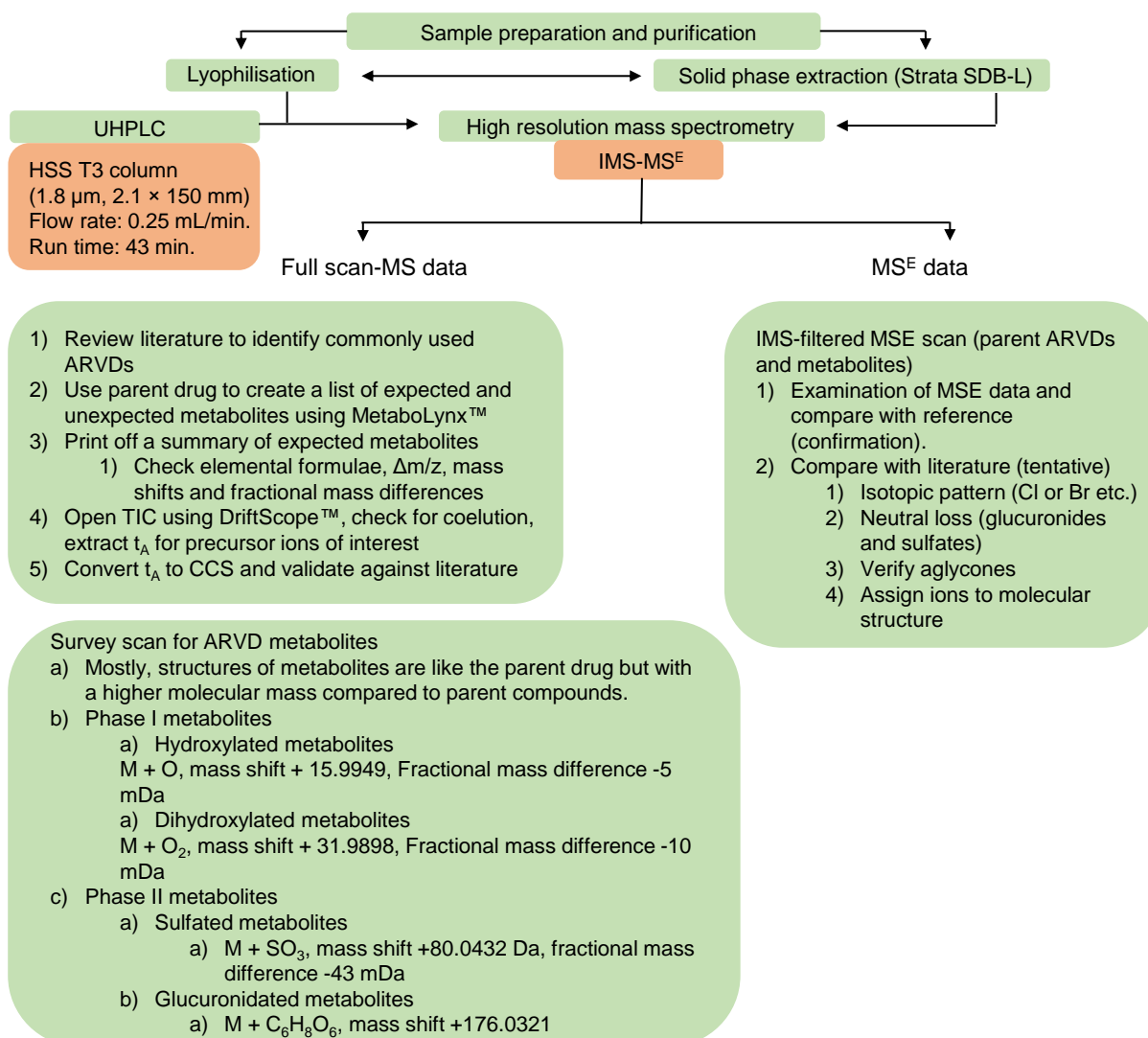


**Figure S5.5:** A detailed workflow used for the identification of ARVDs, their metabolites and other ancillary compounds in wastewater samples by UHPLC-IMS-HR-MS.

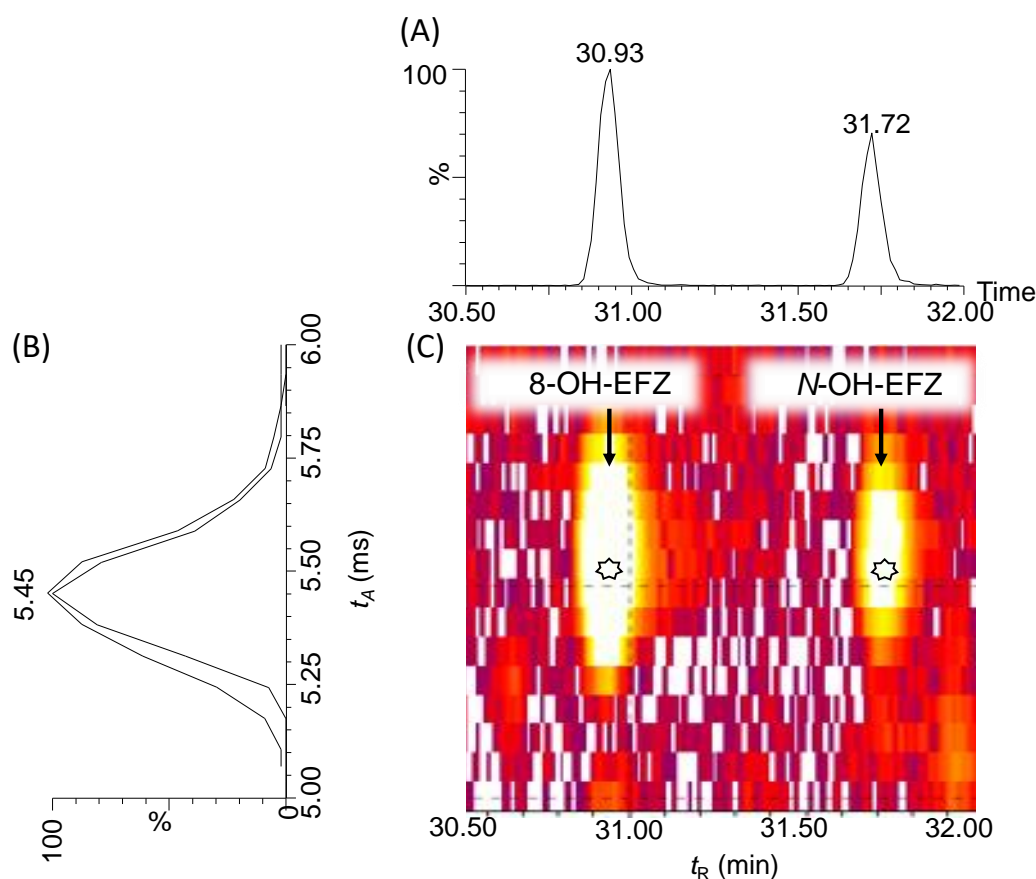


**Figure S5.6:** Contour plot ( $t_R \times t_A$ ) presentation of the UHPLC-IMS-HR-MS data for 7- and/or 8-OH-EFZ and N-OH-EFZ detected in a treated wastewater sample. The XIC for  $m/z$  330 (A) shows well resolved peaks, while the extracted ion mobilogram (B) shows identical arrival times for both compounds. ☆ shows the peak maxima.

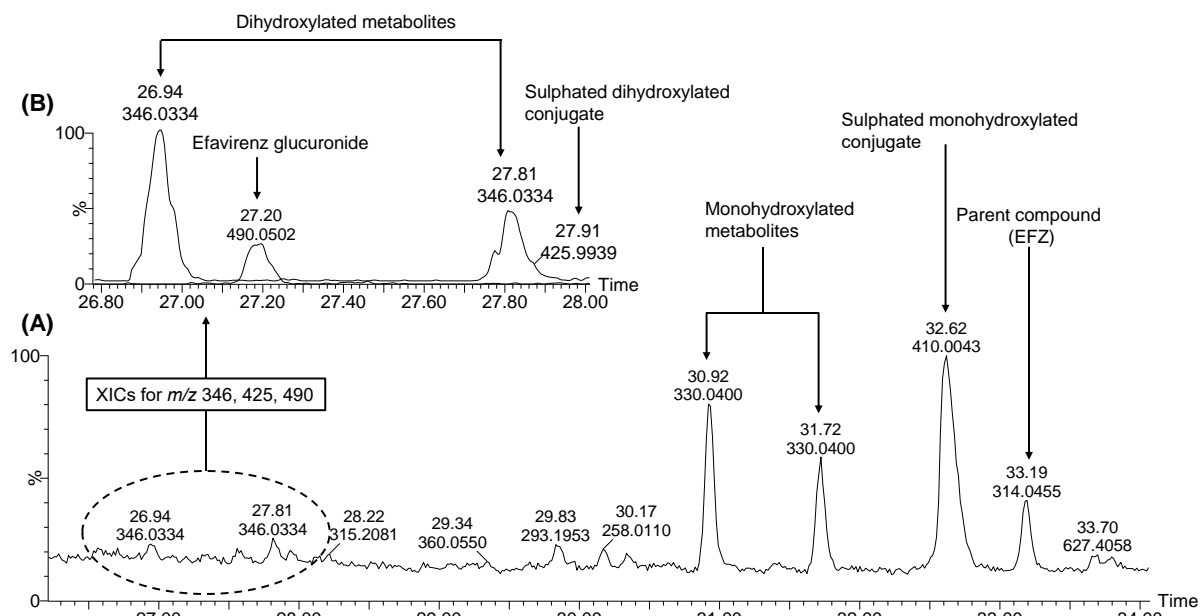


**Figure S5.7:** (A) Region of the TIC chromatogram for a treated wastewater sample processed by SPE showing the detection of EFZ and its metabolites. (B) shows the enlarged region of the TIC where dihydroxy-metabolites and a glucuronide metabolite were detected. These are depicted as overlaid extracted ion chromatograms (XICs) for  $m/z$  346, 425 and 490. Peak annotations represent retention times (top) and base peak ion mass (bottom).

**Table S5.1:** A summary of all the compounds detected in samples processed by SPE and lyophilisation. ✓ and × denote detection and not detected, respectively.

Compound	Influent		Effluent <sup>a</sup>	
	SPE	lyophilization	SPE	lyophilization
<i>Non-ARVD pharmaceutical compounds</i>				
codeine	✓	×	×	×
caffeine	✓	×	×	×
<i>O</i> -desmethyltramadol	✓	✓	×	×
trimethoprim	✓	✓	×	×
tramadol	✓	✓	×	×
carbamazepine	✓	✓	×	×
methaqualone	✓	✓	×	×
diclofenac	✓	✓	×	×
<i>ARVDs and metabolites</i>				
lamivudine	✓	✓	×	×
emtricitabine	✓	✓	×	×
Abacavir	✓	✓	×	×
abacavir-5'-carboxylate	✓	✓	×	×
2-hydroxy efavirenz	✓	✓	✓	✓
12-hydroxy nevirapine	✓	✓	✓	✓
3-hydroxy nevirapine	✓	✓	✓	✓
Nevirapine	✓	✓	✓	✓
8,14-dihydroxy efavirenz	✓	✓	✓	✓
<i>N</i> -hydroxy efavirenz glucuronide	✓	✓	×	×
Atazanavir	✓	×	×	×
7,14-dihydroxy efavirenz	✓	✓	✓	✓
8,14-dihydroxy efavirenz sulphate	✓	✓	✓	✓
hydroxy ritonavir	✓	✓	✓	✓
7- and/or 8-hydroxy efavirenz	✓	✓	✓	✓
<i>N</i> -hydroxy efavirenz	✓	✓	✓	✓
8-hydroxy efavirenz sulphate	✓	✓	✓	✓
ritonavir	✓	✓	✓	✓
efavirenz	✓	✓	✓	✓
lopinavir	✓	✓	✓	✓
<i>Synthetic polymers</i>				
PEG (n = 7)	✓	✓	×	×
PEG (n = 8)	✓	✓	×	×
PEG (n = 9)	✓	✓	×	×
PEG (n = 10)	✓	✓	×	×
PEG (n = 11)	✓	✓	×	×
PEG (n = 12)	✓	✓	×	×
PEG (n = 13)	✓	✓	×	×
PEG (n = 14)	✓	✓	×	×
PEG (n = 15)	✓	✓	×	×
PEG (n = 16)	✓	✓	×	×
PEG (n = 17)	✓	✓	×	×
PEG (n = 16)	✓	✓	×	×
PEG (n = 17)	✓	✓	×	×

<sup>a</sup> Effluent treated by membrane bioreactor with or without subsequent chlorination.

## References

- Mutlib, E., Chen, H., Nemeth, G. a, Markwalder, J. a, Seitz, S.P., Gan, L.S., Christ, D.D., 1999. Identification and characterization of efavirenz metabolites by liquid chromatography/mass spectrometry and high field NMR: species differences in the metabolism of efavirenz. *Drug Metab. Dispos.* 27, 1319–1333.
- Riska, P., Lamson, M., Macgregor, T., Sabo, J., Hattox, S., Pav, J., Keirns, J., 1999. Disposition and biotransformation of the antiretroviral drug nevirapine in humans. *Drug Metab. Dispos.* 27, 895–901.

## **Chapter 6**

---

### **General Conclusions and Recommendations**

## 6.1 General conclusions

ARVDs are administered as a combination of multiple therapeutic classes that are excreted by humans both in intact form and as metabolites into the sewer system, where they are normally measured at ng/L- $\mu$ g/L levels. Despite intense research effort to monitor their occurrence and fate in aquatic environments, most current analytical methods are still targeted at a few ARVDs of selected therapeutic classes suspected to be prevalent in wastewaters. Antiretroviral therapy however often involves constituents of more than one ARVD class, emphasising the need for methods capable of analysing multiclass ARVDs simultaneously. Furthermore, to assess the overall environmental impact of ARVDs, information regarding the occurrence of their metabolites and transformation products in wastewater is required. This is especially relevant considering the lack of published data on this topic.

Despite the merits of targeted LC-tandem mass spectrometric methods mostly used for ARVD analysis, these are not suitable for the analysis of non-target analytes, i.e. compounds for which the methods are not optimised. Notably, the limited availability of ARVD metabolite standards means that no information is available regarding their levels of occurrence in wastewater. Overall, it is clear that no single analytical method is capable of providing all the required information pertaining to the prevalence of ARVDs, metabolites and transformational products in wastewater. Consequently, the main goal of this study was to develop an analytical approach, entailing several complementary methods, to overcome the challenges presented by the analysis ARVDs spanning a vast range of physico-chemical properties in the complex wastewater matrix.

In the first part of the study, an LC-MS/MS method was developed for use in combination with both SPE sample clean-up and direct injection. Validation results showed that the direct injection of wastewater samples could be used to compensate for the poor recoveries obtained by SPE for the polar nucleoside ARVDs. As expected, the direct injection approach suffered from relatively worse sensitivity compared to SPE, as well as vulnerability to matrix effects due to the co-elution with matrix constituents resulting in ion suppression or enhancement. Application of the developed methods to samples from two WWTPs in the Western Cape confirmed their suitability for the analysis of six parent ARVDs of three therapeutic classes, and provided the first confirmation and quantitative data of two ARVD metabolites in wastewater. Quantitative data showed that advanced tertiary stage treatment by *uv*-irradiation was more effective at removing ARVDs than chlorination. ARVD concentrations were generally higher in influent compared to effluent samples and in dry compared to the wet seasons due to rainwater dilution. The differences in the concentrations observed between influent and effluent samples indicates that ARVDs are effectively removed during the treatment process, with the exception of the mid-to-non-polar compounds efavirenz and nevirapine. Generally, the levels of ARVDs in South African wastewater were comparable to global results.



Secondly, the potential of SFC-MS/MS for environmental ARVD analysis was evaluated as a complementary approach to LC-MS/MS. Compared to LC, SFC separation provided a shorter analysis time for the separation of the same compounds, a well-known benefit of the latter technique due to faster analyte diffusion in the supercritical CO<sub>2</sub>-based mobile phases. A BEH silica column was selected based on column screening experiments, and with a gradient of up to 60% methanol as modifier proved suitable for the analysis of six parent ARVDs and a known metabolite of nevirapine. Analyte enrichment by lyophilisation improved recoveries of the polar nucleosidic ARVDs emtricitabine and lamivudine by ~50%, with comparable recoveries to SPE for the remaining target ARVDs. Lyophilisation was however susceptible to more severe matrix effects, as expected for a technique mainly used for pre-concentration as opposed to sample clean-up. The novel SFC-MS/MS method was validated for wastewater analysis, and excellent agreement in quantitative data with LC-MS/MS was demonstrated. This work shows for the first time the applicability of SFC-MS/MS to analysis of pharmaceutical compounds in environmental water samples.

In the final part of this research, an untargeted LC-HR-MS method was developed for the purpose of screening for additional non-target ARVD metabolites. For this method, RP-LC separation was hyphenated to a Q-TOF HR-MS instrument equipped with ion mobility spectrometry. A mass defect filter was implemented to facilitate data analysis, and compounds present in wastewater samples were then identified using selected standards, as well as tentatively identified based on low- and high collision energy HR-MS spectral data, IMS arrival time and derived collisional cross section (CCs) values. Application of the method to wastewater samples allowed the identification of seven efavirenz, three nevirapine, one ritonavir and one abacavir metabolites, nine of which are reported in wastewater for the first time. This work also contributes experimentally determined CCS values for ARVDs and their metabolites to support future research, and highlighted the potential significance of ARVD metabolites in wastewater contamination.

## 6.2 Recommendations for future studies

As outlined in **Chapter 2**, a tremendous amount of work has been performed in the area of ARVD monitoring in wastewater. It is however clear from the work presented in this thesis that the contribution of ARVD metabolites, thus far overlooked, may prove highly significant. This provides an opportunity for future work focusing on the quantitative analysis of a larger number of ARVDs and their metabolites, and possible correlation of concentrations of parent compounds to metabolites in various wastewater streams. To date, wastewater-based epidemiological studies that correlate the observed concentrations in wastewater to the input concentrations expected from human excreta have not been performed. In fact, the concentrations of ARVDs measured in wastewater are often erroneously linked only to human excretion, because disposal of unwanted or expired drugs may be another possible route of entry into the sewer system. Therefore, a reliable way of verifying the contribution of human

excretion of ARVDs to the overall load detected in wastewater is to target human-excreted metabolites, since the polar functional groups of metabolites are specific to human metabolic pathways, therefore eliminating other derivatives that may have formed within the sewer environment. There is also a need to establish the possibility of formation of transformation products that may resemble the chemical structures of metabolites considering that wastewater treatment process largely depends on activities of diverse microorganisms capable of similar oxidative transformations. Therefore, a comparison of metabolites detected in urine obtained from patients taking ART may be compared to the transformation products that are detected in wastewater as this will confirm the origin of metabolites.